Development of an Acid Gas Adsorbent for CO_2 Removal with Increased Performance in the Presence of Moisture

Peter Harlick

Thesis submitted to the
Faculty of Graduate and Postdoctoral Studies
In partial fulfillment of the requirements
For the Ph.D. degree in Chemical Engineering

Faculty of Graduate and Post-Doctoral Studies
University of Ottawa

Abstract

The objective of this work was to evaluate the fundamentals of the currently available CO_2 separation technologies and provide a solution for the efficient capture of carbon dioxide from various point source emitting industries. In order to realize a robust approach to advancing the solution to this global issue, the versatility of the process to the range of compounds contained within the stream(s) to be processed must be maintained.

It is clear that adsorption, membrane, and aqueous amine based processes are all capable. However, only aqueous amine scrubbing appears economically viable at the current stage of development. In order to challenge this, and potentially drive the separation costs lower, this work centered on hybridizing aqueous amine chemistry and dry adsorption based separations to produce a novel nano-porous material capable of efficient removal of CO_2 from flue gas (5% CO_2 balance N_2 with moisture).

In order to combine aqueous amine scrubbing with dry adsorption, a few approaches were considered and evaluated. These included, amine impregnation within the vast pore volume of PE-MCM-41, surface grafting of various amino silane compounds, and finally, a novel approach of volume based amine functionalization (3D grafting).

Application of pore-expanded MCM-41 (PE-MCM-41) mesoporous silica coated with 3-[2-(2-aminoethyl-amino)ethylamino]propyltrimethoxysilane (TRI) has been extensively examined for the adsorption of CO_2 from N_2. A systematic study of the amine loading as a function of the relative amounts of TRI and water used during the grafting procedure, and the temperature of the grafting reaction was carried out. Extremely high levels of active amine content were achieved using prehydrated silica surfaces at grafting temperatures below reflux in order to facilitate thermally controlled water-aided surface polymerization of the aminosilanes.

The CO_2 adsorption capacities and rates were determined for all materials as a function of the amount of TRI and water per gram of support added to the grafting mixture. The optimal TRI grafted PE-MCM-41 adsorbent exhibited a 2.65 mmol/g adsorption capacity at 25 °C and 1.0 atm for a dry 5% CO_2 in N_2 feed mixture, which exceeded all literature reported values, for both meso- and microporous materials under the conditions used in this study. Further, the apparent adsorption and desorption rates with the amine functionalized materials were exceedingly high. When considering the grafted amine quantity, the adsorption capacity and rate were found to be mutually dependent on each other, exhibiting an apparent optimal combination.

In comparison to zeolite 13X, the optimally loaded TRI-PE-MCM-41 was far superior in terms of dynamic adsorption and desorption performance. These results were further enhanced when the adsorbents were challenged with a humid stream of 5% CO_2/N_2. The TRI-PE-MCM-41 exhibited a 10% increase in CO_2 adsorption capacity, whereas the 13X zeolite did not retain any significant CO_2 adsorption capacity.

The novel concept of an internally variably staged permeator was introduced. A theoretical model was developed and used as the basis for simulation studies. The advantage of the internal variably staged design was shown to permit a very high extent of separation similar to a two stage permeator for purity, while maintaining similar flux rates as per a single stage permeator. This IVSP concept has also taken existing membrane materials and mechanically translated their process performance to a higher level. As such, the unit should prove effective for front end process stream cleanup requirements prior to an adsorption process with the novel TRI-PE-MCM-41 nano-porous adsorbent.

Résumé

L'objectif de ce travail était d'évaluer les technologies de séparations du dioxyde de carbone des gaz de combustion pour fournir une solution efficace aux émissions de CO_2 à partir de diverses sources industrielles. La technologie la plus efficace devrait être performante en présence de composés typiques que l'on retrouve dans les gaz de combustion. Il est clair que les procédés à base d'adsorption, de membranes, et de solutions aqueuses d'amines sont tous capables de récupérer le CO_2 de ces gaz de combustion. Toutefois, seuls les procédés à base d'amines aqueuses apparaissent économiquement viables au stade actuel. Ce travail est centré sur l'hybridation de la chimie aqueuse aminique et de séparations à base d'adsorption à sec pour produire un nouveau matériau nanoporeux capable de l'élimination efficace des émissions de CO_2 des gaz de combustion (5% de CO_2 dans l'azote humide).

Quelques approches ont été examinées et évaluées afin de combiner des amines avec l'adsorption à sec. Elles sont: l'imprégnation d'amines dans les pores de PE-MCM-41, le greffage de différents composés à la surface du silane et une nouvelle approche de fonctionnalisation de l'amine (greffage 3D).

L'Application d'absorbant aux pores élargis, MCM-41 (PE-MCM-41) revêtu de silice mésoporeuse 3- [2- (2-aminoéthyl-amino) éthylamino] propyltriméthoxysilane (TRI) a été largement examiné, pour l'adsorption de mélanges de CO_2 et d'azote. Une étude systématique de la charge d'amine en fonction des quantités relatives de TRI, de l'eau utilisée au cours de la procédure de greffage, et de la température de la réaction de greffage a été réalisée. Des niveaux extrêmement élevés d'amines actives ont été obtenus en utilisant des surfaces de silice préhydraté et des températures inférieures au reflux afin de faciliter la polymérisation en surface.

Les capacités et les taux d'adsorption de CO_2 ont été déterminés pour plusieurs matériaux en fonction de la quantité de TRI et d'eau par gramme de support ajoutée au mélange de greffage. L'adsorbant PE MCM 41 greffé du montant optimal de TRI présentait une capacité d'adsorption de 2,65 mmol/g à 25 ° C et 1,0 atm pour une alimentation sèche de N_2 contenant 5% CO_2. Cette capacité est supérieure à celle signalée dans la littérature. En outre, les taux apparents d'adsorption et désorption avec les matériaux fonctionnalisés d'amines étaient extrêmement élevés. Lorsque l'on considère la quantité d'amine greffée, la capacité et la vitesse d'adsorption se sont avérées être mutuellement dépendantes les unes des autres, présentant une combinaison optimale apparente.

Par rapport à la zéolite 13X, le TRI-PE-MCM-41 optimal était de loin supérieur en termes d'adsorption dynamique et de rendement en désorption. Ces résultats ont augmenté lorsque les adsorbants ont été exposés à un flux humide de 5% de CO_2/N_2. Une augmentation de 10% de la capacité d'absorption de CO_2 a été obtenue avec le TRI-PE-MCM-41, tandis que la zéolite 13X n'a pas retenu de capacité d'adsorption importante de CO_2.

Le nouveau concept d'un perméateur à étage interne variable a été introduit. Un modèle théorique a été élaboré et utilisé comme base pour les études de simulation. La variation interne des étages permet un très haut degré de séparation semblable à un perméateur en deux étapes pour la pureté, tout en maintenant des flux semblables à un perméateur ayant une seule étape. Ce concept de IVSP permet d'améliorer la performance de matériaux membranaires existants. L'unité devrait se révéler efficace en tant que prétraitement avant un procédé d'adsorption avec le TRI-PE-MCM-41 nanoporeux.

Acknowledgements

During the course of completing this thesis, and the many research projects which culminated in this document, I have developed many working and personal relationships. However, first and foremost, I must acknowledge my family (two special ladies; Nevada and Beatriz), and although they are in another city, their words were most heard when needed, and I thank them both. Of course, I also thank Dr. A.Y. Tremblay, for whom without, I may not have realized these exciting and challenging areas of chemical engineering involving adsorption and membrane based separations.

Finally, it is an accomplishment in itself; given the journey that led to this point; those close to me will fully understand this point.

Table of Contents

List of Tables

List of Figures

List of Abbreviations (Specific Nomenclature Given in each Chapter where required)

BET	Brunauer Emmett Teller
CA	Canada
CAPEX	Capital Expenditures
CCS	Carbon Capture and Storage
DGC	Dakota Gasification Company
DI	Diamine
DEA	Diethanolamine
EDP	Energais de Portugal
EPA	Environmental Protection Agency
EU	European Union
T_g	Glass Transition Temperature
KJS	Kruk Jaroniec Sayari
LNG	Liquefied Natural Gas
MS	Mass Spectrometry
MDEA	Methyldiethanolamine
MEA	Methylethanolamine
MT	Metric Tonne
MCM-41	Mobil Crystalline Material 41
MONO	Monoamine
OPEX	Operating Expenditures
PCT	Patent Cooperation Treaty
PEI	Polyethylenimine
PE-MCM-41	Pore Expanded Mobil Crystalline Material 41
PSA	Pressure Swing Adsorption
PTSA	Pressure-Temperature Swing Adsorption
RH	Relative Humidity
SBET	Specific Brunauer Emmett Teller
TSA	Temperature Swing Adsorption
TGA	Thermal Gravimetric Analysis
TRI	Triamine
URPSA	Ultra Rapid Pressure Swing Adsorption
USA	United States of America
VSA	Vacuum Swing Adsorption

Chapter 1

Introduction

1.1 – Objective

The thesis has been assembled as a collection of published papers centered on the objective to explore and develop an advantageous pathway to address some of the limitations of current carbon dioxide (CO_2) separation processes. It is clear from the literature that there are several process concepts which are all capable of separating and recovering of CO_2. However, only aqueous phase amine scrubbing appears viable at the current stage of development and level of industrial deployment. However, this process suffers from high capital expense (CAPEX) and operating expense (OPEX), resulting in a challenged economic position given todays drivers. Alternative technologies may prove viable with potential opportunities which may drive CAPEX and OPEX lower. As such, two other potential technologies, membrane based separation and applied adsorption based separations, are examined in detail. Ultimately, the potential of wet amine chemistry and dry adsorption based separations are combined to produce a novel nano-porous material capable of efficient removal of CO_2 from a proxy flue gas (5% CO_2 balance N_2 with and without moisture).

1.2 – Original contribution

The research project involved two major segments. These segments included novel nano-porous materials modification/engineering for CO_2 adsorption, and membrane module development. The membrane modelling was completed with Dr. A.Y. Tremblay and the nano-

porous materials development studies were completed with Dr. A. Sayari. Four of the presented research papers are first authored by myself which attests to my original input and conception in performing and publishing the work.

One additional article presented in Chapter 4, was co-written with Robert Franchi (MASc student at the time), where many concepts were advanced and analysis performed by myself. The concept of ethanol as the carrier for the amine impregnation concept presented in Chapter 4, was forwarded by Robert Franchi.

1.3 – Thesis Structure

This thesis presents selected published and unpublished works which were completed for the research project. The chapters are described as follows:

- **Chapter 2:** Problem Identification.

  Definition of the current issues, drivers for change, and potential applications of the recovered CO_2.

- **Chapter 3:** Technology Solutions

  Overall review of potential separation technologies, and outlay of the decision path which was pursued with respect to three separation processes; aqueous amine based absorption, applied adsorption, and membrane separations.

- **Chapter 4:** Nano-Porous Development – Amine Impregnated Silica

  This chapter examines the potential of impregnating various amine compounds within the pore volume of a pore-expanded nano-porous silica (PE-MCM-41). The intent was to develop and evaluate the potential of this novel adsorbent for dry and humid CO_2 separation, and thus potentially reduce the capital and operating issues of aqueous amine absorption/stripping, and merge into a more manageable dry amine adsorption

based process.

- **Chapter 5**: Nano-Porous Development – Dry Grafted Amine.

  While the adsorption performance of the impregnated amine adsorbent presented in Chapter 4 was promising, observed hybrid material stability issues could limit practical industrial application. As such, the processes of grafting tethered amine compounds to the surface of a pore-expanded silica nano-porous material (PE-MCM-41) were examined. The intent was to demonstrate a stable novel CO_2 specific adsorbent in the presence of moisture.

- **Chapter 6:** Nano-Porous Development – Triamine Grafting Cause/Effect on Performance.

  With the conventional dry grafting amine pathway established in Chapter 5, further improvements were demonstrated via optimization of reactive conditions, in order to increase the amine content and thus the CO_2 adsorption capacity, for both dry and humid CO_2 in N_2 streams.

- **Chapter 7:** Nano-Porous Development – Optimal Triamine Grafting.

  The concept of 3D grafting was explored given the potential of the large pore volume and pore diameters of the nano-porous silica (PE-MCM-41). An unprecedented amine content was demonstrated with an associated exceptionally high CO_2 adsorption capacity. Even in the presence of moisture, the novel adsorbent was shown to exhibit a rapidly attained high equilibrium adsorption capacity, which was easily regenerated with short thermal pulses. This material outperformed the leading zeolite based material, 13X.

- **Chapter 8:** Membrane Module Development.

  Given the nature of the adsorption process, integration with a membrane based gas separation could prove beneficial. However, due to current limitations for the design of these processes and issues with gas membrane separations reduction to practice, a novel module was conceptualized and theoretically modeled; comparisons to other known module types/process lineups are given.

- **Chapter 9:** Summary Discussion.

  Overall summary discussion, conclusions, and recommendations.

1.4 – Significant Contributions

This research project has resulted in a novel acid gas adsorbent that exhibits unprecedented CO_2 adsorption capacity for dry streams at low pressure, and a relative 10% increase in CO_2 capacity in the presence of moisture (27% RH, 25 °C, 1.0 atm). Further, this novel adsorbent 8 years after publication still outperforms all currently available commercial zeolite adsorbents in terms of adsorption rate and equilibrium capacity for a 5% CO_2 in N_2 water saturated stream at 1.0 atm total pressure and 25 °C.

Where applicable, various novel techniques were applied in order to facilitate this goal. These included a novel method for determining binary adsorption isotherms with the rapid analysis method of concentration pulse chromatography (see Harlick and Tezel, 2005, 2004, 2003A, 2003B, 2002, 2001, 2000), improved chromatographic response data reduction, novel approach and materials via amine impregnation (Chapter 4), improved method for grafting (film deposition, Chapter 5) within nano-porous materials, and optimized methodology for 3D grafting within pore-expanded nano-porous silica (PE-MCM-41, Chapter 6, 7).

Review of the open journal literature via google scholar (Google Scholar, scholar.google.com, 2015, Appendix D) resulted in 789 total journal citations with respect to the three journal articles provided within this dissertation (Chapters 4, 5, and 7, average of 263 per article). Further analysis of the literature with respect to amine grafting to meso/nano porous materials provides for a total paper count of about 390 articles since 2007. Given the total citation count for the articles presented in this dissertation and the total articles published to date (April, 2015) shows that the work and concepts shown in this body of work have contributed significantly to the wider global effort for tailoring meso/nano porous materials.

The novel CO_2 tailored meso-porous silica amine impregnated, and amine grafted materials developed and studied within this work have also been granted a US patent, 7 767 004 (2010). Patents have also been issued in Canada, CA 2600751 2012, and EU (under PCT). Since completion of this work, an additional patent under this patent family, (US 8 361 200, 2012) has been issued.

The main cross discipline contribution from this work is the concept of 3D grafting within the porous volume of materials. Prior to the current study, the journal and patent literature taught that amine grafting was limited to the 2D surface functionalization pathways only. By challenging this pathway to functionalize surfaces with the concept of pore filling in terms of pore volume, another dimension has been fundamentally added to this field and enabled novel materials to be developed. This work has vasty increased the amine content in sorbents and lead to several new applications of solid sorbents in acid gas removal, base catalysis, and aqueous phase heavy metal removal (for example see, Chapter 9).

Chapter 2

Problem Identification

2.1 – The Carbon Dioxide Problem

For many decades, combustion processes have been mankind's most common and essential means of releasing energy for comfort, transportation, and industrial processes, and the enabling the greater global economy. With an increasing worldwide population and an increased per capita demand for energy, action has been mandated, proposed, and in certain countries taken to reduce and/or eliminate the airborne pollution resulting from the emission of classified environmentally harmful gaseous by-products from combustion processes. Even carbon dioxide, a gaseous compound produced during combustion by oxidation of carbon and essential to plant life, is being viewed as a pollutant today. Carbon dioxide has been identified as one of many "*greenhouse*" gases and an increased level in the earth's atmosphere has been stated, to some controversy, to contribute to an undesirable global warming effect. While, several other components have also been identified as greenhouse gases, including nitrous oxides (NO_x), fluorocarbons (xCF's), and methane (CH_4), CO_2 remains a high priority target for reduction efforts.

No more than fourty years ago the scientific community was concerned that the earth's atmosphere was cooling and progressing toward the next so-called "*ice age*". Obviously some confusion continues to exist along with a lack of complete understanding of the many factors involved in the thermal energy balance of the earth's crust and the gases comprising the earth's atmosphere. As it is understood today, that measurable changes in the composition of the earth's atmosphere will produce added risk to undesirable changes to the global climate. Until the

complete understanding of the effects of certain ongoing changes, attempts to moderate or eliminate those changes from occurring, and must be exercised. A cause/effect relationship of CO_2 on the atmosphere is given by Solomon et al., (2009), which discussed the linkages in further detail. Control measures have been previously and currently mandated to be met in accordance with the Clean Air Act (U.S. 1990)[1] and the Kyoto Protocol (Kyoto, Japan, 1997)[2], Clean Smokestack Act (U.S. 1999)[3], and the proposed Clean Power Plan Rule (U.S. 2014)[4].

Significant political pressure has been exerted by the World community to cut CO_2 emissions. In the United States, the EPA has attempted to control and reduce CO_2 reductions via the RFS (renewable fuel standards) with second generation biofuel production targets. These are meant to shift the U.S.A. fuel producing CO_2 emissions to a renewable alternative with at least a 60% net reduction in CO_2 emissions. Other alternative energy technologies such as wind and solar power generation markets have also increased in market volume and share significantly over the past decade. However, as a society, we continue to rely upon fossil fuel for our increasing energy demands; a 40% increase in energy usage is expected by 2035 relative to 2015 levels. As such, the carbon dioxide problem will not go away. With increasing world population and rapidly increasing energy demand around the world, the CO_2 issue will only get worse. Therefore, we need to understand what the current technology can do to help reduce the effects of our energy appetite on the environment which we rely upon. Carbon dioxide control strategies is one mechanism which may afford a lower so-called "*carbon footprint*". Continued developments should further enable these technologies to be economically viable and be deployed into the various industrial sectors.

1 – Details of the Clean Air Act can be found at http://www.epa.gov
2 – Details of the Kyoto Protocol can be found at http://unfccc.int/kyoto_protocol
3 – Details of the to the Clean Smokestack Act can be found at http://www.epa.gov
4 – Details of the Clean Power Plan can be found at http://www.epa.gov

As discussed by Figueroa et al., (2008, National Energy Technology Laboratory, US Department of Energy) CO_2 capture/avoidance can be broadly classified into three categories; Pre-Combustion, Oxy-Combustion, and Post-combustion. In this work, the post combustion technology pathway has been selected for study. This is expected to greatly reduce the installation *"pain"* for the operation and thus accelerate industrial adoption.

2.2 – Carbon Dioxide Applications

One method of control is to capture and recover, and beneficially utilize carbon dioxide from combustion processes (Socolow et al., 2004, Song, 2006, Middleton and Eccles, 2013). The oil industry has greatly benefited from the use of CO_2 for enhanced oil recovery (EOR) (Holt et al., 1993, Gelowitz et al., 1995, Tontiwachwuthikul and Chakma, 1997). In particular, the first international CO_2 sequestion project has been operating in Weyburn, Saskachwan, Canada, known as the Weyburn-Midale Monitoring and Storage Project (Weyburn-Midale, 2015). The oil fields in this location have been in operation since about 1955, and have benefited greatly from the use of CO_2 injection and thus extending the life of the oil field. Furthermore, the project has has also sequestered about 40MT of CO_2 since 2000. The CO_2 for this application is largely produced by Dakota Gasification Company (DGC, about 29 MT CO_2) via Oxy-Combustion coal gasification and methanol stripping to produce a 96% pure dry CO_2 stream (50% recovery) for EOR and sequestration pruposes (see Dakota Gasification Company, 2015).

Other small market uses of CO_2 include the beverage industry, refrigeration (*dry ice*), speciality gas supply, pneumatics, fire extinguishers, inert environments, propellants, detoxification of substances contaminated by hazardous hydrocarbons, fire suppression, food preservation and enhanced growth and production from plants in greenhouses.

A few potential large market uses that have been or are continually being investigated include the catalyzed production of ethanol, methanol (Sammells and Ang, 1985, Lee and LeBlanc, 1993), formic acid, methane, and formaldehyde, (Sammells and Ang, 1985). Carbon dioxide has also been studied and used for polymer production and/or polymer processing. For example, the production of urea-formaldehyde resins, and poly(2-pyrone)s (Tsuda et al., 1993). The advantages of using CO_2 in polymer processing include the accelerated inclusion of additives and increased quantities infused (Berens et al., 1992). Carbon dioxide has also been used, in closed systems, for polymer T_g (*glass transition temperature*) modification (Edwards et al., 1998) and micropore foam production (Parks and Beckman, 1996a, b).

Researchers have also been studying the long sought after large market process for electrochemical reduction conversion of CO_2 to the more reactive CO, (for example see Bandi and Kuehne, 1992, Podlovchenko et al., 1994, and Jitaru et al., 1997). Recent advances are beginning to discover the necessary materials and process to economically enable this pathway (Gattrell et al., 2006, Centi, et al.., 2007, Benson et al., 2009, Zhao et al., 2013)

Even with the absence of a proven economical electrochemical route for CO production from CO_2, Audi has created a joint venture with a German company, Sunfire (Dresden, Germany), to scale up a process for a CO_2 product they have termed e-diesel (www.sunfire.de, 2015). The process is based the electrolysis of water to provide a H_2 source and then either an electrochemical route or homogeneous/heterogeneous conventional catalytic process to convert CO_2 to CO (process not disclosed). This stream is combined with the H_2 to produce syngas, and then further conversion with the well known Fischer-Tropch catalysis process to produce value added hydrocarbons. While very promising, this process is currently in the pilot plant stage. A few reviews for the status of other uses of CO_2, see Jiang et al., (2010), Olah et al., (2009), Centi and Perathoner, (2009), and Ganesh, (2013).

2.3 – A Capture Solution

Although CO_2 is emitted by several sources (*natural, residential, automotive, industrial, etc*…), the industrial sector has been targeted by global concerns and politicians. In order to meet the present and future constraints placed on the allowable emissions of CO_2 the solution lies with point source reduction and recovery. The intent of this work was to evaluate the potential for a future technology deployment at the post-combustion stage of power generation. Therefore, a treatment process must be developed. For this treatment process to succeed, it must be capable of effective and efficient removal, concentration and recovery of CO_2 from flue gas for industrial applications in the presence of moisture.

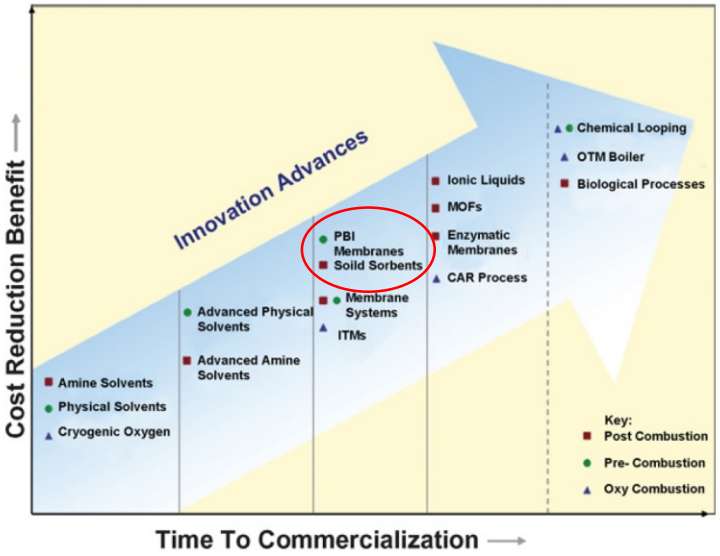

Figure 2.1 Capture technology benefit to time to commercialization comparison as produced by and reproduced from Figueroa et al., (2008), circle indicates the position of this work, http://www.sciencedirect.com./science/article/pii/S1750583607000941.

Figueroa et al., (2008), presented a chart (Figure 2.1) comparing the cost reduction benefit vs the time to commercialization of CO_2 capture technologies. For example, amine based wet scrubbing has a low cost reduction benefit but also low time to commercialization. Whereas, both membrane and adsorbent based separations exhibit, about, medium range for

cost reduction benefit and time to commercialization. As such, these process were examined in this work due to their potential to reduce the capture cost, and be deployed in the near future given the typical time to market for various industrial projects.

2.4 – References

Bandi, A., Kuehne, H.-M., *Electrochemical Reduction of Carbon Dioxide in Water: Analysis of Reaction Mechanism on Ruthenium-Titanium-Oxide*, Journal of the Electrochemical Society, 139 (6), 1992

Benson, E.E., Kubiak, C.P., Sathrum, A.J., Smieja, J.M., *Electrocatalytic and Homogeneous Approaches to Conversion of CO_2 to Liquid Fuels*, Chemical Society Reviews, 38 (1), 2009

Berens, A.R., Huvard, G.S., Korsmeyer, R.W., Kunig, F.W., *Application of Compressed Carbon Dioxide in the Incorporation of Additives into Polymers*, Journal of Polymer Science, 46 (231-242) 1992

Centi, G., Perathoner, S., Winè, G., Gangeri, M., *Electrocatalytic Conversion of CO_2 to Long Carbon-Chain Hydrocarbons*, Green Chemistry, 9 (6), 2007

Centi, G., Perathoner, S., *Opportunities and Prospects in the Chemical Recycling of Carbon Dioxide to Fuels*, Catalysis Today, 148 (3-4), 2009

Dakota Gasification company, www.dakotogas.com

Edwards, R.R., Tao, Y., Xu, S., Wells, P.S., Yun K.S., Parcher, J.F., *Chromatographic Investigation of CO_2-Polymer Interactions at Near-Critical Conditions*, Journal of Physical Chemistry, 102 (7) 1998

Figueroa, J.D., Fout, T., Plasynski, S., McIlvried, H., Srivastava, R.D., *Advances in CO_2 Capture Technology - The U.S. Department of Energy's Carbon Sequestration Program*, International Journal of Greenhouse Gas Control, 2 (1), 2008

Ganesh, I., *Conversion of Carbon Dioxide into Several Potential Chemical Commodities Following Different Pathways - A Review*, Materials Science Forum, 764, 2013

Gattrell, M., Gupta, N., Co, A., *A Review of the Aqueous Electrochemical Reduction of CO_2 to Hydrocarbons at Copper,* Journal of Electroanalytical Chemistry, 594 (1), 2006

Gelowitz, D., Kritpiphat, W., Tontiwachwuthikul, P., *Cogeneration Concepts for CO_2 Separation from Power Plants for Enhanced Oil Recovery Applications*, Energy Conversion & Management, 36 (6-9) 1995

Holt, T., Lindeberg, E., *CO_2 from Industrial Sources as Injection Gas in Oil Reservoirs*, Energy Conversion & Management, 34 (9-11) 1993

Jiang, Z., Xiao, T., Kuznetsov, V.L., Edwards, P.P., *Turning Carbon Dioxide into Fuel*, Philosophical Transactions of the Royal Society A: Mathematical, Physical and Engineering Sciences, 368 (1923), 2010

Jitaru, M., Lowy, D.A., Toma, M., Toma, B.C., Oniciu, L., *Electrochemical Reduction of Carbon Dioxide on Flat Metallic Cathodes*, Journal of Applied Electrochemistry, 27 (8), 1997

Lee, J.M., LeBlanc, J.R., *Integrated Process for Making Methanol and Ammonia*, U.S. Patent # 5,180,570, 1993

Middleton, R.S., Eccles, J.K., *The Complex Future of CO_2 Capture and Storage: Variable Electricity Generation and Fossil Fuel Power*, Applied Energy, 108, 2013

Olah, G.A., Goeppert, A., Prakash, G.K.S., *Chemical Recycling of Carbon Dioxide to Methanol and Dimethyl Ether: From Greenhouse Gas to Renewable, Environmentally Carbon Neutral Fuels and Synthetic Hydrocarbons,* Journal of Organic Chemistry, 74 (2), 2009

Parks, K., Beckman, E.J., *Generation of Microcellular Polyurethane Foams via Polymerization in Carbon Dioxide: 1: Phase Behaviour of Polyurethane Precursors*, Polymer Engineering and Science, 36 (19) 1996a

Parks, K., Beckman, E.J., *Generation of Microcellular Polyurethane Foams via Polymerization in Carbon Dioxide: 2: Foam Formation and Characterization*, Polymer Engineering and Science, 36 (19) 1996b

Podlovchenko, B.I., Kolyadko, E.A., Lu, S., *Electroreduction of Carbon Dioxide on Palladium Electrodes at Potentials Higher than the Reversible Hydrogen Potential*, Journal of Electroanalytical Chemistry, 373 (1-2), 1994

Sammells, A.F., Ang, P.G., *Method for Reducing Carbon Dioxide to Provide a Product*, US Patent #4,545,872, 1985

Socolow, R., Hotinski, R., Greenblatt, J.B., Pacala, S., *Solving the Climate Problem: Technologies Available to Curb CO_2 Emissions*, Environment, 46 (10), 2004

Solomon, S., Plattner, G.-K., Knutti, R., Friedlingstein, P., *Irreversible Climate Change due to Carbon Dioxide Emissions*, Proceedings of the National Academy of Sciences of the United States of America, 106 (6), 2009

Song, C., *Global Challenges and Strategies for Control, Conversion and Utilization of CO_2 for Sustainable Development Involving Energy, Catalysis, Adsorption and Chemical Processing,* Catalysis Today, 115 (1-4), 2006

Tontiwachwuthikul, P., Chakma, A., *R & D on High Efficiency CO_2 Separation Processes for Enhanced Oil Recovery at University of Regina*, Journal of Canadian Petroleum Technology, 36 (2) 1997

Tsuda, T., Kitaike, Y., Ooi, O., *Nickel(0)-Catalyzed 1:1 Cycloaddition Copolymerization of 1,3 and 1,4-Di(2-Hexynl)Benzenes with Carbon Dioxide to Poly(2-Pyrone)s*, Macromolecules, 26 (18) 1993

Weyburn-Midale, 2015, www.ptrc.ca/weyburn-midale

Zhao, H.-Z., Chang, Y.-Y., Liu, C., *Electrodes Modified with Iron Porphyrin and Carbon Nanotubes: Application to CO_2 Reduction and Mechanism of Synergistic Electrocatalysis*, Journal of Solid State Electrochemistry, 17 (6), 2013

Chapter 3

Technology Options and Background

3.1 - Available CO_2 Separation Technologies

Presently, there are several technologies available for removing CO_2 from the exhaust streams before release to the atmosphere (Pruschek and Oeljeklaus, 1990, Figueroa et al., 2008, Meerman et al., 2012A, 2012B). Absorption, cryogenic distillation, fixation by biotechnology, membrane-based processes, and adsorption are technically feasible separation methods. As discussed in Chapter 2, aqueous phase amine scrubbing, adsorption, and membrane separations based process have been chosen to study in further detail.

3.1.1 – General CO_2 Separations

Amine based aqueous phase absorption is the most common technology employed for removing CO_2 from industrial effluents (Sartori, and Leder, 1978, Suzuki et al., 1997, Mariz et al., 1999, Lee and LaBlanc, 1993, Chiesa and Lozza, 1998, Khanmamdov, 1998, Yoshida et al., 2000, Yongling and Yingshu, 2012). The aqueous amine (for example, diethanol amine, DEA) absorption process accounts for approximately 70% of all natural gas upgrading sites. However, this type of amine system is inherently handicapped by economies of scale. Meaning, that the process will produce economic benefit only for large scale operations, and is thus not viable at small scales. While this aspect is well suited for the large scale power industry, the small scale emitters will not realize a payback with respect to CO_2 avoidance. Another impairment relates to the quantity of amine solution as a function of CO_2

concentration. As the CO_2 inlet concentration increases, a convex non-linear increase of the amount of amine is needed to maintain the desired output specification.

Membrane gas separation systems have become more widely used in recent years as reflected by the literature (for example see, Bernardo and Clarizia, 2013). However, the industrial process adoption rate for gas separation using membranes has been slow and typically deployed only within high value specialty product industries. The main cause of this slow adoption rate is the cost impact from effective surface area requirements. Membrane systems rely mainly on the mass transfer rates (*permeabilities*) of the components through a semi-permeable interface, the membrane. In this mode of operation, the flux of the faster permeating component will be the limiting rate mechanism. This will limit the total flowrate that a given membrane surface area can process, in order to maintain a process specification. Presently, there are very few membrane types with the proper morphology capable of handling this type of CO_2 separation on an industrial scale without severe economic penalty due to the initial and replacement membrane costs (Atsonios et al., 2013, Goto et al., 2013, Kazama and Haraya 2013, Nagumo et al., 2013, Lin et al., 2015 ,).

Major advances have been demonstrated with inorganic type membranes either as supports, or with subsequent functionalization (for example see, Yeo et al., 2013, Zulhairun et al., 2015), or as barriers for amine containing fluids such as ionic liquid membranes (for example see, Wu et al., 2013). However, even with all the advances and increased knowledge, economical membrane based gas separation processes for large-scale power producing process is still elusive. Although, membrane materials continue to evolve and support higher separation efficiencies and flux rates, their ability to handle the potential multi-component, so called *"dirty"* effluent streams will continue to be a challenge while maintaining low cost.

Adsorption based systems may be employed in either an isobaric or isothermal mode of operation. These systems do not, generally, operate at steady-state, and have higher capital and energy costs than membrane systems (for example see, Zhai and Rubin, 2013, Heyne and Harvey, 2014, Pritchard et al., 2014). However, a much higher degree of separation can be obtained at a much larger processing rate, and significantly lower media replacement cost relative to membranes. The separation is based on a kinetic or equilibrium difference of the components with a specific or blend of adsorbents, through either physical or chemical binding. Although the process is viable for large-scale separations, it is complicated to operate and currently handicapped by high initial CAPEX. Further, if the process is not properly designed, the setup will not be able adapt to widely changing inlet conditions.

3.1.2 – Membrane Separations

Membrane based gas separation processes have been evolving for the last 70 years (Stern et al, 1964, Pan and Habgood, 1974, 1978, Sirkar, 1984, Perin and Stern, 1986, Sengupta and Sirkar, 1987, Sidholm et al., 1987, Wang and Wang, 1988, Li and Teo, 1992, Sirkar, 1996, Kusakabe et al, 1998, Chen et al., 1999, Yeo et al., 2013, Zulhairun et al., 2015). The productivity of a gas permeation process is jointly controlled by a partial pressure driving force, the mass transfer resistance (*permeability*), and the effective membrane area. Conventionally, membrane modules have a feed and a permeate stream as shown in Figure 3.1.

The feed enters in the upper region at a pressure higher than the lower region. In the feed stream the faster permeating component transverses the membrane and enters into the permeate stream at an enriched level. As the feed is depleted in the faster permeating component, it is enriched in the slower permeating component. At the exit of the module,

two enriched streams are possible, but, typically not attainable in this type of module configuration.

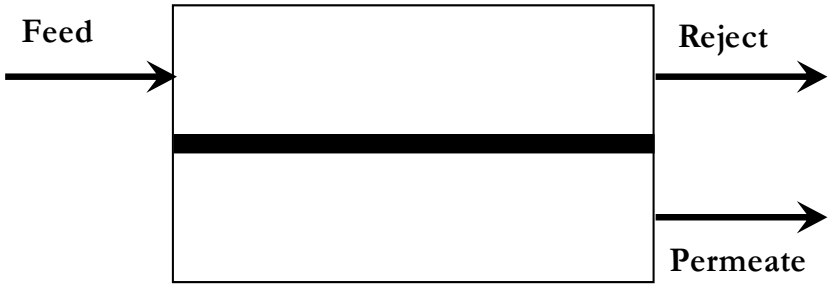

Figure 3.1 A schematic diagram of a conventional membrane gas permeation module in co-current flow.

Various membrane configurations based on this module type have been used. These include flat sheet, tubular, and hollow fibre. All of these membrane types may be employed in a conventional (Pan and Habgood, 1974, Perrin and Stern, 1986), spiral wound, asymmetric (Sirkar, 1984, Sengupta and Sirkar, 1987), and/or an internally staged module (Sidholm et al., 1987, Li and Teo, 1992, Liu et al, 2000, Lui et al., 2001). Further review is available in *Chapter 8* with respect to various membrane module types and process configurations.

The removal of NO/SO_2 from model flue gas was demonstrated using a contained liquid membrane permeator (Majumdar et al., 1994). Chen et al., (1999) also used a contained liquid membrane permeator for separation of CO_2 from N_2. The permeator provided a perm-selectivity >3400 (pure component basis). This is a high degree of separation for CO_2 and N_2. However, the productivity of the system was extremely low. This low productivity is not well suited for industrial integration since the flue gas flowrates are extremely high. The high input flowrate would require a large number of modules to process the requirements. Further, the separation was based on a permeate pressure of near absolute zero pressure, which is not economical for flue gas treatment.

Pilot scale testing of a membrane system for CO_2 removal from coal fired plants was reported by Sandru et al., (2013). Their system consisted of polymeric polyvinylamine carrier membranes with testing completed at the Sines power plant of Energias de Portugal (EDP) in Portugal. Promising results were obtained for continuous operation over 6.5 months. Although only a slipstream was diverted to the pilot skid, neither the real nor synthetic flue gases appeared to negatively effect the membrane performance.

2.1.3 – Adsorption Fundamentals

Adsorption is a process that involves the immobilization of a component or mixture of components (*adsorbate(s)*) to the surface of a porous solid (*adsorbent*). A separation can be achieved by exploiting either kinetic or equilibrium adsorption properties of the components within the porous adsorbent. The pores of the adsorbent can range in equivalent diameter from the macro to micro ranges, or combinations thereof.

The process of adsorption within a zeolite type adsorbent generally occurs in four stages (Figure 3.2). The first step is the introduction of the components (*adsorbates*), to a packed bed of solid particles (*adsorbent*). Next, the components diffuse through the external film layer of the pellet and enter the macroporous regions. Once in the macropores, the components diffuse to the crystalline structure and into the micropores. The bulk of the adsorption occurs in the micropores for zeolite type adsorbents (Taqvi and Levan, 1996).

If the process is properly designed for an equilibrium-based separation, the combined resistance of all of the regions is usually less than the resistance encountered in the microporous region. Therefore, the smallest pore regime will dominate the mass transfer resistance. This is due the relative sizes of the channels, tortuosity, and the kinetic diameters

of the components. The interaction between the components and the surface is the mechanism that will determine the effective rates of mass transfer. In this regard, the role of the adsorbates, and the adsorbent selection, become an important and often overlooked design consideration. For example, it may be more beneficial to have an adsorbent/adsorbate with high adsorption rates yet lower equilibrium capacity than low adsorption rates and high equilibrium capacity.

2.1.4 – Applied Adsorption: Processes

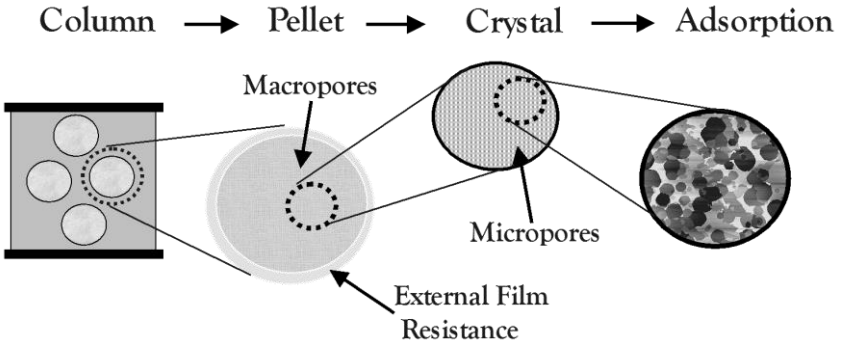

Figure 3.2 A generalized representation of the mechanisms involved with the mass transfer processes of adsorption.

In order to exploit the adsorption properties of adsorbents; the adsorbent must be utilized within a process. This process should exploit the difference in adsorption capacities or component kinetics exhibited by differences in operating conditions. In the field of adsorption, there are three main applied process concepts:

1) - Pressure Swing Adsorption (PSA)

2) - Temperature Swing Adsorption (TSA)

3) - Vacuum Swing Adsorption (VSA)

All other variations of adsorption unit operations are based on one and/or

combinations of the previous three process concepts. A review and teaching of the adsorption-based process is given by Cen and Yang, (*1986*), Yang (*1987*), Kumar and Van Sloun, (*1989*), White and Barkley, (*1989*), Ruthven et al., (*1994*), Harlick and Tezel, *(2004, 2005)*, and Ho et al., *(2008)*.

In the art of adsorption separations, the pressure swing process is the most widely employed (Inui et al., 1988, Shin and Knaebel, 1988, Shin, 1988, Sircar and Kratz, 1988, Sircar, 1988, Kikkinides et al., 1993, Kim et al., 1994, Chue et al., 1995, Dong et al., 1999a, b, and Warmuzinski and Sodzawiczny, 1999). Advances in the design of PSA systems have also greatly enhanced the productivity and capabilities of the separation scheme (Suh and Wannkat, 1989, Dong et al., 1999a, Dong et al., 1999b, Cho et al., 2004).

The process is based on exploiting the difference in adsorption capacity exhibited by an adsorbate-adsorbent system when step changes in the operating pressure are applied. The change in adsorption capacity is termed the working capacity, and is conceptually depicted in Figure 3.3. For a PSA system, the expected working capacity is shown by the difference in the amount adsorbed at the feed pressure and the regeneration pressure from an adsorption isotherm. With this approach, the product purity is highly dependent on the conditions used to obtain low pressure (Warmuzinski and Sodzawiczny, 1999, Gomes and Yee, 2002). In many PSA processes, the desired product is the less adsorbed component, where the more adsorbed component is discarded with no concern of purity. An example of this type of system is natural gas upgrading. The N_2 and CH_4 generally are weakly adsorbed, whereas the CO_2 and other heavy components are strongly adsorbed (Sircar*, 1988*). These more adsorbed components are then desorbed and released to further processing or to the atmosphere as discharge.

When a PSA process requires high product purity of the more strongly adsorbed components, a different regeneration technique must be employed (Sircar and Kratz, 1988). In order to maintain the product purity on the adsorbent surface, the low-pressure step must be used with at least the same composition of gases; i.e., ideally no purge (dilutent) gas. Therefore, by exposing the adsorbent to an environment of this nature, the desorbing gases remain in the state of the adsorbed phase purity.

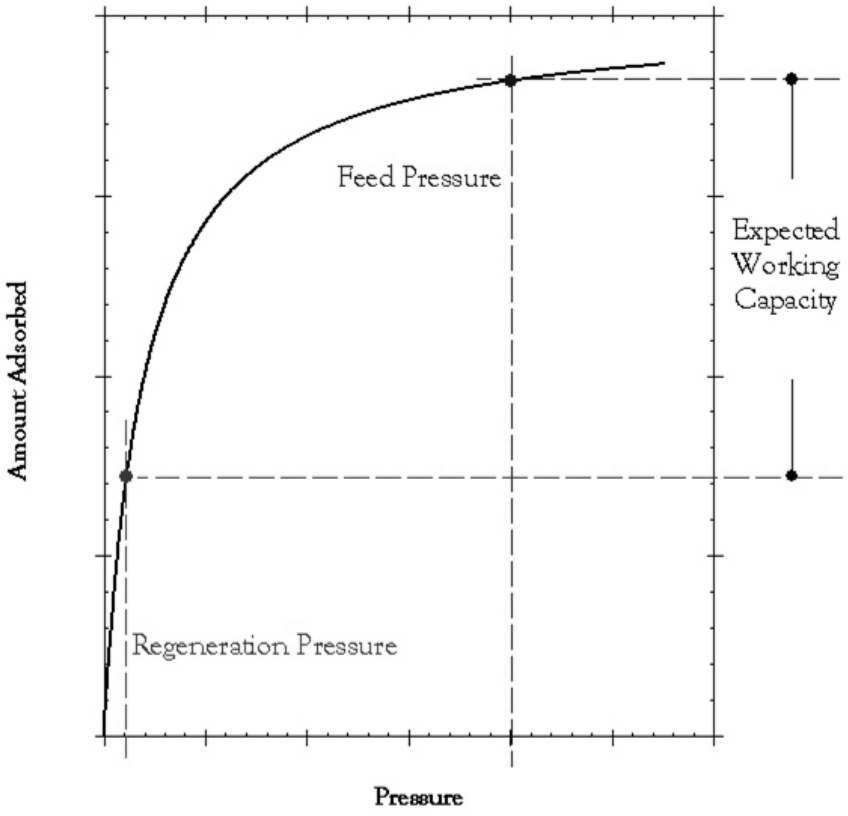

Figure 3.3 A schematic representation of the expected working capacity observed in an equilibrium PSA process.

In order to accomplish a continuous (*cyclic steady-state*) separation, the process must be designed to allow for the regeneration of one adsorbent column while another column is being saturated, with out interruption to the feed rate. The original process was conceptualized by Skarstrom (1959) and was termed the Skarstrom Cycle. The basic Skarstrom cycle only

consists of two adsorption columns, thus affording only one component as the purified product (for example see, Ruthven et. al, 1994). However, the number (limited by size) of columns is defined by the feed flowrate, product purity demands, realized kinetics and adsorption capacities. A modified Skarstrom cycle for the removal and concentration of the more adsorbed component (CO_2) is shown schematically in Figure 3.4.

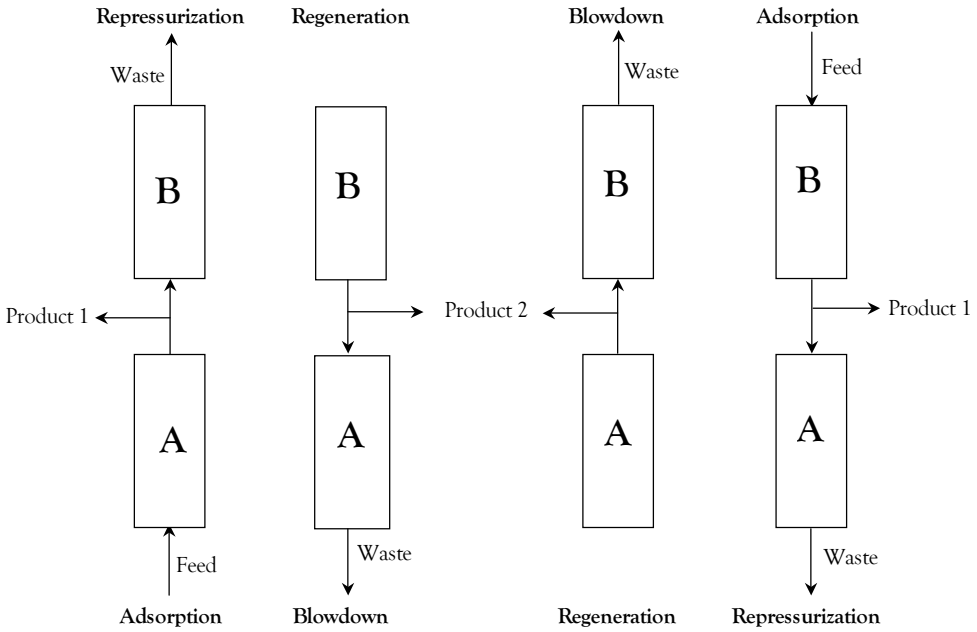

Figure 3.4 A schematic representation of the stages involved in the two-bed pressure swing adsorption design using a modified Skarstrom cycle.

The process occurs in four stages. These include challenging the columns with the feed mixture, blowdown, desorption (regeneration), and repressurization. In the traditional Skarstrom cycle, two adsorption columns are used, and regeneration is accomplished under purge. Figure 3.4 shows the state of each column at various stages in the process, and is designed to allow for high purity component 2 to be obtained.

For simplicity, a two component system will be considered. The cycle starts by

challenging column A with the feed mixture (component 1 and 2), at high pressure. After a very brief time, the less adsorbed component (1) will breakthrough first. At this point, the purity of component 1 is at its highest. The quality of component 1 will remain high until the more strongly adsorbed component (2) starts to breakthrough. When component 2 appears in the effluent, the feed is sent to a second, clean, adsorbent bed, and the first bed is regenerated.

The state of the effluent at which the feed is cycled is a design consideration. Usually, this is set by the desired purity of component 1 (Reynolds et al., 2008), subject to the adsorption capacity/kinetics for component 2, which defines the bed sizing and switching time. As such, high capacity adsorbents, which also exhibit high rates of adsorption/desorption will result in a lower cost process due to the higher performance.

The other stages in the process are more easily described when the process exhibits cyclic steady-state performance. In order to simultaneously challenge and regenerate the columns, a portion of the regeneration effluent from a previous cycle is used to blowdown/purge column B to the regeneration pressure. In this manner the product purity is maintained.

The next step involves the regeneration of column B. This is accomplished by controlled adjustment to a lower pressure. After regeneration is complete, column B is repressurized with a partial bleed of the effluent from column A that is being saturated (at high pressure). The whole cycle continues with the column states reversed. When operated in this manner, the process produces a continuous supply of high purity components 1 and 2, provided that the system kinetics are appropriate for a two-bed system. When the separation demands cannot be satisfied by this design, more adsorbent columns are employed (Dantas et

al., 2001).

Several factors affect the operation of the PSA process. These include particle size and composition effects (Gladden, 1991, Alpay et al., 1994), bed pressure drop (Buzanowski et al., 1989), heat effects (Farooq et al., 1988), feed conditions (Kumar, 1995), incomplete regeneration (Matz and Knaebel, 1988, Na et al., 2002), feed pressure, temperature, and adsorbent characteristics (Harlick and Tezel, 2004, 2005). All of these factors must be considered prior to the design of a PSA process.

The adsorbent particle composition will affect the performance of a PSA process if chemisorption occurs within the matrix and/or the binder. The binder is, typically, a macroporous material that holds the crystals in a suitable pelletized form for use in a packed tower. The kinetics may also be affected by the particle size. When the unit is properly designed, the feed flowrate is high enough to neglect the film diffusion resistance and the macropores are large enough to allow free unhindered gaseous movement. However, if the particle size is sufficiently large, then the assumption of plug flow in the column may not be valid as axial dispersion will dominate the process, and thus reduce the effective adsorption capacities. The effect of axial dispersion, will result in a more disperse mass transfer front (also known as breakthrough curve). This will result in a reduced cyclic operating working capacity, and thus reduced process efficiency. This will have adverse effects on the performance of the process, as the components will not reach an equilibrium state within the adsorbent (Harlick and Tezel, 2005).

The bed pressure drop is a crucial design constraint. The pressure loss should be kept low in order to minimize the compression costs. If a large pressure drop exists in the column,

then the adsorption dynamics will also change. This is due to both the adsorption capacity and diffusivity being functions of pressure.

The internal heat generation effects in the column are largely derived from the adsorption process itself. Since, adsorption is an exothermic process; a quantity of heat is released in relation to the mass transfer transient. If the column is designed to operate at the optimal conditions, then the heat effects must be minimized in order to realize a greater working capacity (Harlick and Tezel, 2005), as adsorption capacity typically decreases as the temperature increases.

The feed conditions have a large effect on applied adsorption performance (Hasan et al., 2012). As the feed composition of the more adsorbed component increases the cycle time will decrease for a fixed design. Similarly, as composition of the less adsorbed component increases, the cycle increases. The effect on the process dynamics can be extremely detrimental. If the kinetics of the system does not favour the new conditions, then the process will not perform as expected. Other feed conditions such as temperature, and flowrate also affect the applied adsorption process in a similar manner (Park et al., 2002).

3.2 – Flue Gas Treatment

The Kyoto Protocol has mandated globally, and the proposed Clean Power Plan (USA) to reduce CO_2, and other pollutants, from flue gas. Presently, technology exists to achieve this goal. The technology permits the reduction of CO_2 at the source and allows for the complete removal of CO_2 in the process effluent. However, in order for industry to adopt a technology that permits a high level of CO_2 control, the economics of the process must be improved.

In most combustion processes, the flue gas consists of many components. These

include N_2/O_2, CO, CO_2, NO_x, SO_x, H_2S, COS, H_2O, and waste hydrocarbons (*fuel, by-product and impurity*). The amount of each component in the flue gas varies greatly based on the process that produced them. Separations of some of these flue gas components have been shown in the literature.

3.2.1 – Absorption Based Treatment

The selective removal of CO_2 from air (*model flue gas*) has been demonstrated using an improved absorption process (Yoshida et al., 2000). In the process a highly selective and high capacity absorbent solvent was used and shown capable of handling the requirements from a liquid natural gas (LNG) fired plant. This has been in pilot use in Japan since 1995, with the goal of eliminating CO_2 from flue gas at fossil fuel power stations. The pilot unit was built and is in use at the Nanko Power Station (Nanko 2015). The process is shown schematically in Figure 3.5.

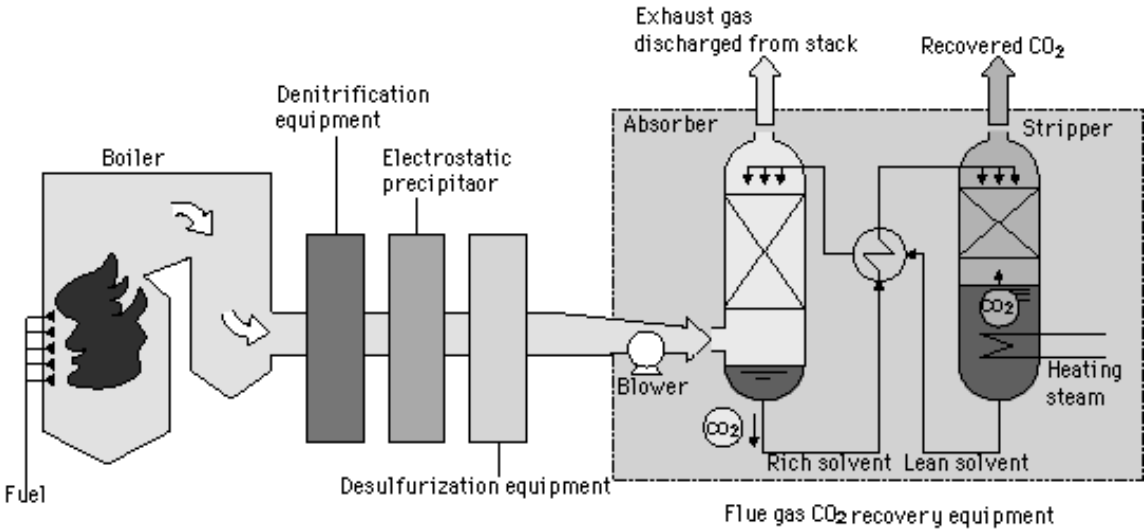

Figure 3.5 A schematic representation of the flue gas separation process in use at the Nanko facilities in Japan (Kansai Electric, 2000).

Another system is about to come on line as part of Shell Canada operations in the

Athabasca oil sands project (Shell Oil Company 2015). This project has been termed Project Quest and has the objective to capture about 1.2 million tonnes of CO_2 per yr. from the Scottford Upgrader, and store this CO_2 underground at a depth of approximately 2500 meters. The basic system components include aqueous amine absorption, dehydration units, and CO_2 compressions. This unit should be in full production in fiscal year 2015, and represents the first of its kind for heavy oil **C**O_2 **C**apture and **S**torage (CCS).

Another major Canadian CO_2 capture and sequestration project is led by Enhance Energy, and also located in Alberta (Enhance Energy 2015). This project aims to have a full faceplate capacity of about 14.6 million tonnes per yr. with start-up in 2015. The capture technology is also based on aqueous amine solutions.

Including these two Canadian based CCS projects, there are currently, three other non-power plant based projects, and two power plant based CCS projects in Canada. The common technology deployed or to be deployed with all these projects is wet amine scrubbing. A full database of CCS projects around the World is available via a few online databases (for example see, sequestration.mit.edu).

Further review on the aqueous amine absorption process chemistry is available in Chapters 4, 5, 6, and 7.

3.2.2 – Adsorption Based Treatment

Very few adsorption based flue gas separations have been shown in the literature (Kikkinides, 1993, Suzuki et al., 1997). The work performed by Kikkinides et al. (1993) simulated the removal of CO_2 from dry flue gas. In their work, the flue gas was assumed to consist of 17% CO_2, 4% O_2 and 79% N_2. They used activated carbon and carbon molecular sieve as possible adsorbent choices due to their higher tolerance to water relative to zeolites. Their

results showed that the pressure swing adsorption process could produce >99% CO_2 at 68% recovery at relatively high inlet flowrates. Although their work was simulated, the results did show that an adsorbent with a low capacity for CO_2 would produce high quality products (N_2/O_2 and CO_2). They also simulated the effect of the feed temperature and found that the recovery and purity of the product were not greatly affected by the feed temperature in the range of 23-70 °C. The independence of temperature on the process is very important for flue gas treatment.

Suzuki et al. (1997) showed that a model flue gas stream (5% CO_2, 95% N_2) could be purified using an ultra-rapid pressure swing adsorption system (URPSA) with zeolite 13X. However, the CO_2 recovery from the process was low. This does not allow any sizeable economic benefit to be realized from the CO_2 product since several adsorption beds would have staged in order to recover the waste CO_2.

One aspect of the work described above which the authors did not evaluate was the effect of moisture. This ubiquitous compound is the adsorbents' weakness due to the strong dipole moment exhibited by water (Berger and Bhown, 2013, Huck et al., 2014). As a result, water dominates the adsorption process and will selectively displace weaker bound molecules such as CO_2, or result in a total loss of CO_2 equilibrium capacity. For example, Harlick and Tezel, (2004), completed a thorough review of commercially available zeolite type adsorbents. All the adsorbents studied exhibited CO_2 adsorption capacities based on Van der Waals interactions, and as a result, will exhibit greatly reduced adsorption capacity in the presence of moisture. This is one aspect of adsorbent screening which often remains unreported.

In order to overcome this adsorbent limitation in the presence of moisture, industry typically installs so-called *"guard beds"* in order to knock out the moisture to very low dew points

as to not affect the CO_2 working adsorption capacity. This will result in a larger energy demand for the separation process, and a significant increase in the CAPEX and OPEX for the scheme.

3.3 – Nano-Porous Silica

The area of nano-porous silica has been largely leveraged through the 1992 disclosure by Mobil Corp. of the M41S family of materials (Kresge et al., 1992, Beck et al., 1992). The area has expanded and grown into a novel area for materials research. Many reviews on the topic are available in the literature (Sayari, 1996, Corma, 1997, Ying et al., 1999, Stein, 2003). Due to the structure of the material, O-Si-O, with occasion imperfections in the wall resulting in reactive OH groups, this type of material is accessible for hydrolysis reactions with appropriate functional groups. One specific member of the M41S family, MCM-41 type silica, the surface area is typically in the 1000-1200 m^2/g with a corresponding near uniform pore diameter of about 1-3 nm, and has garnered much research attention. The pore volume of the material is high with values typically within 0.7 to 1.0 cm^3/g.

Even with these characteristics, there exists an opportunity to further enhance the material towards larger pore diameters and volumes. Many groups have explored these alternative silica based materials. Specifically, Sayari et al. (1999, 2000) has developed a post synthesis technique for various pore expansions with associated pore volume increases. Typical characteristics of this so-called pore expanded MCM-41 are similar to the native MCM-41 with the exception of pore diameter, which can be increased and tuned based on the choice of the swelling agent (surfactant). As a result, the pore volume also increases. Typical results are on the order of 2 to 3.5 times the pore volume without major loss of the available surface area, and a tuneable pore diameter up to 30 nm prior to the eventual pore wall collapse due to excessive wall thinning.

Using this family of materials also affords an opportunity to chemically graft various functional groups within the available pore volume via the hydrolysis reaction with the surface OH groups. As a result, one may develop the material to target specific compounds. The technique has been applied to various meso-porous silicas (for example, see, Stein et al., 2000, Sayari and Hamoudi, 2001). As previously discussed, the aqueous amine chemistry route for CO_2 removal appears beneficial; however, it suffers from high CAPEX and OPEX. Given the characteristics of the silica supports, and the benefits of amine chemistry, several groups have studied the art of grafting amine functional groups within the pore structure, for example see, Chen et al., (2014) for a recent review article.

The first issued US patent for amine grafted meso-porous silica material was granted to Leal et al., 1992, and subsequently published in the journal literature (Leal et al., 1995). The material exhibited a low adsorption capacity for CO_2, but initiated the continuing study and development of such materials.

An amine grafted silica material with exceptional CO_2 adsorption capacity was produced by Harlick and Sayari, (2007); and is described in detail in Chapter 7. The material consisted of triamine functional groups grafted in such a way as to produce a pore filling 3D structure. A family of amine impregnated or grafted materials was also covered by Sayari and Harlick under US patent 7767004 (2010). A full review of amine grafted materials is available in Chapter 4, 5, and more comprehensively in Chapter 7. A more recent review of amine grafted, and other non-zeolite CO_2 adsorbents is available in Chen et al., (2014).

3.3 - Hybrid Separations

In recent years, several initiatives have been taken to increase the efficiency and reduce

the cost of CO_2 separation processes (Neih, 1987, Ray et al., 1991, Farla et al., 1995, Mariz et al., 1999, Hasse et al., 2013, Tomioka et al., 2013, Scholes et al., 2013, Warmuzinski et al., 2013). In general, the approach has been to combine separation processes in order to realize the beneficial characteristics of each in order to exploit all possible synergies through process intensification.

Some examples of commercial hybrid processes include the combination of adsorption with distillation for the separation of propane/propylene (Kumar et al., 1992). The enhanced separation of carbon dioxide-water-oxygen-nitrogen was accomplished with a hybrid membrane-adsorption-cryogenic distillation process (Prasad et al., 1992). A similar process was also successfully employed for the separation of N_2 and CH_4 (Lokhandwala, 1997). Hydrogen purity and production was greatly enhanced by combining an adsorption and membrane process (Sircar et al., 1999). An adsorption process was also combined with cryogenic distillation for the selective removal of low levels of moisture and CO_2 (Kumar et al., 1999).

The pattern observed in all of these examples was that an increase in the product purity and recovery was obtained. However, the processes involving CO_2 did not consider the recovery of this component in a high purity state. Often, the CO_2 and H_2O were collected in the same stage and then discarded.

In order to control flue gas emissions, several separation processes have been studied and shown in the literature. Of all of these processes, only one has been adopted and is in use in industry. Therefore, in order to meet the demands and constraints of the Clean Air Act (U.S.A. 1990), Clean Smokestacks Act, (U.S.A., 1999), Kyoto Protocol (Kyoto, Japan, 1997), and the proposed Clean Power Plan (U.S.A., EPA, 2014), a more economical process must be developed and exploited. More specifically, a novel material must be developed and shown capable of handling flue gas CO_2 removal with minimal processing steps.

3.5 - References

Alpay, E., Kenney, C.N., Scott, D.M., *Adsorbent Particle Size Effects in the Separation of Air by Rapid Pressure Swing Adsorption*, Chemical Engineering Science, 49 (18) 1994

Atsonios, K., Koumanakos, A., Panopoulos, K.D., Doukelis, A., Kakaras, E., *Techno-Economic Comparison of CO2 Capture Technologies Employed with Natural Gas Derived GTCC*, Proceedings of the ASME Turbo Expo, 2, 2013

Beck, J. S.; Vartuli, J. C.; Roth, W. J.; Leonowicz, M. E.; Kresge, C. T.; Schmitt, K. D.; Chu, C. T.-W.; Olson, D. H.; Sheppard, E. W.; McCullen, S. B.; Higgins, J. B.; Schlenker, J. L., *A New Family of Mesoporous Molecular Sieves Prepared with Liquid Crystal Templates*. J. Am. Chem. Soc., 114, 1992

Berger, A.H., Bhown, A.S., *Optimizing Solid Sorbents for CO_2 Capture*, Energy Procedia, 37, 2013

Bernardo, P., Clarizia, G., *30 Years of Membrane Technology for Gas Separation*, Chemical Engineering Transactions, 32, 2013

Buzanowski, M.A., Yang, R.T., Haas, O.W., *Direct Observation of the Effects of Bed Pressure Drop on Adsorption and Desorption Dynamics*, Chemical Engineering Science, 44 (10) 1989

Cen, P., Yang, R.T., *Bulk Gas Separation by Pressure Swing Adsorption*, Industrial & Engineering Chemistry Fundamentals, 25 (4) 1986

Chen, H., Kovvali, A.S., Majumdar, S. Sirkar, K. K., *Selective CO_2 Separation from CO_2-N_2 Mixtures by Immobilized Carbonate-Glycerol Membranes*, Industrial & Engineering Chemistry Research, 38 (9) 1999

Chen, C., Kim, J., and Ahn, W., *CO_2 Capture by Amine-Functionalized Nanoporous Materials: A Review*, Korean Journal of Chemical Engineering, 31 (11), 2014

Chiesa, P., Lozza, G., *CO_2 Emission Abatement in IGCC Power Plants by Semi closed Cycles. Part B: With Air-Blown Combustion and CO_2 Physical Absorption*, American Society of Mechanical Engineers, ASME, Fairfield, NJ, USA., 8p., Report # 98-GT-385, 1999

Cho, S.-H., Park, J.-H., Beum, H.-T., Han, S.-S., Kim, J.-N., *A 2-stage PSA Process for the Recovery of CO_2 from Flue Gas and its Power Consumption*, Studies in Surface Science and Catalysis, 153, 2004

Choudhary, V. R., Mayadevi, S., *Adsorption of Methane, Ethane, Ethylene, and Carbon Dioxide on X, Y, L, and M Zeolites Using a Gas Chromatography Pulse Technique*, Separation Science and Technology, 28 (8) 1993a

Choudhary, V. R., Mayadevi, S., *Adsorption of Methane, Ethane, Ethylene, and Carbon Dioxide on High Silica Pentasil Zeolites and Zeolite-like Materials Using Gas Chromatography Pulse Technique*, Separation Science and Technology, 28 (13-14) 1993b

Corma, A.*, From Microporous to Mesoporous Molecular Sieve Materials and Their Use in Catalysis*. Chem. ReV, 97, 1997

Dantas, T.L.P., Luna, F.M.T., Silva, I.J., Torres, A.E.B., de Azevedo, D.C.S., Rodrigues, A.E., Moreira, R.F.P.M., *Carbon Dioxide-Nitrogen Separation Through Pressure Swing Adsorption*, Chemical Engineering Journal, 172 (2-3), 2011

Dong, F., Lou, H., Kodama, A., Goto, M., Hirose, T., *New Concept in the Design of Pressure-Swing Adsorption Processes for Multicomponent Gas Mixtures*, Industrial & Engineering Chemistry Research, 38 (1) 1999a

Dong, F., Lou, H., Goto, M., Hirose, T., *New PSA Process as an Extension of the Petlyuk Distillation Concept*, Separation & Purification Technology, 15 (1) 1999b

Dune, J. A., Mariwala, R., Rao, M., Sircar, S., Gorte, R. J., Myers, A. L., *Calorimetric Heats of Adsorption and Adsorption Isotherms. 1. O_2, N_2, Ar, CO_2, CH_4, C_2H_6, and SF_6 on Silicalite*, Langmuir, 12 (24) 1996a

Dune, J. A., Rao, M., Sircar, S., Gorte, R. J., Myers, A, L., *Calorimetric Heats of Adsorption and Adsorption Isotherms. 2. O_2, N_2, Ar, CO_2, CH_4, C_2H_6, and SF_6 on NaX, H-ZSM-5, and Na-ZSM-5 Zeolites*, Langmuir, 12 (24) 1996b

El-Nabarawy, Th., Petro, N.Sh., El-Aziz, S.Abd., *Adsorption Characteristics of Coal-Based Activated Carbons. 1. Adsorption of Nitrogen and Carbon Dioxide*, Adsorption Science & Technology, 13 (3) 1996

Enhance Energy 2015, www.enhanceenergy.com visited on May 20, 2015

Farla, J. C.M., Hendriks, C. A., Blok, K., *Carbon Dioxide Recovery From Industrial Processes*, Energy Conversion Management, 36 (6-9) 1995

Farooq, S., Hassan, M.M., Ruthven, D.M., *Heat Effects in Pressure Swing Adsorption Systems*, Chemical Engineering Science, 43 (5) 1988

Farooq, S., Ruthven, D.M., *Effect of Equilibrium Selectivity in a Kinetically Controlled PSA Separation*, Chemical Engineering Science, 47 (8) 1992

Feng, X., Pan, C.Y., Ivory, J., Ghosh, D., *Integrated Membrane/Adsorption Process for Gas Separation*, Chemical Engineering Science, 53 (9) 1998

Figueroa, J.D., Fout, T., Plasynski, S., McIlvried, H., Srivastava, R.D., *Advances in CO_2 Capture Technology - The U.S. Department of Energy's Carbon Sequestration Program*, International Journal of Greenhouse Gas Control, 2 (1), 2008

Gladden, L.F., *Influence of Pellet Structure on Selectivity During Pressure Swing Adsorption Separations*, Chemical Engineering Science, 46 (10) 1991

Golden, T. C., Sircar, S., *Gas Adsorption on Silicalite*, Journal of Colloid and Interface Science, 162 (1) 1994

Gomes, V.G., Yee, K.W.K., *Pressure Swing Adsorption for Carbon Dioxide Sequestration from Exhaust Gases*, Separation and Purification Technology, 28 (2), 2002

Goto, K., Kazama, S., Furukawa, A., Serizawa, M., Aramaki, S., Shoji, K., *Effect of CO2 Purity on Energy Requirement of CO_2 Capture Processes*, Energy Procedia, 37, 2013

Habgood, H. W., *Adsorptive and Gas Chromatographic Properties of Various Cationic Forms of Zeolite X*, Canadian Journal of Chemistry, 42 1964

Harlick, P. J.E., Tezel, F.H., *A Novel Solution Method for Interpreting Binary Adsorption Isotherms from Concentration Pulse Chromatography Data*, Adsorption, 6 (4) 2000

Harlick, P. J.E., Tezel, F.H., *The Importance of Experimental Data Regression for Interpreting Binary Adsorption Isotherms from Concentration Pulse Chromatography Data: A Novel Functional Set*, Canadian Journal of Chemical Engineering, 79 (2) 2001

Harlick, P.J.E., Tezel, F.H., *Adsorption of carbon dioxide, methane and nitrogen: Pure and binary mixture adsorption for ZSM-5 with SiO_2/Al_2O_3 ratio of 280*, Separation and Purification Technology, 33 (2) 2003

Harlick, P.J.E., Tezel, F.H., *Adsorption of carbon dioxide, methane, and nitrogen: Pure and binary mixture adsorption by ZSM-5 with SiO_2/Al_2O_3 ratio of 30*, Separation Science and Technology, 37 (1) 2002

Harlick, P.J.E., Tezel, F.H., *An Experimental Adsorbent Screening Study for CO_2 Removal from N_2*, Microporous and Mesoporous Materials, 76 (1-3), 2004

Harlick, P.J.E., Tezel, F.H., *Equilibrium Analysis of Cyclic Adsorption Processes: CO_2 Working Capacities with NaY*, Separation Science and Technology, 40 (13), 2005

Harlick, P.J.E., Sayari, A.S., *Applications of Pore-Expanded Mesoporous Silica. 5. Triamine Grafted Material with Exceptional CO_2 Dynamic and Equilibrium Adsorption Performance*, Industrial Engineering Chemistry Research, 46 (2) 2007

Hartzog, D.G., Sircar, S., *Sensitivity of PSA Process Performance to Input Variables*, Adsorption, 1 (2) 1995

Hasan, M.M.F., Baliban, R.C., Elia, J.A., Floudas, C.A., *Modeling, Simulation, and Optimization of Postcombustion CO_2 Capture for Variable Feed Concentration and Flow Rate. 2. Pressure Swing Adsorption and Vacuum Swing Adsorption Processes*, Industrial and Engineering Chemistry Research, 51 (48), 2012

Hasse, D., Kulkarni, S., Sanders, E., Corson, E., Tranier, J.-P., *CO2 Capture by Sub-Ambient Membrane Operation*, Energy Procedia, 37, 2013

Heyne, S., Harvey, S., *Impact of Choice of CO_2 Separation Technology on Thermo-Economic Performance of Bio-SNG Production Processes*, International Journal of Energy Research, 38 (3), 2014

Ho, M.T., Allinson, G.W., Wiley, D.E., *Reducing the Cost of CO_2 Capture From Flue Gases using Pressure Swing Adsorption*, Industrial and Engineering Chemistry Research, 47 (14), 2008

Huang, Y. Y., *Quadrupole Interaction of Carbon Dioxide on Silica-Alumina Surface*, Journal of Physical Chemistry, 77 (1) 1973

Huck, J.M., Lin, L.-C., Berger, A.H., Shahrak, M.N., Martin, R.L., Bhown, A.S., Haranczyk, M., Reuter, K., Smit, B., *Evaluating Different Classes of Porous Materials for Carbon Capture*, Energy and Environmental Science, 7 (12), 2014

Hyun, S.H., and Danner, R. P., *Gas Adsorption Isotherms by use of Perturbation Chromatography*, Industrial Engineering Chemistry Fundamentals, 24 (95 – 101) 1985

Inui, T., Okugawa, Y., Yasuda, M., *Relationship Between Properties of Various Zeolites and their CO_2-Adsorption Behaviors in Pressure Swing Adsorption Operation*, Industrial & Engineering Chemistry Research, 27 (7) 1988

Kazama, S., Haraya, K., *Optimization of CO_2 Concentration Captured by Membrane Technology - Possibility of Reduction in CO_2 Capture Energy and Cost*, Energy Procedia, 37, 2013

Khanmamdov, T., *Apparatus for Removal of Contaminants from a Gas Stream*, U.S Patent #5, 716, 587 1998

Kikkinides, E.S., Yang, R.T., Cho, S.H., *Concentration and Recovery of CO_2 from Flue Gas by Pressure Swing Adsorption*, Industrial & Engineering Chemistry Research, 32 (11) 1993

Kim, J.N., Chue, K.T., Kim, K.I., Cho, S.H., Kim, J.D., *Non-Isothermal Adsorption of Nitrogen-Carbon Dioxide Mixture in a Fixed Bed of Zeolite-X*, Journal of Chemical Engineering of Japan, 27 (1) 1994

Ko, D., Siriwardane, R., Biegler, L.T., *Optimization of Pressure Swing Adsorption and Fractionated Vacuum Pressure Swing Adsorption Processes for CO_2 Capture*, Industrial and Engineering Chemistry Research, 44 (21), 2005

Kresge, C. T.; Leonowicz, M. E.; Roth, W. J.; Vartuli, J. C.; Beck, J. S. Ordered Mesoporous Molecular Sieves Synthesized by a Liquid-Crystal Template Mechanism, Nature, 359, 1992

Kumar, R., Van Sloun, J.K., *Purification by Adsorptive Separation*, Chemical Engineering Progress, 85 (1) 1989

Kumar, R., Golden, T.C., White, T.R., Rokicki, A., *Novel Adsorption Distillation Hybrid Scheme for Propane/Propylene Separation*, Separation Science & Technology, 27 (15) 1992

Kumar, R., *Pressure Swing Adsorption Process: Performance Optimum and Adsorbent Selection*, Industrial & Engineering Chemistry Research, 33 (6) 1994

Kumar, R., *Effect of Variable Feed Concentration on the Performance of a Pressure Swing Adsorption Process*, Adsorption, 1 (3) 1995

Kumar, R., Deng, S., Bulow, M., Fitch, F., Ojo, A.F., Gittleman, C.S., *Air Purification Process*, US Patent #5,980,611, 1999.

Leal, O.; Bolivar, C.; Sepulveda, G.; Molleja, G.; Martinez, G.; Esparragoza, L. *Carbon Dioxide Adsorbent and Method for Producing the Adsorbent*, U.S. Patent No. 5,087,597, 1992.

Leal, O.; Bolivar, C.; Ovalles, C.; Garcia, J. J.; Espidel, Y. *Reversible Adsorption of Carbon Dioxide on Amine Surface-bonded Silica Gel.* Inorg. Chim. Acta, 240, 1995

Li, K., W.K. Teo, *Theoretical Analysis of Ternary Gas Mixture Separation in an Internally Staged Permeator*, Chem. Eng. Sci., 47 (15-16) 1992

Lin, H., He, Z., Sun, Z., Kniep, J., Ng, A., Baker, R.W., Merkel, T.C., *CO2-Selective Membranes for Hydrogen Production and CO2 Capture - Part II: Techno-Economic Analysis*, Journal of Membrane Science, 2015

Liu, B., Wu, X., Lipscomb, G.G., Jensvold, J., *Novel Internally Staged Permeator Designs using a Hollow Fiber Fabric*, Separation Science and Technology, 35 (8), 2000

Liu, B., Lipscomb, G.G., Jensvold, J.A., *A Comparison of Optimal Internally Staged Permeator and External Two-Stage Module Designs for O_2 Enrichment From Air*, Separation Science and Technology, 36 (11), 2001

Majumdar, S., Sengupta, A., Cha, J.S., Sirkar, K.K., *Simultaneous SO_2/NO Separation from Flue Gas in a Contained Liquid Membrane Permeator*, Industrial & Engineering Chemistry Research, 33 (3) 1994

Meerman, J.C., Ramírez, A., Turkenburg, W.C., Faaij, A.P.C., *Performance of Simulated Flexible Integrated Gasification Polygeneration Facilities, Part B: Economic Evaluation*, Renewable and Sustainable Energy Reviews, 16 (8), 2012A

Meerman, J.C., Hamborg, E.S., van Keulen, T., Ramírez, A., Turkenburg, W.C., Faaij, A.P.C., *Techno-Economic Assessment of CO_2 Capture at Steam Methane Reforming Facilities using Commercially Available Technology*, International Journal of Greenhouse Gas Control, 9, 2012B

Lokhandwala, K., *Membrane-Augmented Cryogenic Methane/Nitrogen Separation*, US Patent #5,647,227, 1997

Matz, M. J., Knaebel, K.S., *Pressure Swing Adsorption: Effects of Incomplete Purge*, AICHE Journal, 34 (9) 1988

Mariz, C., Chapel, D., Ernst, J., Fluor, D., *Recovery of CO_2 from Flue Gases: Commercial Trends*, Presented at the, 49th Canadian Chemical Engineering Conference. October 3-6, Saskatoon, Saskatchewan, Canada, 1999

Na, B.-K., Lee, H., Koo, K.-K., Song, H.K., *Effect of Rinse and Recycle Methods on the Pressure Swing Adsorption Process to Recover CO_2 from Power Plant Flue Gas using Activated Carbon*, Industrial and Engineering Chemistry Research, 41 (22), 2002

Nagumo, R., Iwata, S., Mori, H., *Simulated Pocess Evaluation of Synthetic Natural Gas Production Based on Biomass Gasifcation and Potential of CO_2 Capture using Membrane Separation Technology*, Journal of the Japan Petroleum Institute, 56 (6), 2013

Nakagawa, K., Ohashi, T., *Novel Method of CO_2 Capture from High Temperature Gases*, Journal of the Electrochemical Society, 145 (4) 1998

Nanko 2015, http://www.kepco.co.jp/english visited on May 15 2015

Nieh, E.C.Y. *Selective Recovery of Carbon Dioxide*, US Patent 4,710,362, 1987

Pan C. Y., H.W. Habgood, *An Analysis of the Single Stage Gaseous Permeation Process*, Industrial Engineering & Chemistry Fundamentals, 13 (4) 1974

Park, J.-H., Beum, H.-T., Kim, J.-N., Cho, S.-H., *Numerical Analysis on the Power Consumption of the PSA Process for Recovering CO_2 from Flue Gas*, Industrial and Engineering Chemistry Research, 41 (16), 2002

Perrin J.E., S.A. Stern, *Separation of a Helium-Methane-Nitrogen Mixture in Permeators with Two Types of Membranes*, AIChE Journal, 32 (11) 1986

Pires, J., Brotas de Carvalho, M., Ramoa Ribeiro, F., Derouane, E. G., *Carbon Dioxide in Y and ZSM-20 Zeolites: Adsorption and Infrared Studies*, Journal of Molecular Catalysis, 85 1993

Prasad, R., Notaro, F., Haas O.W., *Hybrid Prepurifier for Cryogenic Air Separation Plants*, US Patent #5,116,396, 1992

Pritchard, C., Yang, A., Holmes, P., Wilkinson, M., *Thermodynamics, Economics and Systems Thinking: What*

Role for Air Capture of CO_2?, Process Safety and Environmental Protection, 94, 2014

Pruschek, R., Oeljeklaus, G., *Potential CO2-Emission Reduction Processes*, Advances in Solid Fuels Technologies American Society of Mechanical Engineers, Fuels and Combustion Technologies Division, 9 1990

Ray, M.S., *Adsorptive and Membrane Separations. A Bibliographical Guide (1985-1989)*, Adsorption Science & Technology, 7 (1) 1990

Ray, R., Wright Wytcherley, R., Newbold, D., McCray, S., Friesen, D., Brose, D., *Synergistic, Membrane-Based Hybrid Separation Systems*, Journal of Membrane Science, 62 (3) 1991

Reynolds, S.P., Ebner, A.D., Ritter, J.A., *Stripping PSA Cycles for CO_2 Recovery from Flue Gas at High Temperature using a Hydrotalcite-Like Adsorbent*, Industrial and Engineering Chemistry Research, 45 (12), 2006

Reynolds, S.P., Mehrotra, A., Ebner, A.D., Ritter, J.A., *Heavy Reflux PSA Cycles for CO_2 Recovery from Flue Gas: Part I. Performance Evaluation*, Adsorption, 14 (2-3), 2008

Ruthven, D. M., Kumar, R., *An Experimental Study of Single-Component and Binary Adsorption Equilibria by a Chromatographic Method*, Industrial Engineering Chemistry Fundamentals, 19 (27–32) 1980

Ruthven, D.M., *Principles of Adsorption and Adsorption Processes*, John Wiley & Sons Inc., New York, 1984

Ruthven, D.M., Farooq, S., Knaebel, K., *Pressure Swing Adsorption*, VCH Publishers, New York, N.Y., 1994

Sandru, M., Kim, T.-J., Capala, W., Huijbers, M., Hägg, M.-B., *Pilot Scale Testing of Polymeric Membranes for CO_2 Capture From Coal Fired Power Plants*, Energy Procedia, 37, 2013

Sartori, G., Leder, F., *Process for Removing Carbon Dioxide Containing Acidic Gases from Gaseous Mixtures using Aqueous Amine Scrubbing Solutions*, US Patent #4,112,052, 1978

Sayari, A. *Periodic Nanoporous Materials: Synthesis, Characteriza- tion and Potential Applications. In Recent AdVances and New Horizons in Zeolite Science and Technology*; Chong, H., Woo, S. I., Park, S. E., Eds.; Elsevier: Amsterdam, 1996

Sayari, A.; Yang, Y.; Kruk, M.; Jaroniec, M. *Expanding the Pore Size of MCM-41 Silicas: Use of Amines as Expanders in Direct Synthesis and Postsynthesis Procedures*. J. Phys. Chem. B, 103, 1999

Sayari, A. *Unprecedented Expansion of the Pore Size and Volume of Periodic Mesoporous Silica*. Angew. Chem., Int. Ed. Engl., 39, 2000

Sayari, A.; Hamoudi, S. *Periodic Mesoporous Silica-Based Organic-Inorganic Nanocomposite Materials*. Chem. Mater., 13, 2001

Sayari, A.S., and Harlick, P J.E., *Functionalized Adsorbent for Removal of Acid Gases and Use Thereof*, US Patent 7767004, 2010

Scholes, C.A., Anderson, C.J., Stevens, G.W., Kentish, S.E., *Membrane Gas Separation Physical Solvent*

Absorption Combined Plant Simulations for Pre-Combustion Capture, Energy Procedia, 37, 2013

Shah, D. B., Ruthven, D. M., *Measurement of Zeolitic Diffusivities by Chromatography*, AIChE Journal, 23 (6), 1977

Shin, H.S., Knaebel, K.S., *Pressure Swing Adsorption: An Experimental Study of Diffusion-Induced Separation*, AICHE Journal, 34 (9) 1988

Shin, H., *Separation of a Binary Gas Mixture by Pressure Swing Adsorption: Comparison of Different PSA Cycles*, Adsorption, 1 (4) 1995

Sengupta, A. K.K. Sirkar, *Ternary gas Mixture Separation in Two Membrane Permeators*, AIChE Journal, 33 (4) 1987

Sengupta, A. K.K. Sirkar, *Ternary gas Mixture Separation in Two Membrane Permeators*, AIChE Journal, 33 (4)1987

Shell Oil Comapany 2015, www.shell.com visited on May 10, 2015

Sidholm, M.S., S. Majumdar, R.R. Brave, A., Sengupta, and K.K. Sirkar, *Experimental Behaviour of Asymmetric CA Membranes and Its Use in a Novel Separation Schemes*, AIChE Journal, 84 (102) 1987

Sirkar, K.K., *Asymmetric Permeators – A Conceptual Study*, Separation Science & Technology, 15 (73) 1984

Sirkar, K.K., *Membrane Separation Technologies: Current Developments*, Chemical Engineering Communications, 157 1996

Sircar, S., Kratz, W.C., *Simultaneous Production of Hydrogen and Carbon Dioxide from Steam Reformer Off-Gas by Pressure Swing Adsorption*, Separation Science & Technology, 23 (14-15) 1988

Sircar, S., *Separation of Methane and Carbon Dioxide Gas Mixtures by Pressure Swing Adsorption*, Separation Science & Technology, 23 (6-7) 1988

Sircar, S. Waldron, W.E., Rao, M.B., Anand, M., *Hydrogen Production by Hybrid SMR-PSA-SSF Membrane System*, Separation & Purification Technology. 17 (1) 1999

Skarstrom, C.W., Ann. N.Y. Academic Science, 72 1959

Springmann, H., *Economical and Technical Aspects of Cryogenic Plants*. AIChE Symposium Series, 82 (251) 1986

Stein, A.; Melde, B. J.; Schroden, R. C., *Hybrid Inorganic-Organic Mesoporous SilicatessNanoscopic Reactors Coming of Age*, AdV. Mater., 12, 2000

Stein, A., *Advances in Microporous and Mesoporous Solids Highlights of Recent Progress*, AdV. Mater., 15, 2003

Suh, S.S., Wankat, P.C., *New Pressure Swing Adsorption Process for High Enrichment and Recovery*, Chemical Engineering Science, 44 (3) 1989

Suzuki, H., Hayakawa, A., Mimura, T., Shimojo, S., Shimayoshi, H., Iijima, M, Mitsuoka, S, Iwaki, T, *Process for Removing Carbon Dioxide from Gases*, U.S. Patent # 5,618,506, 1997

Suzuki, T., Sakoda, A., Suzuki, M., Izumi, J., *Adsorption of Carbon Dioxide onto Hydrophobic Zeolite Under High Moisture*, Journal of Chemical Engineering of Japan, 30 (5) 1997

Suzuki, T., Sakoda, A., Suzuki, M., Izumi, J., *Recovery of Carbon Dioxide from Stack Gas by Piston-Driven Ultra-Rapid PSA*, Journal of Chemical Engineering of Japan, 30 (6) 1997

Taqvi, S.M., Levan, M.D., *Role of Convection and Diffusion in a Single Pore with Adsorptive Walls*, Adsorption, 2 (4) 1996

Tezel, F. H., Tezel, H. O., and Ruthven, D. M., *Determination of Pure and Binary Isotherms for Nitrogen and Krypton*, Journal of Colloid Interface Science, 149 (1) 1992

Tomioka, T., Sakai, T., Mano, H., *Carbon Dioxide Separation Technology from Biogas by "Membrane/Absorption Hybrid Method"*, Energy Procedia, 37, 2013

Triebe, R.W., Tezel, F.H., *Adsorption of Nitrogen and Carbon Monoxide on Clinoptilolite: Determination and Prediction of Pure and Binary Isotherms*, Canadian Journal of Chemical Engineering, 75 1995

Van der Vlist, E., Van der Meijden, J., *Determination of the Adsorption Isotherms of the Components of Binary Gas Mixtures by Gas Chromatography*, Journal of Chromatography, 79 (1 – 13) 1973

Wang, D., Wang, X., *Carbon Dioxide Separation by Membrane Process and its Recent Development,* Modern Chemical Industry, 8 (6) 1997

Warmuzinski, K., Sodzawiczny, W., *Effect of Adsorption Pressure on Methane Purity during PSA Separations of CH_4/N_2 Mixtures*, Chemical Engineering & Processing, 38 (1) 1999

Warmuzinski, K., Tanczyk, M., Jaschik, M., Janusz-Cygan, A., *A Hybrid Separation Process for the Recovery of Carbon Dioxide from Flue Gases*, Energy Procedia, 37, 2013

White, D.H Jr., Barkley, P.G., *Design of Pressure Swing Adsorption Systems*, Chemical Engineering Progress, 85 (1) 1989

Wu, Y., Zhang, T., Duan, Y., Yu, S., *Supported Ionic Liquid Membranes for CO_2/CH_4 Separation*, Huagong Xuebao/CIESC Journal, 64, 2013

Yamazaki, T, Katoh, M., Ozawa, S., Ogino, Y., *Adsorption of CO_2 over Univalent Cation-Exchanged ZSM-5 Zeolites*, Molecular Physics, 80 (2) 1993

Yang, R.T., *Gas Separation by Adsorption Processes*, Butterworth Publishers, Mass., U.S.A., 1987

Yeo, Z.Y., Chew, T.L., Zhu, P.W., Mohamed, A.R., Chai, S.-P., *Synthesis and Performance of Microporous Inorganic Membranes for CO_2 Separation: A Review*, Journal of Porous Materials, 20 (6), 2013

Ying, J. Y.; Mehnert, C. P.; Wong, M. S. Synthesis and Applications of Supramolecular-Templated Mesoporous Materials. Angew. Chem., Int. Ed., 38, 1999

Yongling, L., Yingshu, L., *Analysis of Separation and Capture Technology for Carbon Dioxide*, International Journal of Advancements in Computing Technology, 4 (23), 2012

Yoshida, K., Mimura, T., Shimojo, S., Karasaki, M., Iijima, M., Seto, T., Mitsuoka, S., *Method for Removing Carbon Dioxide from Combustion Exhaust Gas*, U.S. Patent # 6,036,931, 2000

Zhai, H., Rubin, E.S., *The Effects of Membrane-Based CO_2 Capture System on Pulverized Coal Power Plant Performance and Cost*, Energy Procedia, 37, 2013

Zulhairun, A.K., Fachrurrazi, Z.G., Nur Izwanne, M., Ismail, A.F., *Asymmetric Hollow Fiber Membrane Coated with Polydimethylsiloxane-Metal Organic Framework Hybrid Layer for Gas Separation*, Separation and Purification Technology, 146, 2015

Chapter 4

Applications of Pore-Expanded Mesoporous Silica. 2.

Development of a High-Capacity, Water-Tolerant Adsorbent for CO_2

Robert S. Franchi, **Peter J. E. Harlick,** and Abdelhamid Sayari

Centre for Catalysis Research and Innovation (CCRI), Department of Chemistry, University of Ottawa, 10 Marie Curie, Ottawa, Ontario, Canada K1N 6N5

Department of Chemical Engineering, University of Ottawa, 161 Louis Pasteur, Ottawa, Ontario, Canada K1N 6N5

As Published in (with modification to heading style):

Industrial Engineering and Chemistry Research, 44 (21) 2005

(Citation Count > 240, Google Scholar, 2015)

Further Details:

Sayari, Abdelhamid, **Harlick, Peter J. E.**, *Functionalized Adsorbent for Removal of Acid Gases and Use Thereof*, US 7767004, **2010**

Dharani, D.D., **Harlick, P.J.E.**, Sayari, A., *Applications of Pore-Expanded MCM-41 Silica: 4. Synthesis of a Highly Active Base Catalyst*, Catalysis Communications, **(2007)**, 8 829-833

Harlick, P.J.E., Serna, R., Das, D., Sayari, A., *Application of Modified Pore-Expanded MCM-41 Silica in Catalysis and Adsorption,* International Symposium on Zeolites and Microporous Crystals (ZMPC2006), Yonago, Japan, **2006**

Franchi, R.S., **Harlick, P.J.E.**, Sayari, A., *Applications of Pore-Expanded Mesoporous Silica. 2. Development of a High-Capacity, Water-Tolerant Adsorbent for CO_2*, Industrial and Engineering Chemistry Research, **(2005)**, 44 (21) 2569-2591

Franchi, R.S., **Harlick, P.J.E.**, Sayari, A., *A High Capacity, Water Tolerant Adsorbent for CO_2: Diethanolamine Supported on Pore-Expanded MCM-41,* Studies in Surface Science and Catalysis **(2005)**, 156, 879-886

Harlick, P.J.E., Franchi, R., Yang, Y., Sayari, A., *Hydrophobic MCM-41 Supported Composite Adsorbents for Acid Gas Separation*, 5th Brazilian Meeting on Adsorption, Natal, Brazil, July 18-21, **2004**

Collaboration:

The work presented in this Chapter was completed as a collaboration between R. Franchi and myself under the supervision of Dr. A. Sayari. See section 1.2 for further details.

4.1 - Abstract

A novel high capacity, water-tolerant adsorbent for CO_2 was developed. It consisted of diethanolamine (DEA) loaded pore-expanded MCM-41 silica (PE-MCM-41). Due to its very large pore volume, PE-MCM-41 silica was capable of accommodating a greater quantity of amine resulting in higher CO_2 adsorption capacity compared to the other supports including activated carbon, silica gel, and standard MCM-41 silica. Adsorption measurements were conducted by gravimetry using dry CO_2 to obtain uptake curves and apparent rate data. The capacity and uptake rate reached maxima with respect to amine content and then declined due to the deposition of excess amine on the particle's external surface and within the interparticle voids. At CO_2 partial pressures below 0.15 atm, the current DEA loaded PE-MCM-41 adsorbent was found to be superior to the more conventional zeolite 13X. Adsorption studies with humid CO_2 revealed that the adsorption capacity of the PE-MCM-41-based material was insensitive to the presence of moisture, which represents a major advantage over zeolite 13X. Repeated adsorption- desorption cycles revealed that our novel adsorbent exhibited good cyclic stability.

4.2 - Introduction

Carbon dioxide is a ubiquitous species that has received much attention recently particularly because of its greenhouse gas effect. Concerns over global warming have caused governments to enact regulations aimed at decreasing emissions of CO_2 to the atmosphere caused largely by industrial manufacturing and stationary power sources [1]. Whether because of environmental constraints or technical reasons, various industries are faced with the task of removing CO_2 from gas mixtures containing a wide range of species in different concentrations. The space industry and military establishments require the removal of CO_2 from enclosed areas [2-5] such as space

shuttles and submarines. The natural gas processing and fuel cell industries require CO_2 to be removed from gaseous fuel sources to increase the purity and energy density of the feedstock [6-10].

Amine-CO_2 chemistry has been employed for decades as a method to selectively remove CO_2 from such gas streams, mainly in the form of gas-liquid absorption columns. Aqueous solutions of monoethanolamine (MEA), diethanolamine (DEA), and methyldiethanolamine (MDEA) are commonly used absorbents [11]. Though these systems are effective, they suffer from numerous draw-backs such as corrosion, high-energy consumption, [11] and limited amine concentration in the aqueous phase due to viscosity and foaming issues.

To remedy these problems, recent research has focused on gas-solid adsorption as a promising alternative separation technique. Various zeolitic and non-zeolitic adsorbents have been examined; however, many of the adsorbents developed thus far suffer from problems such as low capacity, poor selectivity, poor tolerance to water, and high-temperature regeneration or also known as activation herein. An example of a commercialized adsorbent for CO_2 removal from gas streams is zeolite 13X. When used for CO_2 separation, this adsorbent requires very stringent moisture control in the inlet gas stream due to its high affinity and adsorption capacity for water. When exposed to water, the material should be regenerated at temperatures between 300 and 400 °C to retain its high CO_2 adsorption capacity.

The idea of combining amines with solid supports to afford CO_2 adsorbents has been examined by several groups [4, 5, 9, 10, 12-15]. The materials were prepared either by grafting of amine containing alkoxysilanes onto the surface of the support or by deposition of amine- containing molecules onto the support. Common problems encountered when

developing amine loaded solid supports are low capacity for CO_2 due the limited quantity of amine retained on the support, operation in a narrow temperature range, and poor thermal stability (i.e., volatility). The rate and capacity of CO_2 adsorption on such adsorbents depend chiefly on the amine loading and the porosity of the material, which are not completely independent since higher amine loadings may be obtained with higher pore volumes. To achieve this goal of dry CO_2 scrubbing (absorption- adsorption hybrid), we used as a support a periodic mesoporous silica whose pores have been further expanded through postsynthesis treatment as described elsewhere by Sayari et al. [16-21].

As shown in Figure 4.1, the PE-MCM-41 silica used in this study was prepared using a two-step methodology consisting of (i) synthesis of MCM-41 at relatively low temperature, typically 70-100°C, and then (ii) postsynthesis hydrothermal treatment of the as-synthesized silica mesophase in an aqueous emulsion of long-chain *N*,*N*-dimethylalkylamine, typically at 120-130 °C for different periods of time. Depending on the conditions of both steps, materials with controlled pore sizes from 3.5 up to 25 nm could be obtained. The pore volume varied accordingly from typically 0.8 up to 3.6 cm^3/g, whereas the specific surface areas were not drastically affected [20, 21]. The two occluded surfactants could be removed stepwise [21] or simultaneously, giving rise to PE-MCM-41 (material **C** in Figure 4.1).

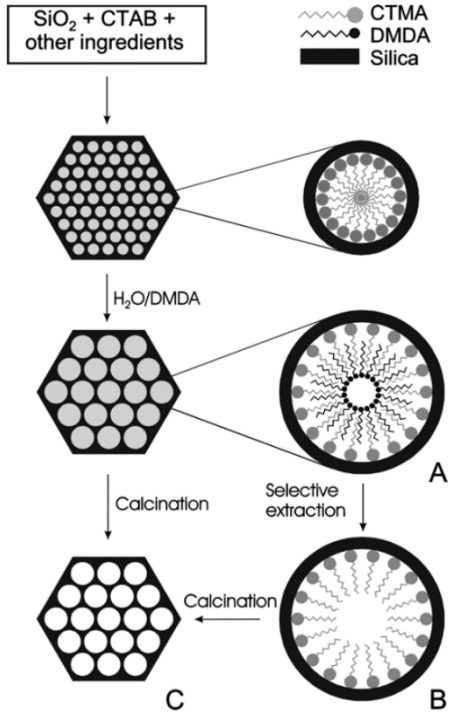

Figure 4.1 Schematic representation of MCM-41 pore expansion.

This investigation is part of an overall effort to develop innovative applications for pore-expanded MCM-41 containing one (material **B**), two (material **A**), or no (material **C**) surfactants. The first part [22] dealt with the use of materials **A** and **B** as adsorbents for the removal of heavy metals and organic pollutants from wastewater, respectively. In the current study, diethanolamine (DEA) was chosen to remove CO_2. In addition to being a typical liquid-phase absorbent, DEA exhibits a lower vapor pressure relative to the commonly applied MEA, making it less susceptible to volatilization, in the temperature range of 20-100 °C. Further, DEA-CO_2 chemistry is generally believed to benefit from the presence of moisture, [4, 9, 11] which presents an advantage since H_2O is frequently found in CO_2-containing gas streams. In addition to PE-MCM-41, three other supports were examined, namely activated carbon, silica gel, and conventional MCM-41 silica. Activated carbon and silica gel were chosen as supports since they are commonly used for various adsorption applications, and their surface properties are such that both are expected to retain DEA in the porous structure. MCM-41 silica was compared to PE-MCM-41 to study the effect of pore size expansion and enhanced pore volume.

4.3 - Experimental Method

4.3.1 – Materials and Synthesis

Norit Darco KB-B activated carbon, Davisil grade 643 silica gel, and zeolite 13X powder were obtained from Sigma-Aldrich. MCM41 and PE-MCM-41 were synthesized in-house using Cab-O-Sil M5 fumed silica (Cabot Corp.). Details of the supports are given in Table 4.1. All other chemicals were obtained from Sigma-Aldrich and used as supplied.

PE-MCM-41 silica was synthesized via a two-step procedure described earlier [16-21]. The first step consisted of preparing an MCM-41 mesophase at a temperature of 100 °C for 40 h as described by Sayari and Yang [23] using Cab-O-Sil M5 fumed silica as the silica source, cetyltrimethylammonium bromide (CTAB) as the surfactant template, and a 25% solution of tetramethylammonium hydroxide in water (TMAOH) for pH adjustment. The molar composition of the gel was 1.0:0.32:0.45:67 SiO_2: TMAOH: CTAB: H_2O. The pore expansion process was carried out by postsynthesis hydrothermal treatment of noncalcined MCM-41 in an emulsion of N, N-dimethyldecylamine (DMDA) at a temperature of 120 °C for 72 h. For the current study, DMDA was used at a ratio of 1.25 g/g of as-synthesized MCM-41. Calcination of the product of the first and second synthesis stages resulted in MCM-41 and PE-MCM-41, respectively.

Table 4.1 Structural Properties of the Supports.

support	S_{BET} (m^2/g)	D_{KJS} (nm)	V (cm^3/g)	particle diam (μm)
activated carbon[a]	1640		1.48	100–150
silica gel[b]	256		0.94	100–150
MCM-41	1138	3.6	1.03	20–30
PE-MCM-41	917	9.7	2.03	20–30
13X[c]	800	0.80		2–5

[a] Noritz Darco KB-B. [b] Davisil grade 643. [c] UOP.

Impregnation of the supports with DEA was carried out by adding various amounts of the amine to distilled, deionized water, followed by the addition of the desired amount of support and evaporating the excess solvent to dryness. Other samples were prepared using ethanol as the solvent. Drying was carried out in a vented oven at 60 °C. The actual amount of DEA retained on the support was measured for each sample by decomposition in nitrogen using a TA

Instruments Q500 thermogravimetric analyzer (TGA) coupled to a Pfeiffer Thermostar mass spectrometer (MS).

4.3.2 – Nitrogen Adsorption Characterization

Nitrogen adsorption measurements were performed at 77 K using a Coulter Omnisorp 100 gas analyzer. Before exposure to nitrogen, the samples were heated to 100 °C (2 h) under high vacuum (10^{-5} Torr). The specific surface area (SBET) was determined from the linear part of the BET plot (P/P_o = 0.05-0.15). The average pore size (DKJS) for the MCM-41 materials was taken as the peak of the pore size distributions as calculated from the adsorption branch using the KJS (Kruk, Jaroniec, Sayari) method [24]. The total pore volume (V) was determined as the volume of liquid nitrogen adsorbed at a relative pressure of 0.995.

4.3.3 – CO_2 Adsorption Studies

CO_2 adsorption uptake curves, uptake rate, and CO_2 adsorption isotherms were obtained using the Q500 TGA-MS system (150 sccm sample and 10 sccm balance purge) and UHP gases supplied by Praxair. Samples of approximately 60 mg were loaded into the instrument and were heated to remove preadsorbed moisture and CO_2. Examination of the TGA-MS data obtained with amine-impregnated samples indicated that heating at 75 °C was sufficient to rapidly desorb any adsorbed moisture and CO_2. Due to the strong adsorption of H_2O on zeolite 13X, this material was initially heated to 400 °C for complete dehydration. Samples were then cooled to 25 °C and exposed to a dry mixture of CO_2 and nitrogen for a period of 1 h (150 sccm), which was sufficient to reach equilibrium. The zeolite 13X samples were then regenerated by heating to 75 °C in dry nitrogen, and adsorption data were collected upon exposure to the same CO_2/N_2 mixture at 25 °C. This was necessary to ensure that the amine-impregnated samples and the zeolite samples were compared after being activated at the

same temperature, i.e., 75 °C. The adsorption capacity was calculated on the basis of the mass increase measured after 1 h of exposure to the gas mixture. The uptake rates were calculated on the basis of the maximum rate of mass gain after exposure to the gas mixture.

To obtain cyclic data, the samples were regenerated by rapid heating to 75 °C (5 min) in dry nitrogen (150 sccm) following the initial adsorption cycle (25 °C, 150 sccm). The samples were then allowed to cool to 25 °C through convection, and the adsorption-desorption cycle was repeated several times. Typical adsorption-desorption cycles were 60 min for adsorption and 90 min for desorption. The time for desorption was longer then the adsorption time due to the cooling behavior of the TGA used for these runs. The amount adsorbed in each cycle was referenced to the mass after the initial activation.

The effect of moisture on the uptake capacity was determined using the same initial treatment procedure and subsequently exposing the samples to humidified gases. This was achieved by passing the dry gases through a gas saturator held at a constant temperature and then passing these humidified gases over the samples. A relative humidity of 28% at 25 °C was used during these tests to investigate the effects of moisture in the low humidity range. This value was chosen to simulate a gas stream that has been dehumidified through a condenser using cooling water to achieve a dew point of 4 – 6 °C. To decouple the adsorption of moisture from the adsorption of CO_2, samples were first exposed to moist nitrogen until the water uptake ceased. Moist CO_2 was then passed over the samples for 1 h to determine the CO_2 adsorption capacity.

4.4 - Results

4.4.1 – Comparison of the Supports

Nitrogen adsorption at 77 K was used to determine the structural characteristics of the supports. The nitrogen adsorption isotherms and calculated pore size distributions for MCM-41 and PE-MCM-41 are shown in Figures 4.2 and 4.3. On the basis of the structural characteristics of the supports as presented in Table 4.1, the various materials were impregnated with DEA to pore saturation by the method previously described. Pore saturation was used since this was assumed to result in the largest quantity of DEA that could be retained by the supports. The samples were then tested for CO_2 adsorption capacity and uptake rate using a dry mixture of 5% CO_2 in nitrogen. These results are shown in Table 4.2. Although the uptake rates of the impregnated activated carbon and the silica gel were higher than those of the MCM-41 and PE-MCM-41 supported materials, PE-MCM-41 achieved the highest capacity since it was able to accommodate the largest quantity of amine. Examination of the carbon dioxide-to-amine ratios (CO_2/DEA) with respect to the specific surface area revealed that the CO_2/DEA ratio decreased as the surface area increased. This observation suggested that some of the DEA may have interacted with the support surface, thus losing its ability to adsorb CO_2. This hypothesis will be discussed in more detail later.

The use of PE-MCM-41 resulted in the highest adsorption capacity and the second highest CO_2/DEA ratio. Further, with pore volumes of up to 3.6 cm^3/g attainable [20, 21] PE-MCM-41 was deemed the most promising support for the amine impregnated adsorbent; hence, it was chosen for further studies.

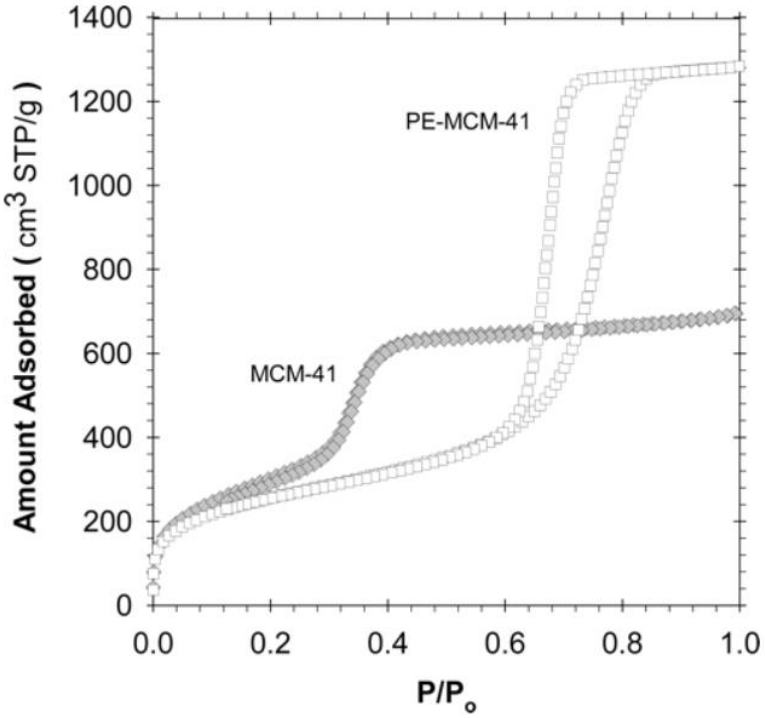

Figure 4.2 Nitrogen adsorption isotherms for MCM-41 and PE-MCM-41

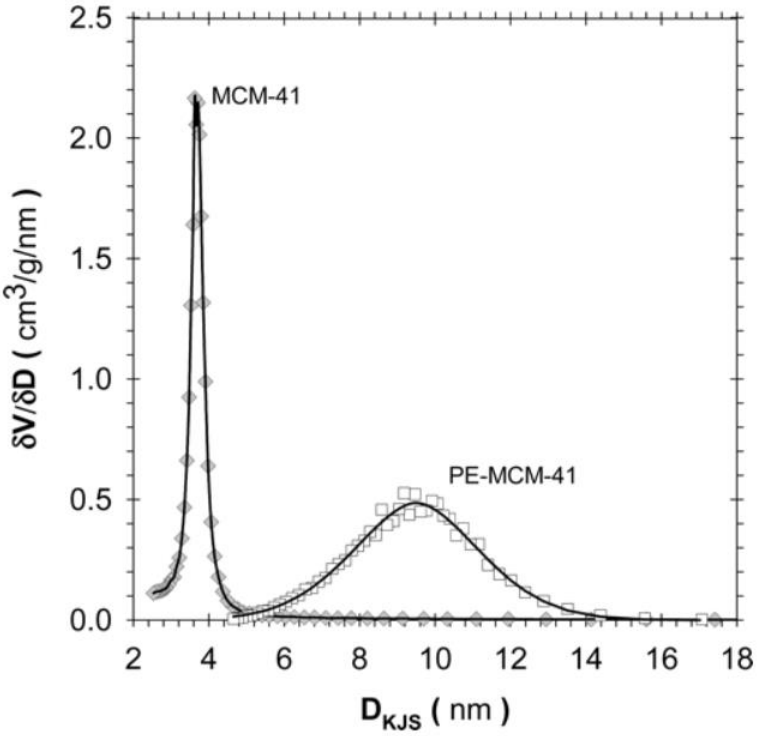

Figure 4.3 KJS pore size distributions for MCM-41 and PE-MCM-41.

Table 4.2 CO_2 Adsorption Data[a] for DEA-Loaded Materials.

support	amine loading ratio[b] (g/g_{sup})	amine content[c] ($mmol/g_{ads}$)	CO_2 capacity ($mmol/g_{ads}$)	CO_2 uptake rate ($mmol/g_{ads}$/min)	CO_2/DEA ratio (mol/mol)
activated carbon[d]	1.62	5.41	1.51	0.95	0.28
silica gel[e]	1.03	4.61	1.88	0.69	0.41
MCM-41	1.13	4.49	1.26	0.57	0.28
PE-MCM-41	2.22	6.34	2.36	0.54	0.37

[a] Obtained with dry 5% CO_2 in N_2. [b] g_{sup}) gram of support. [c] g_{ads}) gram of adsorbent. [d] Norit Darco KB-B. [e] Davisil grade 643.

4.4.2 – DEA Loading

The effect of amine loading on both the maximum adsorption rate and the CO_2 capacity was examined using the PE-MCM-41 support. Samples with amine loadings ranging from 0 to 5.14 g of DEA/g_{sup} were prepared and tested for CO_2 adsorption capacity and rate using a dry mixture of 5% CO_2 in nitrogen (UHP gas supply). This gas mixture was chosen for the bulk of the adsorption tests because it was expected that the amine-impregnated adsorbent would have a high capacity for CO_2 even in the low partial pressure region. Since CO_2 reacts chemically with the amine, higher partial pressures of CO_2 should not greatly increase the CO_2 adsorption capacity.

As shown in Figure 4.4, a maximum capacity of 2.65 mmol of CO_2/g_{ads} was obtained at an amine content of 7.26 mmol of DEA/g_{ads}. Higher amine contents resulted in lower CO_2 capacities as measured after 1 h. The uptake curves of these highly loaded samples showed a high degree of tailing, but for the sake of consistency, the capacity of all samples was compared after 1 h. The tailing in the uptake curves for these samples indicated that beyond an amine loading corresponding to pore saturation, the additional DEA deposited on the adsorbent external surface as well as in the interparticle voids. With large excesses of DEA, film diffusional resistance became a limiting factor for the kinetics of CO_2 uptake, causing the tailing in the uptake curves. This contention was supported by observations of the texture of the impregnated materials, which changed gradually from a free-flowing powder to an agglomerated powder as the amine loading exceeded pore saturation.

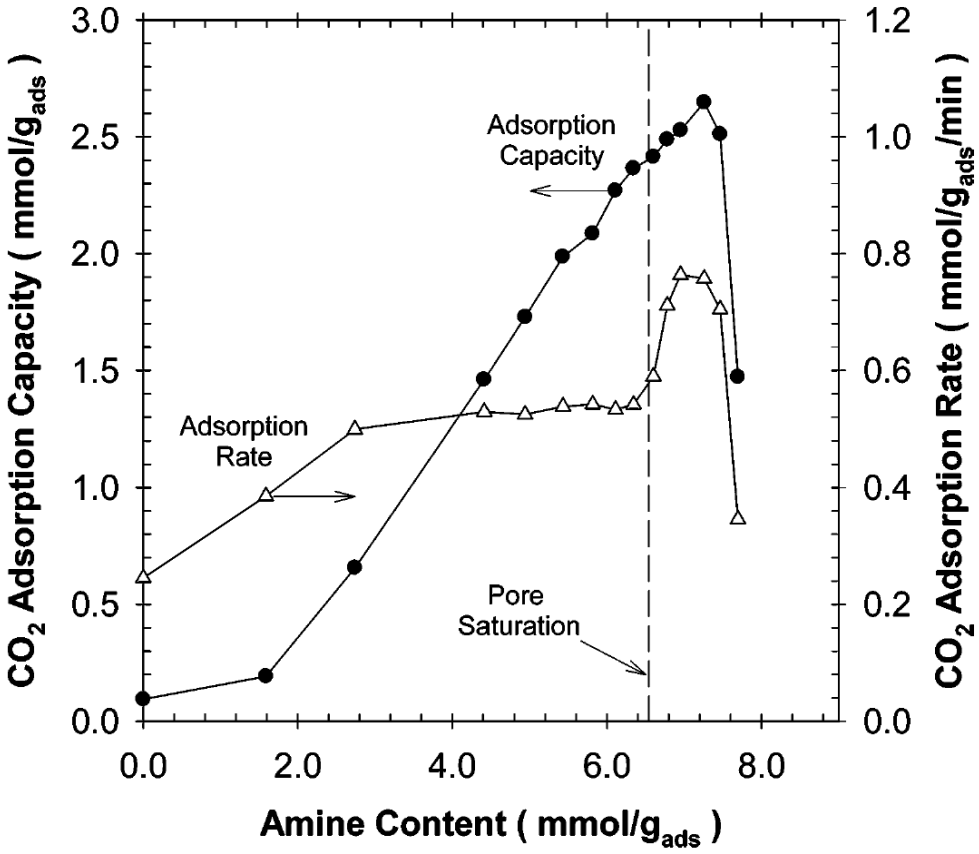

Figure 4.4 CO_2 adsorption capacity and adsorption rate as a function of DEA content on PE-MCM-41 obtained with dry 5% CO_2 in N_2.

The CO_2 uptake rate increased initially and reached a steady value of approximately 0.55 mmol of CO_2/ (g_{ads}/min) between amine contents of 2.74 and 6.34 mmol of DEA/g_{ads}. After exceeding the pore saturation point of 6.54 mmol of DEA/g_{ads}, the uptake rate abruptly increased, reaching a maximum of approximately 0.76 mmol/(g_{ads}/min) at an amine content of 6.95 mmol of DEA/g_{ads}. This sharp increase was attributed to the increase in external deposition of DEA, which initially caused an increase in the adsorption rate due to the easily accessible DEA on the surface and in the inter-particle voids of the adsorbent particles. As the DEA content increased further, the adsorption rate decreased due to mass transfer limitations.

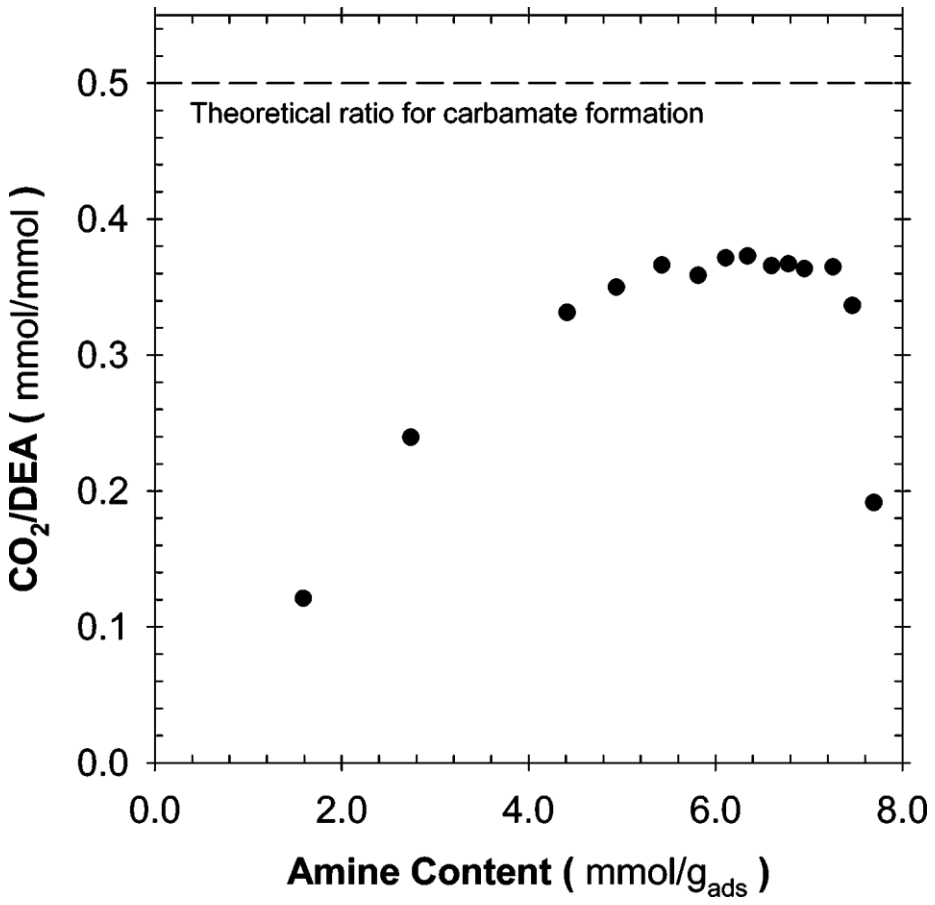

Figure 4.5 CO_2/DEA molar ratio as a function of DEA content on PE-MCM-41 obtained with dry 5% CO_2 in N_2.

Figure 4.5 shows the calculated CO_2/DEA ratios for the DEA impregnated PE-MCM-41. As discussed in the literature [4, 9, 11] in the absence of moisture, DEA and other secondary amines should react with CO_2 in the stoichiometric ratio of 0.5 mol of CO_2/mol of amine. The current study showed that a maximum ratio of 0.37 mol of CO_2/mol of DEA was obtained, which was fairly constant for amine contents between 5 and 7 mmol of DEA/g_{ads}. A possible cause for the low CO_2/DEA molar ratios was revealed by analyzing the TGA decomposition profiles, an example of which is shown in Figure 4.6. The profile was obtained under flowing nitrogen using a thermal ramp of 10 °C/min for a sample impregnated with 6.34 mmol of DEA/g_{ads}. The data revealed that a portion of the DEA loss (5.0 mmol of DEA/g_{ads}) occurred

at temperatures below 280 °C, while another portion (1.34 mmol of DEA/g_{ads}) took place above 300 °C. This second loss, occurring at relatively high temperatures, indicated strong interaction forces between DEA and the support.

To probe the adsorption properties of the material lost at high temperatures, a sample with an amine content of 6.60 mmol of DEA/g_{ads} was tested using the standard procedure, and a CO_2 capacity of 2.41 mmol of CO_2/g_{ads} was obtained (CO_2/DEA = 0.365 mol/mol). The same sample was then rapidly heated in nitrogen to 250 °C and held at this temperature for 15 min, after which time the sample lost 54.1% of its mass (or 5.05 mmol of DEA/gads) and appeared to stabilize. The sample was then cooled to 25 °C and exposed to the dry mixture of 5% CO_2 in nitrogen. The CO_2 capacity was found to be only 0.10 mmol of CO_2/g_{ads} (CO_2/DEA) 0.065 mol/mol). Upon continuation of the decomposition, the sample lost an additional 16.6% of its mass (or 1.55 mmol DEA/gads). This suggested that the DEA decomposing at the higher temperature was almost completely deactivated, which accounted for the lower than stoichiometric CO_2/DEA ratios.

4.4.3 – Impregnation Solvent Effects

It was noticed that samples with very high loadings required a considerably longer time to evaporate the excess water used during the impregnation procedure. To decrease the time required to dry the material, the solvent was changed from water to ethanol, resulting in a reduction in drying time by a factor of 4. As shown in Table 4.3, in addition to the reduction in drying time, the amount of DEA retained on the support increased slightly (ca. 1%), whereas the CO_2 adsorption capacity of the impregnated material increased significantly (ca. 10%). This was accompanied by a noticeable increase in the CO_2/DEA molar ratio, suggesting that the use of ethanol as a solvent resulted in a larger fraction of amine being available for CO_2 adsorption.

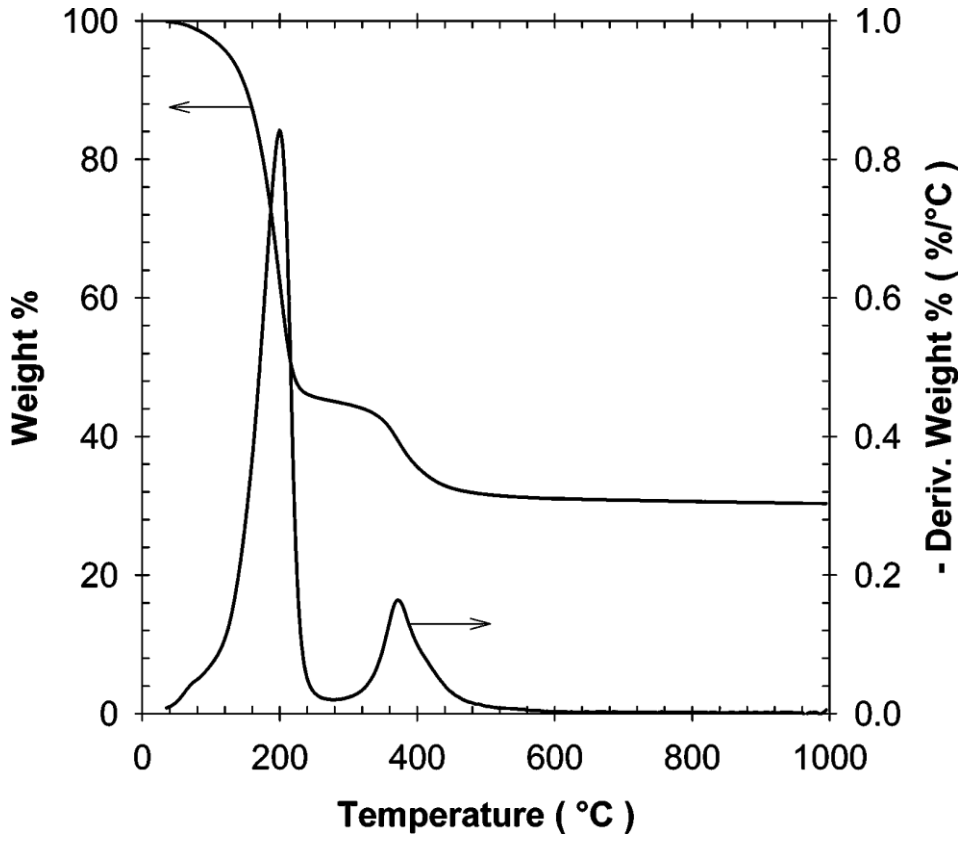

Figure 4.6 Decomposition profile for DEA-impregnated PE-MCM-41 (6.34 mmol of DEA/g_{ads}; temperature ramp of 10°C/min in dry N_2).

Due to the improved performance obtained using ethanol during impregnation, this solvent was used for the preparation of samples for further studies. On the basis of the adsorption capacity, uptake rate, CO_2/DEA molar ratio, and physical texture of the samples impregnated with ethanol as the solvent, it was found that the optimum combination of these parameters was obtained with the sample loaded at a ratio of 3 g of DEA/g_{sup}. This resulted in a sample with an amine content of 6.98 mmol of DEA/g_{ads} (6.98 DEA/PE-MCM-41), approximately 7% higher than pore saturation, which was used for a comparative study with zeolite 13X.

4.4.4 – Comparison Between Amine-Loaded PE-MCM-41 and Zeolite 13X

CO_2 adsorption isotherms were obtained for sample 6.98 DEA/PE-MCM-41 and zeolite 13X at 25 °C. The standard adsorption test method described earlier was used with various concentrations of CO_2 in nitrogen. The resulting isotherm data is shown in Figure 4.7. This study indicated that, under dry conditions, the amine-impregnated material has the most promising potential for applications in the low CO_2 partial pressure region since it has superior adsorption capacity compared to zeolite 13X. The isotherm data suggested that the two materials should have similar CO_2 adsorption capacity in the region of 0.15 atm of CO_2, beyond which point zeolite 13X showed higher equilibrium capacity than the amine-impregnated PE-MCM-41 material. This behavior is the result of the strong chemisorptive interaction between DEA and CO_2 molecules even at very low partial pressures. This type of adsorption does not occur with zeolite 13X since CO_2 molecules are known to be physisorbed to its surface through electrostatic interactions. As the partial pressure of CO_2 increased, the CO_2 capacity of the

Table 4.3 Comparison of DEA-Impregnated PE-MCM-41 Using Water or Ethanol as the Impregnation Solvent.

solvent	amine loading ratio[a] (g/g_{sup})	amine content ($mmol/g_{ads}$)	CO_2 ads capacity[b] ($mmol/g_{ads}$)	CO_2/DEA ratio (mol/mol)
water	2.22	6.34	2.36	0.37
ethanol	2.25	6.42	2.54	0.40
water	2.50	6.60	2.41	0.37
ethanol	2.50	6.68	2.64	0.40
water	2.75	6.78	2.49	0.37
ethanol	2.72	6.84	2.74	0.40
water	2.99	6.95	2.53	0.36
ethanol	3.00	6.98	2.81	0.40
water	3.51	7.26	2.65	0.37
ethanol	3.48	7.31	2.93	0.40
water	4.13	7.47	2.51	0.34
ethanol	3.98	7.54	2.76	0.37

amine-impregnated material was limited by stoichiometry as discussed earlier; hence, only marginal increases in CO_2 adsorption occurred for a large increase in CO_2 partial pressure.

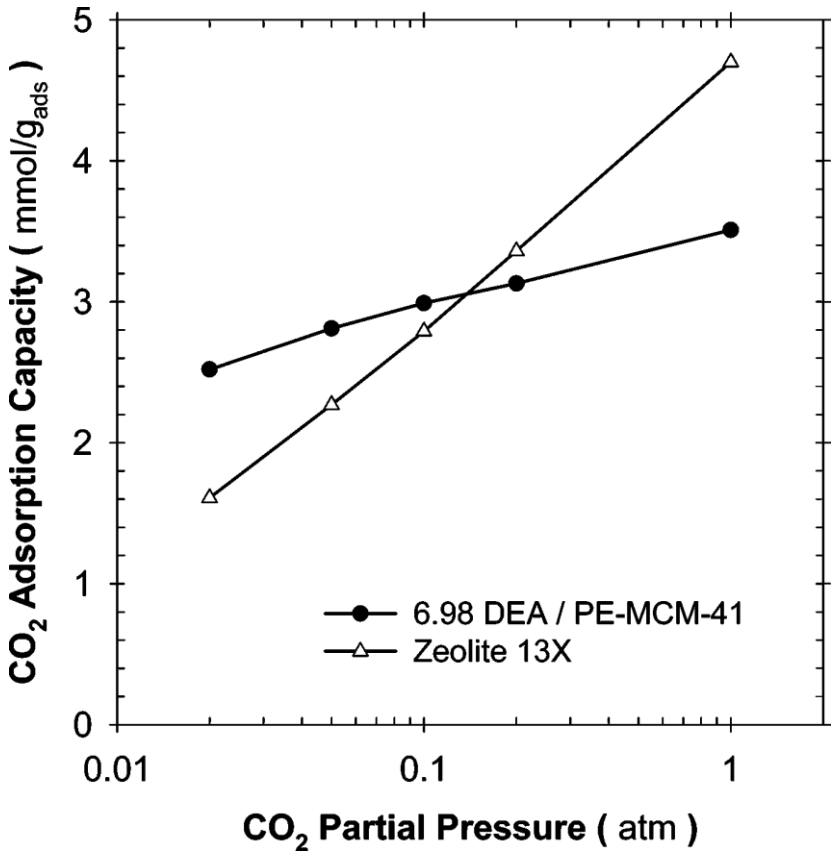

Figure 4.7 CO_2 adsorption isotherms (25°C) for 6.98 DEA/PE-MCM-41 and zeolite 13X.

In addition to high adsorption capacity, any material employed industrially must exhibit favorable kinetics to decrease the length of unused bed in the adsorption column. Figure 4.8 shows the adsorption mass uptake curves obtained with the dry mixture of 5% CO_2 in nitrogen at 25°C and the desorption mass curves obtained with dry nitrogen at 75 °C for both 6.98 DEA/PE-MCM-41 and zeolite 13X. The two materials showed similar favorable adsorption kinetics since 95% of the equilibrium capacity was reached within 6 min (zeolite13X) and 12 min (6.98 DEA/PE-MCM-41) of exposure to the CO_2/N_2 gas mixture. Upon rapid heating to 75

°C in nitrogen (150 sccm), the amine-impregnated material quickly desorbed all the CO_2, whereas zeolite 13X showed evidence of incomplete desorption. In an industrial setting, incomplete desorption would reduce the working capacity of the adsorption bed, resulting in reduced throughput. According to these results, the DEA-impregnated material should allow for more efficient use of the length of an adsorption bed when employed at the industrial scale. Further, the thermal treatment required for desorption consisted only of a heat pulse sufficient to reach 75 °C. Under these conditions, the desorption dynamics and energy requirements favor the amine-impregnated material in comparison to zeolite 13X. These attributes will result in lower operational costs and increased amounts of processed gas.

Since CO_2 is frequently found in gas streams containing varying amounts of water vapor, a highly desirable characteristic of a CO_2 adsorbent is tolerance to moisture. Although zeolite 13X has a high capacity for CO_2 under dry conditions, it cannot tolerate moisture and requires regeneration at high temperatures after exposure to water vapor. According to the literature, [4, 9, 11] moisture should actually increase the CO_2 capacity of the amine-impregnated material by allowing the formation of bicarbonate ions instead of carbamate ions, resulting in a doubling of the CO_2/DEA stoichiometric ratio. The effect of moisture on both of these materials was examined, as described earlier, by exposing the activated samples to a moist stream of nitrogen (28% relative humidity at 25 °C). Once the uptake of moisture ceased, the samples were exposed to a stream of 5% CO_2 in nitrogen under the same humidity conditions. Sample 6.98 DEA/PE-MCM-41 adsorbed 5.37 mmol of H_2O/g_{ads} and was still capable of adsorbing 2.85 mmol of CO_2/g_{ads}. Zeolite 13X adsorbed 15.11 mmol of H_2O/g_{ads} but could subsequently only adsorb 0.09 mmol of CO_2/g_{ads}. The presence of moisture did not significantly enhance the performance of the amine-impregnated material as expected toward the complete bicarbonate formation (CO_2/DEA molar ratio of 1.0). However, the results showed that this material drastically out-

performed zeolite 13X under the humidity conditions of the current study. This suggests that gas streams to be treated with DEA-loaded PE-MCM-41 would not require any moisture control, whereas extensive drying is necessary in the case of zeolite 13X.

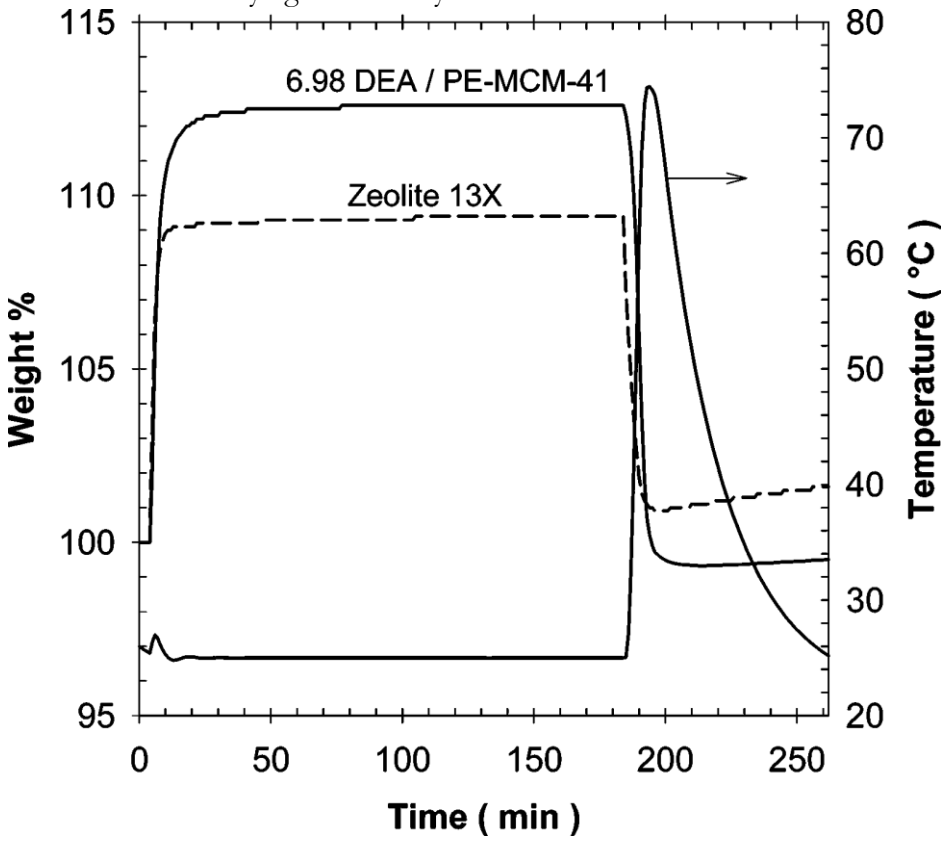

Figure 4.8 Adsorption-desorption mass curves obtained with dry 5% CO_2 in N_2 for 6.98 DEA/PE-MCM-41 and zeolite 13X.

4.4.5 – Cyclic Performance

In order for an adsorbent to be employed industrially, it must provide long-term, stable performance. The cyclic adsorption performance of 6.98 DEA/PE-MCM-41 was examined, and the results are shown in Figure 4.9 along with results obtained using zeolite 13X and others obtained by Xu et al. [14] for polyethylenimine (PEI) impregnated MCM-41.

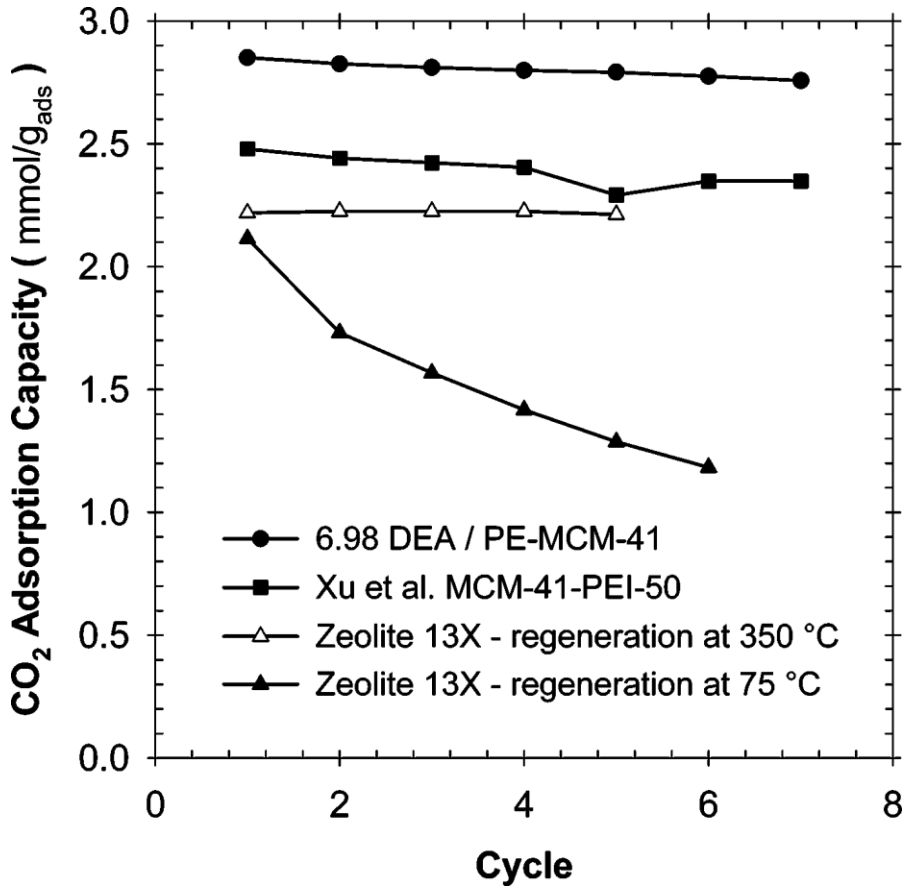

Figure 4.9 CO_2 adsorption capacity as a function of adsorption cycle for 6.98 DEA/PE-MCM-41 and other CO_2 adsorbents.

Examination of Figure 4.9 reveals that the performance of the DEA-impregnated adsorbent is fairly stable, with only a minor decrease in adsorption capacity (0.09 mmol of CO_2/g_{ads}, i.e., 3.3% of initial capacity) after seven adsorption-desorption cycles. The loss in capacity is believed to be due to a slow loss of DEA, which appeared in the TGA data as a loss in adsorbent mass over time. The presence of DEA however could not be detected by the mass spectrometer. According to the work of Satyapal et al. [4] the addition of poly(ethylene glycol) (PEG) to their polymethylmethacrylate supported polyethylenimine CO_2 adsorbent (known as HSC+) resulted in improved thermal stability. Further research could reveal that PEG may also increase the thermal stability of the current DEA-impregnated adsorbent.

Xu et al. [14] reported cyclic performance data for standard MCM-41-impregnated with 50 wt % polyethylenimine (MCM-41-PEI-50). The results were obtained using pure CO_2 and operating between temperatures of 75 and 100 °C. The reported results show a slight decrease in capacity (0.13 mmol of CO_2/g_{ads} after seven cycles, i.e., 5.3% of initial capacity) similar to the decrease obtained in the current study for the DEA-impregnated PE-MCM-41.

Under high-temperature regeneration conditions (350 °C), the cyclic performance of zeolite 13X is stable with virtually no decrease in adsorption capacity occurring. The adsorption capacity decreases very quickly (0.93 mmol/g_{ads} after six cycles, i.e., 44.1% of initial capacity) when the milder regeneration temperature of 75 °C is used. TGA-MS data suggested that the loss in capacity was due to the incomplete regeneration of the zeolite leading to the accumulation of CO_2, N_2, [25] and eventually of water impurities, the latter due to trace moisture in the gas streams. The original adsorption capacity could be obtained after exposing the material to the high-temperature regeneration conditions. These results illustrate both the need for higher temperature regeneration conditions and the importance of moisture control of the inlet gas when using zeolite 13X to remove CO_2, two major disadvantages that do not occur with the adsorbent developed during the current study.

4.5 - Conclusions

DEA was deposited on various porous supports resulting in adsorbents suitable for removing CO_2 from gas streams. The most promising support was found to be PE-MCM-41 due to its high pore volume, which allowed for a higher loading level of DEA compared to the other supports examined. The CO_2 capacity and uptake rate of the DEA-impregnated PE-MCM-41 reached maximum values at loading levels slightly exceeding pore saturation.

The CO_2/DEA ratio did not reach the stoichiometric maximum, i.e., 0.5 under dry conditions, due at least partly to deactivation of a portion of the DEA through interactions with the support surface. Compared to zeolite 13X, the amine-impregnated adsorbent had superior adsorption capacity below a CO_2 partial pressure of 0.15 atm with similar adsorption kinetics. Although the presence of moisture did not improve the performance of the impregnated adsorbent, it did not hinder it as was observed with zeolite 13X. The DEA-impregnated PE-MCM-41 showed good cyclic stability and maintained its capacity for CO_2 better than zeolite 13X tested under the same mild regeneration conditions.

4.6 - Acknowledgements

A.S. is Government of Canada Research Chair in Catalysis by Nanostructured Materials. We thank the Natural Sciences and Engineering Research Council of Canada (NSERC) and the Canadian Foundation for Innovation (CFI) for financial support. R.S.F. thanks the NSERC for a CGSM scholarship.

4.7 - References

[1] Song, C.; Gaffney, A. M.; Fujimoto, K.; Eds., *CO_2 Conversion and Utilization*; American Chemical Society: Washington, DC, 2002; Chapter 1.

[2] Frew, J.; Eaton, *D. J., Report DCIEM 95-16*; Defence and Civil Institute of Medicine: North York, Canada, 1995.

[3] Hodgson, E. W., *Regenerative Carbon Dioxide (CO_2) Removal System*. U.S. Patent 6,709,483, 2004.

[4] Satyapal, S.; Filburn, T.; Trela, J.; Strange, J., *Performance and Properties of a Solid Amine Sorbent for Carbon Dioxide Removal in Space Life Support Applications*. Energy Fuels, 2001, 15, 250.

[5] Birbara, P. J.; Filburn, T. P.; Michels, H.; Nalette, T. A., *Sorbent System and Method for Absorbing Carbon Dioxide (CO_2) from the Atmosphere of a Closed Habitable Environment*. U.S. Patent 6,364,938, 2002.

[6] Little, R. J.; Versteeg, G. F.; Van Swaaij, W. P. M., *Kinetics of CO_2 with Primary and Secondary Amines in Aqueous Solutions- II. Influence of Temperature on Zwitterion Formation and Deprotonation Rates*. Chem. Eng. Sci., 1992, 47, 2027.

[7] Veawab, A.; Tontiwachwuthikul, P.; Chakma, A., *Corrosion Behavior of Carbon Steel in the CO_2 Absorption Process Using Aqueous Amine Solutions*. Ind. Eng. Chem. Res., 1999, 38, 3917.

[8] *Koh, C. A.; Montanari, T.; Nooney, R. I.; Tahir, S. F.; Westacott, R. E., Experimental and Computer Simulation Studies of the Removal of Carbon Dioxide from Mixtures with Methane Using AlPO4-5 and MCM-41*. Langmuir, 1999, 15, 6043.

[9] Huang, H.; Yang, R.; Chinn, D.; Munson, C. L., *Amine-Grafted MCM-48 and Silica Xerogel as Superior Sorbents for Acidic Gas Removal from Natural Gas*, Ind. Eng. Chem. Res., 2003, 42, 2427.

[10] Chang, A. C. C.; Chuang, S. S. C.; Gray, M.; Soong, Y., *In Situ Infrared Study of CO_2 Adsorption on SBA-15 Grafted with γ-(Aminopropyl)triethoxysilane*, Energy Fuels, 2003, 17, 468.

[11] Rinker, E.; Ashour, S. S.; Sandall, O. C., *Absorption of Carbon Dioxide into Aqueous Blends of Diethanolamine and Methyldiethanolamine*, Ind. Eng. Chem. Res., 2000, 39, 4346.

[12] Leal, O.; Bolivar, C.; Ovalles, C.; Garcia, J. J.; Espidel, Y., *Reversible Adsorption of Carbon Dioxide on Amine Surface-bonded Silica Gel*, Inorg. Chim. Acta, 1995, 240, 183.

[13] Nalette, T. A.; Papale, W.; Filburn, T., *Carbon Dioxide Scrubber for Fuel and Gas Emissions*, U.S. Patent 6,755,892, 2004.

[14] Xu, X.; Song, C.; Andresen, J. M.; Miller, B. G.; Scaroni, A. W., *Novel Polyethylenimine-Modified Mesoporous Molecular Sieve of MCM-41 Type as High-Capacity Adsorbent for CO_2 Capture*. Energy Fuels, 2002, 16, 1463.

[15] Contarini, S.; Barbini, M.; Del Piero, G.; Gambarotta, E.; Mazzamurro, G.; Riocci, M.; Zappelli, P., *In Greenhouse Gas Control Technologies-6th International Conference*; Gale, J., Kaya, Y., Eds.; Tribology Series Vol. 41; Elsevier: New York, 2003; Vol. 1, pp 169-175.

[16] Sayari, A.; Yang, Y.; Kruk, M.; Jaroniec, M., *Expanding the Pore Size of MCM-41 Silicas: Use of Amines as Expanders in Direct Synthesis and Postsynthesis Procedures*. J. Phys. Chem. B, 1999, 103, 3651.

[17] Kruk, M.; Jaroniec, M.; Sayari, A., *A Unified Interpretation of High-Temperature Pore Size Expansion Processes in MCM-41 Mesoporous Silicas*, J. Phys. Chem. B 1999, 103, 4590.

[18] Sayari, A.; Kruk, M.; Jaroniec, M.; Moudrakovski, I. L,. *New Approaches to Pore Size Engineering of Mesoporous Silicates*. Adv. Mater., 1998, 10, 1376.

[19] Sayari, A., *Unprecedented Expansion of the Pore Size and Volume of Periodic Mesoporous Silica*. Angew. Chem., Int. Ed., 2000, 39, 2920.

[20] Kruk, M.; Jaroniec, M.; Sayari, *A. New Insights into Pore-size Expansion of Mesoporous Silicates Using Long-chain Amines*. Microporous Mesoporous Mater., 2000, 35-36, 545.

[21] Kruk, M.; Jaroniec, M.; Antochshuk, V., *Sayari, A. Meso-porous Silicate-Surfactant Composites with Hydrophobic Surfaces and Tailored Pore Sizes*. J. Phys. Chem. B, 2002, 106, 10096.

[22] Sayari, A.; Hamoudi, S.; Yang, Y., *Applications of Pore-expanded Mesoporous Silica: 1. Removal of Heavy Metal Cations and Organic Pollutants from Wastewater*. Chem. Mater., 2005, 17, 212.

[23] Sayari, A.; Yang, Y., *Highly Ordered MCM-41 Silica Prepared in the Presence of Decyltrimethylammonium Bromide*. J. Phys. Chem. B, 2000, 104, 4835.

[24] Kruk, M.; Jaroniec, M.; Sayari, A., *Application of Large Pore MCM-41 Molecular Sieves to Improve Pore Size Analysis Using Nitrogen Adsorption Measurements*, Langmuir 1997, 13, 6267.

[25] Chue, K. T.; Kim, J. N.; Yoo, Y. J.; Cho, S. H.; Yang, R. T., *Comparison of Activated Carbon and Zeolite 13X for CO_2 Recovery from Flue Gas by Pressure Swing Adsorption*. Ind. Eng. Chem. Res., 1995, 34, 591-598.

Chapter 5

Applications of Pore-Expanded Mesoporous Silicas. 3.
Triamine Silane Grafting for Enhanced CO_2 Adsorption

Peter J. E. Harlick, and Abdelhamid Sayari

Centre for Catalysis Research and Innovation (CCRI), Department of Chemistry, University of Ottawa, 10 Marie Curie, Ottawa, Ontario, Canada K1N 6N5

Department of Chemical Engineering, University of Ottawa, 161 Louis Pasteur, Ottawa, Ontario, Canada K1N 6N5

As Published (with modification to heading style):

Industrial Engineering Chemical Research, 45 (9) 2006

(Citation Count > 240, Google Scholar, 2015)

Further Details:

Sayari, Abdelhamid, **Harlick, Peter J. E.**, *Functionalized Adsorbent for Removal of Acid Gases and Use Thereof*, US 7767004, **2010**

Dharani, D.D., **Harlick, P.J.E.**, Sayari, A., *Applications of Pore-Expanded MCM-41 Silica: 4. Synthesis of a Highly Active Base Catalyst*, Catalysis Communications, **(2007)**, 8 829-833

Harlick, P.J.E., and Sayari, A., *Amine Grafted, Pore-Expanded MCM-41 for Acid Gas Removal: Effect of Grafting Temperature, Water, and Amine Type on Performance*, , Studies in Surface Science and Catalysis **(2006)**, 158B, 987-994

Serna-Guerrero, R., **Harlick, P.J.E.**, Sayari, A., *Novel Mesoporous Materials for the Adsorption of Volatile Organic Compounds*, 56th CSCHE Conference, Sherbrooke, Quebec, Canada, October 15-18, **2006**

Harlick, P.J.E., Serna, R., Das, D., Sayari, A., *Application of Modified Pore-Expanded MCM-41 Silica in Catalysis and Adsorption,* International Symposium on Zeolites and Microporous Crystals (ZMPC2006), Yonago, Japan, **2006**

Franchi, R.S., **Harlick, P.J.E.**, Sayari, A., *Applications of Pore-Expanded Mesoporous Silica. 2. Development of a High-Capacity, Water-Tolerant Adsorbent for CO_2*, Industrial and Engineering Chemistry Research, **(2005)**, 44 (21) 2569-2591

Franchi, R.S., **Harlick, P.J.E.**, Sayari, A., *A High Capacity, Water Tolerant Adsorbent for CO_2: Diethanolamine Supported on Pore-Expanded MCM-41,* Studies in Surface Science and Catalysis **(2005)**, 156, 879-886

Harlick, P.J.E., Sayari, A., *Unprecented CO_2 adsorption Capacity with Amine Grafted, Pore-Expanded MCM-41*, Presented at the International Chemical Congress of Pacific Basin Societies (Pacifichem), Honolulu, Hawaii, USA, December 1520, **2005**

Harlick, P.J.E., Sayari, A., *Amine Grafted Mesoporous Silica Supports for Acid Gas Removal from Humid Process Streams*, Nano-Porous Materials IV, Niagara Falls, Ontario, Canada, **2005**

Harlick, P.J.E., Franchi, R., Yang, Y., Sayari, A., *Hydrophobic MCM-41 Supported Composite Adsorbents for Acid Gas Separation*, 5th Brazilian Meeting on Adsorption, Natal, Brazil, July 18-21, **2004**

Collaboration:

The work presented in this Chapter was completed by myself under the supervision of Dr. A. Sayari. See section 1.2 for further details.

5.1 - Abstract

Conventional MCM-41 and pore-expanded MCM-41 (PE-MCM-41) silicas have been used as supports for grafting 3-[2-(2-aminoethylamino)ethylamino]propyl trimethoxysilane (TRI) and tested for CO_2 adsorption. The effects of the quantity of triamine silane added to the grafting mixture on the CO_2 adsorption capacity and apparent adsorption rate have been examined. The results showed that when both supports were grafted under the same conditions, PE-MCM-41 was grafted with slightly larger quantities of amine than MCM-41, for all controlled silane additions. Based on the adsorption performance of the materials using a dry 5% CO_2/N_2 feed mixture, the optimal quantity of triamine silane added to the grafting mixture was determined to be ca. 3.0 $cm^3/g(SiO_2)$, for both MCM-41 and PE-MCM-41. The CO_2 adsorption capacity of TRI-PE-MCM-41 was significantly higher than that of TRI-MCM-41. Furthermore, the dynamic adsorption performance of TRI-PE-MCM-41 was far superior to TRI-MCM-41. In comparison to 13X zeolite, TRI-PE- MCM-41 exhibited higher adsorption capacities in the initial timeframe of exposure, even though the 13X zeolite exhibited a higher equilibrium adsorption capacity. The result of this behavior is largely due to the rapid CO_2-amine interaction and the open pore structure of TRI-PE-MCM-41 over that of the 13X zeolite. When these adsorbents were exposed to a humid stream of 5% CO_2/N_2 (28% relative humidity), both grafted materials exhibited a slight increase in the adsorption capacity, whereas, 13X zeolite did not retain any significant CO_2 adsorption capacity. These results suggest that the TRI-PE-MCM-41 material may be most suitable for use in a rapid cyclic adsorption process under humid feed conditions.

5.2 - Introduction

Although there are several compounds that contribute to the greenhouse effect, carbon dioxide has received the most attention, because of its abundance as an effluent in industrial processes. Therefore, because of the global concern over rising atmospheric temperatures, the recent literature has shown that there is a keen interest in developing materials and processes that can efficiently and economically capture and isolate the effluent CO_2. Although the present state-of-the-art methods for CO_2 removal allow for such a process to be applied, the economics of the process may not be favorable enough to offset the capture cost.

Carbon dioxide scrubbing is currently practiced on a large scale for the purification of industrial gases (natural gas, syngas, etc.) and also in life support systems in confined spaces such as submarines, space vehicles, and other inhabited vessels for space exploration platforms). These processes use mainly alkanolamine aqueous solutions, [1] the most common being monoethanolamines and diethanolamines (MEA and DEA) and N-methyl diethanol amine (MDEA). The process is reversible and can be represented as shown in Scheme 5.1. Because the reactions are exothermic, the formation of carbamate and bicarbonate is favored at low temperature, whereas their dissociation into amine and CO_2 prevails at elevated temperatures [2].

The use of aqueous solutions of low-molecular-weight alkanolamines suffers many drawbacks [3, 4]. Under typical scrubbing conditions, (i) a fraction of the amine and its decomposition products is lost by evaporation, which, in addition to reducing the absorption capacity, may cause problems because of their toxicity; (ii) the amine undergoes oxidative

degradation, leading to decreased capacity, increased viscosity, and excessive foaming; and (iii) excessive corrosion occurs, thus posing severe operational problems.

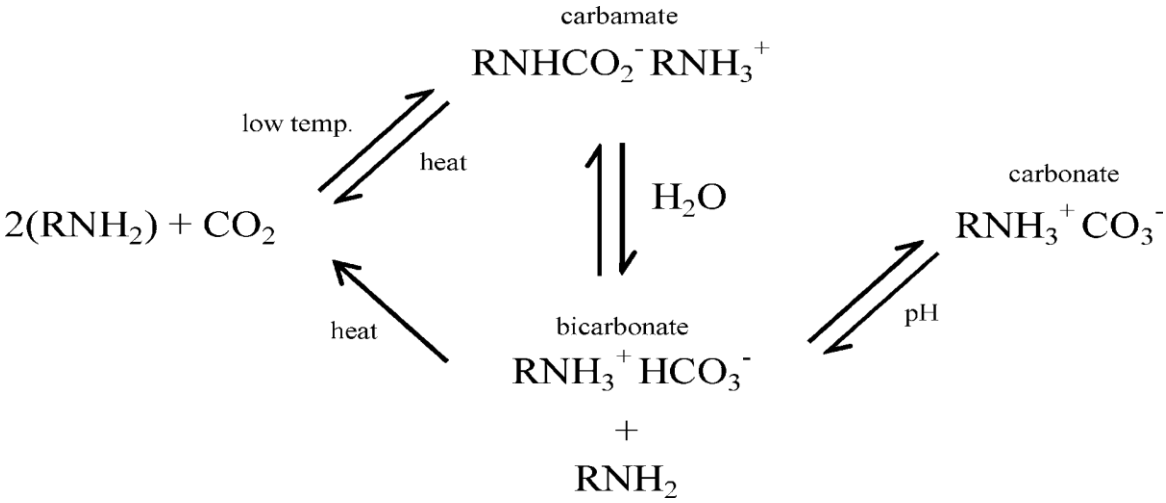

Scheme 5.1 CO_2 Reaction Pathways with Primary Amines.

In addition to liquid-phase systems, there were attempts to use reactive solids or amine-impregnated solids, particularly for air revitalization in manned space shuttles [5-7]. Some of the drawbacks of these impregnated materials were the quantity of amine that could be occluded. Because of the nature of the support material, only limited quantities could be loaded, and, thus, the materials did not exhibit sufficiently high adsorption capacities. In our previous work, [8] we developed a material that could occlude a large quantity of amine (up to 7.5 mmol(N)/g, based on diethanol amine), and thus exhibit a high adsorption capacity. However, since the amine loading was achieved through impregnation, the material could only be applied in low- temperature applications, i.e., <100 °C.

In this study, the development of novel adsorbent materials has been achieved with the specific task of CO_2 separation from N_2 by combining the favorable properties of liquid

amine absorption and gas-solid adsorption. The main goal was to develop a material with CO_2 adsorption characteristics that would not be hindered by the presence of moisture in the feed stream. Furthermore, this material should exhibit high adsorption capacity at low CO_2 partial pressure. Therefore, to put our work into context, it was felt that a short review of the pertinent literature was necessary.

5.3 - Background and Literature Review

The area of periodic mesoporous materials has gained widespread attention since the discovery in 1992 by Mobil Corp. of the M41S family of materials [9,10]. During this short period, this area has grown into a separate research field. Many authoritative reviews of this topic are readily available [11-14]. These materials can be prepared with tailor made pore sizes from 3 nm to 30 nm [9,15]. Our research group has developed a postsynthesis method to significantly increase the pore size and volume of MCM-41 periodic mesoporous silica in a controlled manner [16-18]. This technique affords mesoporous silicas, which may have 3-4 times the pore diameter and 2-3.5 times the pore volume of the typical MCM-41 mesoporous silica (i.e., pore size of 3-4 nm, and pore volume of 0.7-1.0 cm^3/g) without a major loss of surface area. This achievement allows us to exploit the internal space of the material to levels that are not possible with more-conventional porous supports such as zeolites, silica gels, aluminosilicates, and other periodic mesoporous materials [8,19].

Because the literature that concerns CO_2 removal is vast, the current review will be limited to data that are pertinent to this investigation, i.e., periodic mesoporous silica supports grafted with amine-containing species for the selective removal of CO_2. There are several zeolites that adsorb CO_2 from low-concentration feeds, [20] but the most effective and most

commonly used, as indicated by the patent and journal literature, are based on the 13X zeolite [21-27]. However, as discussed by Brandani and Ruthven [28] and in our previous work, [8] the presence of moisture greatly reduces the adsorption performance of the 13X zeolite toward CO_2, to the point where very high-temperature regeneration is necessary and/or a layer of desiccant preceding the zeolite is required, to adsorb high levels of CO_2 from a humid mixed feed.

The art of grafting active groups to the surface of a support has been exploited for many years and is well established in the literature (for example, see, refs [29] and [30]). However, in regard to amine grafting for CO_2 removal, there are limited amounts of published data. To our knowledge, the first instance of amine grafting onto a silica surface for CO_2 removal was reported in the patent literature by Leal et al. [31] and was later published in the journal literature [32]. In the patent document, disclosure was made for an aminosilane functionalized silica gel and was applied to the separation of CO_2 from air in confined spaces. The support material was characterized by a pore diameter of 6-18 nm, pore volume of 0.4-0.8 cm^3/g, and a surface area of 120-240 m^2/g. A further claim of the adsorption capacity of the material being 7.5-11.7 cm^3/g (1.47 and 2.30 wt % gain), when exposed to a pure dry CO_2 environment, was made. The patent also disclosed the method to produce the functionalized material. Specifically, the solvent should be from the alkane or aromatic hydrocarbon family or mixtures thereof, and the reaction should occur in an oxygen-deficient atmosphere. A claim of 0.50-1.26 mmol/g of alkylamine, specifically, $CH_2CH_2CH_2NH_2$, was made in regard to the organic content of the adsorbent.

Huang et al. [33] demonstrated the highest CO_2 adsorption capacities for a monoamine grafted material in the open literature. They evaluated the adsorption

performance with two high-surface-area, silica-based support materials MCM-48 (1389 m^2/g) and silica xerogel (816 m^2/g). These materials were grafted at 70 °C for 18 h under the conditions of an inert gas headspace (N_2), toluene as the solvent, excess (aminopropyl)triethoxysilane, and vapor reflux. The resulting amine grafted quantities were 1.7 mmol/g (9.9 wt %) for the xerogel and 2.3 mmol/g (13.3 wt %) for the MCM-48, based on the propylamine chain ($CH_2CH_2CH_2NH_2$). Using a dry 5% CO_2/N_2 mixture, the corresponding adsorption capacities were determined as 1.14 mmol/g (5.0 wt %) for the aminoMCM-48, and 0.45 mmol/g (1.96 wt %) for the amino-xerogel. When the supports were exposed to a humid stream of 5% CO_2/N_2, the authors claimed the adsorption capacity for CO_2 doubled, in comparison to the capacity obtained in the presence of a dry stream. This type of adsorption behavior is reminiscent of the amine-CO_2 chemistry in the liquid phase at high pressures.

Hiyoshi et al. [34] studied the effect of amine type and moisture on the CO_2 adsorption performance of various amines grafted onto SBA-15. The SBA-15 support exhibited a surface area of 910 m^2/g and a pore volume of 1.06 cm^3/g; the pore diameter was not reported. This SBA-15 was grafted with monoamino, diamino, and triamino ethoxysilanes, with resulting amine contents of 2.7, 4.2, and 5.1 mmol(N)/g, respectively. The CO_2 adsorption capacity, using a dry 15% CO_2/N_2 mixture, were reported as 0.52, 0.87, and 1.10 mmol/g for the monoamino, diamino, and triamino grafted SBA-15 supports, respectively. In the presence of a humid stream (15% CO2, 12% H2O, with the balance being N2), the monoamine grafted support exhibited a slight decrease in CO_2 adsorption capacity, whereas the diamino and triamino grafted supports both exhibited a slight increase, c.a., 3% and 10%, respectively. Hiyoshi et al. [34] also studied the SBA-15 material as a support for

impregnating the monoamine triethoxysilane to pore saturation. This material exhibited very low CO_2 adsorption capacity in the absence of moisture. However, when exposed to a 15% CO_2, 12% H_2O, balance N_2 feed mixture, the adsorption capacity was very high, ca. 2.32 mmol/g. Although this impregnated material seemed promising for CO_2 removal in the presence of moisture, the rate of adsorption was very low, and, thus, in an applied process, premature breakthrough will occur. From these results, the authors concluded that the density of the grafted species had an important role in the efficient adsorption of CO_2, where higher surface density favored higher amine efficiency and, thus, higher CO_2 adsorption capacities.

Through these cited works, it is apparent that the adsorption performance is directly related to the surface density of amine groups. Therefore, the use of the triamine silane should be preferred as the grafted species, because it contains three amine groups per organic chain. A similar conclusion was drawn based on the adsorption of metallic anions [35] and cations [36] using triamine grafted MCM-41 and SBA-15. However, previous studies have not examined the effect of the surface density on the adsorption efficiency of the material. This efficiency can be defined as the point at which the rate of adsorption is optimal while considering the magnitude of the adsorption capacity. Furthermore, the relative amount of silane required to reach this level of grafting should also be considered. The general approach has been to add the silane in excess. However, the amount of silane added and subsequently grafted to the surface may not result in the optimal material for dynamic CO_2 adsorption and, thus, for application in a cyclic-adsorption process. Therefore, in this study, the effect of the quantity of triamine silane addition on the amount of amine grafted and the dynamic and equilibrium adsorption performance have been critically examined using MCM-41 and PE-MCM-41 as supports.

5.4 – Materials and Methods

5.4.1 – Mesoporous Silicas Synthesis and Triamine Silane Grafting

The MCM-41 silica was prepared according to the procedure of Sayari and Yang [37]. The pore-expanded MCM-41 material, referenced hereafter as PE-MCM-41, was prepared by post-synthesis treatment of the as-synthesized MCM-41 silica, as described by Franchi et al. [8]. All materials in 1.0 kg batches were calcined in flowing N_2 (2.0 slpm) under a thermal ramp of 1 °C/min to 550 °C, and then held at 550 °C in air for 5 h. The materials were then transferred, hot, to a sealed container until their use. These support materials were characterized by N_2 adsorption at 77 K using an Omnisorp-100 instrument.

The reagents used for the synthesis of all the grafted materials were purchased from Sigma-Aldrich and used as supplied with no further treatment. These compounds were toluene (99% ACS grade), pentane (99% ACS grade), and 3-[2-(2-aminoethylamino) ethylamino] propyl trimethoxysilane (Tech), herein referenced as TRI.

To introduce the amine functionality to the MCM-41 materials, the conventional grafting technique was applied. Specifically, a batch of the support material was first dehydrated at 150 °C for 2 h in air under static conditions. A suspension of 1.0 g of this dried material then was dispersed in 150 cm^3 of toluene in a 250 cm^3 multi-neck flask by mixing for 30 min at room temperature. Next, the temperature was increased rapidly to 110 °C and then the desired quantity of TRI was added (0.3-8 $cm^3(TRI)/g(SiO_2)$), and the system was then held for 16 h with vapor reflux. These grafted materials were then filtered in a Buchner funnel and washed with copious amounts of toluene, followed by pentane. The materials were dried at 120 °C in a natural convection oven for 4 h and subsequently stored in capped vials until use. The obtained adsorbents have been designated as TRI-MCM-41 and TRI-PE-MCM-41, depending on the support that was used.

To determine the amount of amine that was grafted, a thermal decomposition method using the thermogravimetric analysis mass spectroscopy (TGA-MS) was developed and applied. Because not all of the alkoxy groups have been hydrolyzed, leading to surface Si-O-Si bridges, determination of the amount of grafted amine is not straightforward. From a set of exploratory experiments, it was determined that the unbound methoxy ligands were removed up to a temperature of 200 °C, thereafter, a second decomposition product, caused by the decomposition of the amine chain, started to evolve. Thus, the amount of grafted amine should correspond to the total weight loss beyond 200 °C. To correctly determine this amount, the material was first treated in a flow of ultrahigh-pressure (UHP) helium at 200 °C for a period of 1 h. At the completion of this initial heat treatment, a thermal ramp of 10 °C/min in UHP helium was imposed, up to 900 °C, then, in air up to 1000 °C to remove any residual coke from the support material. To validate this approach, a few samples were also examined by elemental analysis using a Carlo Erba model EA1100 CHNS instrument, and the error was determined to be no more than 2%-5% (on a dry basis), relative to the amount determined by TGA.

5.4.2 – CO_2 Adsorption Properties

To determine the adsorption capacity, a modified thermogravimetric balance (model Q500TGA, TA Instruments) coupled to a 1-300 amu mass spectrometer (Thermostar, Pfeiffer Vacuum) was used and is shown schematically in Figure 5.1. Typical sample weights of ca. 50 mg were loaded into a 100-μL platinum sample pan and used for both the adsorption and decomposition studies. Using this balance, the grafted materials response to a step change in CO_2 concentration (from 0% to 5% in N_2) was measured, as a weight change relative to the condition of each material after initial activation (regeneration) with a N_2 purge. The initial activation condition imposed on the materials was determined, in a separate experiment, by

examining the thermal stability of the material in a N_2 atmosphere ramped at 10 °C/min to 1000 °C with the above-mentioned modified TGA-MS instrument.

The pure gases used in this study were purchased from Praxair Canada and were specified as UHP grade. The 5% CO_2/N_2 mixture was also purchased from Praxair Canada as a certified UHP-grade mixture. The feed flow rates used with the TGA-MS were controlled at 150 sccm into the sample chamber and mixed with 10 sccm of purge gas through the balance assembly (see Figure 5.1), for both the adsorption and regeneration steps of the study.

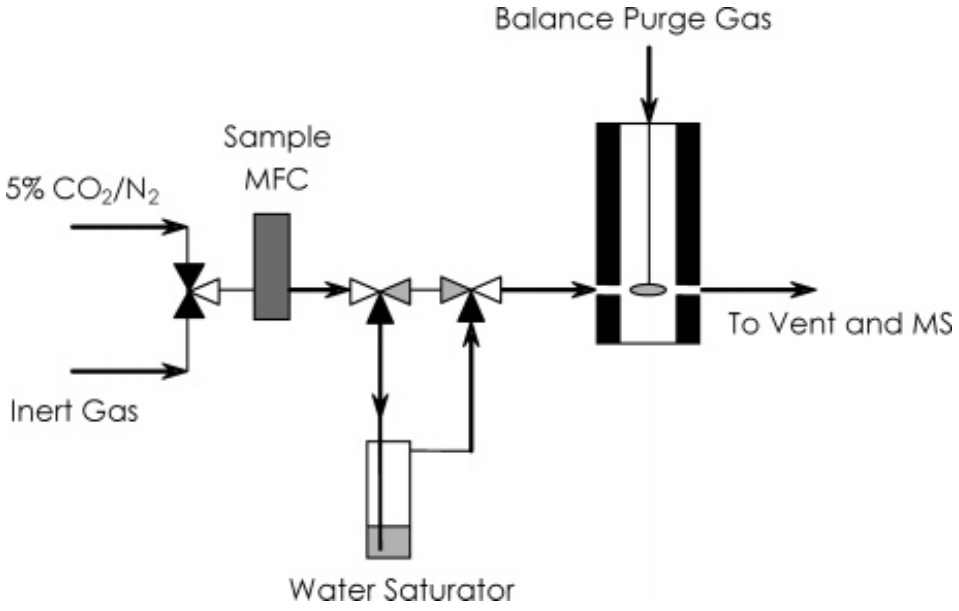

Figure 5.1 Schematic diagram of the modified thermogravimetric analysis- mass spectroscopy (TGA-MS) system used for equilibrium and dynamic adsorption studies.

To examine the effects of moisture on the adsorption capacity of CO_2 with the grafted materials, the following procedure was used, where the term humid refers to 5 °C saturation of water with the carrier gas (26% relative humidity (RH) at 25 °C): (i) initial thermal regeneration under dry N_2 purge (200 °C, 45 min), (ii) isothermal humid N2 adsorption to equilibrium (25 °C, H_2O/N_2), (iii) isothermal humid 5% CO_2/N_2 adsorption to equilibrium (25 °C), and (iv)

thermal regeneration in humid N_2 to 100 °C for 30 min. The procedure for dry CO_2 adsorption was similar, with the removal of humidity from all the streams and step (ii) omitted. The regeneration temperature of 100 °C was determined from a TGA profile of a fresh material that was subsequently loaded with 5% CO_2/N_2, and thermally ramped (5 °C/min) up to 200 °C to determine the temperature profile for CO_2 desorption. In addition to the grafted materials, extensive comparison was also made with the 13X zeolite, supplied by UOP in the powder form.

5.5 - Results

Support Structural Characterization. A brief summary of the material structural properties, as obtained by N_2 adsorption at 77 K, is shown in Table 5.1. From these data, it is evident that the pore-expansion process affords materials with a much larger pore size and pore volume than the typical MCM-41 silica. For the synthesis procedure applied in this study, the pore-expansion process resulted in a 2.7× increase in the pore diameter, and a 2.1× increase in the pore volume, whereas the surface area decreased by only 17%. Therefore, it is anticipated that PE- MCM-41 will be capable of accommodating bulkier organic molecules than the typical MCM-41 silica.

Table 5.1 Material Characteristics

support	BET surface area (m^2/g)	pore diameter (nm)	volume (cm^3/g)
MCM-41	1140	3.7	1.03
PE-MCM-41	950	10	2.2

5.5.1 – Thermal Stability

The thermal stability of the TRI-MCM-41 and TRI-PE-MCM-41 materials was examined to determine the upper operating thermal limit without decomposition of the grafted

amine. The results for TRI-MCM-41 and the TRI-PE-MCM-41 with a 10 °C/min thermal ramp in dry N_2 are shown in Figure 5.2A for the weight loss and derivative responses (DTG) and in Figure 5.2B as the corresponding mass spectrometry profiles of select amu/e values, as a function of time for TRI-MCM-41 only; the TRI-PE-MCM-41 material exhibited similar trends.

From the data shown in the TG-DTG plot, both grafted supports exhibited similar weight losses as a function of temperature. In combination with the mass spectrometry (MS) data shown in Figure 5.2B, the various species contributing to the weight loss can be determined. First, at temperatures below 250 °C, the MS profiles show that the dominant species evolving are water and methanol. This observation supports the fact that not all methoxy ligands bond with the surface, and, thus, some are left unreacted. As the temperature increased, the methoxy ligands react most probably with adjacent free-hydroxyl groups and, therefore, produce CH_3OH, as shown in the MS profile (Figure 5.2B), as 31 amu/e. The release of trace amounts of H_2O (shown as 18 amu/e) in this same thermal range may be due to the rearrangement of the grafted silane, and/or the release of strongly bound water on the surface. Above 250 °C, the amine chain starts to decompose and is removed from the surface in three stages. The first stage occurs in the temperature range of 250-400 °C, where the decomposition of the amine chain occurs. At temperatures above 400 C, the decomposition of the amine chain increases and is complete by 650 °C. For temperatures above 650 °C, coke formation is slowly burned off, due to the trace amounts of oxygen from the UHP gases, which are inherently present in an instrument of this nature. This partial coke burn-off is shown by the increase in the MS profiles of 44 and 18 amu/e, which represent CO_2 and H_2O, respectively. Overall, the grafted amine species seems to be stable up to 250 °C in a nitrogen atmosphere.

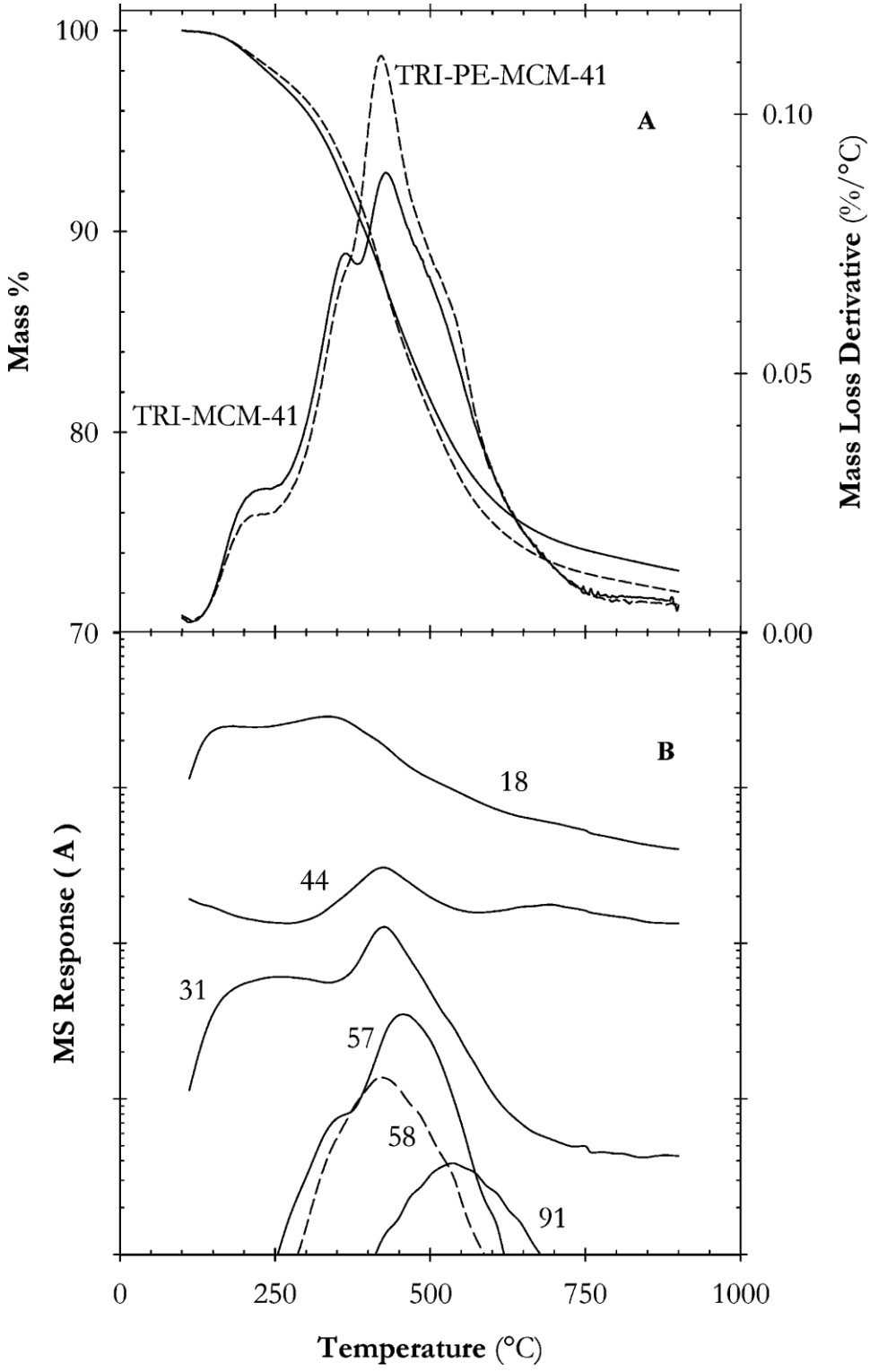

Figure 5.2 (A) Decomposition curves and associated derivative curves and (B) MS response profiles for TRI-MCM-41 and TRI-PE-MCM-41 materials that were grafted at 110 °C, with a TRI addition of 3.0 $cm^3/(SiO_2)$.

5.5.2 – Effect of Silane Quantity on Amine Loading and CO_2 Adsorption Performance

The optimization of the material for CO_2 adsorption capacity involved multiple constraints. The criteria for optimization was the minimization of the silane addition to achieve a maximum amine loading without adverse effect on the dynamic adsorption performance; i.e., the apparent adsorption rate and adsorption capacity. The choice to minimize the silane addition was driven by the cost/benefit ratio for manufacturing considerations. To explore the effect of the silane quantity added to the reaction mixture on these response parameters, samples were prepared with various amounts of TRI (0.3-8 $cm^3/g(SiO_2)$), at constant reaction temperature (110 °C) and time (16 h). The results are shown in Figure 5.3 for both the TRI-MCM-41 and TRI-PE-MCM-41 materials.

It is interesting to note that, in comparison to the MCM-41 support, the PE-MCM-41 support exhibited a slightly higher loading of triamine silane grafted for the same amount of silane added. Because the surface areas of the two supports are similar, this result may be due to the density of reactive hydroxyl groups or the beneficial effect of the pore size and pore volume on the amount and nature of the grafted species. Because of the limiting effect of silane additions beyond 3.0 cm^3/g, materials grafted with 3.0 cm^3/g were examined in detail.

Because the target separation for these materials was CO_2 removal from N_2 (air), it was important to examine the response of these adsorbents to N_2 alone. With both materials, the N_2 adsorption capacity at 25 °C was determined by regenerating the material in a flow of UHP-grade helium to 200 °C, and then exposing it to a pure stream of UHP-grade N_2, under the same flow conditions described previously for the CO_2 adsorption study, and it was allowed to equilibrate for a period of 180 min. The adsorption response of both materials was negligible, and, therefore, the N_2 adsorption capacity was considered to be zero. This behavior

is very beneficial for CO_2 separation from N_2, or air sources, since the system can be treated as pure rather than multicomponent. Furthermore, the losses of N_2 product due to adsorption will be negligible when the material is used in a cyclic adsorption process. This should offset the void volume product loss that is due to the increase in the porosity, relative to zeolite materials: increased overall void volume, as related to the packed bed density. In contrast, because our materials do not adsorb N_2, very-high-purity CO_2 should be recovered during the process cycle with the appropriate regeneration method.

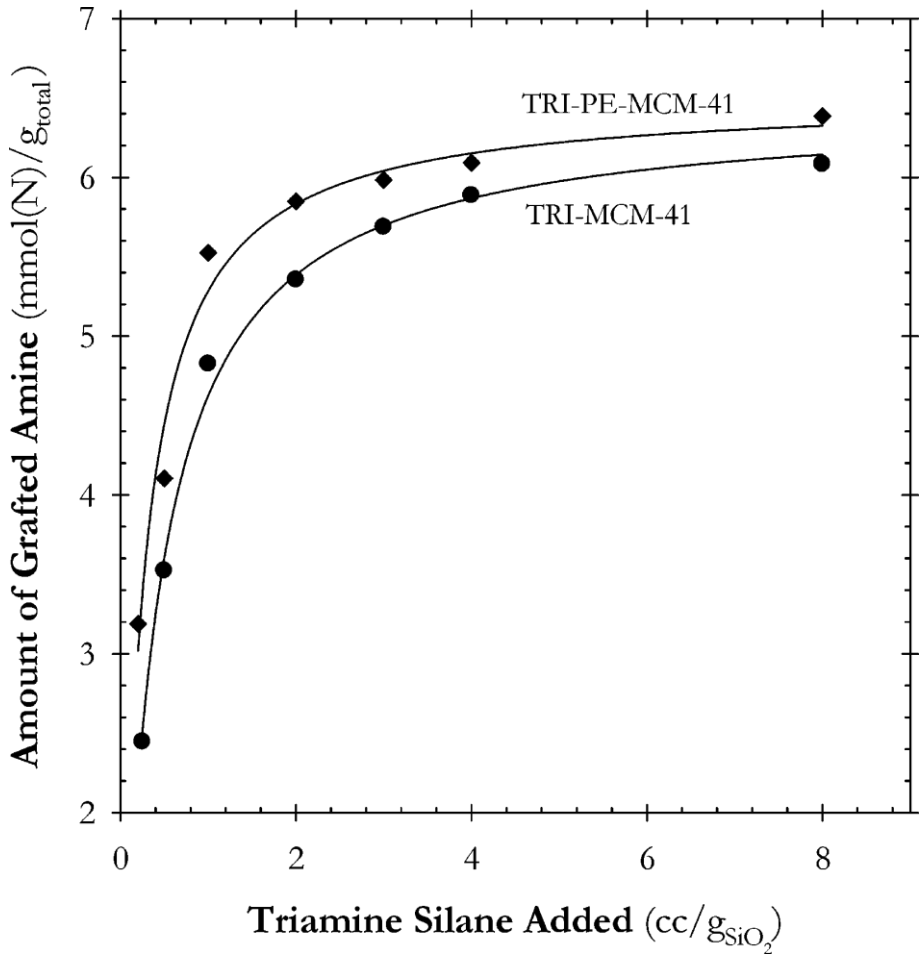

Figure 5.3 Effect of the amount of TRI added to the grafting mixture on the amount of TRI grafted on MCM-41 and PE-MCM-41 at 110 °C.

The N_2 adsorption capacity of the most commonly used CO_2 adsorbent, 13X zeolite, was also determined, using the method previously described, and was equivalent to 0.40 mmol/g. Essentially, this adsorption capacity will result with competitive adsorption behavior with CO_2, where the more quadrupolar CO_2 should dominate. However, when applied in a cyclic adsorption process, the CO_2 purity will be effectively reduced.

In terms of CO_2 adsorption performance, the various materials were challenged with a 5% CO_2/N_2 mixture, to determine the adsorption capacity and adsorption rate. By examining the adsorption in relation to the amount of added silane, and the amount of silane grafted, the optimal material could be determined, as synthesized under the conditions imposed in this work. The results are shown as a function of the amount of silane added in Figure 5.4, and as a function of the amount of grafted silane in Figure 5.5.

As shown in Figure 5.4, the TRI-PE-MCM-41 material exhibited much higher adsorption capacities and apparent rates than the TRI-MCM-41 material. Most importantly, TRI-MCM-41 exhibited a decrease in the apparent CO_2 adsorption rate as the amount of silane added was increased above 4.0 cm^3/g. In contrast, the TRI-PE-MCM-41 material did not show any decrease in the adsorption rate or the adsorption capacity. Therefore, it is concluded that, at high triamine silane loading, the surface density affects the rate of adsorption. This behavior is largely due to high surface density and the possible aminosilane polymerization at the pore openings. It can also be inferred from these data that the rate decrease is not due to complete pore blockage, because the adsorption capacity continued to increase.

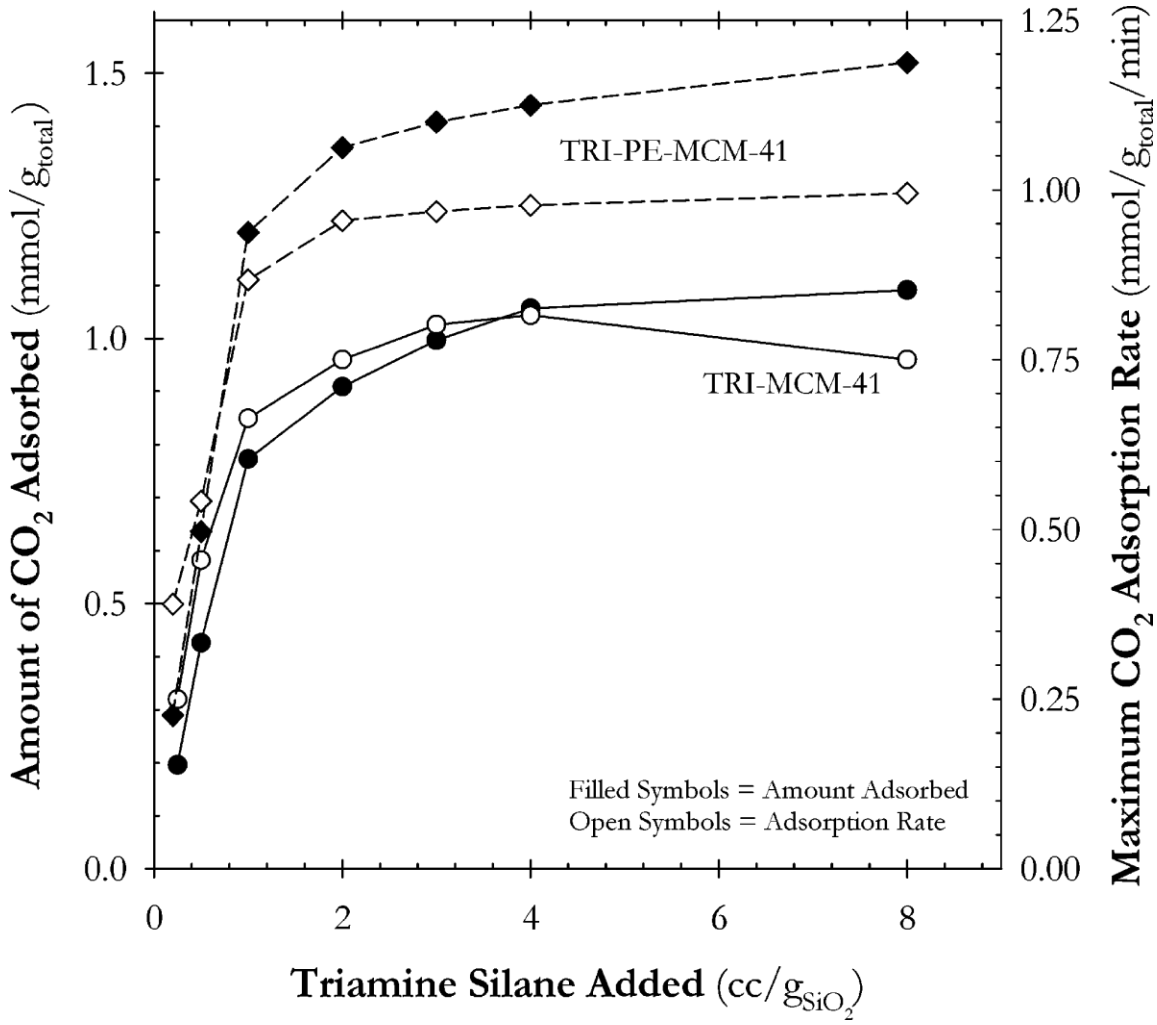

Figure 5.4 Effect of the amount of TRI added to the grafting mixture on the resulting 5% CO_2/N_2 adsorption capacity and apparent maximum adsorption rate for various levels of grafted TRI on MCM-41 and PE-MCM-41 at 110 °C.

These effects were not observed with the TRI-PE- MCM-41 material; rather, an adsorption rate plateau was reached. This plateau may be related to the mobility of the CO_2 within the pore; caused by the openness of the pore. The grafted amine species and the diffusing compound (CO_2) are both small, in comparison to the pore diameter; therefore, this limitation may be related to the kinetics of the CO_2-amine reaction.

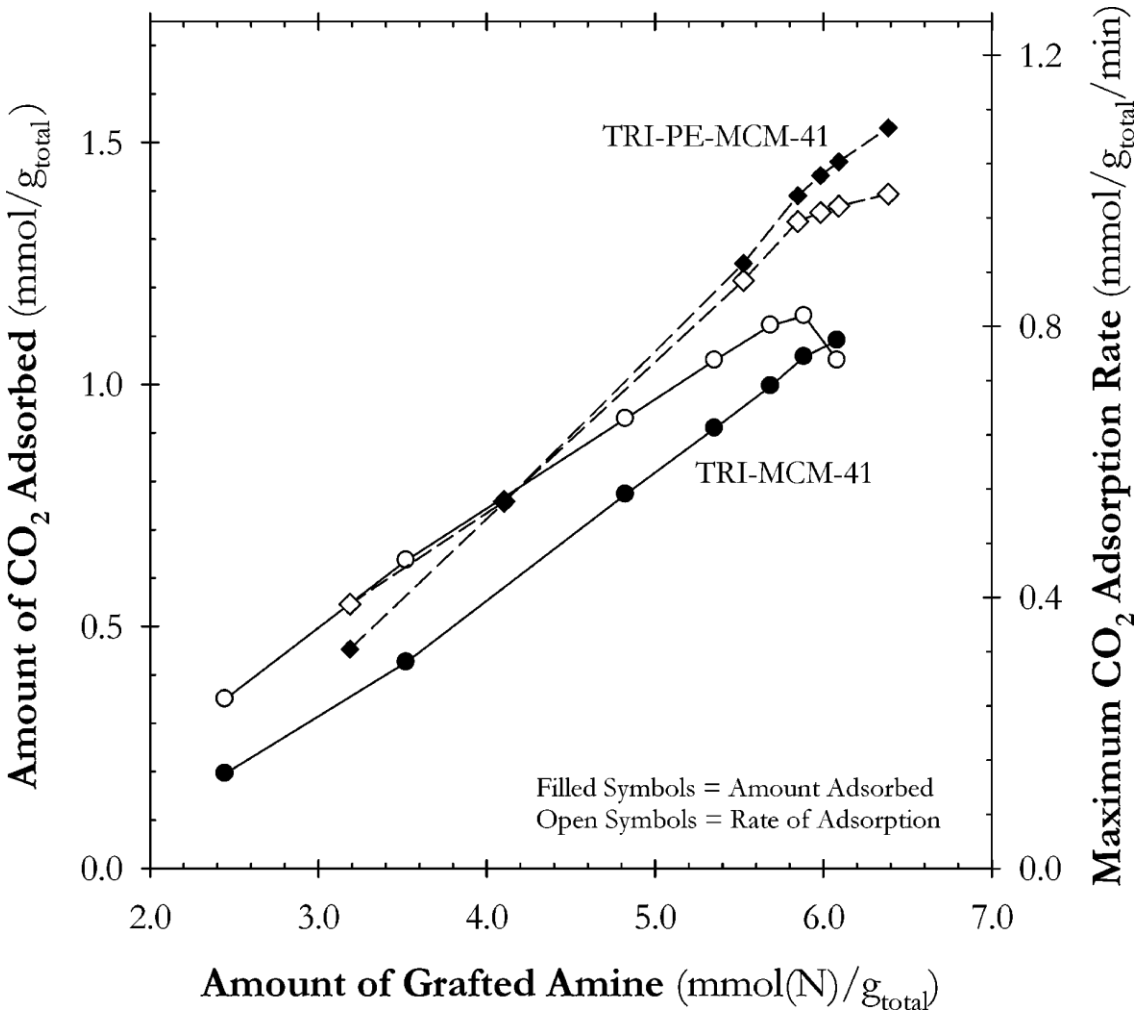

Figure 5.5 Plot of the 5% CO_2/N_2 adsorption capacity and maximum adsorption rate as a function of the amount of grafted amine on MCM-41 and PE-MCM-41.

When the adsorption performance data are compared on the basis of the amount of grafted amine, similar trends are observed, as shown in Figure 5.5. In this figure, the amine loading is expressed as the amount of nitrogen per gram of total material (support + amine). From these data, it is apparent that the PE-MCM-41 support material is capable of extending the amount of amine that can be grafted without negative effects on the materials performance.

The adsorption data were also examined in terms of the amine efficiency, i.e., moles of CO_2 adsorbed per moles of amine present, the CO_2/N ratio, and is shown in Figure 5.6.

Under the assumption of carbamate formation, this ratio should be 0.5 for dry CO_2 adsorption, and it approaches 1.0 for wet CO_2 adsorption, because of the formation of carbonate and bicarbonate (see Scheme 5.1). The actual CO_2/N ratios obtained under dry conditions (Figure 5.6) are significantly less than 0.5. This behavior may be due to several reasons. First, the reaction is weakly sensitive to the partial pressure of CO_2; in this study, a low partial pressure of CO_2 (5.1 kPa) was used. Furthermore, the amine-CO_2 chemistry may be hindered by the possibility of amine hydrogen bonding, leading to a reduced amount of amine groups available for CO_2 adsorption. However, the TRI- PE-MCM-41 materials did exhibit higher CO_2/N ratios than the TRI-MCM-41 materials, which is most likely due to the increased pore volume and pore diameter, which could lead to the amine chain conforming in such a way as to interact with the surface via the amine functional group.

In comparison to aqueous phase amine scrubbing, the CO_2/N ratios obtained in this study are similar. Typically, CO_2/N ratios of 0.15-0.30 are obtained with aqueous phase systems under the CO_2 inlet conditions used in this work (for example, see ref 1). In terms of amine grafted materials, the CO_2/N ratios vary widely in the literature. For monoamine grafted materials, Leal and co-workers [31,32] obtained a CO_2/N ratio of 0.42 with silica gel as the support, and Huang et al. [33] obtained a CO_2/N ratio of 0.50 with MCM-48 as the support and a CO_2/N ratio of 0.27 with silica xerogel as the support. Hiyoshi et al. [34] used SBA-15 as the support and obtained CO_2/N ratios of 0.19 for monoamine, 0.21 for diamine, and 0.22 for triamine grafted materials. In this study, the CO_2/N ratio varied from 0.08 to 0.18 for TRI-MCM-41, and 0.14-0.24 for TRI-PE-MCM-41, as a function of the amine loading.

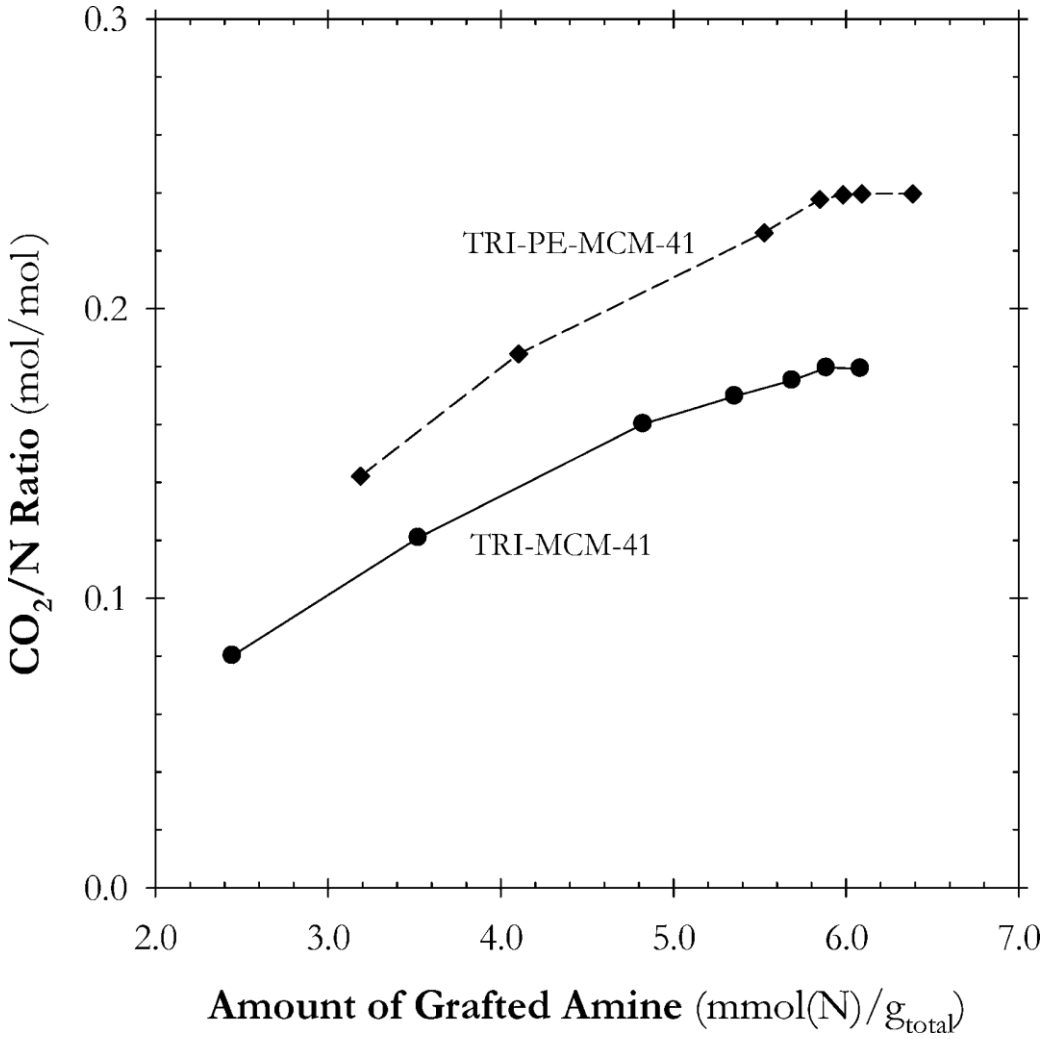

Figure 5.6 Relationship between the adsorption efficiency (CO_2/N ratio) as a function of the amount of amine grafted for various levels of TRI loading on MCM-41 and PE-MCM-41.

5.5.3 – Dynamic Adsorption Capacity

Most of the literature data have examined adsorption capacity on an equilibrium basis only. However, the dynamic regime of operation is equally (if not more) important as a material characteristic; most applications of adsorption are only run to partial bed saturation, because of the adsorption dynamics. Therefore, in this work, the CO_2 adsorption capacity was determined as a function of time in all runs, and an example is shown

in Figure 5.7 for the TRI-MCM-41 and TRI-PE-MCM-41 materials. The dynamic data were calculated based on the weight gain versus time, as measured by the previously described TGA-MS. Each material shown in this figure was grafted using a 3.0 cm^3/g addition of the triamine silane. From the data shown in Figure 5.7, the TRI-PE-MCM-41 material outperformed the TRI-MCM-41 material, from both the dynamic and equilibrium points of view. Specifically, TRI-PE-MCM-41 exhibited a higher adsorption rate than the TRI-MCM-41 material. This increase in rate resulted in a slight increase in the amount of CO_2 adsorbed in the initial exposure time frame. As a consequence, the adsorption capacity of TRI-PE-MCM-41 was superior to TRI-MCM-41 at exposure times of >0.80 min. This behavior demonstrated the dynamic processing ability of the PE-MCM-41 support over the standard MCM-41 support. Furthermore, the desorption of CO_2 (not shown) was also rapid and complete at 100 °C with a N_2 purge (purge/feed ratio of 1.0). Typically, <5 min of purge at 100 °C was required to completely regenerate the material, which could be considered as the equivalent of a short-time thermal pulse.

Since the TRI-PE-MCM-41 material exhibited a high rate of adsorption, its performance was compared to 13X zeolite and is shown in Figure 5.8. The 13X zeolite adsorbent was also regenerated at 200 °C for 45 min prior to the CO_2 adsorption run, to maintain the same initial regeneration thermal history as the TRI-grafted MCM-41 and PE-MCM-41 materials (see the section on CO_2 adsorption properties). From the data shown in this figure, it is evident that the TRI-PE-MCM-41 outperformed the 13X zeolite material within the first 2 min of exposure. The offset of the amount adsorbed curve for the 13X zeolite to the TRI-PE-MCM-41 material is largely due to the N_2 adsorption capacity, and weakly on the mass-transfer barriers of the two adsorbents. It is important to recall that each material was regenerated in pure N_2 prior to the introduction of the 5% CO_2/N_2 gas mixture.

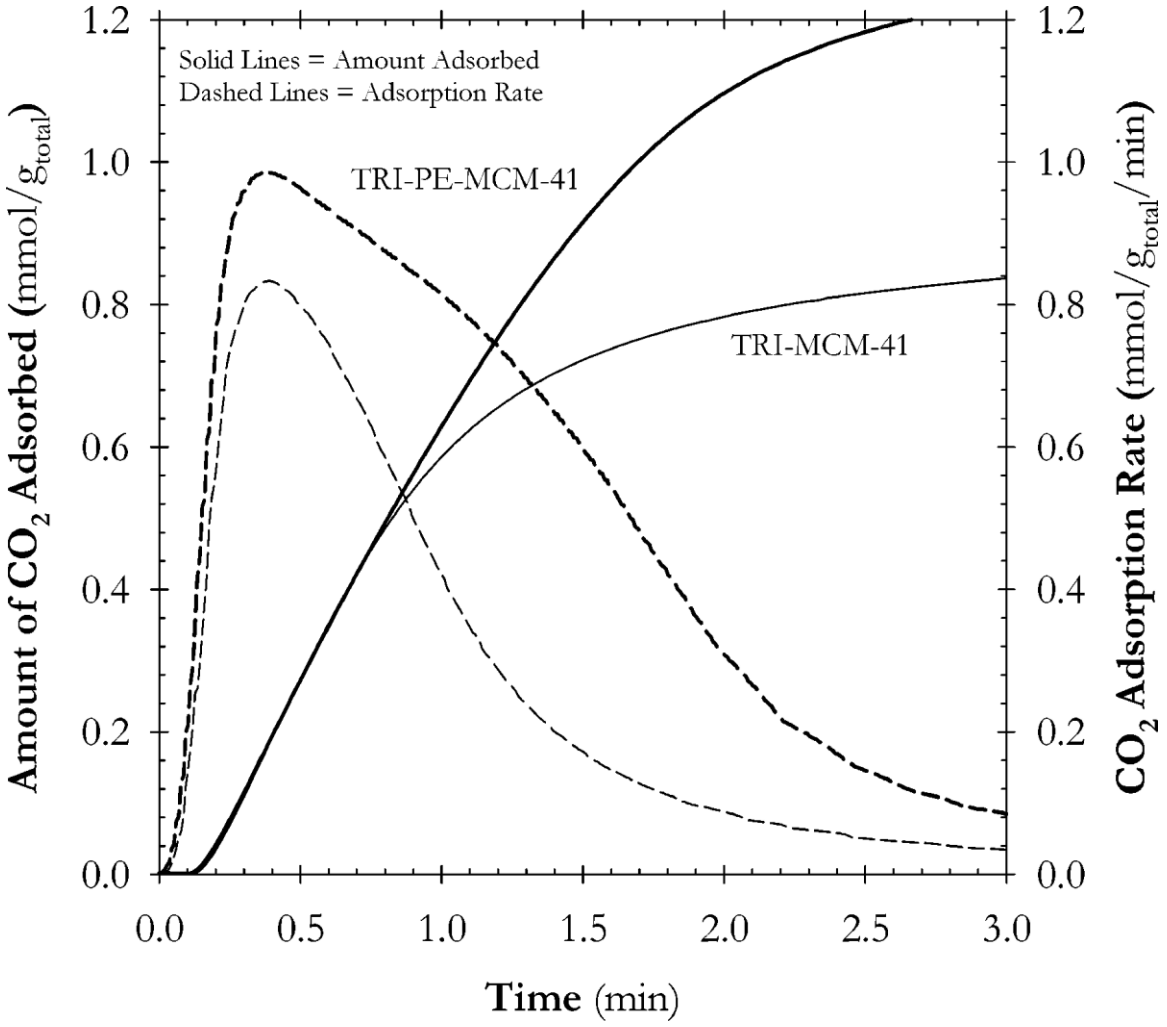

Figure 5.7 Dynamic 5% CO_2/N_2 adsorption performance of TRI-MCM-41 with TRI-PE-MCM-41 grafted with 3.0 $cm^3/g(SiO_2)$ TRI at 110 °C.

Therefore, for the 13X zeolite, ~0.40 mmol/g of N_2 was present on the adsorbent. When the CO_2 gas mixture was introduced, a competitive adsorption mechanism would dominate, where the CO_2 would displace the preadsorbed N_2. In the initial stages of CO_2 exposure, the weight gain due to CO_2 adsorption is counterbalanced by the weight loss due to desorption of preadsorbed N_2. Furthermore, because the pores of the 13X zeolite are much smaller than those of the PE-MCM-41 (i.e., 0.8 nm, compared to 10 nm, respectively), a small lag could also exist, because of the diffusional resistance. Therefore, in the initial time frame of exposure, the

CO_2 adsorbate will encounter a greater resistance to mass transfer and, thus, a delay in the uptake curve. By combining these arguments, the difference in uptake performance was demonstrated by the slow increase in the adsorption rate curve for the 13X zeolite from time zero, whereas TRI-PE-MCM-41 exhibited an almost- immediate adsorption rate response.

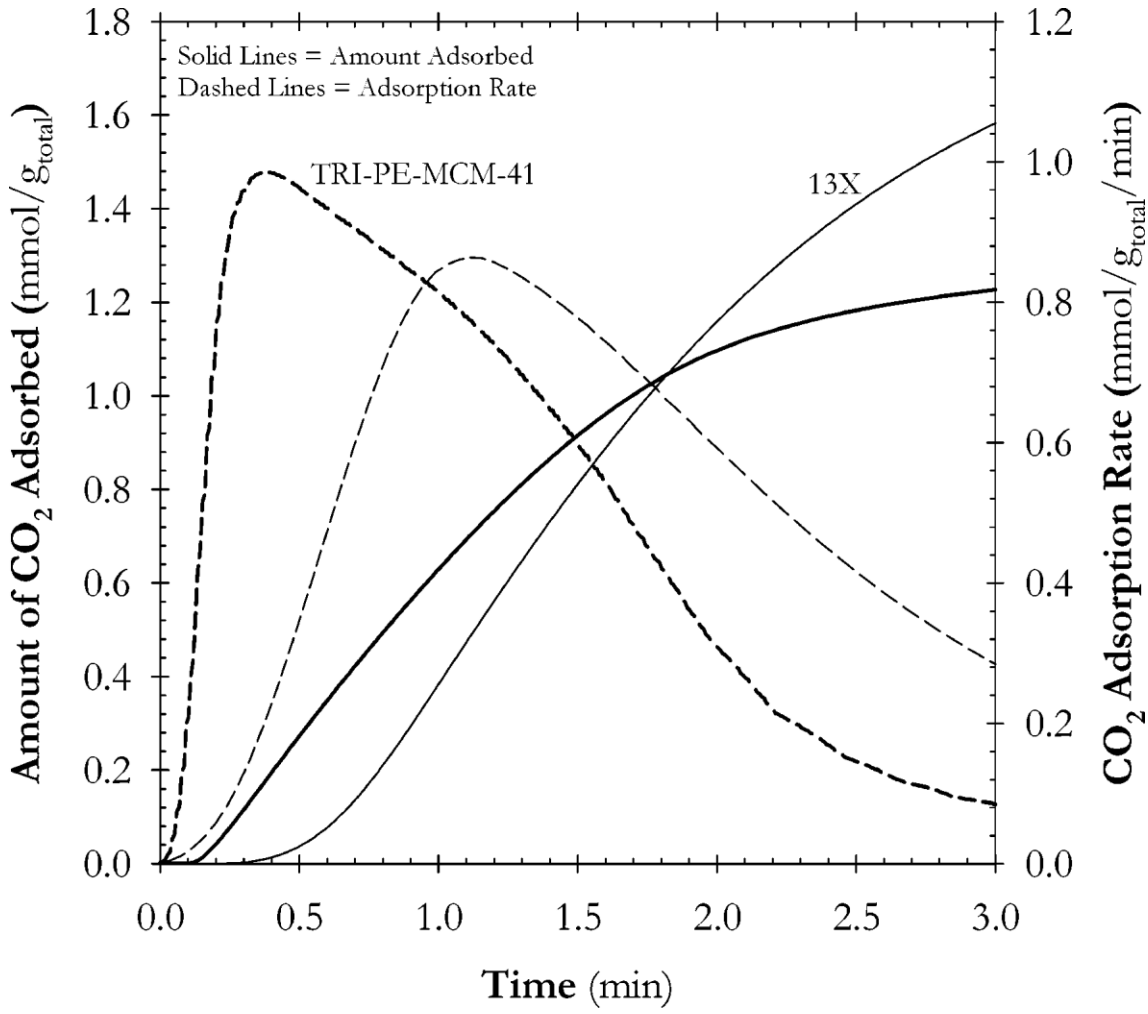

Figure 5.8 Comparison of the dynamic 5% CO_2/N_2 adsorption capacity and adsorption rate of TRI-PE-MCM-41 grafted with 3.0 $cm^3/g(SiO_2)$ TRI at 110 °C and 13X zeolite (regenerated at 200 °C).

Because the grafted material exhibited a lower equilibrium adsorption capacity than the 13X zeolite, a further comparison was made on the basis of the fractional uptake (i.e., [amount adsorbed at time t]/[amount adsorbed at equilibrium]) and is shown in Figure 5.9. From these

data, it is still evident that, in the initial exposure to CO_2, the grafted material outperformed the 13X zeolite. This behavior will be most beneficial when applying the material for the separation of CO_2 in a rapid (cycle time of <1.0 min), or ultrarapid (cycle time of <5 s) cyclic adsorption process,38 because the CO_2 uptake within a very small time frame (ca. 1.5 min) is greater for the TRI-PE-MCM-41 material than the 13X zeolite.

When the exposure time was equal to 4.2 min, the TRI-PE- MCM-41 and 13X zeolite adsorbents both exhibited the same fractional uptake of ca. 90%. Beyond this point, the 13X zeolite material reached a higher fractional uptake than the TRI-PE- MCM-41. This behavior

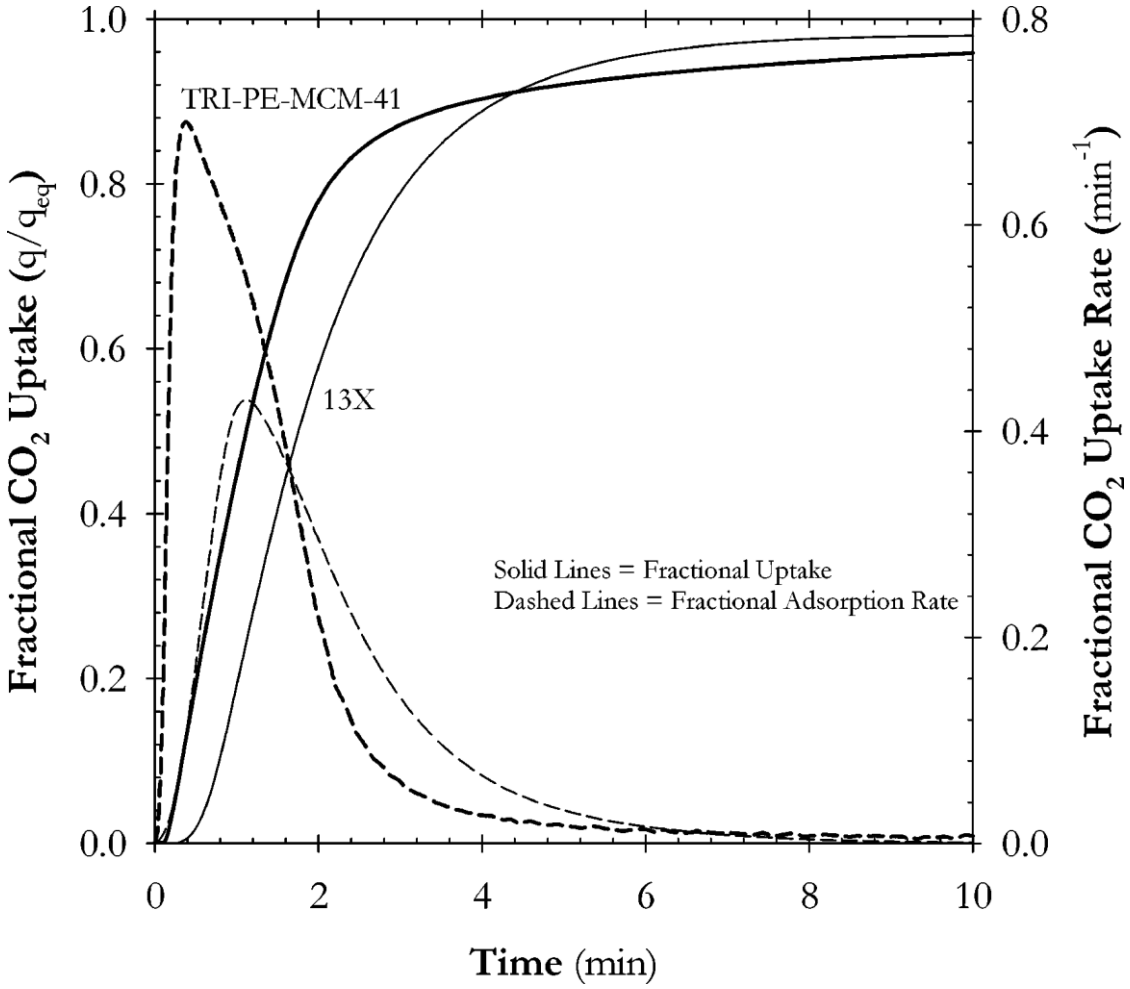

Figure 5.9 Comparison of the dynamic 5% CO_2/N_2 fractional uptake and fractional uptake rate of TRI-PE-MCM-41 grafted with 3.0 $cm^3/g(SiO_2)$ TRI at 110 °C and 13X zeolite (regenerated at 200 °C).

is largely due to the slow secondary mechanisms of adsorption, which may be occurring with the TRI-PE-MCM-41 material. For example, the primary amine site is known to react with CO_2 very rapidly, whereas the secondary amine sites are slower and the tertiary amine sites are very slow. Therefore, it is conceivable that the high initial adsorption rate is the result of CO_2 interaction with the primary amines, and the subsequent slow uptake is due to the CO_2 interaction with the secondary amines. This contention is consistent with the dual-mode response of the adsorption rate curve shown in Figure 5.8 for the TRI-PE-MCM-41, as an inflection point at a time of 1.5 min, and is not observed with the 13X zeolite. Admittedly, a direct observation of the stepwise interaction of CO_2 with the primary and secondary amine functional groups would be desirable.

5.5.4 – Effect of Moisture

The effect of moisture on the adsorption of CO_2 was considered in this study to be an important factor, because most process streams contain moisture, to a certain extent. For this study, the effect of moisture was evaluated by passing the feed mixture (either N_2, or 5% CO_2/N_2) through a H_2O saturator that was held isothermal at 5 °C, corresponding to a relative humidity (RH) of 26% at 25 ° C (see the section on CO_2 adsorption properties for details). It was determined that this temperature would best model the moisture content of a gas stream after being chilled with cooling water in a condenser. For both materials, the grafting was performed as previously described, where the triamine silane addition was 3.0 cm^3/g.

The adsorption runs were performed by first adsorbing the moisture from the N_2 feed, to equilibrium, and then switching to the humid 5% CO_2/N_2 stream for the adsorption of CO_2. It was determined by MS that, upon the introduction of the humid 5% CO_2/N_2 stream, there was negligible desorption of the preadsorbed moisture; therefore, the adsorption of H_2O

and CO_2 could be considered to be non-competitive. The results of the CO_2 + H_2O runs are summarized in Table 5.2. From these data, it is evident that the CO_2 adsorption capacity does not decrease in the presence of moisture; rather, there is a slight increase in capacity. Furthermore, in comparison to the 13X zeolite (regenerated at 200 °C), the adsorption performance of TRI- PE-MCM-41 is far superior, in the presence of moisture.

Table 5.2 Summary of the Dry and Humid 5% CO_2/N_2 Adsorption Data

material	amount grafted (mmol(N)/g)	Adsorption Capacity (mmol/g)		
		dry CO_2	H_2O	humid CO_2
TRI−MCM-41	5.69	0.97	2.56	1.01
TRI−PE-MCM-41	5.98	1.41	3.11	1.52
13X zeolite		2.05	15.11	0.09

The effect of moisture on the CO_2 adsorption capacity determined in this study compares well with the literature data. For example, Hiyoshi et al. [34] determined that the CO_2 adsorption capacity increased by 10% with a triamine grafted MCM-41, whereas Huang et al. [33] surprisingly claimed that the CO_2 adsorption capacity doubled (CO_2/N = 1.0) with a monoamine grafted MCM-48. However, even with liquid-phase amine absorption, the CO_2/N ratio of 1.0 is not achieved at low pressure for various amine types and concentrations (for example, see ref [1]). Therefore, the fact that the data in this work showed that the CO_2/N ratio increased only slightly (from 0.24 to 0.25) is a very positive result, in comparison to the 13X zeolite material, which exhibited almost no CO_2 adsorption capacity after saturation with H_2O.

5.6 - Conclusions

The results of this work have shown that the pore-expanded MCM-41 (PE-MCM-41) material can be grafted with a slightly higher quantity of triamine silane than the conventional MCM-41. However, in terms of actual CO_2 adsorption performance, PE-MCM-41 resulted in a significant increase of the equilibrium adsorption capacity and apparent adsorption rate. These benefits are mainly due to the larger pore diameter and pore volume of the PE-MCM-41, in comparison to the conventional MCM-41. The amount of silane added to the grafting mixture was observed to directly affect the quantity of amine that could be grafted, and, for both materials, the grafted quantities followed a Langmuir-type curve. Marginal increases in the quantity of grafted amine were observed for silane additions beyond 3.0 cm^3/g(silica). In comparison to 13X zeolite, the optimally grafted PE-MCM-41 exhibited superior adsorption performance in the initial stages of exposure to the 5% CO_2/N_2 feed. In contrast, the 13X zeolite did exhibit a higher equilibrium adsorption capacity. When exposed to a humid stream of 5% CO_2/N_2, the optimally grafted MCM-41 and PE-MCM-41 materials exhibited a slight increase in the CO_2 adsorption capacity. However, the 13X zeolite did not retain any significant CO_2 adsorption capacity. This result shows that the grafted materials are capable of adsorbing CO_2 in a humid environment and, therefore, outperforming the 13X zeolite.

5.7 – Acknowledgements

A.S. is the Government of Canada Research Chair in Catalysis by Nanostructured Materials. We thank the Natural Sciences and Engineering Research Council of Canada (NSERC), the Canadian Foundation for Innovation (CFI), and the Ontario Research & Development Challenge Fund (ORDCF) for financial support.

5.8 - References

[1] Rinker, E.; Ashour, S. S.; Sandall, O. C., *Absorption of Carbon Dioxide into Aqueous Blends of Diethanolamine and Methyldiethanolamine*, Ind. Eng. Chem. Res. 2000, 39, 4346.

[2] Little, R. J.; Versteeg, G. F.; Van Swaaij, W. P. M., *Kinetics of CO_2 with Primary and Secondary Amines in Aqueous SolutionssII. Influence of Temperature on Zwitterion Formation and Deprotonation Rates*, Chem. Eng. Sci. 1992, 47, 2027.

[3] Veawab, A.; Tontiwachwuthikul, P.; Chakma, A., *Corrosion Behavior of Carbon Steel in the CO_2 Absorption Process Using Aqueous Amine Solutions*, Ind. Eng. Chem. Res. 1999, 38, 3917.

[4] Hook, R. J., *An Investigation of Some Sterically Hindered Amines as Potential Carbon Dioxide Scrubbing Compounds*, Ind. Eng. Chem. Res.1997, 36, 1779.

[5] Satyapal, S.; Filburn, T.; Trela, J.; Strange, J., *Performance and Properties of a Solid Amine Sorbent for Carbon Dioxide Removal in Space Life Support Applications*. Energy Fuels, 2001, 15, 250.

[6] Birbara, P. J.; Filburn, T. P.; Michels, H.; Nalette, T. A., *Sorbent System and Method for Absorbing Carbon Dioxide (CO_2) from the Atmosphere of a Closed Habitable Environment*, U.S. Patent No. 6,364,938, 2002.

[7] Hodgson, E. W., *Regenerative Carbon Dioxide (CO_2) Removal System*, U.S. Patent No. 6,709,483, 2004.

[8] Franchi, R. S.; Harlick, P. J. E.; Sayari, A., *Applications of Pore- Expanded Mesoporous Silica. 2. Development of a High-Capacity, Water- Tolerant Adsorbent for CO_2*. Ind. Eng. Chem. Res., 2005, 44, 8007.

[9] Kresge, C. T.; Leonowicz, M. E.; Roth, W. J.; Vartuli, J. C.; Beck, J. S., *Ordered Mesoporous Molecular Sieves Synthesized by a Liquid-Crystal Template Mechanism*, Nature, 1992, 359, 710.

[10] Beck, J. S.; Vartuli, J. C.; Roth, W. J.; Leonowicz, M. E., Kresge, C. T., Schmitt, K. D., Chu, C. T.-W.; Olson, D. H.; Sheppard, E. W.; McCullen, S. B.; Higgins, J. B.; Schlenker, J. L., *A New Family of Mesoporous Molecular Sieves Prepared with Liquid Crystal Templates*. J. Am. Chem. Soc., 1992, 114, 10834.

[11] Sayari, A., *Periodic Nanoporous Materials: Synthesis, Characterization and Potential Applications*. In Recent AdVances and New Horizons in Zeolite Science and Technology; Chong, H., Woo, S. I., Park, S. E., Eds.; Elsevier: Amsterdam, 1996; p 1.

[12] Corma, A., *From Microporous to Mesoporous Molecular Sieve Materials and Their Use in Catalysis*. Chem. ReV, 1997, 97, 2373.

[13] Ying, J. Y.; Mehnert, C. P.; Wong, M. S., *Synthesis and Applications of Supramolecular-Templated Mesoporous Materials*. Angew. Chem., Int. Ed., 1999, 38, 56.

[14] Stein, A., *Advances in Microporous and Mesoporous Solids Highlights of Recent Progress*. AdV. Mater., 2003, 15, 763.

[15] Zhao, D.; Huo, Q.; Feng, J.; Chmelka, B. F.; Stucky, G. D., *Triblock Copolymer Syntheses of Mesoporous Silica with Periodic 50 to 300 Å Pores*. Science, 1998, 279, 548.

[16] Sayari, A.; Kruk, M.; Jaroniec, M.; Moudrakovski, I. L., *New Approaches to Pore Size Engineering of Mesoporous Silicates*. AdV. Mater., 1998, 10, 1376.

[17] Sayari, A.; Yang, Y.; Kruk, M.; Jaroniec, M., *Expanding the Pore Size of MCM-41 Silicas: Use of Amines as Expanders in Direct Synthesis and Postsynthesis Procedures*. J. Phys. Chem. B, 1999, 103, 3651.

[18] Sayari, A., *Unprecedented Expansion of the Pore Size and Volume of Periodic Mesoporous Silica*. Angew. Chem., Int. Ed. Engl., 2000, 39, 2920.

[19] Sayari, A.; Hamoudi, S.; Yang, Y., *Applications of Pore-Expanded Mesoporous Silica: 1. Removal of Heavy Metal Cations and Organic Pollutants from Wastewater*. Chem. Mater., 2005, 17, 212.

[20] Harlick, P. J. E.; Tezel, F. H., *An Experimental Adsorbent Screening Study for CO_2 Removal from N_2*, Microporous Mesoporous Mater., 2004, 76, 71.

[21] Chue, K. T.; Kim, J. N.; Yoo, Y. J.; Cho, S. H.; Yang, R. T., *Comparison of Activated Carbon and Zeolite 13X for CO_2 Recovery from Flue Gas by Pressure Swing Adsorption*. Ind. Eng. Chem. Res., 1995, 34, 591.

[22] Golden, T. C.; Taylor, F. W.; Johnson, M. L.; Malik, N. H.; Raiswell, C. J., *Purification of Air*, U.S. Patent No. 6,106,593, 2000.

[23] Rege, S. U.; Yang, R. T.; Buzanowski, M. A., *Sorbents for Air Prepurification in Air Separation*. Chem. Eng. Sci., 2000, 55, 4827.

[24] Golden, T. C.; Taylor, F. W.; Malik, N. H.; Raiswell, C. J.; Salter, E. H., *Process for Reducing the Level of Carbon Dioxide in a Gaseous Mixture*, U.S. Patent No. 6,506,236, 2002.

[25] Gomes, V. G.; Yee, K. W. K., *Pressure Swing Adsorption for Carbon Dioxide Sequestration from Exhaust*. Sep. Purif. Technol., 2002, 28, 161.

[26] Kumar, R.; McIlroy, C. B.; Schluter, R. W.; Pulsinelle, J.; Mitariten, M. J., *Pressure Swing Adsorption Process for Removing Carbon Dioxide and Water Vapor from a Gas Mixture*, Eur. Patent No. 1,221,337, 2002.

[27] Wegeng, R. S.; Rassat, S. D.; TeGrotenhuis, W. E.; Drost, K.; Vishwanathan, V. V., *Method and Apparatus for Thermal Swing Adsorption and Thermally-Enhanced Pressure Swing Adsorption*, U.S. Patent No. 6,746,515, 2004.

[28] Brandani, F.; Ruthven, D. M., *The Effect of Water on the Adsorption of CO_2 and C_3H_8 on Type X Zeolites*. Ind. Eng. Chem. Res., 2004, 43, 8339.

[29] Sayari, A.; Hamoudi, S., *Periodic Mesoporous Silica-Based Organic-Inorganic Nanocomposite Materials*. Chem. Mater., 2001, 13, 3151.

[30] Stein, A.; Melde, B. J.; Schroden, R. C., *Hybrid Inorganic-Organic Mesoporous SilicatessNanoscopic Reactors Coming of Age*. AdV. Mater., 2000, 12, 1403.

[31] Leal, O.; Bolivar, C.; Sepulveda, G.; Molleja, G.; Martinez, G.; Esparragoza, L., *Carbon Dioxide Adsorbent and Method for Producing the Adsorbent*, U.S. Patent No. 5,087,597, 1992.

[32] Leal, O.; Bolivar, C.; Ovalles, C.; Garcia, J. J.; Espidel, Y., *Reversible Adsorption of Carbon Dioxide on Amine Surface-bonded Silica Gel.* Inorg. Chim. Acta, 1995, 240, 183.

[33] Huang, H. Y., Yang, R. T.; Chinn, D.; Munson, C. L., *Amine Grafted MCM-48 and Silica Xerogel as Superior Sorbents for Acidic Gas Removal from Natural Gas*. Ind. Eng. Chem. Res., 2003, 42, 2427.

[34] Hiyoshi, N.; Yogo, D K.; Yashima, T., *Adsorption of Carbon Dioxide on Amine Modified SBA-15 in the Presence of Water Vapor*. Chem. Lett., 2004, 33, 510.

[35] Yoshitake, H.; Yokoi, T.; Tatsumi, T., *Adsorption of Chromate and Arsenate by Amino-Functionalized MCM-41 and SBA-1*. Chem. Mater., 2002, 14, 4603.

[36] Yokoi, T.; Yoshitake, H.; Tatsumi, T., *Synthesis of Amino- Functionalized MCM-41 via Direct Co-Condensation and Post-Synthesis Grafting Methods Using Mono-, Di- and Tri-Amino-Organoalkoxysilanes*. J. Mater. Chem. 2004, 14, 951.

[37] Sayari, A.; Yang, Y., *Highly Ordered MCM-41 Silica Prepared in the Presence of Decyltrimethylammonium Bromide*. J. Phys. Chem. B 2000, 104, 4835.

[38] Ackley, M. W.; Smolarek, J., *Enhanced Rate PSA Process*, U.S. Patent No. 6,790,260, 2004.

Chapter 6

Amine grafted, Pore-Expanded MCM-41 for Acid Gas Removal:
Effect of Grafting Temperature, Water, and Amine Type on Performance

P. J.E. Harlick, and A. Sayari

Centre for Catalysis Research and Innovation (CCRI), Department of Chemistry, University of Ottawa, 10 Marie Curie, Ottawa, Ontario, Canada K1N 6N5

Department of Chemical Engineering, University of Ottawa, 161 Louis Pasteur, Ottawa, Ontario, Canada K1N 6N5

As Published (with modification to heading style):

Studies in Surface Science and Catalysis, volume 158B, 2006

(Citation Count > 20, Google Scholar, 2015)

http://www.sciencedirect.com/science/article/pii/S0167299105804392

Further Details:

Sayari, Abdelhamid, **Harlick, Peter J. E.**, *Functionalized Adsorbent for Removal of Acid Gases and Use Thereof*, US 7767004, **2010**

Dharani, D.D., **Harlick, P.J.E.**, Sayari, A., *Applications of Pore-Expanded MCM-41 Silica: 4. Synthesis of a Highly Active Base Catalyst*, Catalysis Communications, **(2007)**, 8 829-833

Harlick, P.J.E., and Sayari, A., *Amine Grafted, Pore-Expanded MCM-41 for Acid Gas Removal: Effect of Grafting Temperature, Water, and Amine Type on Performance*, , Studies in Surface Science and Catalysis **(2006)**, 158B, 987-994

Serna-Guerrero, R., **Harlick, P.J.E.**, Sayari, A., *Novel Mesoporous Materials for the Adsorption of Volatile Organic Compounds*, 56th CSCHE Conference, Sherbrooke, Quebec, Canada, October 15-18, **2006**

Harlick, P.J.E., Serna, R., Das, D., Sayari, A., *Application of Modified Pore-Expanded MCM-41 Silica in Catalysis and Adsorption,* International Symposium on Zeolites and Microporous Crystals (ZMPC2006), Yonago, Japan, **2006**

Franchi, R.S., **Harlick, P.J.E.**, Sayari, A., *Applications of Pore-Expanded Mesoporous Silica. 2. Development of a High-Capacity, Water-Tolerant Adsorbent for CO_2*, Industrial and Engineering Chemistry Research, **(2005)**, 44 (21) 2569-2591

Franchi, R.S., **Harlick, P.J.E.**, Sayari, A., *A High Capacity, Water Tolerant Adsorbent for CO_2: Diethanolamine Supported on Pore-Expanded MCM-41,* Studies in Surface Science and Catalysis **(2005)**, 156, 879-886

Harlick, P.J.E., Sayari, A., *Unprecented CO_2 adsorption Capacity with Amine Grafted, Pore-Expanded MCM-41*, Presented at the International Chemical Congress of Pacific Basin Societies (Pacifichem), Honolulu, Hawaii, USA, December 1520, **2005**

Harlick, P.J.E., Sayari, A., *Amine Grafted Mesoporous Silica Supports for Acid Gas Removal from Humid Process Streams*, Nano-Porous Materials IV, Niagara Falls, Ontario, Canada, **2005**

Harlick, P.J.E., Franchi, R., Yang, Y., Sayari, A., *Hydrophobic MCM-41 Supported Composite Adsorbents for Acid Gas Separation*, 5th Brazilian Meeting on Adsorption, Natal, Brazil, July 18-21, **2004**

Collaboration:

The work presented in this Chapter was completed by myself under the supervision of Dr. A. Sayari. See section 1.2 for further details.

6.1 - Abstract

The application of pore-expanded MCM-41 mesoporous silica coated with various aminosilanes has been examined by the adsorption of CO_2 from N_2. Extremely high levels of active amine content were achieved with pre-hydrated surfaces and reaction at temperatures below reflux in order to facilitate surface polymerization of the silanes. The various coated materials exhibited CO_2 adsorption capacities, which all exceeded the literature reported values, for both meso-porous and micro-porous materials. Further, the apparent adsorption/desorption rate with the amine functionalized materials was exceedingly high even at low regeneration temperatures. When considering the amine type, the adsorption capacity was found to be dependent on the type and quantity of grafted amine. However, the difference between the diamine and triamine silane was only significant in the apparent adsorption rate as the triamine outperformed the diamine. These properties will result in a large decrease in the cyclic temporal and thermal parameters, and therefore an increase in the gas processed per unit time, when exploited in an adsorption process.

6.2 - Introduction

The term greenhouse gas has been mentioned quite often in the recent literature, as a result of society's global concern over rising atmospheric temperatures. While there are several compounds which contribute to the greenhouse effect, carbon dioxide (CO_2) has received the most attention, due to its abundance as an effluent in industrial processes. Therefore, the literature has shown a concentration on developing a separation scheme. While the present state of the art for CO_2 removal allows for such a process to be applied, the economics of the

process are not favorable enough to offset the capture cost. The major obstacle to these processes is the dynamic efficiency of the separation medium being employed. Various techniques have been applied which exploit the properties of membranes, absorbents, or adsorbents. The most common method of CO_2 removal presently used on a large scale is via wet scrubbing (liquid phase absorption).

To meet the present and future constraints placed on the allowable emissions of CO_2 the solution lies with point source reduction and recovery. Therefore, a treatment process must be developed. For this approach to succeed, it must be capable of effective and efficient removal, concentration, and recovery of CO_2 from various sources for industrial applications. Periodic cyclic adsorption processes can be designed to overcome these constraints if a suitable adsorbent is available. In this study, the development of novel adsorbent materials has been completed with the specific task of CO_2 separation from N_2 by exploiting the favorable properties of wet absorption and dry adsorption.

The main goal was to develop a material having a number of desirable properties. This material should exhibit excellent thermal behavior and an adsorption capacity higher than that of the most commonly employed zeolite based material, 13X. It should also be suitable for low CO_2 partial pressure applications. In addition, the CO_2 adsorption characteristics, ideally, should not be hindered by the presence of moisture in the feed stream. While these properties have been sought in CO_2 adsorbents, in the open literature to date, they have not been met simultaneously. In our previous work [1], we exploited a MCM-41 material with high pore volume, which could occlude a large quantity of amine, and thus exhibit a large adsorption capacity. However, since the amine was loaded by simple impregnation, the interaction between the support and the occluded species was weak, hence the material could be operated

only at relatively low temperature. The current work describes improved CO_2 adsorbents prepared using a different amine loading procedure with meso-porous silica as the support.

Periodic mesoporous silicas, discovered in 1992 by Mobil researchers [2, 3] and extensively studied by others [4, 5, 6, 7] appeared to be an excellent starting point for the synthesis of silicas with large pore volume and pore size. Previously our research group has developed a synthesis method to further extend the pore size and volume of MCM-41 silica from typically 4 nm and 0.8 cc/g up to 25 nm and 3 cc/g, respectively through a post-synthesis hydrothermal treatment in the presence of long chain alkyldimethylamines [8, 9, 10]. This profound transformation takes place without any significant loss of surface area. This achievement allows us to exploit the internal space of this type of material for different adsorption applications [1, 11]

Modification of periodic mesoporous silica surfaces has been extensively examined [12, 13]). However, the grafting of amine ligands for CO_2 removal has only been examined by a few groups [14, 15, 16]. The most promising results were reported by Huang et al., [14]. Using the common dry grafting method, Huang et al. [14] grafted y-aminopropyl-triethoxysilane on periodic mesoporous MCM-48 silica. They obtained an amine loading of 2.30 mmol/g (based on total adsorbent weight). When exposed to a 5% CO_2 in N_2 feed mixture, an equilibrium adsorption capacity of 1.14 mmol/g (50 mg/g) was obtained. In their work, they also demonstrated that regeneration of the adsorbed CO_2 could be accomplished at a relatively low temperature (75 °C). To explore this promising CO_2 adsorption behaviour, we have adopted our pore-expanded MCM-41 material as the support for various aminosilanes. Since this support material has a large pore volume and pore diameter, the approach of Feng

et al. [17], of using water aided surface functionalization, has also been incorporated to achieve unprecedented amine loadings and CO_2 adsorption capacity under comparable conditions.

6.3 – Materials and Method

6.3.1 - Support Synthesis and Grafting

The MCM-41 and pore-expanded MCM-41 (PE-MCM-41) materials used in this study were prepared as reported earlier [7, 9]. Specifically, the PE-MCM-41 material was prepared in a two-step procedure. The first step consisted of preparing a MCM-41 mesophase at a temperature of 100 °C for 40 h as described by Sayari and Yang [7]. This procedure required using Cab-O-Sil M5 fumed silica as the silica source, cetyltrimethylammonium bromide (CTAB) as the surfactant template, and a 25% solution of tetramethylammonium hydroxide in water (TMAOH) for pH adjustment. The molar composition of the gel was: 1.0 SiO_2: 0.32 TMAOH: 0.45 CTAB: 67 H_2O. The pore expansion process was carried out by post-synthesis hydrothermal treatment of non-calcined MCM-41 in an emulsion of N,N-dimethyldecylamine (DMDA) at a temperature of 120 °C for 72 h [9]. For the current study, DMDA was used at a ratio of 1.25 g per g of as-synthesized MCM-41. All materials were calcinated in flowing N_2 under a thermal ramp rate of 1 °C/min to 550 °C, and then held in air for 5 h. The materials were then transferred, hot, to a sealed container until their use. The calcination of the product of the first and second synthesis stages resulted in MCM-41 and PE-MCM-41, respectively.

All reagents used for the synthesis of grafted materials were purchased from Sigma-Aldrich and used as supplied with no further treatments. The following lists the compounds that were used with their respective purities and the acronym applied for identification in this study, water (distilled and di-ionized), Toluene (99% ACS grade), Pentane (99% ACS Grade), 3-(aminopropyl)trimethoxysilane, (97%, referred to as Mono), [3-(2-aminoethylamino)

propyl]trimethoxysilane (97%, referred to as DI), 3-[2-(2-aminoethylamino)ethylamino]propyl-trimethoxysilane (Tech, referred to as TRI).

The amine functionality was introduced into the PE-MCM-41-based materials via the post synthesis grafting technique. Two grafting procedures were used; dry and wet. The first, and most common method is referred to as the dry technique (for example see [12]), and uses dry solvents under reflux. For a typical synthesis, a suspension 1.0 g of the PE-MCM-41 material in 150 cc of dry toluene (250 cc multi-neck flask) at room temperature was prepared. Then a quantity of the amine-based silane was added and the temperature was increased rapidly to the desired set temperature where it was held for 16 h, with reflux. The wet technique involved addition of a measured quantity of water to 150 cc of toluene and mixing for 15 min. Then 1.0 g of the PE-MCM-41 material was added and allowed to equilibrate under stirring for 60 min. Finally, the required quantity of amine-based silane was added and the temperature was increased to the desired set temperature and held for 16 h, with reflux. All of the grafted materials were then filtered in a Buchner funnel with copious amounts of toluene and then pentane. The materials were subsequently dried at 120 °C in a natural convection oven for 4 h and stored in capped vials until use.

6.3.2 - Material Characterization and CO_2 Adsorption Measurements

The support materials were characterized by N_2 adsorption-desorption measurements using a Coulter Omnisorp 100 instrument. The standard BET method and the KJS method [18] were used to determine the specific surface area and the pore size distribution, respectively. The thermal stability of all materials was investigated using a thermal gravimetric analyzer coupled with an in-line mass spectrometer (TGA-MS, Q500 TA Instruments). The weight loss was monitored under flowing nitrogen, while the temperature was increased to

1000 °C at a rate of 10 °C/min. In order to quantify the grafted content, the TGA weight loss profile, normalized to 100% at 200 °C, was corrected to account for the losses exhibited by the support material alone; in the temperature range of 200-1000 °C. Using this corrected weight-loss, the amount of amine loading was calculated based on the amine-organic chain alone per gram of material.

Table 6.1 Summary of the Support Characteristics

Material	Surface Area (m^2/g)	Pore Diameter (nm)	Pore Volume (cc/g)
MCM-41	1138	3.6	1.03
PE-MCM-41	917	9.7	2.03

The adsorption capacity and apparent rate were obtained using the same TGA-MS instrument mentioned earlier. For these adsorption runs, the feed flowrate was controlled at 150 sccm sample and 10 seem balance purge. Using this balance, the materials response to a step change in CO_2 concentration (from 0.0 to 5% in N_2) was measured as the weight change relative to the condition of the material after thermal regeneration with N_2 purge. Thermal stability studies showed that with a regeneration condition of 200 °C, there were no losses of the grafted amine. All the pure gases used in this study were purchased from Praxair Canada, and were specified as UHP grade. The 5% CO_2/N_2 mixture was also purchased from Praxair Canada as a certified UHP grade mixture.

6.4 – Results and Discussion

6.4.1 - Material Properties

The structural properties calculated from nitrogen adsorption data are summarized in Table 6.1. From these data, it is evident that the pore expansion process has greatly increased

the pore diameter and pore volume, relative to the standard MCM-41 starting material, but without significant effect on the surface area.

With regard to thermal stability, TGA-MS experiments showed that under flowing nitrogen, all the grafted amines were stable up to 250 °C (results not shown). All grafted materials exhibited only minor losses up to 300 °C, in N_2. The materials did release the free methoxy side ligands (as shown by MS) in the temperature range of 150-200 °C, which accounted for 3-4 wt% of the total material mass. When each material was examined in air, the organic species were stable up to the decomposition temperature of 200 °C.

6.4.2 - CO_2 Adsorption Studies on Dry vs. Wet Grafted Materials

The first aspect examined in this study was the use of water during the grafting procedure. Conceptually, the dry grafting procedure can be considered as a reaction between the surface hydroxyl groups and the alkoxy ligands of the silane compound leading ultimately to the formation of a surface layer of tethered amine functionalities. Accordingly, it is assumed that all of the alkoxy ligands would ideally react with the surface hydroxyl groups to liberate an alcohol, leading to the formation of multiple Si-O-Si bridges with the silica surface.

Ideally, this reaction would occur with a ratio of 3 OH groups per molecule grafted; however, this is often not achieved. If grafting does occur, the alkoxy ligands will form at least one link to the surface, since the probability is highest for obtaining a single reactive OH site on the surface. However, this probability decreases as the requirement for the number of adjacent reactive OH sites increase. Therefore, it should be expected that not all the alkoxy ligands will be consumed to produce an alcohol, and consideration should be given to the free alkoxy group(s) which may be still attached to the Si center of the amino-silane. In order to consume the free alkoxy ligands and complete the surface coverage, water may be added to the

support material to produce a hydrated support material. Therefore, the surface water would facilitate the hydrolysis of the un-reacted alkoxy groups with the free silane and thus surface coverage would be enhanced. In this manner, the grafting should be considered as coating, since there is a possibility that some of the amino-silanes are not attached to the surface directly, rather, only through Si-O-Si bridges to other grafted amino-silanes. Since the objective of the present study was to obtain a material with a high CO_2 adsorption capacity, the constraint of the surface amine functionalization to be limited to a uniform mono-layer was not required. Rather, a high density of accessible amine sites without significant pore-blockage was essential.

The first issue of grafting in the presence of water was to examine the effect of the quantity of water added on the amount of amine which could be grafted, at a given reaction temperature. For this two parameter analysis (water and temperature), the quantity of each type of amine silane added to the post-synthesis mixture was kept constant and in excess (3.0 cc/g(SiO_2)). For this report, the triamine silane (TRI) was used for illustration in detail and is shown in Fig. 6.1. From the data shown, it is evident that the amount of added water has a profound impact on the quantity of TRI that can be grafted, for all reaction temperatures examined. In all cases, as the amount of added water exceeded 0.30 cc/g(SiO_2), the amount grafted increased only slightly. However, if the amount of added H_2O is constrained to 0.30 cc/g(SiO_2), as shown in Fig. 6.1B, it is clear that the highest amount of amine grafted was obtained with a temperature of 85 °C. The reasoning for this result could be due to the dependence on the rate of alkoxy consumption, both in the pores where the silane is able to react with the surface, and in the bulk solution, where the silane may polymerize (condense) due to the water content.

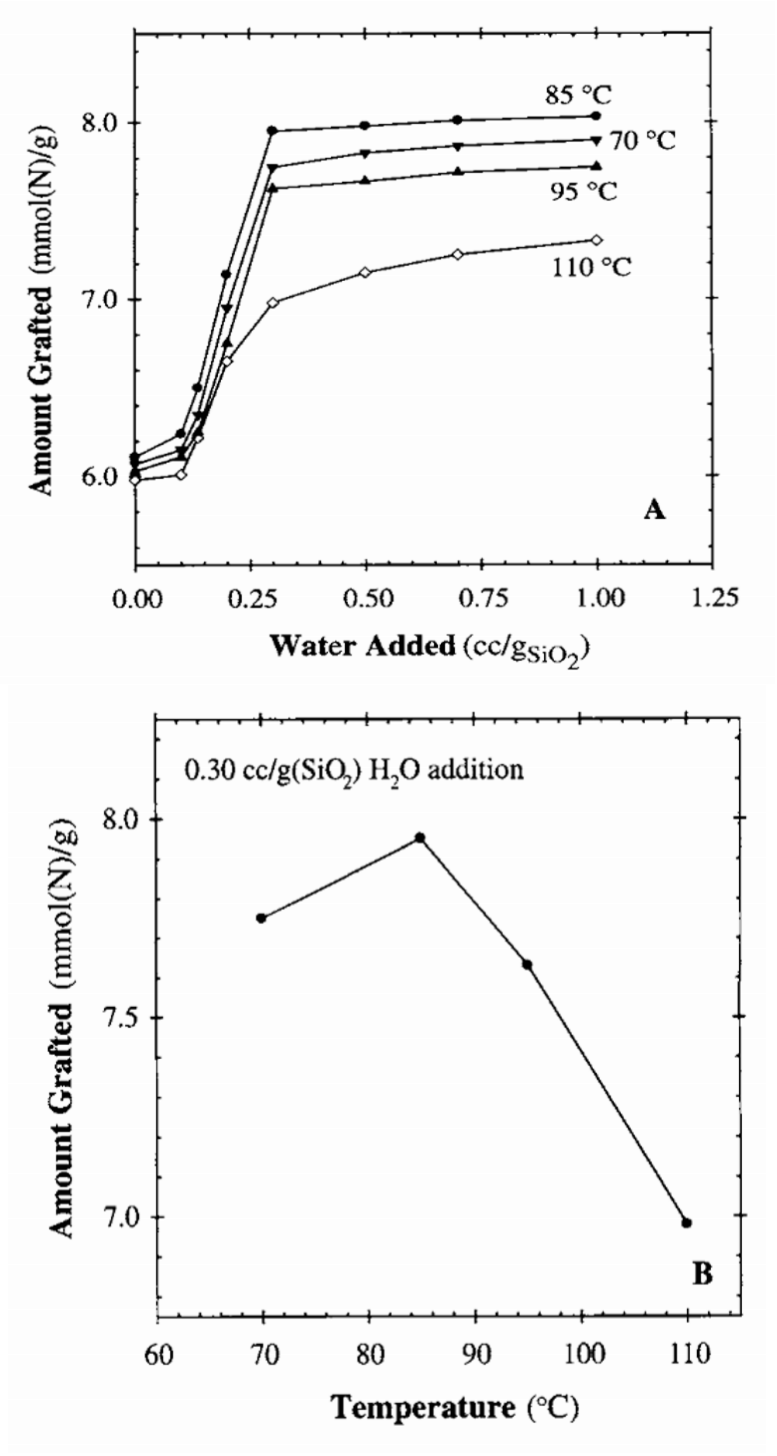

Fig 6.1 Effect of the grafting, temperature and water content, on the resulting amine content for PE-MCM-41, in the presence of 3.0 cc/g(SiO_2) of TRI.

In order to verify that the grafted amine was accessible and active, adsorption tests were performed using a 5% CO_2 in N_2 gas mixture. The results are shown in Fig. 6.2A in terms of adsorption capacity vs. amount of water added. Prior to each adsorption test, the material was regenerated at 200 °C for 45 min. It is seen that as the amount of water added increased above 0.30 cc/g(SiO_2), the CO_2 adsorption performance decreased, even though the amount of grafted amine was increasing (Fig. 6.1A). To examine these trends further, the apparent adsorption rate obtained from the adsorption runs was plotted as a function of water added (Fig. 6.2B). From this data, it is evident that as the adsorption capacity decreased, the adsorption rate also decreased. By combining these results, the general conclusion is that for water additions above 0.30 cc/g(SiO_2) pore blockage may occur due to the polymerization (condensation) of the silane in the bulk solution, and subsequent deposition on the external surface of the support.

6.4.3 - Effect of Grafted Aminosilane Type Under Optimal Reaction Conditions

For all amine types, the optimal grafting temperature was found to be 85 °C. However, the optimal amount of water added to the reaction mixture was higher for the mono-amine (0.44 cc/g(SiO_2)) silane than the di and tri-amine silanes (0.3 cc/g(SiO_2)). Overall, the results of the study showed that very high amine loadings, and associated adsorption capacities of the various materials were obtained when exposed to a 5% CO_2/N_2 gas mixture. For the mono-amine, an optimal grafted quantity of 4.31 mmol(N)/g (5.75 mmol(N)/gSiO_2) was obtained with a corresponding 2.35 mmol/g (104 mg/g) of 5% CO_2 in N_2 adsorbed at equilibrium. The maximum apparent adsorption rate for this material was also very high; 1.16 mmol/g/min (51 mg/g/min).

The optimal active grafting with DI produced an amine content of 6.16 mmol(N)/g (8.94 mmol(N)/gSiO_2), with a corresponding CO_2 adsorption equilibrium capacity of 2.58 mmol/g (113 mg/g), and the apparent adsorption rate increased to 1.57 mmol/g/min (69 mg/g/min). The results for this material show that the increase in the active amine content per grafted chain only produced a slight increase in the equilibrium CO_2 adsorption capacity, and the maximum apparent adsorption rate, with a subsequent decrease in the CO_2/amine ratio.

When TRI was optimally grafted, an amine loading of 7.95 mmol(N)/g (12.9 mmol(N)/gSiO_2) was obtained. In comparison to the diamine-coated material, the equilibrium adsorption capacity increased to 2.67 mmol/g (117 mg/g), and the maximum rate increased to 1.79 mmol/g/min (88 mg/g/min).

The dynamic response of the material containing the optimum amount of grafted triamine is shown in Fig. 6.3. This material was challenged with a 5% CO_2/N_2 feed mixture, and the dynamic amount adsorbed was recorded and is compared to the same response exhibited by zeolite 13X. As shown in Fig 6.3A, the fractional uptake for the triamine-grafted material is superior when the exposure time is less than 5 min. Beyond this time, the two materials exhibit similar approaches to complete saturation. However, the triamine grafted material adsorbed a larger amount of CO_2 (2.67 mmol/g) than the 13X material (2.05 mmol/g), when regenerated at 200 °C. The specific amount adsorbed and the associated adsorption rates are shown in Fig. 6.3B. From these data, it is evident that the triamine-grafted material is far superior in terms of the specific amount adsorbed, especially, upon initial contact with the feed gas mixture.

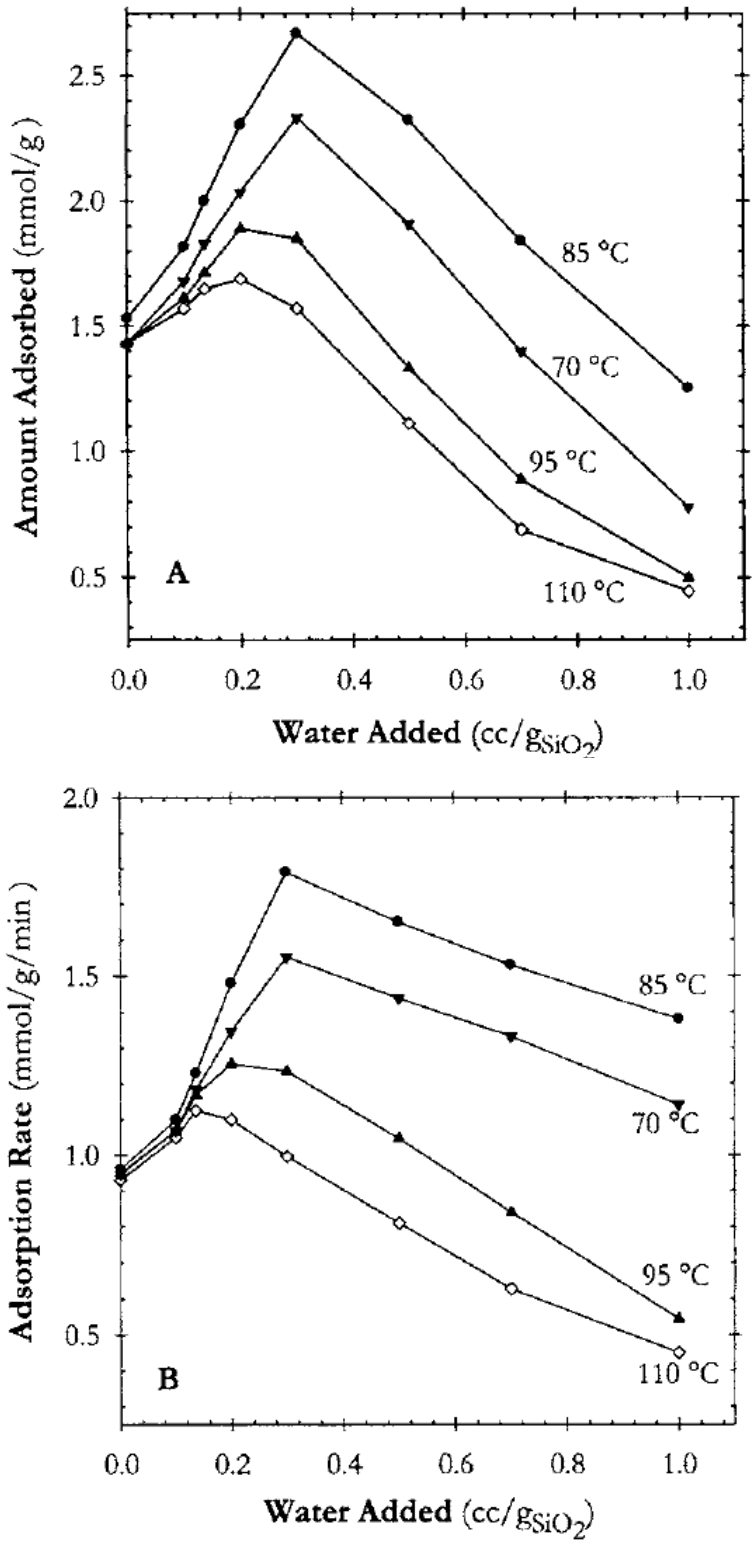

Fig 6.2 Effect of the grafting, temperature and water content, on the CO_2 adsorption capacity (A), and the adsorption rate (B) at 25 °C with 5% CO_2/N_2, for triamine-silane grafted with PE-MCM-41.

It is also interesting to observe that the 13X zeolite exhibited a delayed response to the 5% CO_2 feed mixture, as noted by the offset of the uptake curve and the slow increase in the rate. This behaviour may be due to the competitive effects of N_2, which was pre-adsorbed on the material, or by the result of pore diffusion. This type of behaviour was not observed with the triamine-grafted material since it does not exhibit N_2 adsorption, and the pore structure is such that diffusion limitations are greatly reduced.

By exposing the material to a N_2 stream saturated at 4-5 °C with water (27-28 % relative humidity), and then switching the gas supply to the 5% CO_2/N_2 gas mixture at the same humidity, the effects of both adsorbed components were examined. The results showed that the CO_2 adsorption capacity only slightly increased in the presence of this level of moisture; c.a. 3% increase with Mono, 7% with DI and 10% with TRI. Further analysis revealed that the materials were cyclically capable of regenerating both the adsorbed moisture and CO_2 completely at 75 °C with a dry N_2 purge. When the 13X was exposed to the same cyclic conditions, only a portion of the water could be regenerated, and the CO_2 equilibrium capacity remained unchanged (0.08 mmol/g).

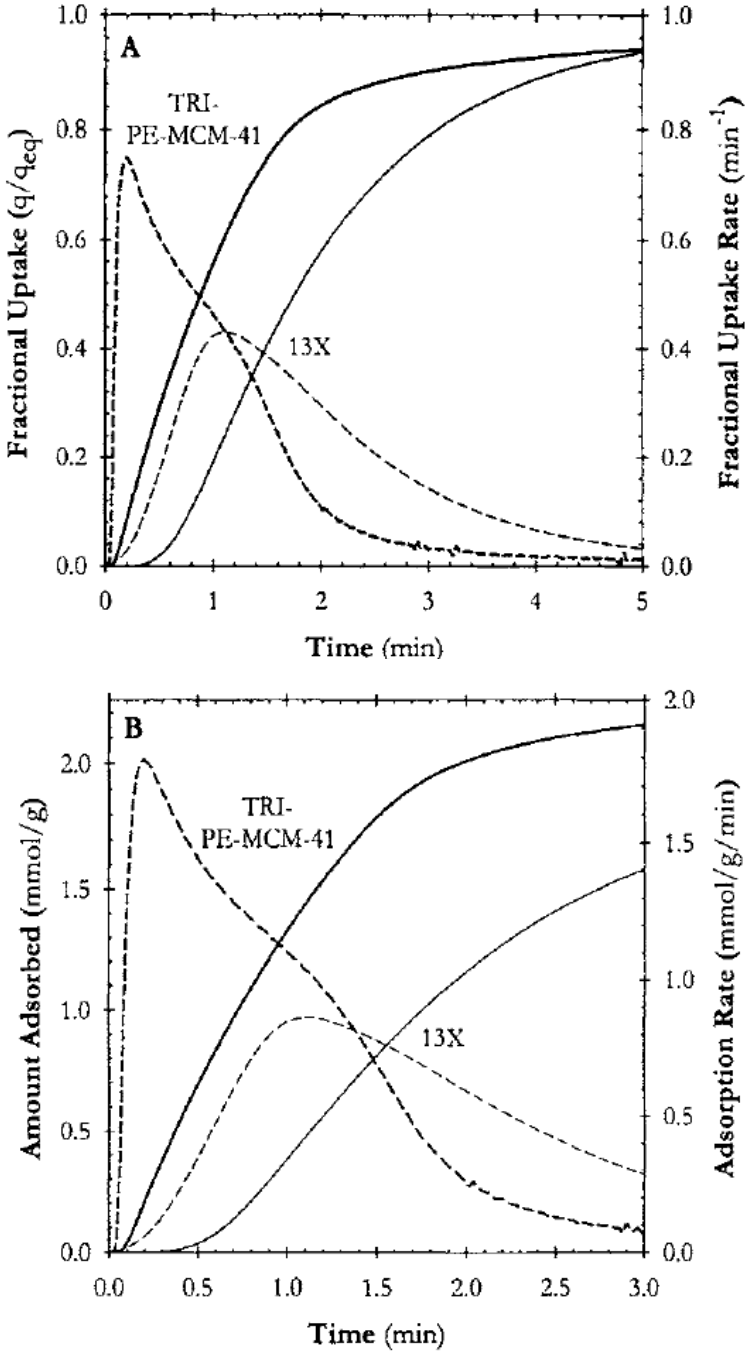

Fig 6.3 Dynamic adsorption response of the optimal TRI-PE-MCM-41 material and 13X zeolite to a 5% CO_2/N_2 feed mixture, as a fractional uptake (A), and specific amount adsorbed (B), where the solid lines represent the adsorption quantities and the dashed lines represent the adsorption rates.

6.5 - Conclusion

The grafting of amines to the surface of pore-expanded MCM-4 I was examined through the use of mono, di, and triamine alkoxy-silanes. The effects of reaction temperature, and the quantity of water added to the grafting mixture, were investigated in terms of the amount of amine grafted and CO_2 adsorption performance. The optimal reaction temperature for grafting was found to be 85 °C, which was significantly lower than the temperature of 110 °C, typically applied during grafting with toluene as the solvent. Under optimal reaction conditions, all amines types were grafted to very high contents. All materials exhibited high adsorption capacities and adsorption rates when exposed to a 5% CO_2/N_2 gas mixture. Further, each grafted material outperformed zeolite 13X with dry CO_2 adsorption and vastly outperformed zeolite 13X with humid CO_2 adsorption. These characteristics demonstrate the ability of the pore-expanded MCM-4l support to accommodate a large quantity of aminosilane and still allow high adsorbate mobility, which translates into an adsorbent with a high CO_2 adsorption capacity and an unprecedented adsorption rate.

6.6 - Acknowledgements

The financial support of the Natural Science and Engineering Research Council of Canada through the Strategic Grant program is acknowledged.

6.7 - References

[1] R. Franchi, P.J.E. Harlick, A. Sayari, Ind. Eng. Chem. Res., submitted (2005).

[2] C.T. Kresge, M.E. Leonowicz, W.J. Roth, J.C. Vartuli, J.S. Beck, Nature, 359 (1992) 710.

[3] J.S. Beck, J.C. Vartuli, W.J. Roth, M.E. Leonowicz, C.T. Kresge, K.D. Schmitt, C.T-W. Chu, D.H. Olson, E.W. Sheppard, S.B. McCullen, J.B. Higgins, J.L. Schlenker, J. Am. Chem. Soc., 114 (1992) 10 834.

[4] M. Kruk, M. Jaroniec, A. Sayari, J. Phys. Chem. B, 103 (1999) 4590.

[5] M. Kruk, M. Jaroniec, A. Sayari, Microporous Mesoporous Mater., 35-36 (2000) 545.

[6] M. Kruk, M. Jaroniec, V. Antochshuk, A. Sayari, J. Phys. Chem. B, 106 (2002) 10096.

[7] A. Sayari, Y. Yang, J. Phys. Chem. B, 104 (2000) 4835.

[8] A. Sayari, M. Kruk, M. Jaroniec, I.L. Moudrakovski, Adv. Mater., 10 (1998) 1376.

[9] A. Sayari, Y. Yang, M. Kruk, M. Jaroniec, J. Phys. Chem. B, 103 (1999) 3651.

[10] A. Sayari, Angew. Chem. Int. Ed. Engl, 39 (2000) 2920.

[11] A. Sayari, S. Hamoudi, Y. Yang, Chem. Mater, 17 (2005) 212.

[12] A. Sayari, S. Hamoudi, Chem. Mater., 13 (2001) 3151.

[13] A. Stein, B.J. Melde, R.C. Schroden, Adv. Mat., 12 (2000) 1403.

[14] H.Y. Huang, R.T. Yang, D. Chinn, C.L. Munson, Ind. Eng. Chem. Res., 42 (2003) 2427.

[15] 0. Leal, C. Bolivar, C. Ovalles, J. J. Garcia, Y. Espidel, Inorg. Chim. Acta, 240 (1995) 183.

[16] N. Hiyoshi, K. Yogo, T. Yashima, Chem. Letters, 33 (2004) 510.

[17] X. Feng, G.E. Fryxell, L.Q. Wang, A.Y. Kim, J. Liu, K.M. Kemner, Science, 276 (1997) 923.

[18] M. Kruk, M. Jaroniec, A. Sayari, Langmuir, 13 (1997) 6267.

Chapter 7

Applications of Pore-Expanded Mesoporous Silicas. 5.
Triamine Silane Grafted Material with Exceptional CO_2 Dynamic and Equilibrium Adsorption Performance

P. J.E. Harlick, and A. Sayari

Centre for Catalysis Research and Innovation (CCRI), Department of Chemistry, University of Ottawa, 10 Marie Curie, Ottawa, Ontario, Canada K1N 6N5

Department of Chemical Engineering, University of Ottawa, 161 Louis Pasteur, Ottawa, Ontario, Canada K1N 6N5

As Published (with modification to heading style):

Industrial Engineering Chemical Research, 46 (2) 2007

(Citation Count > 310, Google Scholar, 2015)

Further Details:

Sayari, Abdelhamid, **Harlick, Peter J. E.**, *Functionalized Adsorbent for Removal of Acid Gases and Use Thereof*, US 7767004, **2010**

Dharani, D.D., **Harlick, P.J.E.**, Sayari, A., *Applications of Pore-Expanded MCM-41 Silica: 4. Synthesis of a Highly Active Base Catalyst*, Catalysis Communications, **(2007)**, 8 829-833

Harlick, P.J.E., and Sayari, A., *Amine Grafted, Pore-Expanded MCM-41 for Acid Gas Removal: Effect of Grafting Temperature, Water, and Amine Type on Performance*, , Studies in Surface Science and Catalysis **(2006)**, 158B, 987-994

Serna-Guerrero, R., **Harlick, P.J.E.**, Sayari, A., *Novel Mesoporous Materials for the Adsorption of Volatile Organic Compounds*, 56th CSCHE Conference, Sherbrooke, Quebec, Canada, October 15-18, **2006**

Harlick, P.J.E., Serna, R., Das, D., Sayari, A., *Application of Modified Pore-Expanded MCM-41 Silica in Catalysis and Adsorption,* International Symposium on Zeolites and Microporous Crystals (ZMPC2006), Yonago, Japan, **2006**

Franchi, R.S., **Harlick, P.J.E.**, Sayari, A., *Applications of Pore-Expanded Mesoporous Silica. 2. Development of a High-Capacity, Water-Tolerant Adsorbent for CO_2*, Industrial and Engineering Chemistry Research, **(2005)**, 44 (21) 2569-2591

Franchi, R.S., **Harlick, P.J.E.**, Sayari, A., *A High Capacity, Water Tolerant Adsorbent for CO_2: Diethanolamine Supported on Pore-Expanded MCM-41,* Studies in Surface Science and Catalysis **(2005)**, 156, 879-886

Harlick, P.J.E., Sayari, A., *Unprecented CO_2 adsorption Capacity with Amine Grafted, Pore-Expanded MCM-41*, Presented at the International Chemical Congress of Pacific Basin Societies (Pacifichem), Honolulu, Hawaii, USA, December 1520, **2005**

Harlick, P.J.E., Sayari, A., *Amine Grafted Mesoporous Silica Supports for Acid Gas Removal from Humid Process Streams*, Nano-Porous Materials IV, Niagara Falls, Ontario, Canada, **2005**

Harlick, P.J.E., Franchi, R., Yang, Y., Sayari, A., *Hydrophobic MCM-41 Supported Composite Adsorbents for Acid Gas Separation*, 5th Brazilian Meeting on Adsorption, Natal, Brazil, July 18-21, **2004**

Collaboration:

The work presented in this Chapter was completed by myself under the supervision of Dr. A. Sayari. See section 1.2 for further details.

7.1 - Abstract

Application of pore-expanded MCM-41 (PE-MCM-41) mesoporous silica coated with 3-[2-(2-aminoethyl-amino)ethylamino]propyltrimethoxysilane (TRI) has been extensively examined for the adsorption of CO_2 from N_2. A systematic study of the amine loading as a function of the relative amounts of TRI and water used during the grafting procedure and the temperature of the grafting reaction was carried out. Extremely high levels of active amine content were achieved using prehydrated silica surfaces at grafting temperatures below reflux in order to facilitate thermally controlled water-aided surface polymerization of the aminosilanes. The CO_2 adsorption capacities and rates were determined for all materials as a function of the amount of TRI and water per gram of support added to the grafting mixture. The optimal TRI grafted PE-MCM-41 adsorbent exhibited a 2.65 mmol/g adsorption capacity at 25 °C and 1.0 atm for a dry 5% CO_2 in N_2 feed mixture, which exceeded all literature reported values, for both meso- and microporous materials under the conditions used in this study. Further, the apparent adsorption and desorption rates with the amine functionalized materials were exceedingly high. When considering the grafted amine quantity, the adsorption capacity and rate were found to be mutually dependent on each other, exhibiting an apparent optimal combination. In comparison to zeolite 13X, the optimally loaded TRI-PE-MCM-41 was far superior in terms of dynamic adsorption and desorption performance. These results were further enhanced when the adsorbents were challenged with a humid stream of 5% CO_2/N_2. The TRI-PE-MCM-41 exhibited a 10% increase in CO_2 adsorption capacity, whereas the 13X zeolite did not retain any significant CO_2 adsorption capacity.

7.2 - Introduction

The term greenhouse gas has been mentioned quite often in the recent literature, as a result of society's concern over rising atmospheric temperatures. While there are several compounds which contribute to the greenhouse effect, carbon dioxide (CO_2) has received the most attention, because of its abundance as part of the effluent from many industrial processes. Carbon dioxide emission is largely based on the combustion of carbon containing fuels, as in the heating and transportation markets. Therefore, much effort has been focused on developing viable separation schemes. While the present state of the art for CO_2 removal offers feasible processes for certain applications, the process economics are often not favorable enough to offset the capture cost. The major obstacle to separation processes is the dynamic efficiency of the separation medium being employed. Various techniques have been applied that exploit the properties of membranes, absorbents, or adsorbents, while the most common method of CO_2 removal presently used on a large scale is wet scrubbing (liquid-phase absorption).

To meet the present and future constraints placed on the allowable emissions of CO_2, an immediate solution lies with point-source reduction and recovery. Therefore, a treatment process must be developed. For this separation process to succeed, it must be capable of effective and efficient removal, concentration, and recovery of CO_2 from various sources for industrial applications. Periodic cyclic adsorption processes can be designed to overcome these process requirements if a suitable adsorbent is available. In this study, the development of novel adsorbent materials has been achieved with the specific task of CO_2 separation from N_2 by exploiting the favorable properties of gas-liquid absorption and gas-solid adsorption via the grafting of amine functionality to a mesoporous solid support.

Periodic mesoporous silicas, discovered in 1992 by Mobil researchers [1, 2] and extensively studied by others (for example, see refs [3-7]), appeared to be an excellent starting point for the synthesis of silicas with large pore volume and pore size. Previously, our research group developed a method to further enlarge the pore size and volume of MCM-41 silica from typically 4 nm and 0.8 cm^3/g up to 25 nm and 3.5 cm^3/g, respectively, through a postsynthesis hydrothermal treatment in the presence of long chain alkyldimethylamines [8-11]. This profound transformation occurs without any significant loss of surface area. This achievement allows us to exploit the internal space of this type of material for different adsorption [12-14] and catalytic applications [15-17].

In our initial work dealing with CO_2 removal, [13] we exploited the high pore volume and diameter of pore-expanded MCM-41 silica (PE-MCM-41) to impregnate a large quantity of diethanolamine (ca. 8.0 mmol/g). With this material, very high amine loadings were obtained and resulted in CO_2 adsorption capacities as high as 2.93 mmol/g for a 5% CO_2/N_2 feed at 25 °C and 101 kPa total pressure. However, since the amine was loaded by simple impregnation, the interaction between the support and the occluded species was weak; hence, the material could be operated only at relatively low temperature.

In order to overcome the limitations of the amine impregnated PE-MCM-41, we focused our attention on the design of more robust amine containing PE-MCM-41 adsorbents via the grafting of aminosilanes [14]. In this work, we showed that the effect of the amine surface density of the material has a profound impact on the adsorption efficiency. Intuitively, a high amine density would be desirable; however, we demonstrated that a high amine loading does not necessarily allow for the optimal use of the grafted amine for CO_2 adsorption from

N_2. This efficiency was defined as the point at which the rate of adsorption was optimal while considering the magnitude of the adsorption capacity.

Further, the relative amount of aminosilane to silica required to reach this level of grafting was found to be significantly lower than the amounts that are typically used (see ref [14]). The general approach has been to add the silane in large excess. Therefore, in this study, the effect of the quantity of triaminesilane added on the amount of amine grafted in the presence of controlled amounts of water and the resulting dynamic and equilibrium CO_2 adsorption performance have been critically examined using PE-MCM-41 as the support.

To explore this promising CO_2 adsorption behavior, typical MCM-41 and pore-expanded MCM-41 materials have been used as the support for triaminesilane grafting. On the basis of our earlier results, [14] and since the PE-MCM-41 exhibits a large pore volume and pore diameter, it is expected that much higher quantities of triamine may be loaded within the volume of the pore channels through a combination of surface grafting and condensation. In order to achieve this, the classical approach of water-aided surface functionalization for enhancing the surface coverage of grafted species on flat substrates and thin films (for example, see ref [18]), and later extended to mesoporous materials by Feng et al. [19] and Li et al. [20] has been modified and applied to PE-MCM-41. By utilizing this approach and optimizing the grafting conditions, the aim was to achieve unprecedented amine loading and CO_2 adsorption capacity.

7.3 – Literature Review

Modification of periodic mesoporous silica surfaces has been extensively examined (for example, see refs [21] and [22]). A review of the literature concerning amine grafting on

silica- based supports under dry conditions (anhydrous solvents and materials) with the goal of enhanced CO_2 adsorption is available in our previous work [14]. From this review, the most promising result reported was that of Huang et al. [23]. Using the common dry grafting method, Huang et al. [23] grafted 3-aminopropyltriethoxysilane on periodic mesoporous MCM-48 silica and obtained an amine loading of 2.30 mmol/g (based on total adsorbent weight). When exposed to a 5% CO_2 in N_2 feed mixture, an equilibrium adsorption capacity of 1.14 mmol/g (50 mg/g) was obtained. For 100% CO_2 at 1.0 atm total pressure, the adsorption capacity was determined to be ca. 2.05 mmol/g. It was also suggested in this work that the presence of water vapor (64% RH) produces an adsorption capacity for CO_2 of twice as much as the capacity in dry streams. In a more recently published article, Knowles et al. [24] grafted 3-aminopropyltrimethoxysilane onto a hexagonal mesoporous silica support (HMS) and obtained a loading of 2.29 mmol(N)/g. The corresponding adsorption capacity from a 90% CO_2/Ar gas feed at 20 °C was 1.59 mmol/g. In comparison to the data presented by Huang et al. [23] the material prepared by Knowles et al. [24] exhibited a significantly lower adsorption capacity for the same monoamine loading. Further, when the grafted material was challenged with a humid (30% RH) stream of CO_2, the adsorption capacity slightly decreased.

In our previous study on dry TRI grafting with PE-MCM-41 silica, we obtained an amine loading of 5.98 mmol(N)/g (1.99 mmol(organic)/g) with a corresponding dry 5% CO_2/N_2 adsorption capacity of 1.41 mmol/g (62 mg/g) [14]. However, unlike the data presented by Huang et al. [23] the triamine grafted material did not exhibit a doubling of the CO_2 adsorption capacity in the presence of a moist feed of CO_2, but rather only exhibited a modest increase, ca. 8%.

The following review will be limited to data relevant to the current study; in particular, the use of water during the grafting of aminosilanes with silica-based supports for the adsorption of CO_2. The approach has been used by a few research groups, [25-27] and most likely inadvertently by a few others, by relaxing the anhydrous conditions during the grafting procedure. Each of the techniques applied by these workers are slightly different, yet all are based on the methods described by Feng et al. [19] and Li et al. [20]. The original concept reported by Feng et al. [19] involved boiling the silica support in water for 4 h and subsequent drying to a constant weight over several days. In a separate method, they replaced the drying step by removing the excess water by azeotropic distillation with benzene [19]. In both cases, the hydrated material was used as the support and applied to the conventional approach for grafting, i.e., in refluxing toluene (110 °C). However, Li et al. [20] found that the procedures were too time-consuming and, therefore, developed a different approach to achieving the desired level of support hydration. The new approach to achieve the few monolayers of preadsorbed water on the silica support consisted of determining the quantity of water required based on the available surface area of the silica support (m^2/g) to form 2-2.5 monolayers of surface hydration and adding this quantity of water to the suspension of silica in toluene at room temperature, which is herein termed the coaddition technique. This mixture was allowed to equilibrate for a few hours, and then the silane to be grafted was added and allowed to react with the silica at room temperature for several hours; ultimately, the temperature was increased to achieve reflux (ca. 110 °C) for 4 h. At the end of the time frame allotted to the grafting process, the reflux condenser was replaced with a Dean-Stark still head and distillation continued until the effluent temperature reached that of boiling toluene. The authors claimed that this additional step aids in the formation of a ideal monolayer by helping

to overcome defects in the surface. In all cases, the head space of the grafting chamber was purged with an inert gas.

The approach used by Hiyoshi et al. [25] was adapted from the technique of preboiling the silica support in water, as described by Feng et al. [19]. They used SBA-15 as the support and grafted mono-, di-, and triamine based silanes in separate experiments with refluxing toluene as the solvent. The result of preboiling the SBA-15 in water was not quantified in terms of the amount of water retained on the surface. The grafting work performed by Kim et al. [27] employed the coaddition technique described by Li et al. [20] to graft aminopropyltriethoxysilane onto hydrated MCM-48 in toluene under reflux. However, this group added a molar amount of water equal to the number of moles of alkoxy groups, i.e., 3 mol of water per mol of silane. The authors did not report the amount of MCM-48 used during the grafting procedure. Likewise, Zheng et al. [26] added 0.32 $cm^3(H_2O)/g(silica)$ to a suspension of SBA-15 in toluene, allowing for an assumed equilibrium to be reached (1 h). To this mixture, a diamine based silane was added in excess and reacted at 110 °C for several hours.

The main goal in the current study was to develop an adsorbent having a number of desirable properties. This adsorbent should exhibit an adsorption capacity higher than that of the most commonly employed zeolite-based material, 13X. It should also be suitable for low CO_2 partial pressure applications. Most importantly, the material should exhibit very rapid adsorption and desorption rates in order to be efficiently and effectively applied in a cyclic adsorption process, i.e., pressure- or temperature-swing adsorption or a combination thereof. In addition, the adsorbent's CO_2 capacity should not be hindered by the presence of moisture

in the feed stream. While the literature shows that these properties have been sought in CO_2 adsorbents, they have not been met simultaneously with a reusable adsorbent.

7.4 – Materials and Methods

7.4.1 – Mesoporous Silicas Synthesis and Triamine Silane Grafting

The pore-expanded MCM-41 material, referred to as PE- MCM-41, was prepared in a 1.0 kg scale, by postsynthesis treatment of the as-synthesized MCM-41 silica [13]. The initial MCM-41 silica was prepared according to Sayari and Yang [28]

All materials were calcined in flowing N_2 under a thermal ramp of 1 °C/min to 550 °C and then held at 550 °C in flowing air for 5 h. The materials were then transferred hot, to a container, and sealed until their use. These support materials were characterized by N_2 adsorption at 77 K using an Omnisorp-100 instrument. The surface area was determined in the range of P/P_o of 0.05-0.15 according to the Brunauer-Emmett-Teller (BET) method, and the pore diameter was determined by the Kruk-Jaroniec-Sayari (KJS) method from the adsorption branch of the isotherm [29]. The pore volume was calculated as the amount of liquid nitrogen adsorbed at P/P_o of 0.99.

The reagents used for the synthesis of all the grafted materials were purchased from Sigma-Aldrich and used as supplied with no further treatment. These compounds were toluene (99% ACS grade), pentane (99% ACS Grade), and 3-[2-(2-aminoethylamino) ethylamino] propyl trimethoxysilane (Tech), herein referred to as TRI.

In order to introduce the amine functionality to the PE-MCM-41, the conventional grafting technique was adapted to include water during the procedure. Specifically, a batch of the support material was first dehydrated at 150 °C for 2 h in static air. This drying procedure was necessary so that the quantity of water on the surface of the support was solely due to the controlled addition during grafting and not from water physically adsorbed during preparation or storage. From this dried batch, 1.0 g was dispersed in 150 cm^3 of toluene in a 250 cm^3 multineck flask by mixing for 30 min at room temperature. Next, a specific quantity of water (0.1 to 1.0 cm^3/g(silica)) was rapidly added to the mixture and allowed to equilibrate at room temperature for 2-3 h. After this time frame, the temperature was increased rapidly to the desired grafting temperature (in the range of 70-110 °C), a quantity of TRI (3.0 $cm^3/g(SiO_2)$) was added, and the system was held for 16 h with vapor reflux. The amount of 3.0 cm^3 of TRI per gram of silica was determined in a separate series of experiments as the optimum amount for grafting under dry conditions, [14] and it has been used throughout this work. These grafted materials were then filtered in a Buchner funnel and washed with copious amounts of toluene followed by pentane. The materials were dried at 120 °C in a natural convection oven for 4 h and subsequently stored in capped vials until use.

In order to determine the amount of amine that was grafted, a thermal decomposition method using a thermogravimetric analyzer (Q500 TGA, TA Instruments) coupled with a mass spectrometer (Thermostar, Pfeiffer Vacuum) was developed and applied. From our earlier observations, [14] we showed that, during grafting, not all alkoxy groups are hydrolyzed, leading to surface Si-O-Si bridges, and therefore, determination of the amount of grafted amine based on weight loss is not straightforward. From a set of exploratory experiments with the TGA-MS, it was determined that the unreacted methoxy ligands were removed below 200

°C. Above this temperature, the decomposition of the amine chain starts to take place. Thus, the amount of grafted amine should correspond to the total weight loss beyond 200 °C. To correctly determine this amount, the TGA experiment was carried out as follows: the sample was heated under flowing helium up to 200 °C, kept for 1 h, and then heated to 900 °C before switching to air and heating to 1000 °C to remove any residual coke from the support material. To validate this approach, a few samples were also examined by elemental analysis using a Carlo Erba EA1100 CHNS instrument. The TGA-MS results were found to be no more than 2-5% lower (on a dry basis) relative to the amount determined by elemental analysis.

7.4.2 – CO_2 Adsorption Properties

To determine the adsorption capacity, the previously described thermal gravimetric unit coupled with the mass spectrometer (TGA-MS) was employed using the experimental setup shown schematically in Figure 7.1. Typical sample weights of ca. 50 mg (~30 μm diameter particles) were loaded into a 100 μL platinum sample pan and used for both the adsorption and decomposition studies. Using this balance, the grafted materials response to a step change in CO_2 concentration (from 0 to 5% in N_2) was measured, as a weight change relative to the condition of each material after initial activation (regeneration) with a N_2 purge. The initial activation condition imposed on the materials was determined, in a separate experiment, by examining the thermal stability of the material in a N_2 atmosphere ramped at 10 °C/min to 1000 °C with the previously mentioned TGA-MS instrument.

The pure gases used in this study were purchased from Praxair Canada and were specified as UHP (ultrahigh purity) grade. The 5% CO_2/N_2 mixture was also purchased from Praxair Canada as a certified UHP grade mixture. The feed flowrates used with the TGA-MS were controlled at 150 sccm into the sample chamber and mixed with 10 sccm of purge gas

through the balance assembly (see Figure 7.1), for both the adsorption and regeneration steps of the study.

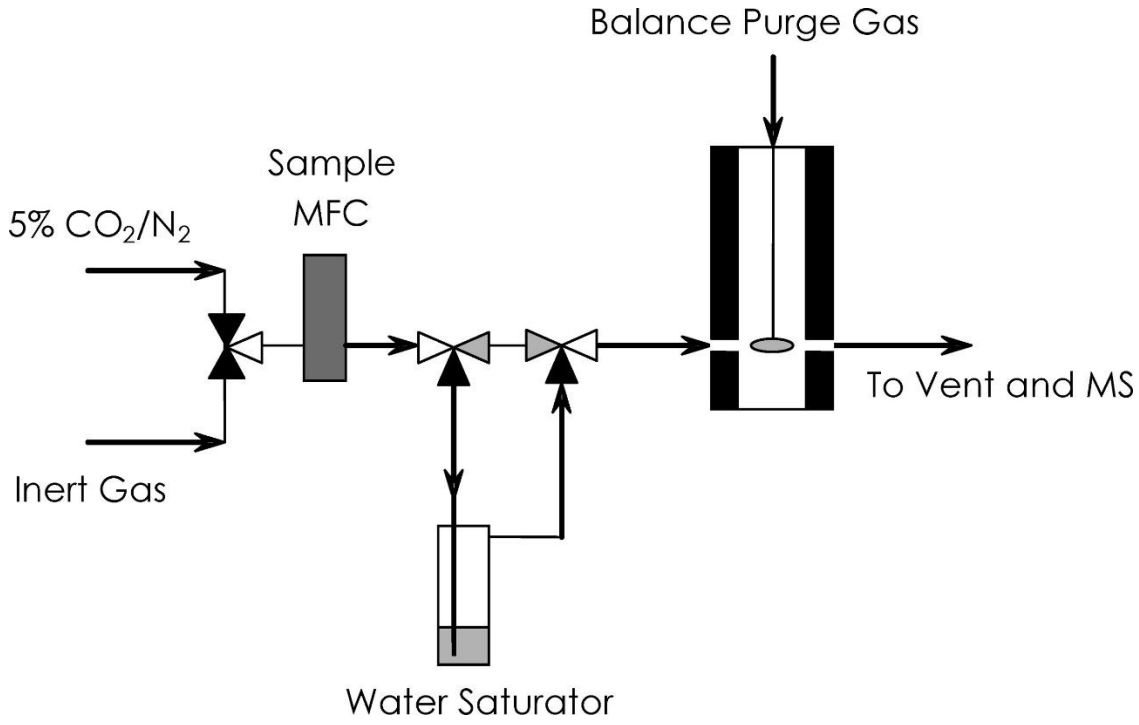

Figure 7.1 Schematic diagram of the modified TGA instrument used for CO_2 adsorption measurements.

In order to examine the effects of moisture on the adsorption capacity of CO_2 with the grafted materials, the following procedure was employed, where the term humid gas refers to the gas saturated with water at 5 °C, i.e., 27% relative humidity (RH) @ 25 °C:

(i) Initial thermal regeneration under dry N_2 purge (200 °C, 45 min);

(ii) Isothermal humid N_2 adsorption to equilibrium (25 °C, H_2O/N_2)

(iii) Isothermal humid 5% CO_2/ N_2 adsorption to equilibrium (25 °C)

(iv) Thermal regeneration in humid N_2 to 100 °C for 30 min.

The procedure for dry CO_2 adsorption was similar; with the removal of humidity from all the streams and the omission of step (ii), as the grafted materials did not exhibit any adsorption affinity for N_2 under these conditions. The regeneration temperature of 100 °C was determined from a TGA profile of a fresh material, which was saturated from a 5% CO_2/N_2 gas mixture feed and then thermally ramped (5 °C/min) up to 200 °C in N_2, in order to determine the temperature profile for CO_2 desorption. For comparison, similar experiments were carried out using the most common CO_2 commercial adsorbent, zeolite 13X (UOP, ~2 μm diameter powder). Moreover, extensive comparison was made with CO_2 adsorption data over amine grafted silicas reported in the literature.

7.5 – Results and Discussion

The first aspect examined in this study was to compare anhydrous grafting and the use of water during the grafting procedure on the resulting amine loading. Conceptually, the dry grafting procedure can be considered as a reaction between the surface hydroxyl groups and the alkoxy ligands of the silane compound, leading to the formation of a surface layer of tethered amine functionalities. Accordingly, it is assumed that all of the alkoxy ligands would ideally react with the surface hydroxyl groups to liberate the corresponding alcohol, leading to the formation of $(SiO)_3Si$-R species; see Chart 7.1. This reaction should occur with a ratio of three surface OH groups per silane compound grafted. However, this is often not achieved. One or two alkoxy groups per silane may not react; see Chart 7.2. In order to consume the free alkoxy ligands and complete the surface coverage, water may be added to the support material to produce a hydrated surface. This surface water would increase the surface density of hydroxyl groups or initiate the hydrolysis of the unreacted alkoxy groups with the free silane still present in the solvent phase and, thus, enhance the surface coverage of amine bearing

species. Unlike the perfect monolayer concept put forward by Feng et al. [19] (see Chart 7.3), we believe that the process of grafting under these conditions is more complex. In this regard, the grafting should be considered as a coating, since it is likely that some of the aminosilanes are not attached to the surface directly, but rather only through Si-O-Si bridges to other grafted aminosilanes; see Chart 7.4. Since the objective of the present study was to obtain a material with a high CO_2 adsorption capacity, the constraint of the surface amine functionalization to be limited to a uniform monolayer, as shown in Chart 7.3, was not required. Rather, a high density of accessible amine sites without significant pore blockage was essential.

A few other research groups have studied amine grafted silica for use as an adsorbent for CO_2 [14, 23-27, 30-32]. Summaries of the support materials characteristics, the grafting conditions, and the resulting amine contents are shown in Tables 7.1 and 7.2 for the materials grafted under dry conditions and the water-aided grafted materials, respectively.

Typically, only the most studied material disclosed in the corresponding reference was included in Table 7.1. However, where multiple materials are reported in the same reference, a second entry from the same reference was included if a higher performing material was described but was not the main focus of the study. The entries in bold represent the highest loading of aminosilane grafted for each type, i.e., mono-, di-, and triaminesilane. It is obvious from this compilation that the most widely studied type of amine functionalization is the grafting of monoamine silane, as six different research groups have studied this type of functionalized material for CO_2 adsorption.

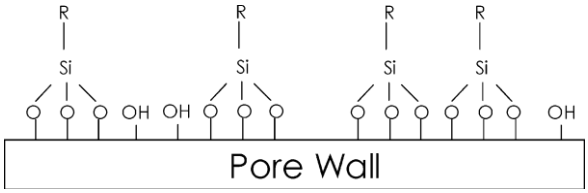

Chart 7.1 Idealized pore surface obtained for anhydrous alkoxy-silane grafting, under the often assumed formation of $(SiO)_3SiR$ surface species, where the support chemistry $(SiO)_x$ has been schematically represented as pore wall for simplicity.

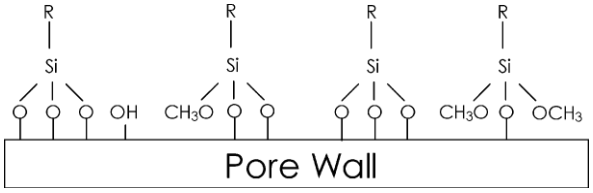

Chart 7.2 Proposed surface structure obtained with anhydrous grafting, where the support chemistry $(SiO)_x$ has been schematically represented as pore wall for simplicity.

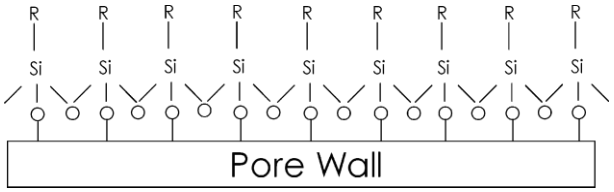

Chart 7.3 Idealized fully cross-linked pore surface obtained for alkoxy-silane grafting in the presence of water as proposed by Feng et al., [19] where the support chemistry $(SiO)_x$ has been schematically represented as pore wall for simplicity.

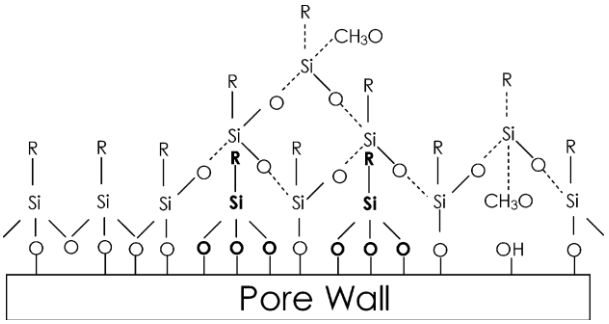

Chart 7.4 Proposed early stage growth of a 3-D polyaminosiloxane layer that occurs during the grafting of alkoxy-silane compounds in the presence of water. The R group represents the triamine chain, and the dashed lines represent orientation out of plane of the bold groups; approximating depth, where the support chemistry $(SiO)_x$ has been schematically represented as pore wall for simplicity.

As shown in Figure 7.2, by comparing the support material surface area and the amount of amine grafted under anhydrous conditions, it appears that the surface area affects the resulting amount of silane that can be grafted. However, as a few data points are significantly outside of the general correlation, it is possible that the amount of amine grafted may be affected by another material property or by the imposed conditions during grafting. For example, the results which are slightly below the general correlation may be due to the lack of available surface active OH groups for covalent bonding with the aminosilane. Overall, the results demonstrate the effect of temperature and silane concentration during grafting on the amount of amine that can be functionalized. For example, Hiyoshi et al. [25] obtained the highest loading of monoamine grafted but also used the highest starting ratio of aminosilane to the weight of support (8.5 cm^3/g).

The question to be explored further within these results is whether the surface area is the dominant property that affects the degree of functionalization or whether it may be more strongly affected by the grafting conditions and thermal history of the support material. In our previous study [14], we showed that the quantity of triaminesilane added to the grafting mixture affects the resulting amount grafted but appears to reach a plateau at high silane-to-silica ratios (>8 cm^3/g). Therefore, it should be reasonable to assume that this saturation effect will be similar for other types of aminosilanes, i.e., mono- and diamine. From the data shown in Table 7.1 for the monoamine- silane grafting, all the other research groups used aminosilane additions that were below the quantity used by Hiyoshi and et al. [25]. Therefore, if the other research groups had also used this high level of aminosilane addition, the amount of amine grafted for each of these groups may slightly increase. However, the increase in the amine content may not result in the most benefit for the intended application, because of steric

hindrance and/or overloading phenomena, which cause inefficiencies in the amine-CO_2 chemistry [14].

Table 7.1 Summary of Amine-Grafted Silica-Based Adsorbents Prepared Under Anhydrous Conditions and Applied for CO_2 Adsorption [a].

		initial support properties			grafting condition			amount grafted			
									amine content[e]		
support material	amine type[b]	BET SA[c] (m^2/g)	pore diameter (nm)	pore volume[c] (cm^3/g)	silanex added[c] (cm^3/g)	concentration[c] (vol %(silane)/g)	temp (°C)	organic[d] (mmol/g)	(mmol(N)/g)	(μmol(N)/m^2)	reference
silica gel	mono-ethoxy	340	12.0	1.4	0.45	0.00	138	1.20	1.20	3.53	30
xerogel	mono-ethoxy	816			5.0	10.0	70	1.70	1.70	2.08	23
HMS	mono-methoxy	762	3.0	1.02	4.0	4.0	25	1.93	1.93	2.53	24
HMS	mono-methoxy	1198	2.1	0.97	4.0	4.0	25	2.29	2.29	1.91	24
MCM-48	mono-ethoxy	1389			5.0	10.0	70	2.30	2.30	1.66	23
MCM-48	mono-ethoxy	1290	2.6	1.15		0.0	110	2.45	2.45	1.90	27
SBA-15	**mono-ethoxy**	**910**	**5.9**	**1.11**	**8.5**	**3.4**	**110**	**2.57**	**2.57**	**2.82**	**25**
MCM-48[f]	tert	1290	2.6	1.15		0.0	110	1.48	1.48	1.15	27
HMS	di	762	3.0	1.02	3.9	3.9	25	1.54	3.07	4.03	31
HMS	di	1268	2.4	0.98	3.0	3.0	25	1.82	3.64	2.87	31
SBA-15	**di**	**910**	**5.9**	**1.11**	**8.5**	**3.4**	**110**	**1.88**	**3.76**	**4.13**	**25**
MCM-48[f]	PEI	1290	2.6	1.15		0.0	110		5.20	4.03	27
SBA-15	tri	910	5.9	1.11	8.5	3.4	110	1.62	4.85	5.33	25
HMS	tri	762	3.0	1.02	4.9	4.9	25	1.29	3.86	5.06	32
HMS	tri	1268	2.4	0.98	3.0	3.0	25	1.52	4.57	3.61	32
MCM-41	tri	1140	3.7	1.03	3.0	2.0	70	1.92	5.75	5.04	present study
MCM-41	tri	1140	3.7	1.03	3.0	2.0	85	1.98	5.95	5.22	present study
MCM-41	tri	1140	3.7	1.03	3.0	2.0	95	1.94	5.83	5.11	present study
MCM-41	tri	1140	3.7	1.03	3.0	2.0	110	1.90	5.69	4.99	14
PE-MCM-41	tri	950	10.0	2.21	3.0	2.0	70	2.02	6.07	6.39	present study
PE-MCM-41	**tri**	**950**	**10.0**	**2.21**	**3.0**	**2.0**	**85**	**2.04**	**6.11**	**6.43**	**present study**
PE-MCM-41	tri	950	10.0	2.21	3.0	2.0	95	2.01	6.03	6.35	present study
PE-MCM-41	tri	950	10.0	2.21	3.0	2.0	110	1.99	5.98	6.29	14

[a] Materials shown in the table reflect the most studied material if a group of materials was presented by the authors. In some cases, a second entry is shown for the highest perfoming material. [b] Mono = either aminopropyltriethoxysilane or aminopropyltrimethoxysilane; di = aminoethlyaminopropyltrimethoxysilane; tri = aminoethylaminoethlyaminopropyltrimethoxysilane; tert = tertiary functionality, see *f*; PEI = polyethyleneimine. [c] Units are per gram of SiO_2 (support). [d] Units are mmol of organic chain per gram of final material (organic + SiO_2), in the absence of alkoxy groups. [e] Units are mmol of amine (nitrogen) per gram of final material (aminosilane + SiO_2) or per m^2 of the initial support surface area. [f] Chloropropyltrimethoxysilane was grafted first (110 °C), then pyrrolidine or PEI was reacted with the CI group to produce the desired tethered amine functionality.

Table 7.2 Summary of Water-Aided Amine-Grafted Silica Adsorbents Applied to CO_2 Adsorption [a].

		initial support properties			grafting conditions				amine content[d]		
support material	amine type[b]	BET SA[c] (m^2/g)	pore diameter (nm)	pore volume[c] (cm^3/g)	silane added[c] (cm^3/g)	water[c] (cm^3/g)	H_2O/alkoxy (mol/mol)	temp (°C)	(mmol(N)/g)	(μmol(N)/m^2)	reference
MCM-48	mono-ethoxy	1290	2.6	1.15			1.00	110	3.99	3.09	27
SBA-15	mono-ethoxy	820	5.9	1.07	8.5	preboiled		110	2.61	3.18	25
SBA-15	di	700	6.7		1.0	0.32	1.28	110	2.64	3.77	26
SBA-15	di	820	5.9	1.07	8.5	preboiled		110	4.61	5.62	25
SBA-15	tri	820	5.9	1.07	8.5	preboiled		110	5.80	7.07	25
PE-MCM-41	tri	950	10.0	2.21	3.0	0.30	0.48	70	7.75	8.16	present study
PE-MCM-41	**tri**	**950**	**10.0**	**2.21**	**3.0**	**0.30**	**0.48**	**85**	**7.98**	**8.40**	**present study**
PE-MCM-41	tri	950	10.0	2.21	3.0	0.20	0.32	95	6.75	7.11	present study
PE-MCM-41	tri	950	10.0	2.21	3.0	0.20	0.32	110	6.65	7.00	present study

[a] Materials shown in the table reflect the most studied material if a group of materials was presented by the authors. In some cases, a second entry is shown for the highest perfoming material. [b] Mono = either aminopropyltriethoxysilane or aminopropyltrimethoxysilane; di = aminoethlyaminopropyltrimethoxysilane; tri = aminoethylaminoethlyaminopropyltrimethoxysilane. [c] Units are per gram of SiO_2 (support). [d] Units are mmol of amine (nitrogen) per gram of final material (aminosilane + SiO_2) or per m^2 of the initial support surface area.

On the basis of the initial surface area of each support used for monoamine grafting given in Table 7.1, the amount of amine grafted can be generally correlated to exhibit diminishing surface area utilization as the support surface area increases; see Figure 7.2. For example, if the amount of amine grafted is considered on a per gram basis, the total content increases with increasing surface area. However, when these same quantities are transformed to a per m^2 basis, increases in surface area do not translate into proportional increases in loading. Therefore, it appears that the amount of monoamine grafted under anhydrous conditions will be limited to values <3.0 mmol/g and that the available surface area is not being completely, and thus effectively, exploited. However, adding to the complexity of the data shown in Table 7.1, several groups have applied different grafting temperatures, and although not always clearly stated in the publications, various silane-toluene concentrations per weight of support material have been added. These last two points have not been fully studied in the literature and may have implications on the resulting amine loadings.

The data shown in Table 7.1 also demonstrate that the logical route to increase the amine content with the presently available silica based mesoporous materials is to use silanes with multiple amine groups per organic chain, diamine and triamine based silanes. To this extent, only a few research groups have examined the use of these types of aminosilanes. These groups have shown that the total amine content can be increased; however, the actual silane loading has decreased relative to that obtained through the use of monoamine silane. However, based on our earlier work, [14] the PE-MCM-41 support material appears to be an excellent candidate for exploring the limits of amine grafting for application as a highly effective CO_2 adsorbent and has, therefore, been used in this study.

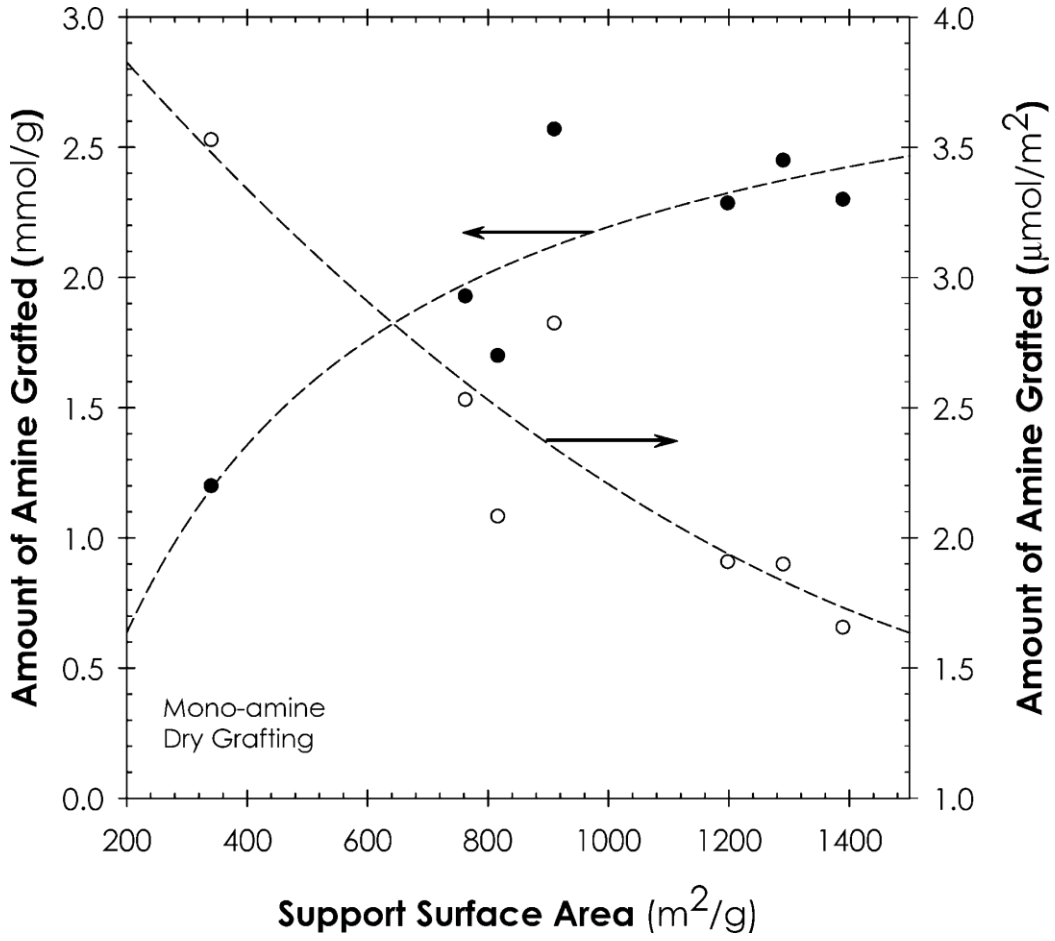

Figure 7.2 Effect of the support surface area on the amount of monoamine silane grafted under dry conditions (references given in Table 7.1).

7.5.1 – Support Characteristics

The BET surface area, KJS pore diameter, and pore volumes of the PE-MCM-41 and MCM-41 silicas are given in Table 7.1, under the reference present study. The adsorption-desorption isotherms, and the pore size distributions, are shown in parts A and B of Figure 7.3, respectively. As seen in Figure 7.3A, PE-MCM-41 exhibits a much higher N_2 adsorption uptake than the MCM-41 close to $P/P_o = 1$, thus demonstrating the increased pore volume. Also, the point of inflection of the adsorption isotherm has shifted from ca. P/P_o = 0.30 for MCM-41 to 0.65 for PE-MCM-41, which is directly related to the increased pore

diameter of the PE-MCM-41 over the MCM-41 support. Therefore, it is expected that the PE- MCM-41 should be capable of accommodating bulky compounds and exhibiting less mass-transfer resistance and, thus, higher diffusional constants. In terms of grafting aminosilanes, this property should result in an increased loading of triamine-silane from a dynamic and static point of view.

7.5.2 – Thermal Stability of Grafted AminoSilane

In order to study the thermal behavior of the grafted triaminesilane, TGA- MS decomposition experiments were performed. When the TGA experiment was run in air, the amine bearing chain was stable up to the initial point decomposition temperature of 200 °C. To further examine the nature of the evolving species, TGA experiments were performed with UHP He as the sample gas (see Figure 7.1). These results showed that all the grafted amines were stable up to 200 °C (Figure 7.4). As shown in Figure 7.4, both the dry and wet grafted triamine materials exhibited only minor losses up to 300 °C, at 10 °C/min in He. The corresponding MS responses (not shown) for both materials showed the release of the unreacted methoxy species in the temperature range of 150-200 °C. For the dry grafted TRI-PE-MCM-41, the methoxy release accounted for 5-6 wt % of the total initial material mass, whereas for the wet grafted TRI-MCM-41, the weight loss was significantly lower, ca. 2-3 wt %. The correlation between the amount of methoxy released upon thermal curing and the grafting technique can be viewed as a consequence of the degree of hydrolysis of the silane methoxy ligands during the grafting procedure. The dry grafting process is based on the reaction of the methoxy chains with the pore wall hydroxyl groups, whereas the wet technique also involves water, which may facilitate silane polymerization and, thus, produce a degree of silane condensation in the grafting solution prior to surface functionalization. Therefore, it is

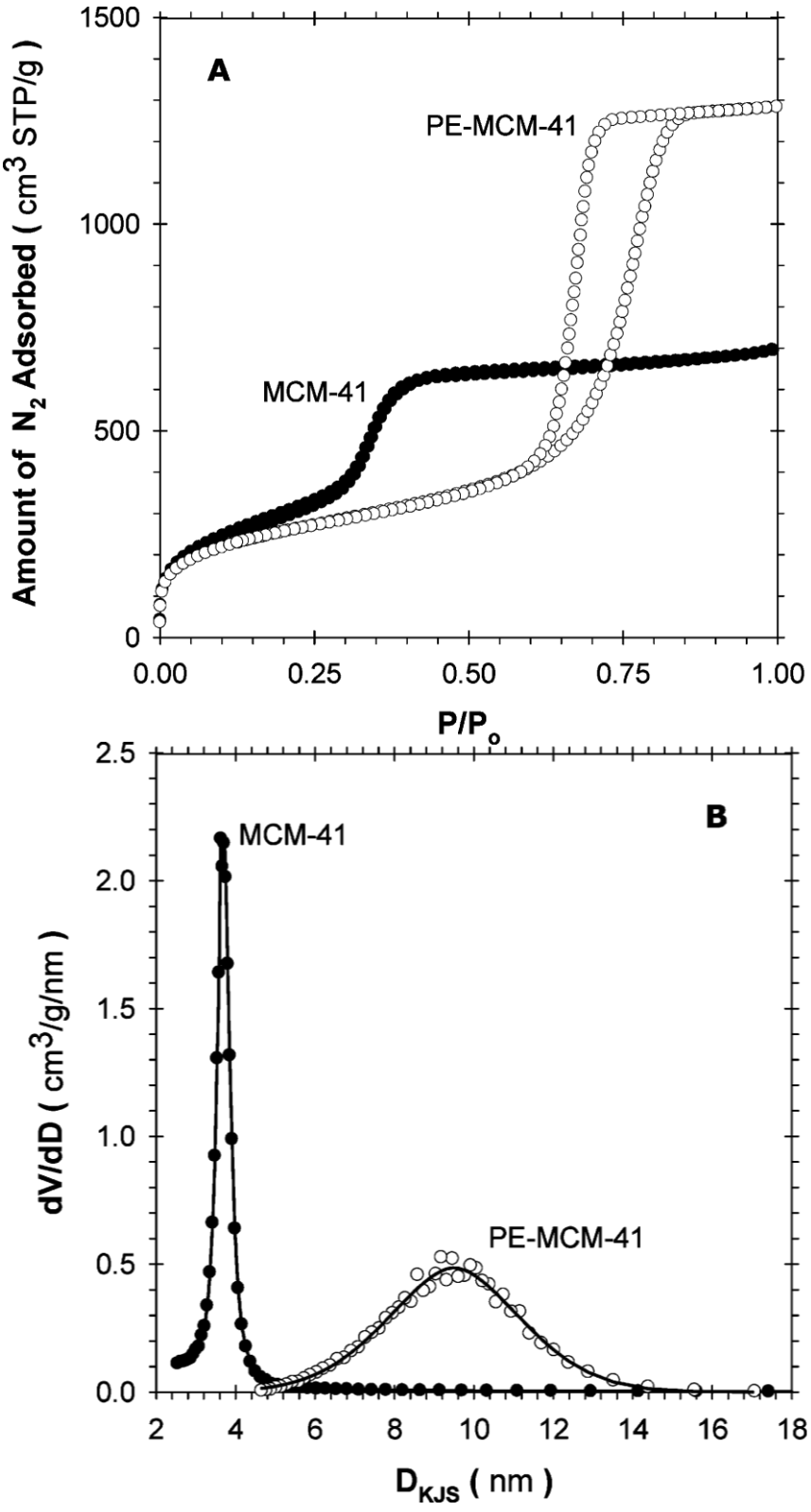

Figure 7.3 Nitrogen adsorption and desorption isotherms and KJS pore size distribution for MCM-41 and PE-MCM-41.

expected that the wet technique will afford a much higher quantity of grafted silane, either directly on the surface or as part of an island-type silane polymerization in the solution phase with subsequent surface attachment. In addition, the relative amount of alkoxy groups will be lower, as demonstrated by the TGA-MS data shown in Figure 7.4.

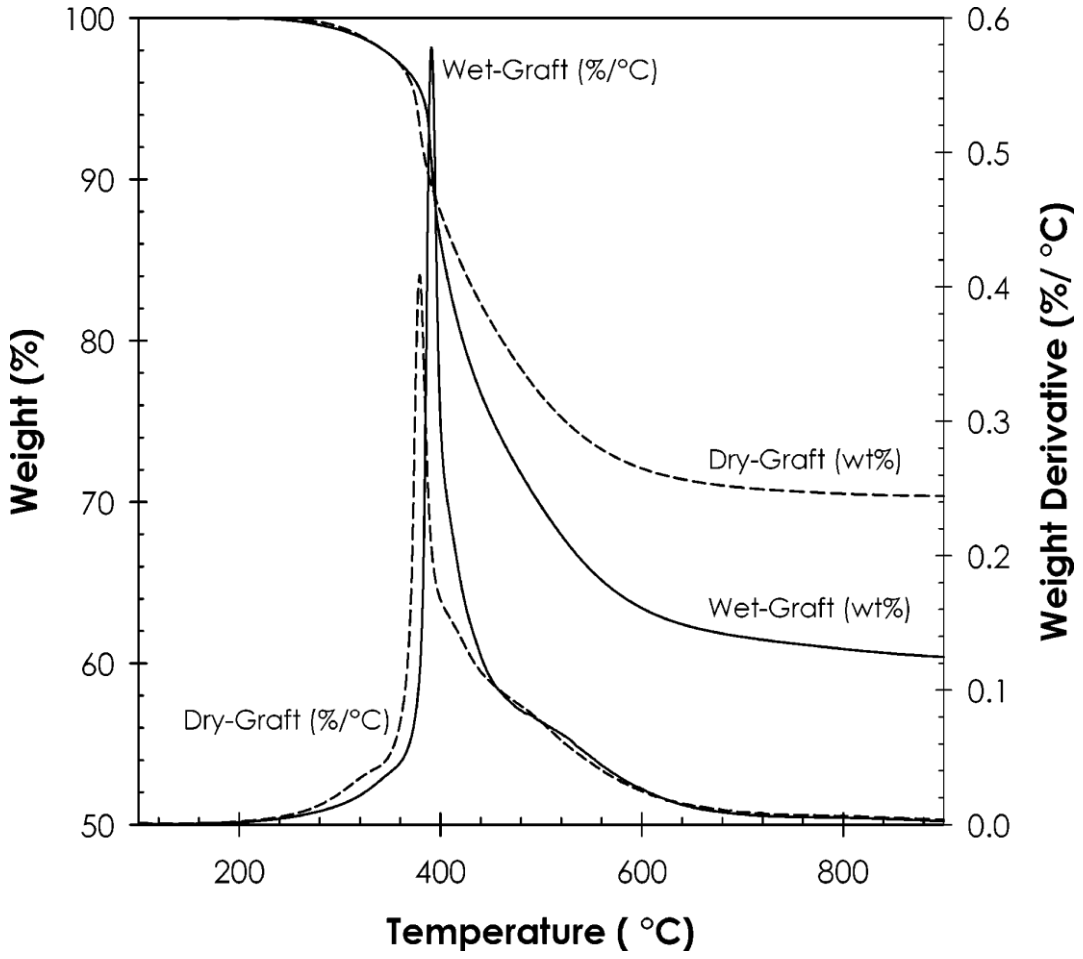

Figure 7.4 Decomposition profiles at 10 °C/min in He for TRI-PE-MCM-41 grafted under dry conditions and TRI-PE-MCM-41 grafted in the presence of 0.30 $cm^3(H_2O)/g(SiO_2)$; both materials with 3.0 $cm^3/g(SiO_2)$ silane at 85 °C. Both materials previously treated in He for 2 h at 200 °C.

7.5.3 – Effect of Grafting Conditions

As shown in our previous work, [14] the relative amount of aminosilane added to the grafting mixture exhibited a significant impact on the quantity of amine groups accessible to CO_2. In comparison to the typical MCM-41 material, the PE-MCM-41 was capable of accommodating a slightly higher amount of grafted TRI. However, the results showed that a controlled 3.0 $cm^3/g(SiO_2)$ silane was appropriate, as further increases in silane quantity did not afford any significant increase in the amount grafted or the CO_2 adsorption performance. Further comparison of the TRI grafting efficiency between MCM-41 and PE-MCM-41 can be made based on the amount of TRI grafted as a function of the amount of TRI added, as shown in Figure 7.5. The data in this figure demonstrates that the PE-MCM-41 material is superior to MCM-41 in terms of TRI uptake. Therefore, in this study, the TRI addition was also constrained to 3.0 $cm^3/g(SiO_2)$.

The first issue of grafting in the presence of water was to examine the effect of the relative quantity of water added on the amount of amine that could be grafted, at a given reaction temperature. For this two-parameter analysis (water and temperature), the quantity of aminosilane added to the grafting solution was kept constant and in excess (3.0 $cm^3/g(SiO_2)$), and the results are shown in Figure 7.6.

From these data, it is evident that the amount of added water has a profound impact on the quantity of TRI that can be grafted, for all grafting temperatures examined. The amount of grafted amine increased significantly as the amount of water added increased to 0.30 $cm^3/g(SiO_2)$, then leveled off as the amount of water increased further. However, if the amount of added H_2O is constrained to 0.30 $cm^3/g(SiO_2)$, as shown in Figure 7.7, it is clear

that the highest amount of amine grafted was obtained at a temperature of 85 °C. The obtained amine loading was significantly higher than the amounts grafted under anhydrous conditions with both MCM-41 and PE-MCM-41. In all cases of water addition from 0 to 1.0 $cm^3/g(SiO_2)$, the apparent optimal grafting temperature appeared to be ca. 85 °C. This finding could be due to the functionalization dependence on the rate of alkoxy consumption, both at the solid-liquid interface where the silane is able to react with the surface and in the bulk solution, where the silane may polymerize (through methoxy hydrolysis/condensation) because of the presence of free water.

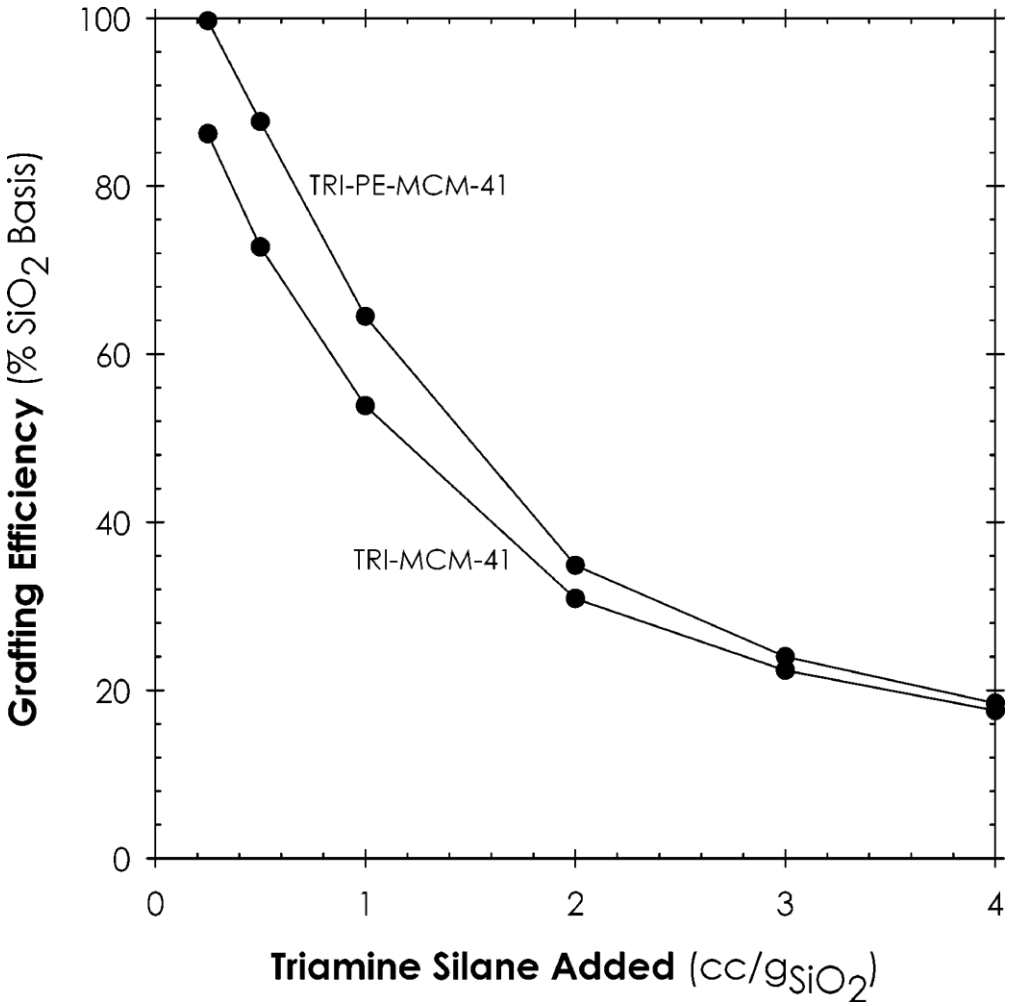

Figure 7.5 Grafting efficiency as a function of the amount of triamine silane added to the grafting mixture on the amount of grafted amine.

It is also interesting to note that the amount of amine grafted under the more typical reaction temperature of 110 °C (reflux condition) is considerably lower than the amount grafted at the other temperatures studied. The effect of temperature on the amount of amine loaded under dry conditions was small; however, as water was added, the difference increased dramatically. For example, when 0.30 cm^3/ g(SiO_2) water was added, the ratio of the amount grafted at 85-110 °C was ca. 1.15. Therefore, we can obtain a 15% increase in amine loading by applying a lower temperature and ca. 31% increase (over dry grafting at 85 °C) by employing a controlled amount of water.

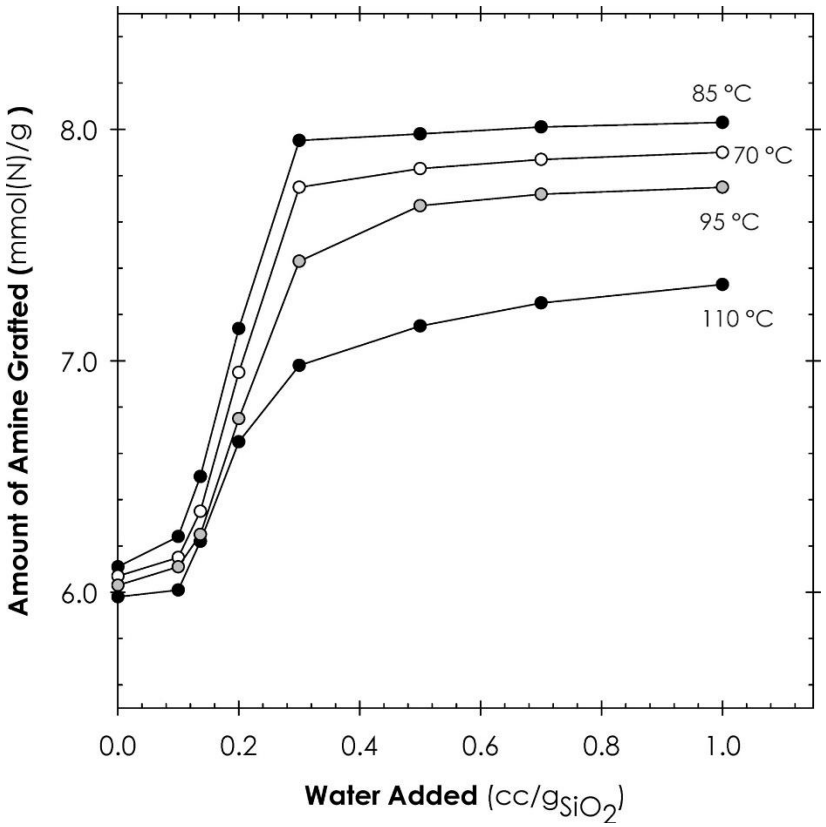

Figure 7.6 Effect of the amount of water added to the grafting mixture on the amount of amine grafted as a function of the reaction temperature for a controlled 3.0 cm^3/g(SiO_2) silane addition.

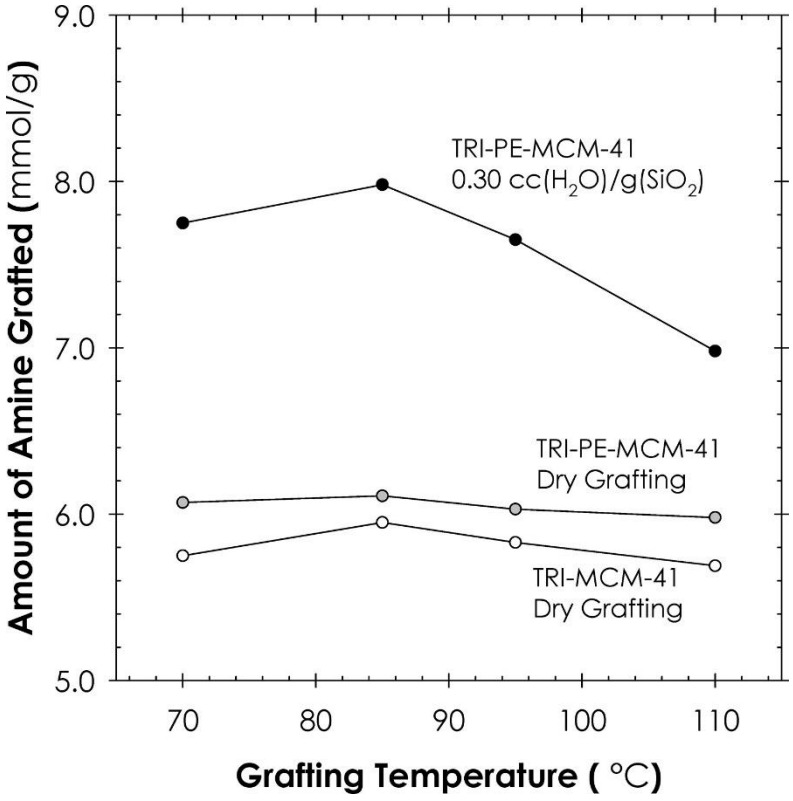

Figure 7.7 Effect of grafting temperature on the amount of amine grafted for a 3.0 $cm^3/g(SiO_2)$ silane and 0.30 $cm^3/g(SiO_2)$ water addition.

7.5.4 – CO_2 Adsorption Studies

To verify that the grafted amine was accessible and active for CO_2 adsorption, tests were performed using a 5 vol % CO_2 in N_2 gas mixture at 101 kPa total pressure and 25 °C. The results are shown in Figure 7.8 in terms of adsorption capacity vs amount of water added per gram of silica at an assumed equilibrium at 60 min run time. Prior to each CO_2 adsorption test, each material was regenerated at 200 °C for 45 min under a flow of UHP N_2 (see Materials and Method section). The data showed that, as the amount of water added increased above 0.30 $cm^3/g(SiO_2)$, the CO_2 adsorption performance decreased, even though the amount of grafted amine was increasing (Figure 7.6). To examine these trends further, the

apparent maximum adsorption rates obtained during the adsorption runs were plotted as a function of water added and are shown in Figure 7.9. From these data, it is evident that, as the adsorption capacity decreased (Figure 7.8), the adsorption rate also decreased (Figure 7.9). By examining the adsorption data from a dynamic and equilibrium point of view, the conclusion is that, for water additions above 0.30 $cm^3/g(SiO_2)$, pore choking and/or complete blockage may occur because of the polymerization (through methoxy hydrolysis/condensation) of the aminosilane in the bulk solution and subsequent deposition on the external surface of the support. Therefore, there exists an optimal condition under which the PE-MCM-41 should be grafted in order to obtain the most efficient use of the grafted amine in conjunction with the targeted CO_2 adsorption application. By critically examining the data shown in Figures 7.6-7.9, the apparent optimal grafting conditions for TRI with PE-MCM-41 are as follows: 3.0 $cm^3/g(SiO_2)$ silane, 0.30 $cm^3/g(SiO_2)$ water, and 85 °C grafting temperature. Admittedly, there is room for the fine-tuning of these conditions.

Under the optimal grafting conditions, the TRI-PE-MCM-41 amine loading was 7.95 mmol(N)/g (12.9 mmol(N)/g(SiO_2)), whereas in the absence of water (dry grafting), TRI-PE-MCM-41 was loaded with 5.98 mmol(N)/g (6.95 mmol(N)/g(SiO_2)) with a corresponding increase in the 5% CO_2 adsorption capacity by ca. 90% to 2.65 mmol/g (117 mg/g) vs 1.41 mmol/g (62 mg/g). The maximum CO_2 adsorption rate also increased by 80% to 1.79 mmol/g/min (78 mg/g/min) in comparison to the dry grafted TRI-MCM-41 adsorption rate of ca. 0.96 mmol/g/ min (42 mg/g/min).

Another factor to examine when using amines to adsorb CO_2 is the CO_2/N ratio, which represents the molar amount of CO_2 adsorbed per the molar amount of grafted amine groups. Under the assumption of carbamate formation, this ratio should be 0.5 for dry CO_2

adsorption and 1.0 for humid CO_2 adsorption due to the formation of carbonate and bicarbonate. The ratios obtained for this work are shown in Figure 7.10 as a function of the amount of amine grafted and the grafting temperature. The data points represent the various amine loadings obtained by varying the amount of water added to the grafting mixture, from 0 to 1.0 cm3/g(SiO_2).

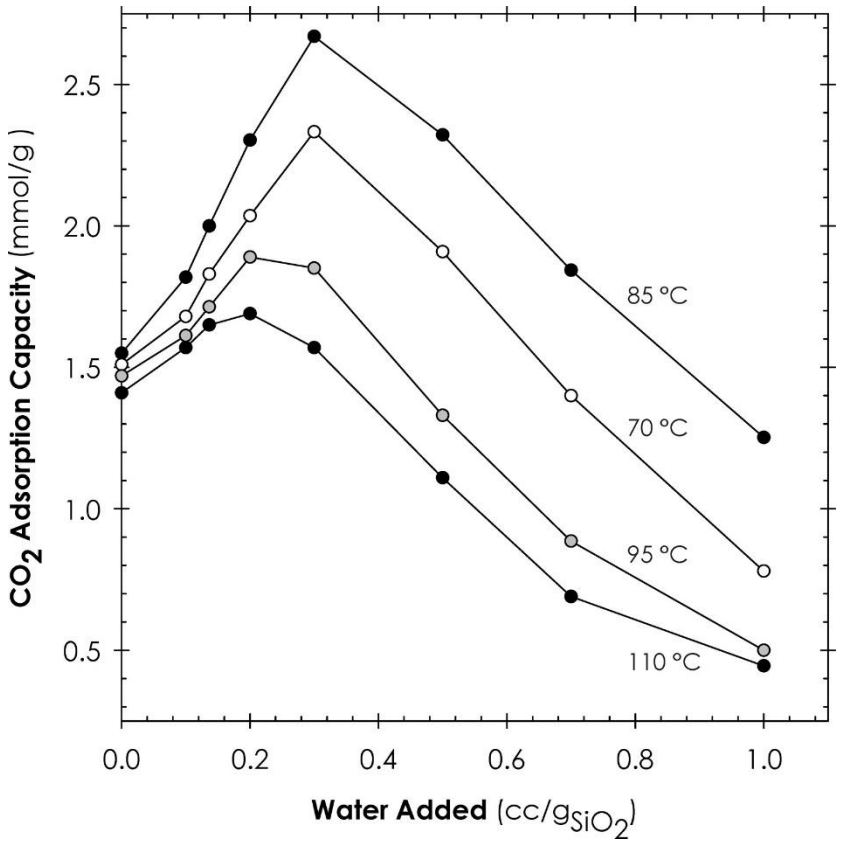

Figure 7.8 Effect of grafting temperature and water content on the 5% CO_2 adsorption capacity for 3.0 $cm^3/g(SiO_2)$ silane addition.

From this data, it is evident that the grafting temperature of 85 °C produced a superior functionalized state than those obtained at the other temperatures applied. However, the CO_2/N ratios are still significantly below the ideal 0.50 value for dry CO_2 adsorption. At each grafting temperature, the addition of water resulted in materials with higher CO_2/N ratios than

the dry grafted materials (the initial point for each curve), up to a certain temperature-dependent level as follows: for 85 °C, <0.50 cm^3/g; for 70 and 95 °C, <0.30 cm^3/g; and for 110 °C, <0.135 cm^3/g.

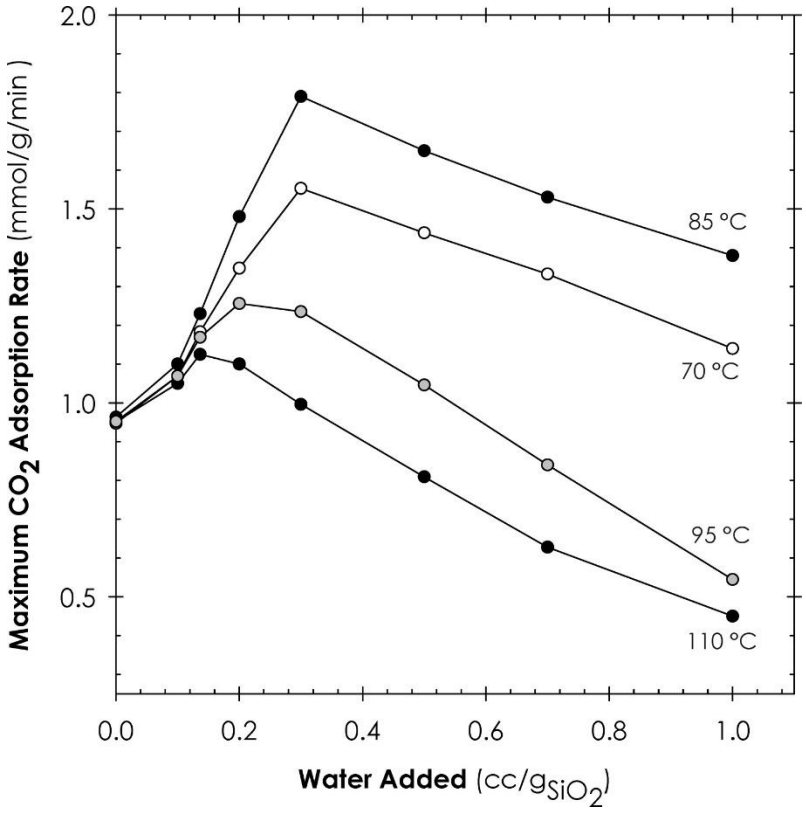

Figure 7.9 Effect of the grafting temperature and water added on the maximum 5% CO_2 adsorption rate for 3.0 $cm^3/g(SiO_2)$ silane addition.

Although the stoichiometric CO_2/N ratio of 0.5 is seldom observed, the lower values obtained in this work may be due to several reasons. First, the reaction is sensitive to the partial pressure of CO_2; in this study, low partial pressure CO_2 (5.1 kPa) was used. Further, the amine-CO_2 interaction may be hindered by the possibility of amine hydrogen bonding between amine groups or with the remaining surface hydroxyl groups, leading to a reduced amount of

amine groups available for CO_2 adsorption. However, the TRI-PE-MCM-41 materials did exhibit higher CO_2/N ratios then the TRI-MCM-41 materials (see Table 7.3), which is most likely due to the increased pore volume and pore diameter, which lead to less possibility of the amine chain conforming in such a way as to interact with the surface via the amine functional group. Conversely, the increase in CO_2/N ratio, over the materials grafted under dry conditions, could be due to the higher density of grafted amine and could thus afford the carbamate based intermediate more readily.

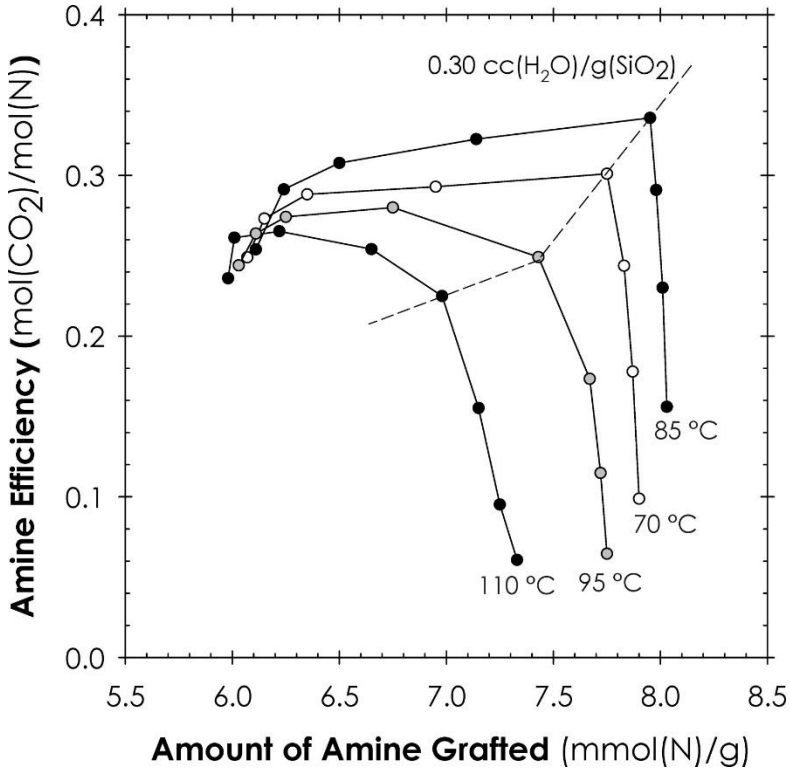

Figure 7.10 Amine adsorption efficiency (CO_2/N, mol/mol) as a function of the grafted amine content and the grafting temperature for a 3.0 cm^3/ $g(SiO_2)$ silane addition and various water quantities. The dashed line shows the tie line for a 0.30 $cm^3(H_2O)/g(SiO_2)$ water addition.

Table 7.3 Summary of amine grafted silica adsorbents CO_2 adsorption performance [a, b].

			CO_2 adsorption performance						humid CO_2		CO_2/N ratio		
	support material	amine type[c]	CO_2 partial pressure[d] (kPa)	balance gas	temp (°C)	dry capacity (mmol/g)	max rate (mmol/g/min)	adsorption parameter (mmol/g/Pa)	R.H. (%)	adsorption capacity (mmol/g)	dry ads (mol/mol)	wet ads (mol/mol)	reference
anhydrous grafting	silica gel	mono	101		295	0.41		4.02	98	0.89	0.338	0.744	30
	xerogel	mono	101		298	1.12		11.0			0.656	0.000	23
	HMS	mono	91	Ar	293	0.86		9.47	30	1.04	0.448	0.537	24
	HMS	mono	91	Ar	293	1.59		17.5			0.696		24
	MCM-48	**mono**	**5**	**He**	**298**	**1.14**		**223**	**64**	**2.30**	**0.494**	**1.000**	**23**
	MCM-48	mono	101		298	0.80		7.92			0.327		27
	SBA-15	mono	15	N_2	333	0.52		34.7	61	0.50	0.202	0.195	25
	MCM-48[e]	tert	101		298	0.30		2.97			0.145		27
	HMS	di	91	Ar	293	0.89		9.74	30	0.45	0.289	0.148	31
	HMS	**di**	**91**	**Ar**	**293**	**1.66**		**18.2**			**0.455**		**31**
	SBA-15	di	15	N_2	333	0.87		58.0	61	0.90	0.231	0.239	25
	MCM-48[e]	PEI	101		298	0.40		3.96			0.077		27
	SBA-15	tri	15	N_2	333	1.10		73.3	61	1.21	0.227	0.249	25
	HMS	tri	91	Ar	293	1.20		13.2	30	0.98	0.312	0.253	32
	HMS	tri	91	Ar	293	1.34		14.7			0.293		32
	MCM-41	tri	5	N_2	298	1.04	0.841	203	27	1.12	0.180	0.195	present study
	MCM-41	tri	5	N_2	298	1.08	0.865	211	27	1.18	0.181	0.198	present study
	MCM-41	tri	5	N_2	298	1.01	0.823	198	27	1.09	0.173	0.186	present study
	MCM-41	tri	5	N_2	298	0.97	0.802	190	27	1.01	0.170	0.185	14
	PE-MCM-41	tri	5	N_2	298	1.51	0.947	296	27	1.60	0.249	0.264	present study
	PE-MCM-41	**tri**	**5**	**N_2**	**298**	**1.55**	**0.963**	**304**	**27**	**1.66**	**0.254**	**0.272**	**present study**
	PE-MCM-41	tri	5	N_2	298	1.47	0.952	288	27	1.58	0.244	0.263	present study
	PE-MCM-41	tri	5	N_2	298	1.41	0.951	276	27	1.52	0.236	0.254	14
water-aided grafting	MCM-48	mono	101		298	0.10		0.990			0.025		27
	SBA-15	mono	15	N_2	333	0.66		44.0	61	0.65	0.253	0.249	25
	SBA-15	di	15	N_2	298	0.57		37.9	64	0.57	0.215	0.215	26
	SBA-15	di	15	N_2	333	1.36		90.7	61	1.51	0.295	0.328	25
	SBA-15	tri	15	N_2	333	1.58		105	61	1.80	0.272	0.310	25
	PE-MCM-41	tri	5	N_2	298	2.33	1.553	457	27	2.58	0.301	0.333	present study
	PE-MCM-41	**tri**	**5**	**N_2**	**298**	**2.65**	**1.790**	**520**	**27**	**2.94**	**0.332**	**0.368**	**present study**
	PE-MCM-41	tri	5	N_2	298	1.89	1.256	371	27	2.08	0.280	0.309	present study
	PE-MCM-41	tri	5	N_2	298	1.69	1.1	331	27	1.85	0.254	0.278	present study
zeolite	13X[f]		5	N_2	298	2.05	0.840	402	27	0.09			13
	13X[f]		101		298	4.70		46.5	27	0.09			13

[a] Materials shown in the table reflect the most studied material if a group of materials was presented by the authors. In some cases, a second entry is shown for the highest performing material. [b] The material order is identical in Tables 2 and 3 for each type of grafting. [c] Mono = either aminopropyltriethoxysilane or aminopropyltrimethoxysilane; di = aminoethlyaminopropyltrimethoxysilane; tri = aminoethylaminoethlyaminopropyltrimethoxysilane; tert = tertiary functionality, see *e*; PEI = polyethyleneimine. [d] Total system polyethyleneimine. [e]Chloropropyltrimethoxysilane was grafted first (110 °C), then pyrrolidine or PEI was reacted with the CI group to produce the desired tethered amine functionality. [f] Regenerated at 200 °C for 1 h in flowing N_2.

Although lower than the stoichiometric ratio, the current CO_2/N ratios are comparable to those obtained in aqueous-phase amine scrubbing. Typically, CO_2/N ratios of 0.15-0.30 are obtained with aqueous-phase systems at the CO_2 inlet conditions used in this work (for example, see ref [33]). As for the amine grafted materials described in the literature, the CO_2/N ratios vary widely, and as shown in Table 7.3, they rarely exceed 0.30. For

monoamine grafted materials, the ratios varied from 0.20 to 0.70 for dry adsorption and from 0.20 to 1.0 for humid adsorption. For the diamine grafted materials, the ratios varied in the range of 0.22-0.46 and 0.15-0.33 under dry and humid conditions, respectively. For the triamine grafted materials, the ratios varied from 0.17 to 0.33 for dry adsorption and from 0.19 to 0.37 for humid adsorption.

7.5.5 – Adsorption of Humid CO_2

By exposing the optimally grafted TRI-PE-MCM-41 material to a N_2 stream saturated at 4-5 °C with water (ca. 27-28% relative humidity at 25 °C) and then switching the gas supply to the 5% CO_2/N_2 gas mixture at the same humidity, the mutual effects of both adsorbates (H_2O + CO_2) were examined. The results showed that the CO_2 adsorption capacity only increased slightly (ca. 10%) in the presence of this level of moisture.

Further analysis revealed that the material was capable of releasing both the moisture and CO_2 completely at 100 °C with a dry N_2 purge within a very short period of thermal exposure, <5 min. When the 13X zeolite was exposed to the same adsorption test conditions, only a portion of the water could be removed, and as a result, the CO_2 equilibrium capacity remained unchanged and extremely low (0.09 mmol/g) because of the higher adsorption affinity of water over CO_2. Therefore, it can be concluded that the CO_2 adsorption capacity of the TRI-PE-MCM-41 is not hindered by the presence of moisture but does not possess the proper amine environment to produce carbonate or bicarbonate in stoichiometric quantities. Further, the competitive nature of the binary H_2O/CO_2 adsorption with preference to water exhibited by the 13X zeolite was not observed with the triamine grafted materials. Therefore,

unlike the single-site adsorption mechanisms operating within the 13X zeolite, the grafted materials exhibit distinct sites for adsorption of water and CO_2.

7.5.6 – Comparison to Literature Data

As shown in Table 7.3, the water-aided grafted materials developed in this study outperformed all other amine grafted silicas reported in the literature. The effect of using water during the grafting procedure greatly enhanced the amine content and the resulting CO_2 adsorption performance. However, to put the results into a clearer context, the present results and literature data were plotted in terms of the CO_2 adsorption capacity and amine efficiency (CO_2/N molar ratio) as a function of the amount of amine grafted and are shown in Figures 7.11 and 7.12, respectively. The data in Figure 7.11 represent the CO_2 adsorption capacity obtained by the various research groups (from Table 7.3) at different CO_2 inlet concentrations; the filled symbols represent dry CO_2 adsorption, and the open symbols tied by dashed lines to the filled symbols represent the corresponding humid CO_2 adsorption. Since all the data correspond to various CO_2 inlet concentrations, direct interpretation of the results is not straightforward, as the CO_2 adsorption capacity increases as the inlet concentration increases. However, from the trends shown in Figure 7.11, it is apparent that the CO_2 adsorption capacity is almost independent of the amount of amine loaded; adsorption capacities obtained with mono-, di-, or triamine grafting can produce the same result, even though the amine content has increased. This observation may be solely due to the method of grafting, as the approach taken by the various groups varies greatly. However, in light of the results presented in this study, we have demonstrated that a properly optimized grafting procedure can produce a highly active material.

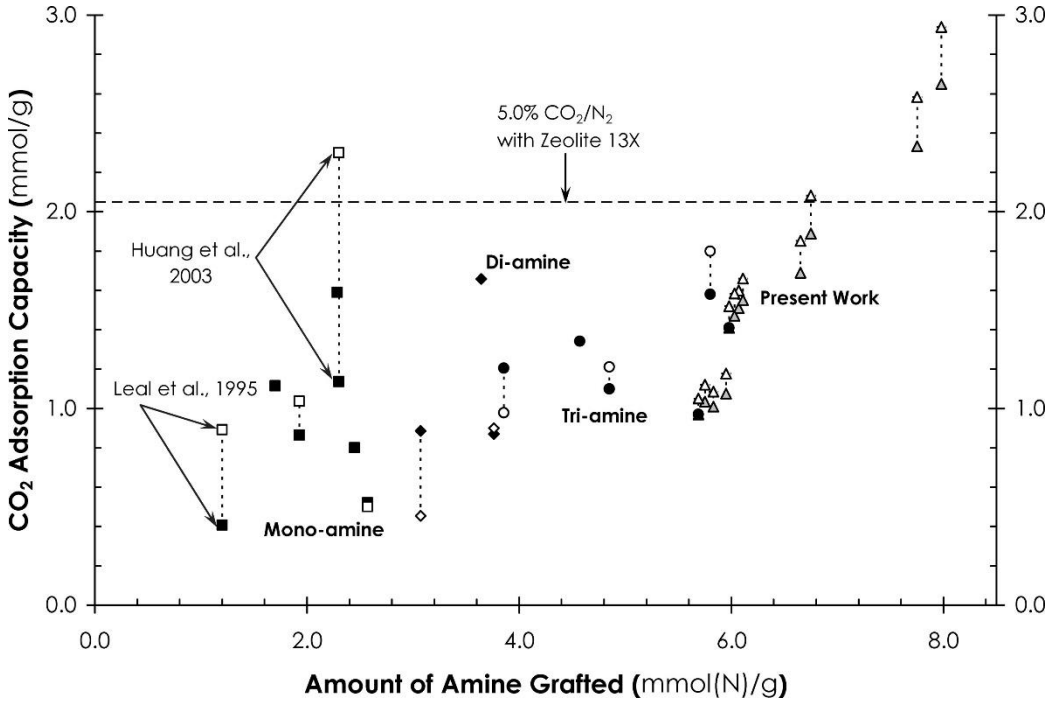

Figure 7.11 Summary of the literature and current data, for amine-grafted mesoporous silicas applied as CO_2 adsorbents; adsorption capacity as a function of the amount of amine grafted for various amino-silane types. The filled symbols represent dry CO_2 adsorption, and the open symbols represent humid CO_2 adsorption, where applicable. The squares, diamonds, and circles represent the mono-, di-, and triamine grafted materials reported in the literature, respectively. The gray filled triangles represent triamine grafted materials described in the present study.

In terms of amine adsorption efficiency (Figure 7.12), most CO_2/N ratios obtained in the current investigation are within the range of 0.20-0.35. Moreover, in most cases, water vapor has only a marginal effect on the adsorption of CO_2. However, there are a few intriguing exceptions. Two research groups, Huang et al. [23] and Knowles et al. [24] reported CO_2/N ratios equal to or higher than the stoichiometric value based on carbamate formation under dry conditions (Table 7.2). It is also interesting to note that, from all the data presented in the literature, only the two earliest investigations dealing with monoamine grafted materials

reported that the adsorption of humid CO_2 resulted in an approximate doubling of the dry adsorption capacity [23, 30].

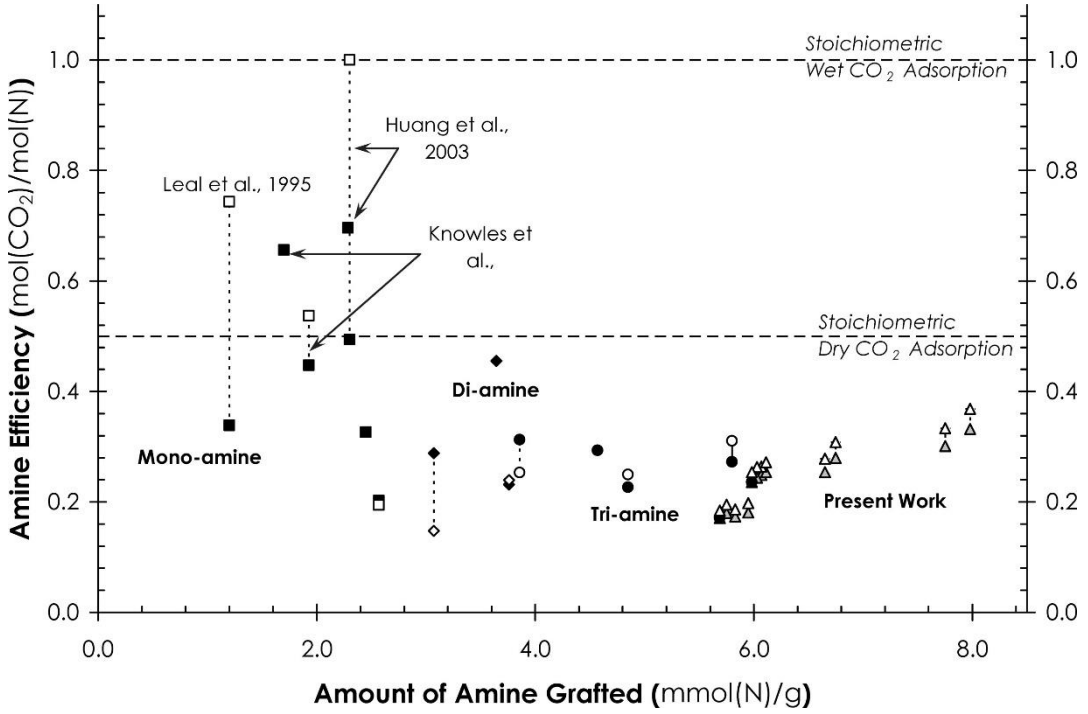

Figure 7.12 Summary of the literature and current data, for amine-grafted mesoporous silicas applied as a CO_2 adsorbent; amine efficiency as a function of the amount of amine grafted for various amino-silane types. The filled symbols represent dry CO_2 adsorption, and the open symbols represent humid CO_2 adsorption, where applicable. The squares, diamonds, and circles represent the mono-, di-, and triamine grafted materials reported in the literature, respectively. The gray filled triangles represent triamine grafted materials described in the present study.

In order to put the adsorption capacities shown in Figure 7.11 into perspective, an adsorption parameter was defined and represents the amount of CO_2 adsorbed divided by the inlet partial pressure of CO_2 (mmol/g/Pa). Although this parameter resembles Henry's Law constant and the slope of the adsorption isotherm, it is not intended to convey such similarities, within the spirit of this work, but rather is only an attempt to rationalize the various data presented in the literature.

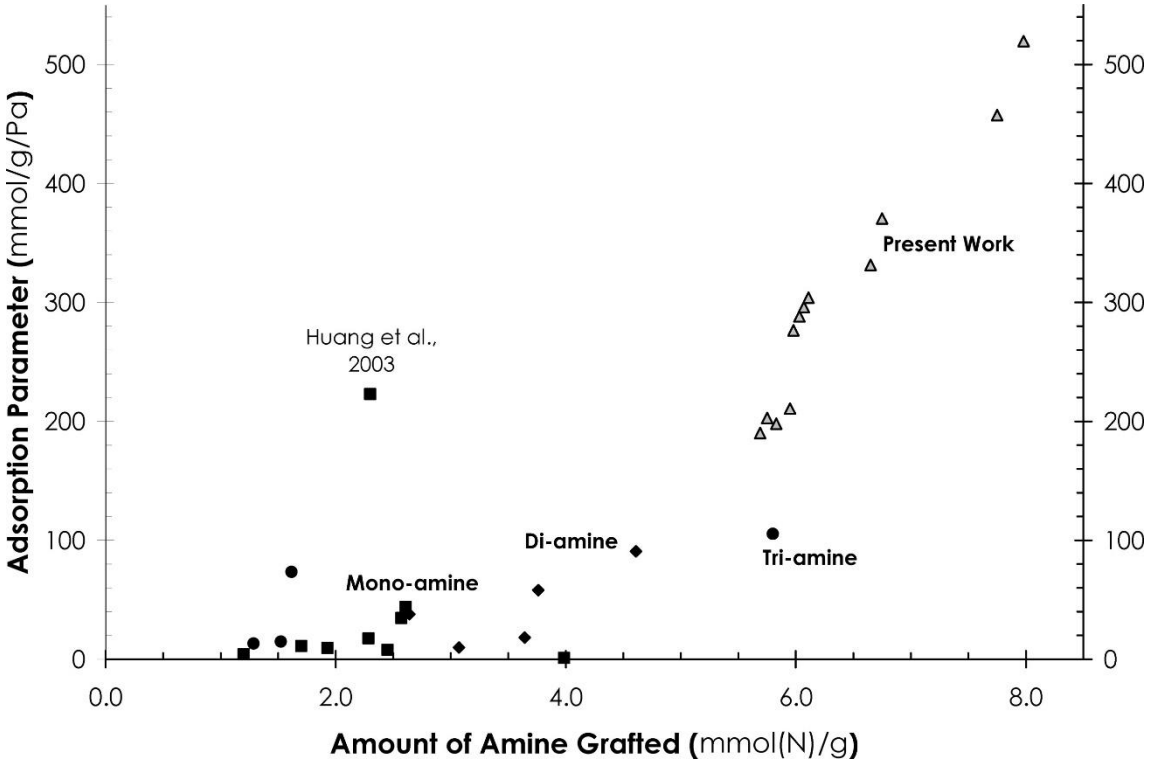

Figure 7.13 Summary of the literature and current data, for amine-grafted mesoporous silicas applied as a CO_2 adsorbent under dry CO_2 conditions; adsorption parameter as a function of the amount of amine grafted for various amino-silane types. The squares, diamonds, and circles represent the mono-, di-, and triamine grafted materials shown in the literature, respectively. The gray filled triangles represent triamine grafted materials described in the present study.

The CO_2 adsorption process with amine sites occurs predominately via chemical reaction, and it is often assumed that the adsorption capacity should not vary to a high degree with changes in the inlet pressure. However, the data presented by several groups [23, 25, 26, 30] all showed a strong dependence of the amount of CO_2 adsorbed as a function of CO_2 pressure. In all cases, comparison of the 5% to 100% CO_2 inlet concentration (where available) exhibited a 2-3 fold increase in the CO_2 adsorption capacity with the various amine grafted materials. Therefore, by defining this adsorption parameter, the effects of the wide

range of inlet CO_2 pressures will be normalized, and materials that exhibit a high CO_2 adsorption capacity at low CO_2 inlet pressures will become more evident.

As shown in Figure 7.13, our materials presented in this study stand out in terms of the adsorption parameter, with values in the 400-500 range compared to the bulk of values below 100 for the literature data. Further, even though a few other groups have obtained relatively high adsorption capacities (Figure 7.11), the adsorption parameter reveals that they may not be as impressive as they appeared to be at first glance. Therefore, data at low CO_2 partial pressures are needed in order to exploit the favorable amine-CO_2 interaction in comparison to other typical physisorption- based adsorbents such as zeolite 13X.

7.5.6 – Dynamic Adsorption Performance of Optimally Grafted PE-MCM-41

The dynamic response of the material containing the optimum amount of grafted triamine is shown in Figure 7.14. This material was challenged with a 5% CO_2/N_2 feed mixture, and the dynamic amount adsorbed was recorded and compared to data obtained with zeolite 13X under replicate operating conditions. As shown in Figure 7.14A, the fractional uptake for the triamine grafted material is superior when the exposure time is <5 min. Beyond this time, the two materials exhibited similar approaches to complete saturation. However, at equilibrium, the triamine grafted material adsorbed a larger amount of CO_2 (2.65 mmol/g) than the 13X zeolite (2.05 mmol/g), when both adsorbents are initially regenerated at 200 °C. The specific amount adsorbed and the associated adsorption rates are shown in Figure 7.14B. From these data, it is evident that the triamine grafted material is far superior in terms of the specific amount adsorbed, especially upon initial contact with the feed gas mixture.

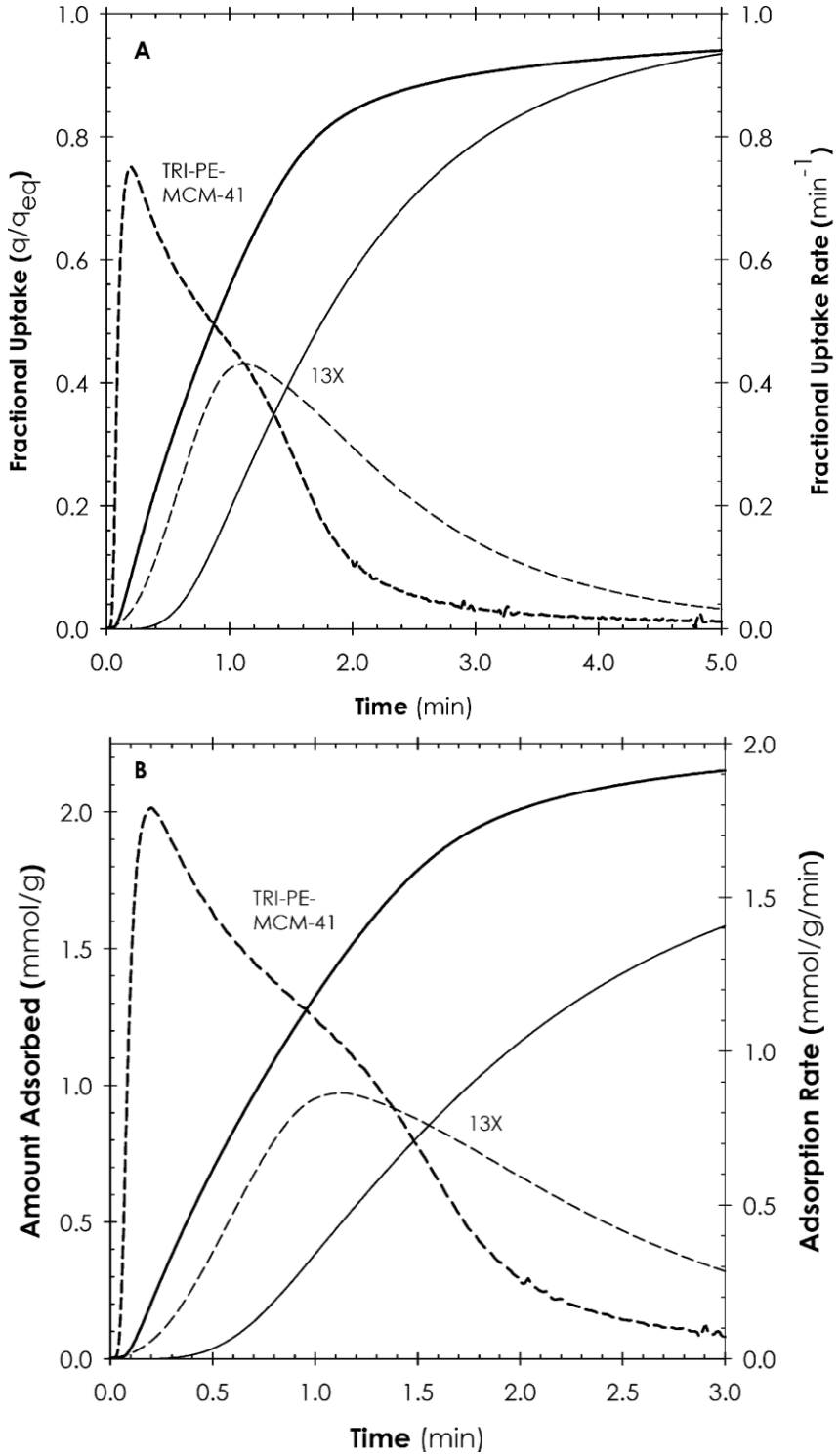

Figure 7.14 Dynamic adsorption response of the optimal TRI-PE-MCM-41 material and 13X zeolite to a 5% CO_2/N_2 feed mixture, as a fractional uptake(A) and a specific amount adsorbed (B), where the solid lines represent the adsorption quantities and the dashed lines represent the adsorption rates.

It is also interesting to observe that the 13X zeolite exhibited a delayed response to the

5% CO_2 feed mixture, as noted by the offset of the uptake curve and the slow increase in the rate. This behavior may be due to the competitive effect of N_2, which was preadsorbed on the material, as separate experiments showed that zeolite 13X adsorbs ca. 0.40 mmol/g of pure N_2 at 25 °C, or to the slower pore diffusion. This behavior was not observed with the triamine grafted material since it does not exhibit N_2 adsorption, and the pore structure is such that diffusion limitations are greatly reduced.

7.6 - Conclusion

The grafting of 3-[2-(2-aminoethylamino)ethylamino]propyltrimethoxysilane to the surface of pore-expanded MCM-41 was parametrically examined through the control of the amount of water added to the grafting mixture and the grafting temperature. The effects of these parameters were profiled in terms of the amount of amine grafted and the CO_2 adsorption performance. The optimal reaction temperature for grafting was found to be 85 °C, which was significantly lower than the temperature of 110 °C typically applied when grafting with toluene as the solvent.

Under appropriate grafting conditions, the PE-MCM-41 was loaded to very high amine contents. The optimally grafted TRI- PE-MCM-41 was obtained under the conditions of 3.0 $cm^3/g(SiO_2)$ silane, 0.30 $cm^3/g(SiO_2)$ water, and 85 °C grafting temperature. This optimal TRI-PE-MCM-41 adsorbent exhibited unprecedented high adsorption capacities and adsorption rates when exposed to a 5% CO_2/N_2 gas mixture. Coaddition of water to the grafting mixture also exhibited a pronounced effect on the adsorption performance. In comparison to the dry grafting procedure, the wet technique afforded a 33% increase in total amine content and a 43% increase in active amine content, i.e., CO_2/N molar ratio, resulting in a 90% overall improvement. Further, the TRI-PE-

MCM-41 material outperformed zeolite 13X with dry 5% CO_2 adsorption and vastly outperformed zeolite 13X with humid 5% CO_2 adsorption. These characteristics demonstrate the ability of the pore-expanded MCM-41 support to accommodate a large quantity of aminosilane and still allow high adsorbate mobility, which translates into an adsorbent with a high CO_2 adsorption capacity and an unprecedented adsorption rate.

7.7 - Acknowledgements

The financial support of the Natural Science and Engineering Research Council of Canada through the Strategic Grant and the Idea to Innovation programs is acknowledged. Support from the Ontario Research Fund (ORDCF program) is also acknowledged. A.S. is a Canada Research Chair in Catalysis by Nanostructured Materials (2001-2008).

7.8 - References

[1] Kresge, C. T.; Leonowicz, M. E.; Roth, W. J.; Vartuli, J. C.; Beck, J. S., *Ordered Mesoporous Molecular Sieves Synthesized by a Liquid-Crystal Template Mechanism*. Nature, 1992, 359, 710.

[2] Beck, J. S.; Vartuli, J. C.; Roth, W. J.; Leonowicz, M. E.; Kresge, C. T.; Schmitt, K. D.; Chu, C. T. W.; Qlson, D. H.; Sheppard, E. W.; McCullen, S. B.; Higgins, J. B.; Schlenker, J. L., *A New Family of Mesoporous Molecular Sieves Prepared with Liquid Crystal Templates*. J. Am. Chem. Soc., 1992, 114, 10 834.

[3] Sayari, A., *Periodic Nanoporous Materials: Synthesis, Characterization and Potential Applications*. In Recent AdVances and New Horizons in Zeolite Science and Technology; Chong, H., Woo, S. I., Park, S. E., Eds.; Elsevier: Amsterdam, The Netherlands, 1996; p 1.

[4] Sayari, A., *Catalysis by Crystalline Mesoporous Molecular Sieves*. Chem. Mater., 1996, 8, 1840.

[5] Corma, A., *From Microporous to Mesoporous Molecular Sieve Materials and Their Use in Catalysis*. Chem. ReV., 1997, 97, 2373.

[6] Hoffmann, F; Cornelius, M.; Morell, J.; Froba, M, *Silica-Based Mesoporous Organic-Inorganic Hybrid Materials*. Angew. Chem. Int. Ed., 2006, 45, 3216.

[7] Stein, A., *Advances in Microporous and Mesoporous Solids Highlights of Recent Progress*. AdV. Mater., 2003, 15, 763.

[8] Sayari, A., *Unprecedented Expansion of the Pore Size and Volume of Periodic Mesoporous Silica*. Angew. Chem. Int. Ed. Engl. 2000, 39, 2920.

[9] Sayari, A.; Kruk, M.; Jaroniec, M.; Moudrakovski, I. L., *New Approaches to Pore Size Engineering of Mesoporous Silicates*. AdV. Mater., 1998, 10, 1376.

[10] Sayari, A.; Yang, Y.; Kruk, M.; Jaroniec, M., *Expanding the Pore Size of MCM-41 Silicas: Use of Amines as Expanders in Direct Synthesis and Postsynthesis Procedures*. J. Phys. Chem. B, 1999, 103, 3651.

[11] Kruk, M.; Jaroniec, M.; Sayari, A., *New Insights into Pore-Size Expansion of Mesoporous Silicates using Long-Chain Amines*. Microporous Mesoporous Mater., 2000, 35-36. 545.

[12] Sayari, A.; Hamoudi, S.; Yang, Y., *Applications of Pore-Expanded Mesoporous Silica. 1. Removal of Heavy Metal Cations and Organic Pollutants from Wastewater*. Chem. Mater., 2005, 17, 212.

[13] Franchi, R.; Harlick, P. J. E.; Sayari, A., *Applications of Pore- Expanded Mesoporous Silica. 2. Development of a High-Capacity, Water-Tolerant Adsorbent for CO_2*. Ind. Eng. Chem. Res., 2005, 44, 8007.

[14] Harlick, P. J. E.; Sayari, A., *Applications of Pore-Expanded Mesoporous Silica. 3. Triamine Silane Grafting for Enhanced CO_2 Adsorption*. Ind. Eng. Chem. Res., 2006, 45, 3248

[15] Reynhardt, J. P. K.; Yang, Y.; Sayari, A.; Alper, H., *Periodic mesoporous silica-supported recyclable rhodium-complexed dendrimer catalysts*. Chem. Mater., 2004, 16, 4095.

[16] Reynhardt, J. P. K.; Yang, Y.; Sayari, A.; Alper, H., *Rhodium Complexed C2-PAMAM Ddendrimers*

Supported on Large Pore Davisil Silica as Catalysts for the Hydroformylation of Olefins. AdV. Synth. Catal., 2005, 347, 1379.

[17] Reynhardt, J. P. K.; Yang, Y.; Sayari, A.; Alper, H., *Polyamidoamine Dendrimers Prepared Inside the Channels of Pore-Expanded Periodic Mesoporous Silica.* AdV. Funct. Mater., 2005, 15, 1641.

[18] Bunker, B. C.; Haaland, D. M.; Michalske, T. E.; Smith, W. L., *Kinetics of Dissociative Chemisorption on Strained Edge-Shared Surface Defects on Dehydroxylated Silica*. Surf. Sci., 1989, 222, 95.

[19] Feng, X.; Fryxell, G. E.; Wang, L. Q.; Kim, A. Y.; Liu, J.; Kemner, K. M., *Functionalized Monolayers on Ordered Mesoporous Supports*. Science, 1997, 276, 923.

[20] Liu, J.; Feng, X.; Fryxell, G. E.; Wang, L. Q.; Kim, A. Y.; Gong, M., *Hybrid Mesoporous Materials with Functionalized Monolayers*. AdV. Mater., 1998, 10, 161.

[21] Stein, A.; Melde, B. J.; Schroden, R. C., *Hybrid Inorganic-Organic Mesoporous Silicates Nanoscopic Reactors Coming of Age*. AdV. Mater., 2000, 12, 1403.

[22] Sayari, A.; Hamoudi, S., *Periodic Mesoporous Silica-Based Organic-Inorganic Nanocomposite Materials*. Chem. Mater., 2001, 13, 3151.

[23] Huang, H. Y.; Yang, R. T.; Chinn, D.; Munson, D. L., *Amine- Grafted MCM-48 and Silica Xerogel as Superior Sorbents for Acidic Gas Removal from Natural Gas*. Ind. Eng. Chem. Res., 2003, 42, 2427.

[24] Knowles, G. P.; Graham, J. V.; Delaney, S. W.; Chaffee, A. L., *Aminopropyl-Functionalized Mesoporous Silicas as CO_2 Adsorbents*. Fuel Process. Technol., 2005, 86, 1435.

[25] Hiyoshi, N.; Yogo, K.; Yashima, T., *Adsorption of Carbon Dioxide on Amine Modified SBA-15 in the Presence of Water Vapor*. Chem. Lett., 2004, 33, 510.

[26] Zheng, F.; Tran, D. N.; Busche, B. J.; Fryxell, G. E.; Addleman, R. S.; Zemanian, T. S.; Aardahl, C. L., *Ethylenediamine-Modified SBA-15 as Regenerable CO_2 Sorbent*. Ind. Eng. Chem. Res., 2005, 44, 3099.

[27] Kim, S.; Ida, J.; Guliants, V. V.; Lin, J. Y. S., *Tailoring Pore Properties of MCM-48 Silica for Selective Adsorption of CO_2*. J. Phys. Chem. B, 2005, 109, 6287.

[28] Sayari, A.; Yang, Y., *Highly Ordered MCM-41 Silica Prepared in the Presence of Decyltrimethylammonium Bromide*. J. Phys. Chem. B, 2000, 104, 4835.

[29] Kruk, M.; Jaroniec, M.; Sayari, A., *Application of Large Pore MCM-41 Molecular Sieves To Improve Pore Size Analysis Using Nitrogen Adsorption Measurements*. Langmuir, 1997, 13, 6267.

[30] Leal, O; Bol´ıvar, C.; Ovalles, C.; Garc´ıa, J. J.; Espidel, Y., *Reversible Adsorption of Carbon Dioxide on Amine Surface-Bonded Silica Gel*. Inorg. Chim. Acta, 1995, 240, 183.

[31] Knowles, G. P.; Delaney, S. W.; Chaffee, A. L., *Amine-Functionalised Mesoporous Silicas as CO2 Adsorbents*. Stud. Surf. Sci. Catal., 2005, 156, 887.

[32] Knowles, G. P.; Delaney, S. W.; Chaffee, A. L., *Diethylenetriamine-[propyl(silyl)]-Functionalized (DT) Mesoporous Silicas as CO_2 Adsorbents*. Ind. Eng. Chem. Res. 2006, 45, 2626.

[33] Rinker, E. B.; Ashour, S. S.; Sandall, O. C., *Absorption of Carbon Dioxide into Aqueous Blends of Diethanolamine and Methyldiethanolamine*. Ind. Eng. Chem. Res., 2000, 39, 4346.

Chapter 8

Development of a Novel Dual Membrane Gas Permeator Module:
Internally Variably Staged Permeator

Harlick, P.J.E., and Tremblay, A.Y

Department of Chemical Engineering, University of Ottawa, 161 Louis Pasteur, Ottawa, Ontario, Canada K1N 6N5

Harlick, P.J.E., and Tremblay, A.Y., *Development of a Novel Dual Membrane Gas Permeator*, Proceedings of the 6th World Congress of Chemical Engineering **(2001)**, Melbourne, Australia, Sept. 23-27

The work presented in this Chapter was completed by myself under the supervision of Dr. A.Y. Tremblay. See section 1.2 for further details.

8.1 - Abstract

Membrane based gas separation has recently seen a drastic increase in industrial applicability. The growth has largely been due to the of membrane material development which has resulted with increased selectivity and component flux. However, very little work has been completed on the development of modules that contain these membranes. In this study, a novel dual membrane gas permeator has been developed, modelled and termed an Internal Variably Staged Permeator (IVSP).

For a binary CO_2-N_2 mixture, the results show that the IVSP provided high permeate purity of the faster permeating component, while maintaining a high permeate stage-cut. Simultaneously, the purity of the slower permeating component was also increased. Parametric analysis of the module proved that the degree of trade-off between the permeate purity and stage-cut could be controlled. Comparison of the conventional, two-stage cascade and ISP designs to the IVSP, showed that the IVSP produces higher permeate purity for a given permeate stage-cut with less membrane area than a two stage series or an ISP.

8.2 - Introduction

For many centuries, combustion processes have been mankind's most common and essential means of releasing energy for comfort and preparation of food. In recent times, those same processes have additionally become essential for transportation, industrial commerce, and the disposal of organic refuse. With an increasing worldwide population and an increased per capita demand for energy, concern is now being raised over the environmental pollution resulting from the emission of gaseous by-products from combustion processes. Even carbon dioxide, a gaseous compound produced during combustion by oxidation of carbon

and essential to plant life, is being viewed as a pollutant today. Carbon dioxide has been identified as one of many "*greenhouse*" gases and an increased level in the earth's atmosphere is known to contribute to an undesirable global warming effect.

Although carbon dioxide is emitted by several sources (natural, residential, automotive, industrial, etc…), the industrial sector has been targeted by global concerns. In order to meet the present and future constraints placed on the allowable emissions of CO_2 the solution lies with point source reduction and recovery. Therefore, an economical treatment process must be developed. For this treatment process to succeed, it must be capable of effective and efficient removal, concentration and recovery of CO_2 from flue gas for industrial applications.

Membrane based gas separation processes have been evolving for the last 35 years. The productivity of a gas permeation process is jointly controlled by a partial pressure driving force, the mass transfer resistance (permeability) across the membrane, and the effective membrane area. Conventionally, membrane are contained within modules and are provided a feed, feed rejuect, and a permeate stream as shown in Figure 8.1.

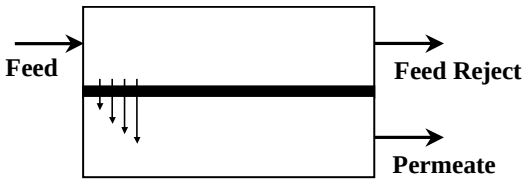

Figure 8.1 – Schematic diagram of a conventional permeator.

The feed enters in the lower region at high pressure. In this stream the faster permeating component transverses the membrane and enters into the permeate stream at an enriched level. For a binary feed mixture, the feed is depleted in the faster permeating

component; it is enriched in the slower permeating component. At the exit of the module, two enriched streams are possible but typically not attainable in this type of configuration.

Various membrane configurations have been used. These include flat sheet, hollow fiber, annular hollow fiber (Li et al., 1998), and hollow fiber fabric (Lui et al., 2000). The flat sheet and hollow fiber type membranes have been employed in conventional, multi stage cascade permeators (Blaisdell and Kammermeyer, 1973, Pan and Habgood, 1974, 1978 a, b, Sirkar, 1996) and an internally staged permeator (Sidhoum et al., 1988, Sidhoum et al., 1989, Li et al., 1991, Li and Hughes, 1992, Li et al., 1994, Chen et al., 1995, Li et al., 1998) . The hollow fiber fabric has only been shown in an ISP design (Lui et al., 2000).

In order to improve the separation efficiency in a single stage, the concept of the ISP was introduced by Sidhoum et al. (1988), shown schematically in Figure 8.2. The internal staging of this permeator offered advantages over conventional and two-stage series type permeators, in that permeate from the feed was locally fed to a second membrane in the permeator via a shell space. Sidhoum and co-workers confirmed the feasibility of such a unit by the numerical simulation of O_2-N_2 and CO_2-N_2 mixtures (Sidhoum et al., 1988) and experimental work (Sidhoum et al., 1989). Their simulations where performed for a hollow fiber configuration with a co-current flow pattern. They concluded that the ISP performed better than a two-stage cascade and that two enriched product streams where possible, at reasonable overall stage-cuts. One enriched stream emerged as permeate from the second membrane, and the other as the feed reject.

A hollow fiber, ISP module was later assembled by Sidhoum et al., (1989). In this module, the mixture to be separated was fed into the lumen of several hollow fibber membranes. The feed gases, which had not permeated through the membrane, exited the module as a feed reject stream. The permeate from the first membrane entered the shell

space of the module and exited the module as the shell reject stream. The permeate from this membrane (second membrane) exited as the permeate stream.

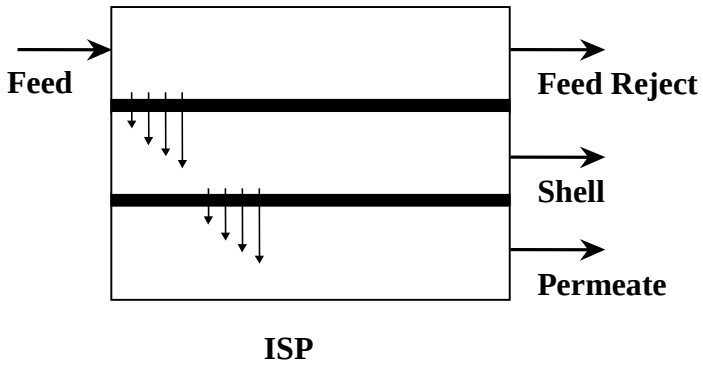

Figure 8.2 – Schematic diagram of an internally staged permeator (ISP).

Sidhoum et al. (1989) extended their work to co-current, and counter-current flow pattern comparison, by experimentation and numerical simulation that included the lumen pressure drop equations. They concluded that when the ideal separation factor for the mixture to be processed was low, as is the case for known O_2-N_2 selective membranes, a better separation is always achieved with an ISP.

Sidhoum et al. (1989) also concluded that the co-current flow pattern would result in a better separation over the counter-current flow pattern. This conclusion is in contrast with the conventional membrane type permeator, for which a counter-current flow pattern is superior (Blaisdell and Kammermeyer, 1973, Pan and Habgood, 1974, 1978 a,b, Sirkar, 1996). Li and co-workers (1991, 1992, 1993, 1994) also examined the ISP design and reached the same conclusions advanced by Sidhoum et al. (1988, 1989).

Further studies of binary separations using the ISP were performed by Chen et al. (1995) and Li et al. (1998). Their studies were based on a hollow-fiber configuration. They evaluated the performance of the ISP concerning co-current, counter-current and perfect mixing flow patterns. They found that an optimal stage-cut and pressure ratio could be

found that would ultimately fine-tune the performance of the ISP. They also showed that the ratio of pressures across the low to medium pressure regions to that of the high to medium pressure regions would provide no further increase in the initial permeate stream mole fraction when the ratio was above one. However, even with the optimal parameters chosen, the productivity of the ISP was low when compared to the conventional module; high purity but low stage-cut. They concluded that the area requirement of the ISP is considerably higher than the conventional permeator.

Lui and co-workers (2000) constructed a hollow fiber fabric for use in an ISP. With this novel material a variety of flow patterns were examined. They also found that the area requirements of the ISP are considerably higher than those with a conventional permeator. They suggested that the ISP be used for a process were the gas to be processed is abundantly available and disposal of the waste is not problematic, such as air separation.

Lim and Li, (2001), evaluated the ISP concept with focus on the development and modelling of the annulus pressure for a module configured with hollow fibers. Although no experimental results are presented, the effect of the shell side pressure drop is shown to be significant on the module performance.

Lui et al., (2001), compare the performance of an ISP with an external 2-stage conventional module design. They conclude that an optimal ISP design is comparable to the performance from an optimal external 2-stage module design, when operated with co-current flow. They also conclude that the experimental results from the external 2 stage module system are in good agreement with the theoretical model.

In the all the studies of an ISP in the literature, the same conclusion of low productivity has been reached, regardless of the flow pattern. In order for the design to be economical, the feed rate to area ratio parameter of the ISP must be increased while

maintaining a higher permeate purity than the conventional or cascade permeator designs. Therefore, the purpose of this study was to parametrically examine the ISP and determine the design parameter which could be controlled to result with enhanced performance.

8.3 - Module Development

The purpose of the module for the permeation process is to provide intimate contact of the two gases with the membrane in order to promote relative diffusion. The flux rate is partly dependent upon the effective use of the interfacial surface exposed between the respective streams. In this respect, the module design can broadly be classified according to the extent of separation that can be achieved within its bounds. Presently, high purity permeate can only be achieved with highly selective membranes, or multi membrane permeators.

The first step towards a novel membrane permeator is with the module layout and operating characteristics. In order to understand the modules' effect on the separation, the most dependent characteristics of the permeation process must be established. The following have been judged to affect the degree of separation,

1) - The number, type and configuration of membranes used.

2) - The operating pressures.

3) - The effective area requirements for desired product(s) flowrate at the specified feed flowrate.

Several authors have shown that the separation was dependent on the area, such that increasing the membrane area would reduce the permeate purity, while increasing the overall stage-cut, for the conventional permeator and the ISP. This is the trade-off syndrome.

Initially the permeate purity is at its highest, yet always decreases as the permeate stage-cut increases. Although the ISP produces higher permeate purities, the rate of decline of permeate purity with respect to permeate stage-cut is significantly higher than the conventional permeator. Even with this behaviour, the dual membrane design of the ISP is the most promising as a result of more control over the permeation process.

8.4 - Theoretical Model

To fully describe the gas permeator, the governing differential equations must be established for the flow patterns being analyzed. The following assumptions were used in the model derivations:

1) - Permeation obeys Fick's First Law of diffusion.

2) - Bulk diffusion controls, i.e., axial and transverse diffusion are negligible.

3) - The permeability of each species is independent of pressure and composition.

4) - Plug flow exists in the feed, shell and permeate streams.

5) - The effective membrane thickness is constant along the flow path.

6) - Flow induced pressure drops in each stream are negligible.

7) - Isothermal operation.

Each of these assumptions, as applied to each of the modules, has been validated by many authors, (Blaisdell and Kammermeyer, 1973, Pan and Habgood, 1974, 1978 a, b, Sirkar, 1996).

For the cross-flow pattern being studied, the variables of interest are the local mole fractions in both the shell and permeate streams, the collective mole fractions, and flow rates in each of the feed, shell and permeate streams, as well as the pressure ratio's across each membrane. Detailed descriptions of the model equations for an ISP can be elsewhere, and are not repeated here (Sidhoum et al., 1988, Sidhoum et al., 1989, Li et al., 1991, Li and Hughes, 1992, Li et al., 1994, Chen et al., 1995, Li et al., 1998). The model equations describing a conventional permeator and a two-stage cascade have also been described in the literature (, Blaisdell and Kammermeyer, 1973, Pan and Habgood, 1974, 1978 a, b). Some important parameter relationships are given as follows.

1) - The dimensionless membrane area is represented as the traversed area(distance) to total membrane area ratio.

$$A^* = \frac{A}{A_{Total}} \tag{8.1}$$

2) - The ideal selectivity is defined as the ratio pure component permeability's of the faster to slower component.

$$\alpha_I = \frac{Q_I^{CO_2}}{Q_I^{N_2}}, \quad \alpha_{II} = \frac{Q_{II}^{CO_2}}{Q_{II}^{N_2}} \tag{8.2}$$

3) - The trans-membrane pressure ratio is defined as the high pressure to low-pressure ratio across each membrane.

$$\gamma_{FS} = \frac{P_F}{P_S}, \quad \gamma_{SP} = \frac{P_S}{P_P} \tag{8.3}$$

4) - The overall pressure ratio is defined as the feed pressure to permeate pressure.

$$\gamma_{Ov} = \frac{P_F}{P_P} \tag{8.4}$$

5) - The feed, shell and permeate stage-cut are defined as the stream flow rate over the inlet flow rate.

$$\Phi_F = \frac{L_F}{L_F^o}, \quad \Phi_S = \frac{L_S}{L_F^o}, \quad \Phi_P = \frac{L_P}{L_F^o} \tag{8.5}$$

6) - The permeate mole fraction for a conventional permeator at zero stage-cut,

$$y_P^i = \frac{a\left(\gamma_{Ov} y_F^o - y_P^i\right)}{a\left(\gamma_{Ov} y_F^o - y_P^i\right) + \gamma_{Ov}\left(1 - y_F^o\right) - \left(1 - y_P^i\right)} \tag{8.6}$$

The shell and permeate mole fractions at zero stage-cut are represented by a coupled system as follows.

$$y_S^i = \frac{a_I\left(\gamma_{II}\left(\gamma_I y_F^o - y_S^i\right) - \left(\gamma_{II} y_S^i - y_P^i\right)\right)}{\left(\gamma_I\left(a_I\left(\gamma_I y_F^o - y_S^i\right) - \gamma_I\left(1 - y_F^o\right) - \left(1 - y_S^i\right)\right) - \left(a_{II}\left(\gamma_{II} y_S^i - y_P^i\right) + \gamma_{II}\left(1 - y_S^i\right) - \left(1 - y_P^i\right)\right)\right)} \tag{8.7}$$

$$y_P^i = \frac{a_{II}\left(\gamma_{II}\, y_S^i - y_P^i\right)}{a_{II}\left(\gamma_{II}\, y_S^i - y_P^i\right) + \gamma_{II}\left(1 - y_S^i\right) - \left(1 - y_P^i\right)} \qquad \textbf{(8.8)}$$

Upon internal examination, it was deduced, that the shell pressure (functional on γ_I and γ_{II}) acted as an interfacial dual acting driving force between the feed stream and the permeate stream.

With the internally staged gas permeator, each local flux component from the first membrane is locally fed to the second, via the driving force centred on the shell stream. The permeate stream then collectively combines all of these components together along the effective length, to final stage-cut and purity for each of the streams. If the internally staged gas permeator was then set into a cascade of ISP's (permeate stream is used as feed for module n+1), then the separation in terms of permeate purity, would improve. However, with industrial applications, the objectives are to optimize for both permeate purity and permeate stage-cut, while recovering the feed stream with high purity of the slower permeating gases, and reject stage-cut. Therefore, if each of these local flux components were also locally fed across to another ISP in a series approach, the realization of the *Internal*

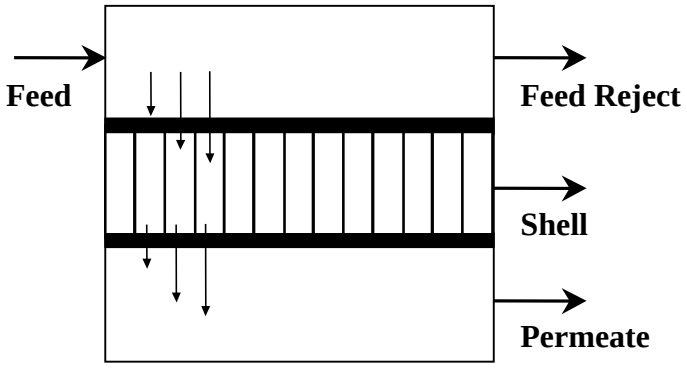

Figure 8.3 – Schematic diagram of an internally variably staged permeator (IVSP).

Variably Staged gas Permeator (IVSP) is established, Figure 8.3.

With this type of module design, it would be necessary to vary the operational properties of the inter-module contact region if its performance is to be different then the ISP. This requires that the shell volume would be operated at a different pressure with respect to module area. The shell pressure is a typically a controlling parameter for both purity and flowrate. By transforming this parameter into a design variable as a function of module area, the module will allow for a permeate enrichment when the permeating flux is most concentrated, and a slow build-up of the flowrate throughout the effective length of the module. The inclusion of the shell pressure distribution and magnitude of the pressure will directly affect the parametric trends. Therefore, the optimization of this module will allow for another degree of freedom.

8.4.1 - Shell Pressure

The shell pressure distribution is the centre of the design and very sensitive to change. For this study, a linear increase in the shell pressure was assumed, Eq. 8.9.

$$P_S = \left(P_S^{Max} - P_S^{Min} \right) \mathcal{A}^* + P_S^{Min} \tag{8.9}$$

In order for the equations to be incorporated into the permeation model for the IVSP, they must be transformed into the form of pressure ratios, since these ratios represent the individual driving forces in the module, Eqs. 8.10-8.11.

$$\frac{d\gamma_{FS}}{d\mathcal{A}^*} = \frac{P_F}{\left(P_S^{Max} - P_S^{Min} \right)}, \quad \gamma_{FS}\big|_{\mathcal{A}^*=0} = \frac{P_F}{P_S^{Min}} \tag{8.10}$$

$$\frac{d\gamma_{SP}}{d\mathcal{A}^*} = \frac{\left(P_S^{Max} - P_S^{Min} \right)}{P_P}, \quad \gamma_{SP}\big|_{\mathcal{A}^*=0} = \frac{P_S^{Min}}{P_P} \tag{8.11}$$

The distribution in the shell region that is used can be achieved practically by several methods, for example with a spiral wound membrane type module with specifically designed spacer matrices.

8.5 - Results and Discussion

In order to evaluate novel permeator (IVSP), simulations were performed to compare the performance to a conventional, two-stage cascade and an internally staged permeator (ISP). Several authors have previously validated the use of the model equations with experimental results (Sidhoum et al., 1989, Li et al., 1992, 1994, Li and Hughes, 1993, Chen et al., 1998). Therefore, the applicability of these present results should also hold to experimental results.

The parameters used in the simulations are given in Table 8.1. The membrane type and contact area for each module was assumed constant, i.e.,

$$Area_{Conv} = Area_{Ser1} = Area_{Ser2} = Area_{ISP_I} = Area_{ISP_{II}}$$

Table 8.1 Simulation parameters and conditions.

Membrane Type	CA Type*	
CO_2 Permeability	90	GPU*
N_2 Permeability	6.7	GPU*
Perm-Selectivity	13.5	
Membrane Area (I and II)	0-1.5	m^2
Feed Composition CO_2	0.15	
Feed Rate	13	sL/min
Feed Pressure	25	atm
Shell Pressure (ISP)	5	atm
Shell Pressure (IVSP)	5-20	atm
Permeate Pressure	1	atm

* - Li and Hughes, 1993

The overall pressure ratio for the separation process was kept constant at 25:1 for each module, and the applied pressure in each stream, for each module are given in Table 8.2.

These pressures were obtained by using an internal pressure ratio (γ_{II}/γ_{I}) of one. This condition was applied since several authors have stated that an internal pressure ratio of approximately one would result with optimal ISP performance, but is dependent on the feed conditions; pressure and mole fraction (Sidhoum et al., 1989, Li et al., 1991, Chen et al., 1995, Li et al., 1998).

Table 8.2 Effect of the internal pressure ratio on the zero stage-cut purity

	γ_{II}/γ_{I} =1.0	γ_{II}/γ_{I} =0.30
P_F	25	25
P_S	5	2.7
P_P	1	1
y_S^i	0.387	0.546
y_P^i	0.837	0.879

In order to validate the use of an internal pressure ratio of one, a parametric study on the effect the pressure ratio's was performed for zero stage-cut permeation. Data were generated by varying γ_{II} at constant γ_{I} within the solution space of $1.0 \le \gamma_{I,II} \le 30.0$. The grey contours represent lines of constant γ_{II}. When γ_{II} = 1.0, Eqs. 8.7 and 8.8 reduce to Eq. 8.6, the conventional permeator, and is shown by the blue line. In order to examine the effect of changing P_S, data was also generated for various P_F values where P_S was varied from P_P to P_F, and are shown as black contours. The results for the shell mole fraction, y_S^i, are shown in Figure 8.4, and the permeate mole fraction, y_P^i, are shown in Figure 8.5.

The effect of the internal pressure ratio on the shell mole fraction indicate that a high level of shell space enrichment can be achieved when the internal pressure ratio is low. In order for this condition to be achieved, the feed pressure must be high or the shell pressure must be low, Figure 8.4. However, as the feed pressure increases, the magnitude of change in y_S^i decreases.

The permeate mole fraction is also dependent on the shell mole fraction and shell pressure, Figure 8.5. Therefore, as the shell mole fraction increases, the permeate mole fraction should also increase. However, since high shell purity is obtained when the internal pressure ratio is low, this translates into a very low-pressure ratio across the second membrane (shell-permeate). The result is decreasing permeate purity as the shell purity increases, shown in Figure 8.5 as the black contours. Therefore, for a given membrane type and feed pressure, an optimal internal pressure can be found such that the permeate purity is maximum. It is also important to note that the magnitude of change of the permeate purity also decreases as the feed pressure is increased. For example, the maximum point in the solution space for the permeate purity, Figure 8.5, was obtained using values of γ_{I}=30 and γ_{II}=30. If a permeate pressure of 1.0 atm was specified, then these values would translate into a feed pressure of 900 atm, and a shell pressure of 30 atm. For this system (P_F = 25 atm), the optimal was found where $\gamma_{\mathrm{II}}/\gamma_{\mathrm{I}}$ = 0.30.

Based on this information, data were generated for an internal pressure ratio of one and the optimal found in Figure 8.5, shown in Table 8.2. Although the results are larger, the values are only optimal in terms of purity; the stage-cut parameter has been neglected. Since a low pressure was specified for the shell stream, the flux across the shell-permeate membrane will be very low. Therefore, in order to increase the flux higher pressures must be specified.

However, as the shell pressure is increased, the permeate purity will decrease, Figure 8.5. Therefore, a solution lies with pressure control.

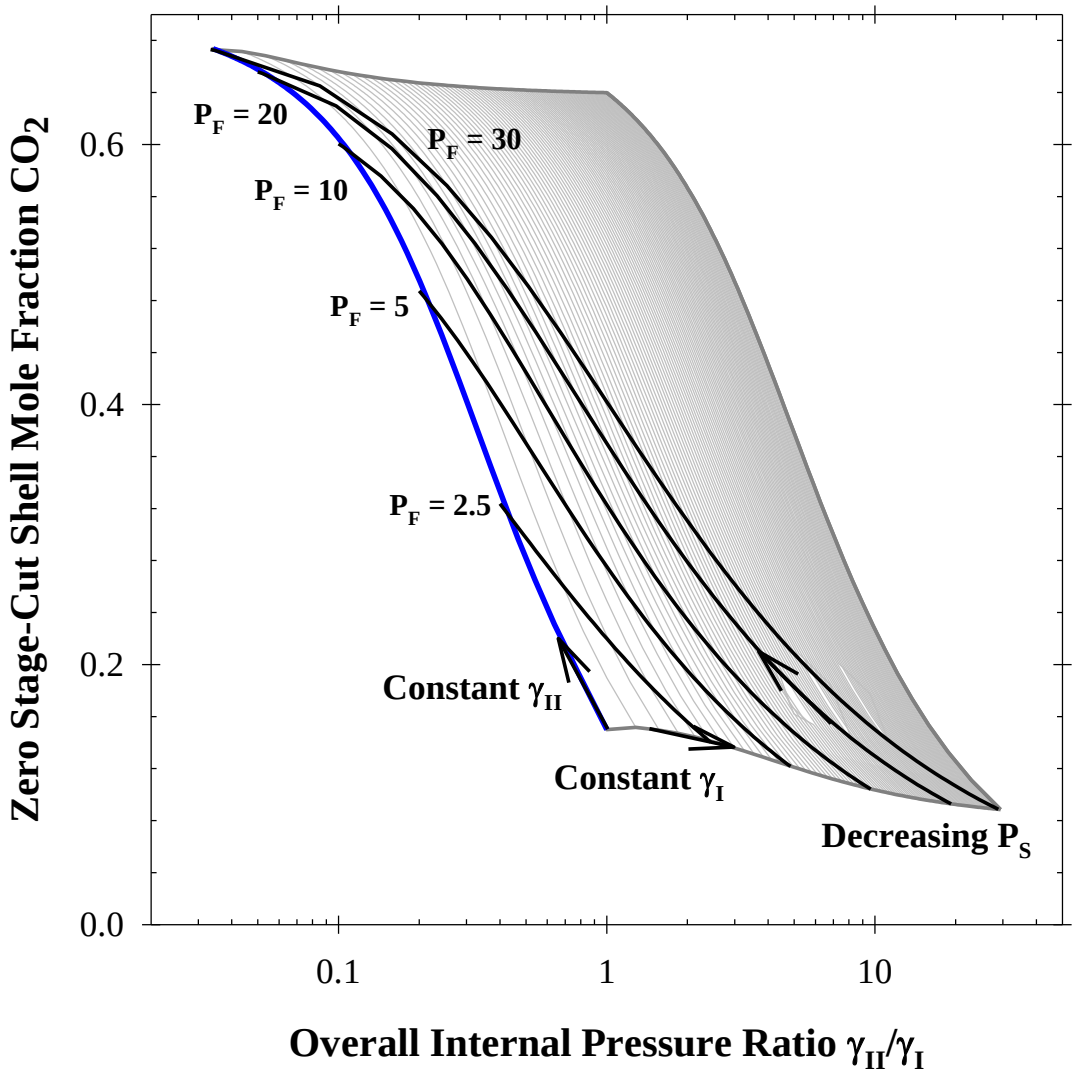

Figure 8.4 Effect of internal pressure ratio on the shell mole fraction of CO_2 at zero stage-cut. The grey lines are contours of constant γ_{II} : $\forall\, \gamma_{II} \in \{1..30\}$ *and* $\gamma_I \in \{1..30\}$ and the black lines are contours of decreasing $P_S : \forall\, P_S \in \{1..P_F\}$. The blue line represents the solution for the conventional permeator (γ_{II} =1.0).

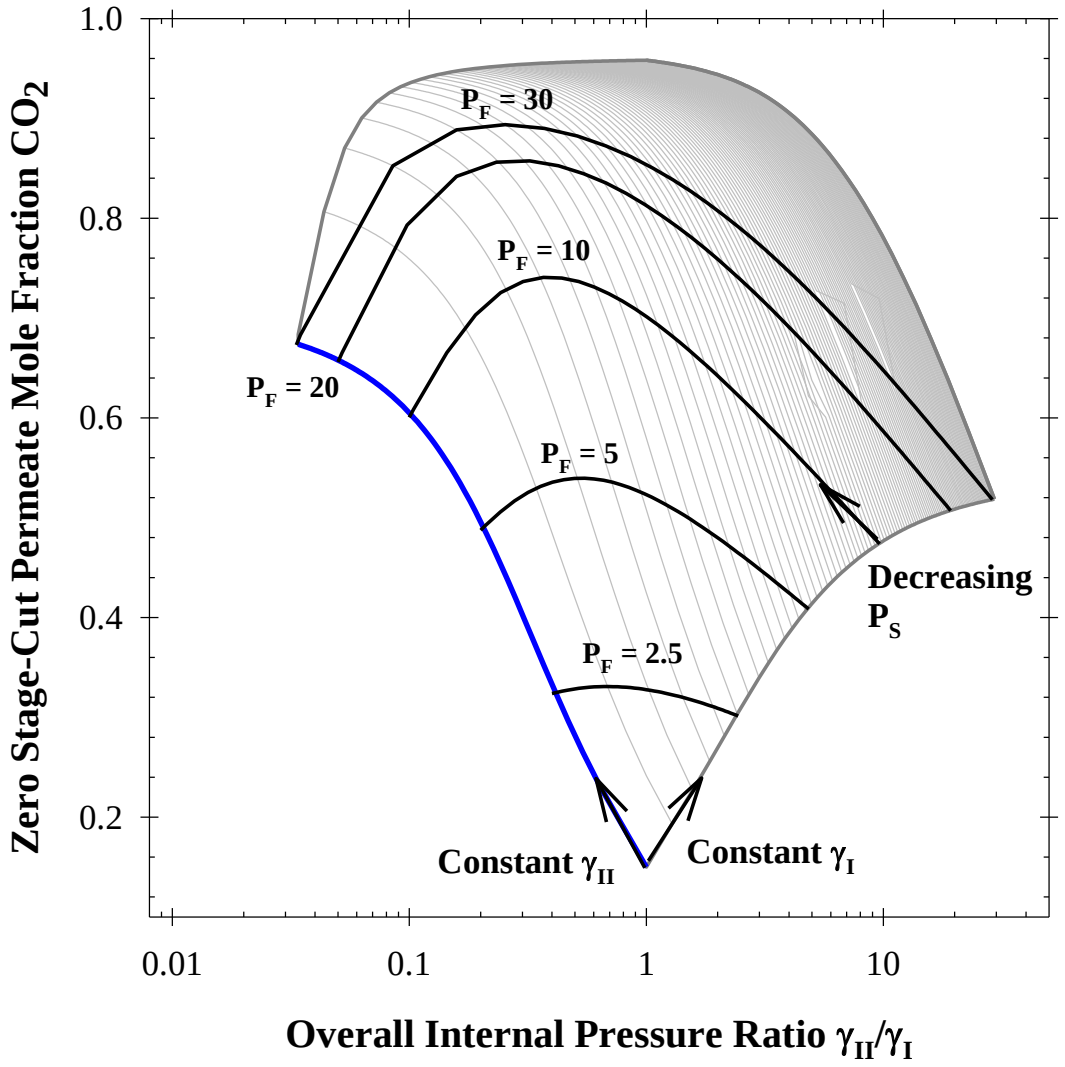

Figure 8.5 Effect of internal pressure ratio on the permeate mole fraction of CO_2 at zero stage-cut. The grey lines are contours of constant γ_{II} : $\forall\, \gamma_{II} \in \{1..30\}$ *and* $\gamma_I \in \{1..30\}$ and the black lines are contours of decreasing $P_S : \forall\, P_S \in \{1..P_F\}$. The blue line represents the solution for the conventional permeator (γ_{II} =1.0).

The effect of pressure control is depicted in Figures 8.6 and 8.7 for the shell and permeate streams respectively. The data shown in these figures are contours based on the variation of γ_I and γ_{II} in the solution space of $1.0 \le \gamma_{I,II} \le 30.0$. The arrows represent how the purity will vary depending on which pressure is controlled and in which direction.

In both figures, the most obvious benefit is realized form feed pressure control. However, unless the feed mixture is abundantly available at high pressure, controlling this pressure becomes a major economical consideration. If the permeate pressure were controlled, then the most benefit would be realized from decreasing this pressure. Since a decrease in the permeate pressure translates into positive vertical movement in Figure 8.6,

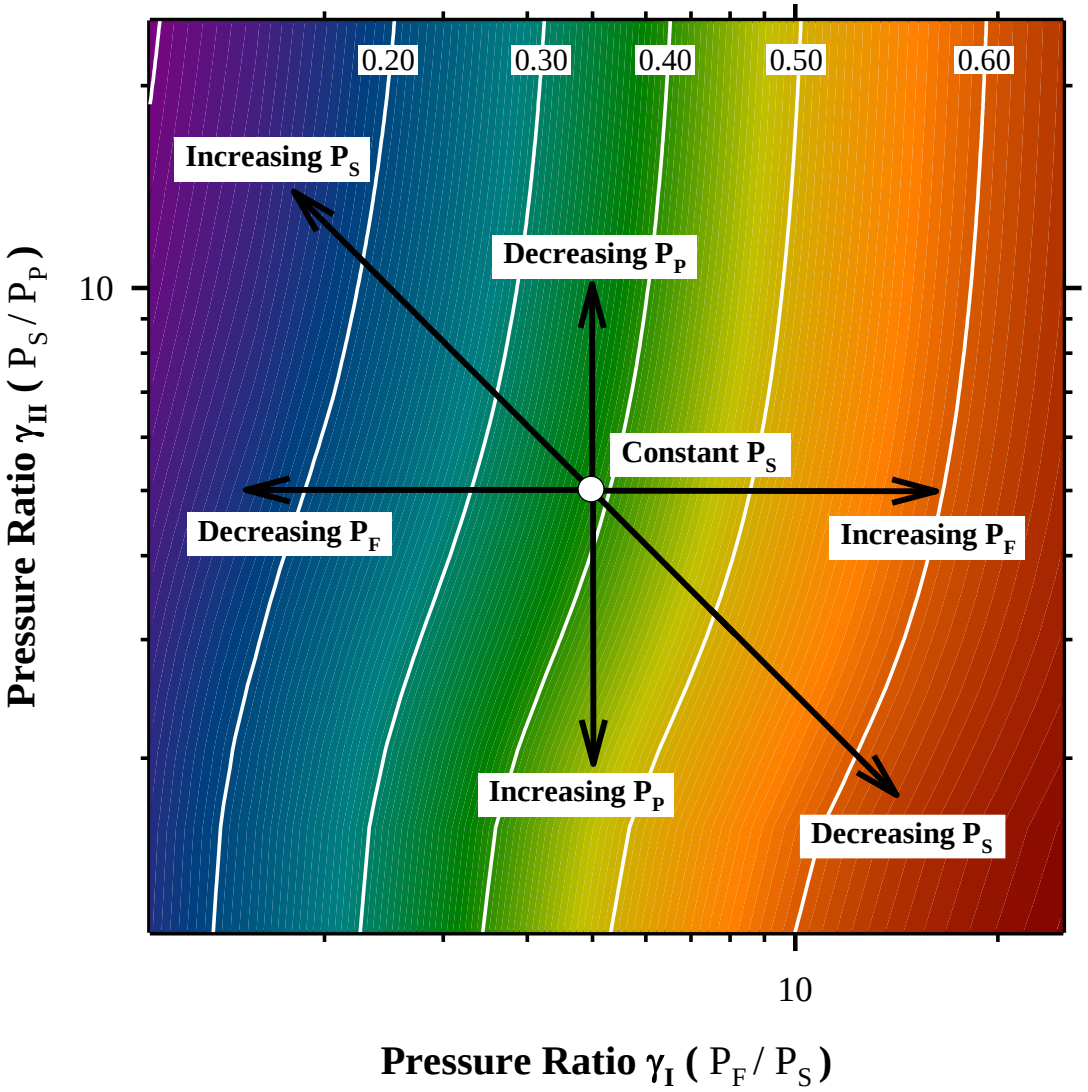

Figure 8.6 Effect of each membrane pressure ratio on the shell mole fraction of CO_2 at zero stage-cut. The shading and white lines represent contours of constant $y_S^i : \forall \gamma_{II} \in \{1..30\}$ *and* $\gamma_I \in \{1..30\}$ and the black lines represent directions of varying the specified pressure.

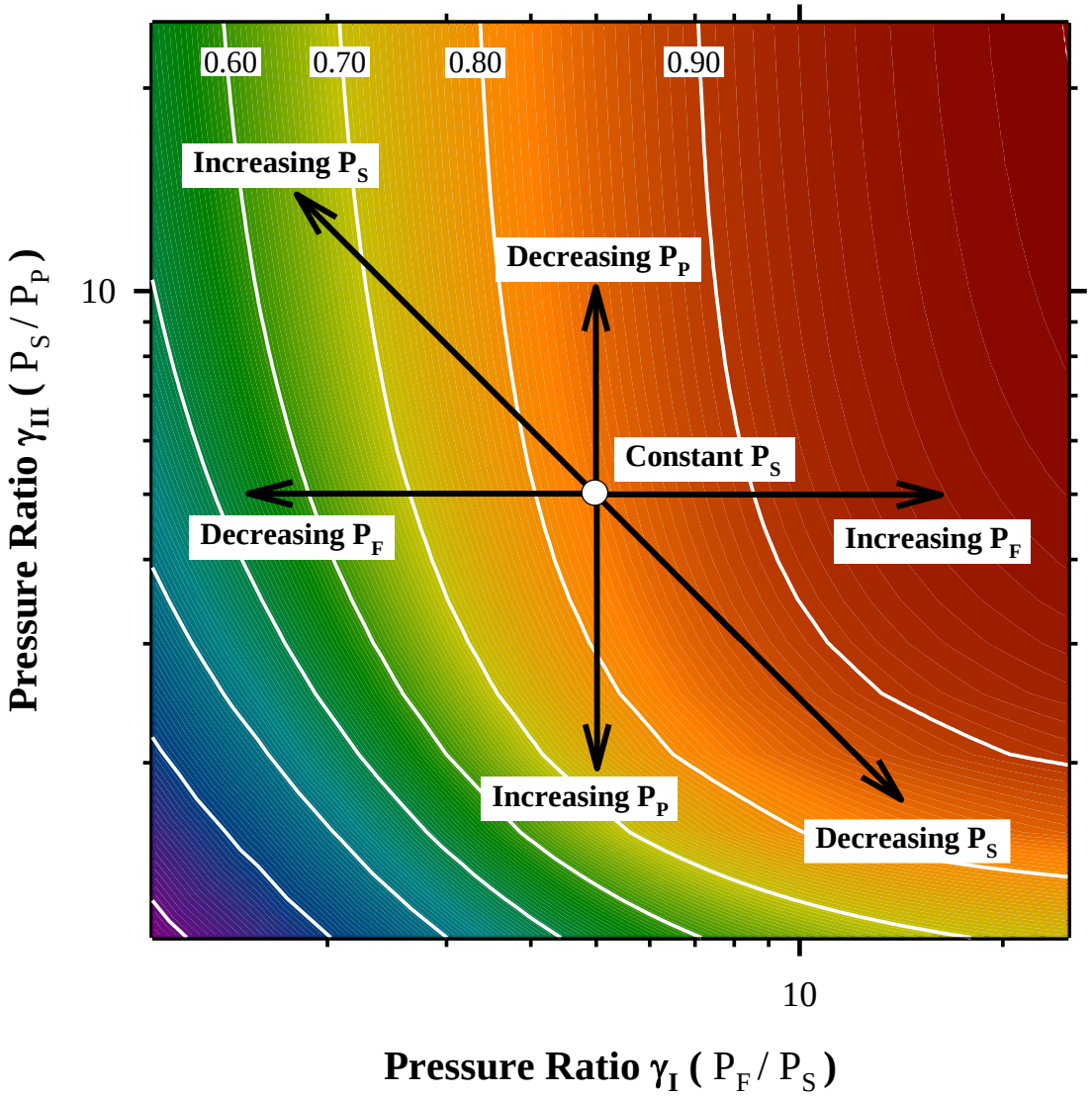

Figure 8.7 Effect of each membrane pressure ratio on the permeate mole fraction of CO_2 at zero stage-cut. The shading and white lines represent contours of constant $y_p^i : \forall \gamma_{II} \in \{1..30\}$ *and* $\gamma_I \in \{1..30\}$ and the black lines represent directions of varying the specified pressure.

and 8.7, the result is almost constant y_S^i and y_P^i. Although, controlling the permeate pressure appears to be promising, this would require the stream to operate under vacuum, since most permeators take the permeate at 1.0 atm pressure. Although an increase in the shell pressure results with decreased permeate purity, the flux through the shell-permeate membrane will increase dramatically.

Based on this information, a parametric study of a conventional, two-stage cascade, ISP and the novel IVSP permeators was conducted. The results of the study are shown in Figures 8.8 and 8.9, in terms of mole fraction CO_2 and stage-cut for the feed reject and permeate streams. The data were generated under the conditions stated in Table 8.1.

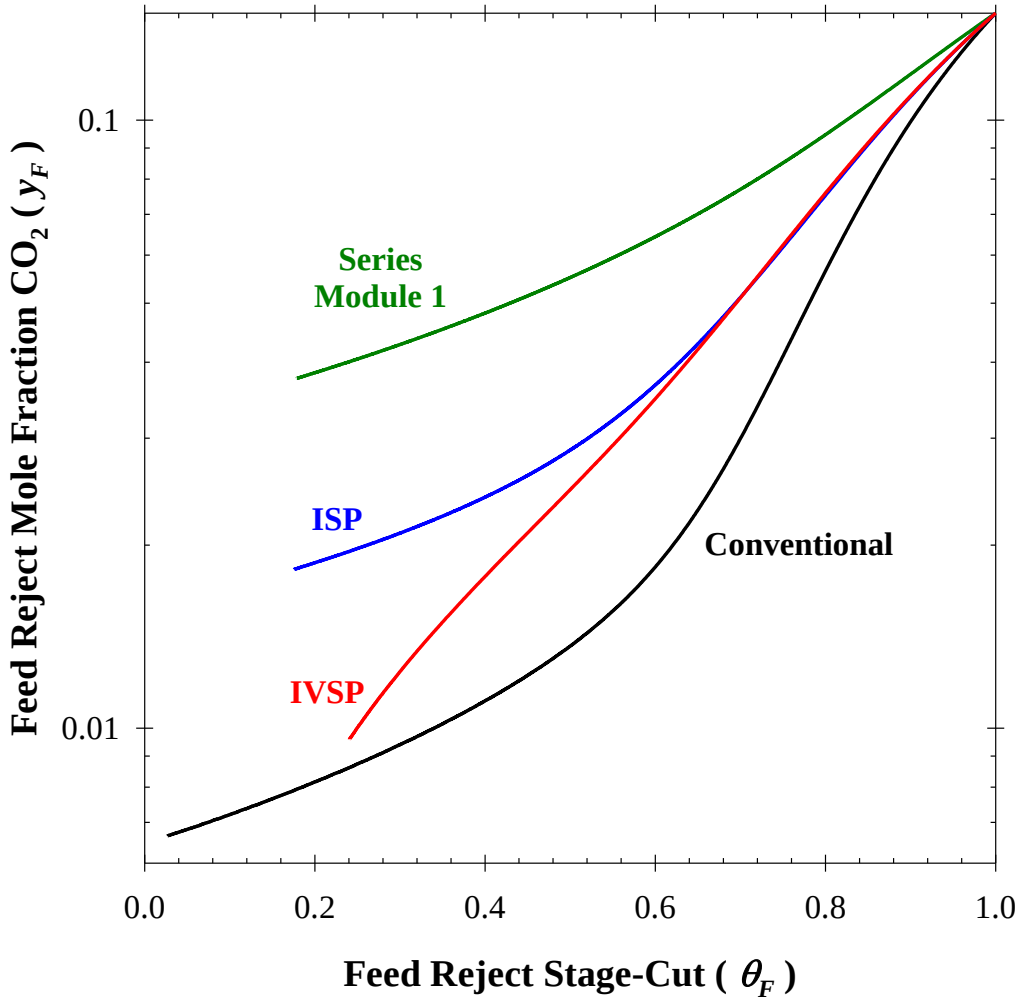

Figure 8.8 Effect of permeation area on the feed reject purity and stage-cut for $\gamma_I=\gamma_{II}=13.5$ and $P_F=25$, $P_S=5.0$ (ISP and Series) and $P_P=1.0$. Total membrane area varied from 0.0001 – 1.5 m^2 with a federate of 13 sL/min. The IVSP incorporated the linear relationship given by Eq. 8.9.

The feed reject conditions (Figure 8.8) of the conventional permeator produce the lowest purity and stage-cut, whereas the first module of the two-stage cascade produced the highest purity. In this stream, the objective would be to recover the slower (N_2) permeating

gas at high stage-cut and purity. The IVSP out-performs the ISP in this regard. The depleting characteristics of variable shell pressures are the cause of this behaviour. Whereas, when the shell pressure is constant, ISP, the permeator does not perform as well.

The effect of the pressure variation is shown in Figure 8.9 as the shell mole fraction CO_2 as a function of the shell stage-cut. In this linear pressure configuration, the IVSP is capable of reducing the shell stage-cut, to a point where the mole fraction of CO_2 is reduced to a value below that of the feed gas. This behaviour could be beneficial when used in a hybrid process, or used as a recycle to the feed stream.

The permeate stream conditions are shown in Figure 8.10. Since the ISP and the IVSP locally couple the membranes, they produce the highest purity in a single stage. The conventional permeator initially produces the lowest purities, but does perform better than the ISP (at stage-cuts above 0.20) and the two-stage cascade (at stage-cuts above 0.12). However, the internal shell pressure control of the IVSP outperforms the ISP at stage-cuts above 0.15 and performs the same as the conventional permeator at stage-cuts above 0.25.

Although the data shown in Figure 8.8 and 8.9 show that the IVSP will outperform the ISP, two stage cascade and bridge the gap between the conventional and ISP designs, it is important to note the curves were generated by varying the permeation area. Therefore, the location where the ISP curve ends is for an area of 1.5 m^2. In comparison, the IVSP at that stage-cut would require less membrane area to produce the same purity. The effect of area on the permeate recovery is shown in Figure 8.11 A and B.

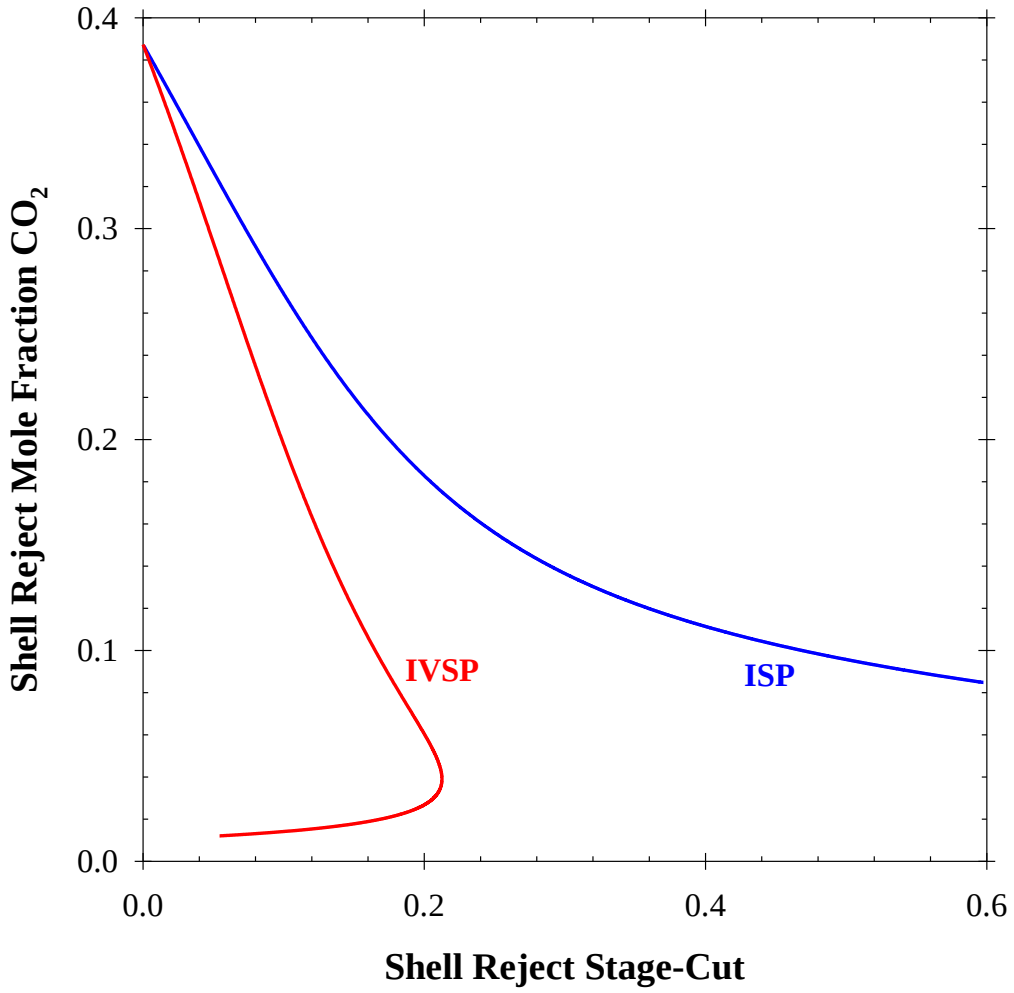

Figure 8.9 Effect of permeation area on the shell purity and stage-cut for $\gamma_I=\gamma_{II}=13.5$ and $P_F=25$, $P_S=5.0$ (ISP and Series) and $P_P=1.0$. Total membrane area varied from 0.0001 – 1.5 m^2 with a federate of 13 sL/min. The IVSP incorporated the linear relationship given by Eq. 8.9.

The data in these figures shows how the IVSP, in the simple linear pressure configuration, is capable of producing higher permeate stage-cuts and purities at a lower area to feed flowrate ratio.

Another performance indicator is the extent of separation, and is defined by as follows:

$$\zeta_P = \frac{\left(y_p - x_f\right)}{\left(x_f\left(1 - x_f\right)\right)} V_p \qquad \textbf{(8.12)}$$

This function shows effect of the permeate purity and stage-cut as a function of the feed conditions. By evaluating this value for the various feed conditions used in this study, an operating curve has been constructed for each of the modules, and is shown in Figure 8.12.

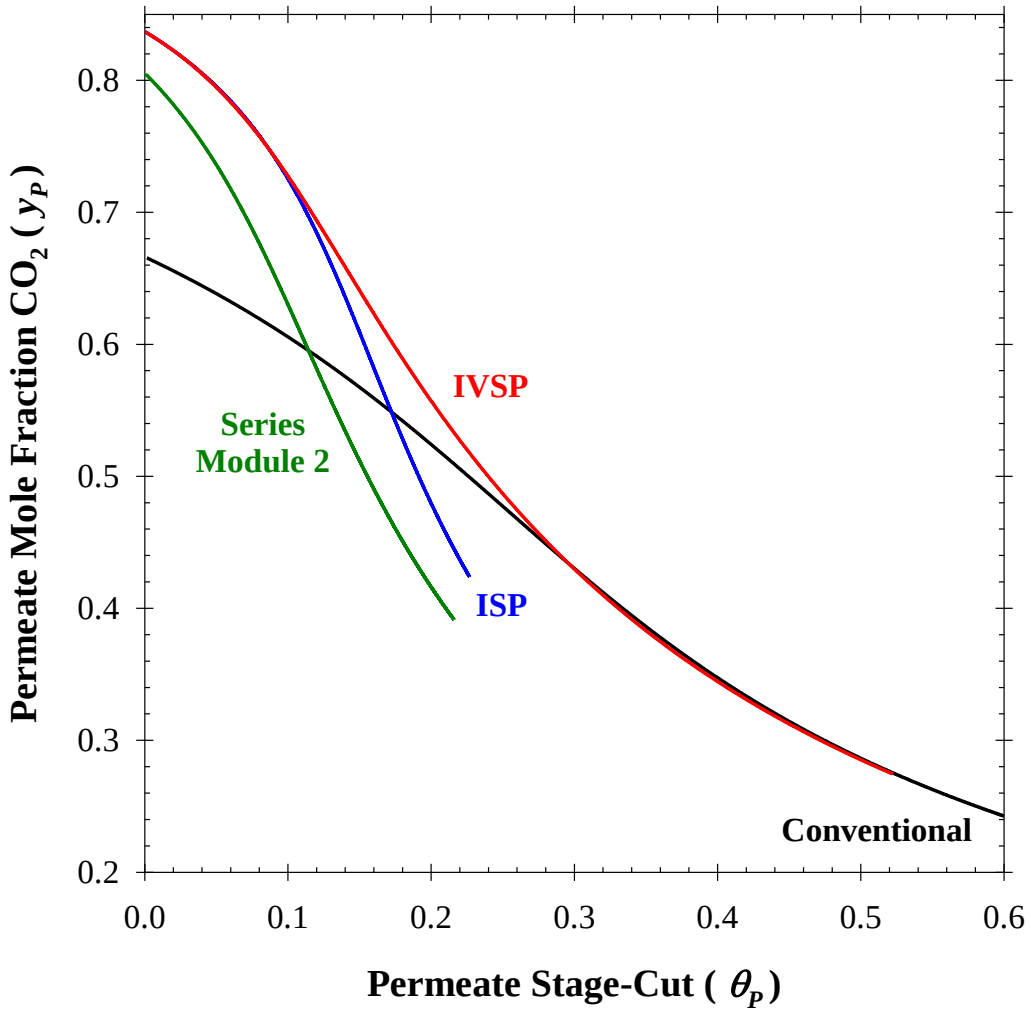

Figure 8.10 Effect of permeation area on the permeate purity-stage-cut [B] for $\gamma_I=\gamma_{II}=13.5$ and $P_F=25$, $P_S=5.0$ (ISP and Series) and $P_P=1.0$. Total membrane area varied from 0.0001 – 1.5 m^2 with a federate of 13 sL/min. The IVSP incorporated the linear relationship given by Eq. 8.9.

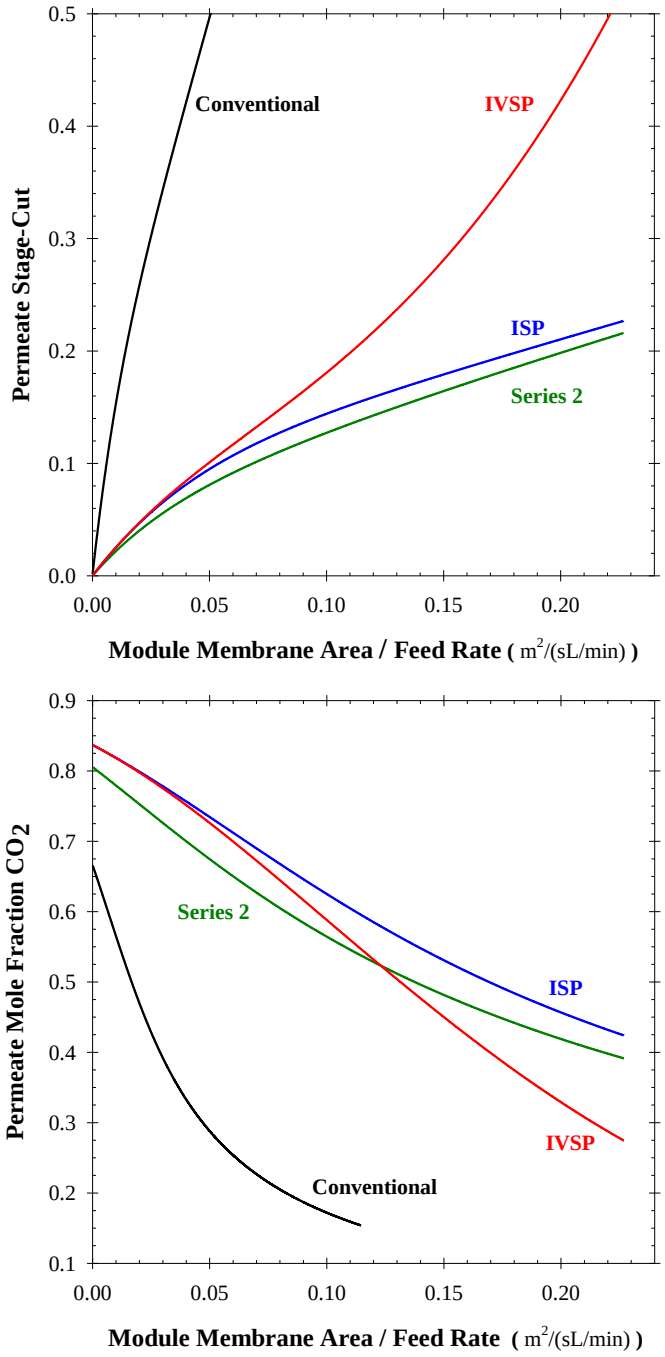

Figure 8.11 Effect of permeation area and flowrate on the permeate purity and stage-cut for $\gamma_I=\gamma_{II}=13.5$ and $P_F=25$, $P_S=5.0$ (ISP and Series) and $P_P=1.0$. Total membrane area varied from 0.0001 – 1.5 m^2 with a federate of 13 sL/min. The IVSP incorporated the linear relationship given by Eq. 8.9.

The results show that under the conditions applied, an optimal extent of separation exists for each of the modules. It is interesting to note that the optimal value for the conventional module is close to the optimal value for the IVSP. However, the IVSP does provide the highest extent of separation with a single module. However, it does require more membrane area or a lower feedrate in order to achieve this. However, recall that the

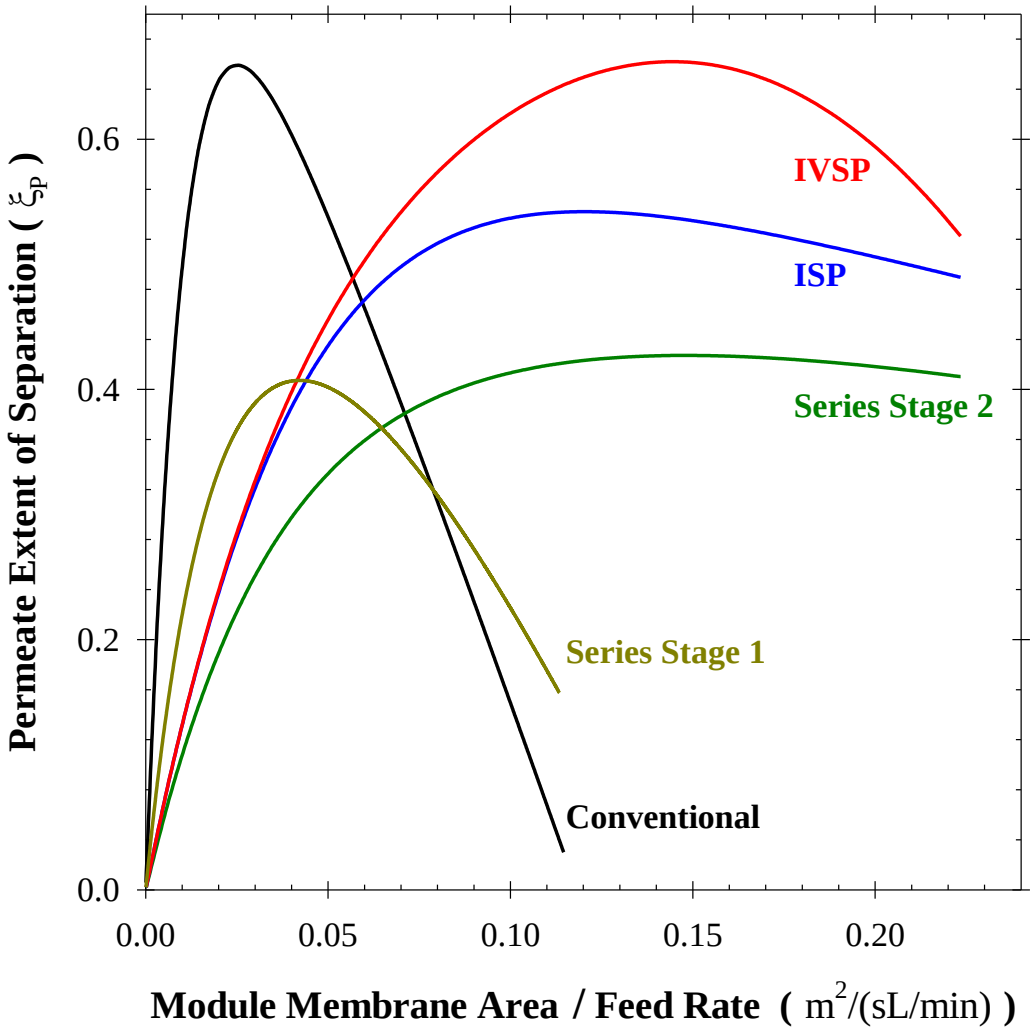

Figure 8.12 Effect of permeation area and flowrate on the extent of separation for $\gamma_I=\gamma_{II}=13.5$ and $P_F=25$, $P_S=5.0$ (ISP and Series) and $P_P=1.0$. Total membrane area varied from 0.0001 – 1.5 m^2 with a federate of 13 sL/min. The IVSP incorporated the linear relationship given by Eq. 8.9.

conventional module was modeled based on the overall pressure ratio of P_P/P_F. This does introduce a very large driving force for the permeation process, and thus the observed high flux.

8.6 - Conclusion

In this study, the effects of the internal pressure ratio on the performance of an internally staged permeator were investigated. The results were used to develop a novel dual membrane permeator, the IVSP, which controlled this ratio. Parametric analysis of the conventional, two-stage cascade, ISP, and IVSP designs proved that shell pressure control would enhance the separation capabilities of a dual membrane permeator. Further, the IVSP was also capable of producing two streams of greater purity than the ISP or two-stage cascade at all stage-cuts. The IVSP also outperformed the conventional permeator at permeate stage-cuts less than 0.25 and provided the same performance at stage-cuts above 0.25.

8.7 - References

Blaisdell, C.T., Kammermeyer, K., *Counter-Current and Co-Current Gas Separation*, Chemical Engineering Science, 28 1973

Chen, Y.S., Li, K., Teo, W.K., *Performance of Co/Counter-Current and Counter/Co-Current Flow Patterns in an Internally Staged Permeator for Gas Separation*, Trans IChemE, 73 Part A 1995

Li, K., Acharya, D.R., Hughes, R., *Simulation of Gas Separation in an Internally Staged Permeator*, Trans IChemE, 69 Part A 1991

Li, K., Teo, W.K., *Theoretical Analysis of Ternary Gas Mixture Separation in an Internally Staged Permeator*, Chemical Engineering Science, 47 1992

Li, K., Hughes, R., *Internal Staging for Membrane Gas Separation: Comparison with Conventional Membrane Permeators*, Chemical Engineering Science, 48 1993

Li, K., Lau, W. W.Y., Teo, W.K., *Theoretical and Experimental Evaluation of an Internally Multi-Staged Permeator for Oxygen Enrichment*, Chemical Engineering Science, 49 1994

Li, K., Wang D., Li, D., Teo, W.K., *Internally Staged Permeator Prepared from Annular Hollow Fibers for Gas Separation*, AIChE Journal, 44 1998

Liu, B., Wu, X., Lipscomb, G.G., Jensvold, J., *Novel Internally Staged Designs Using a Hollow Fiber Fabric*, Separation Science and Technology, 35 2000

Liu, B., Lipscomb, G.G., Jensvold, J.A., *A Comparison of Optimal Internally Staged Permeator and External Two-Stage Module Designs for O_2 Enrichment from Air*, Separation Science and Technology, 36 (11), 2001

Lim, S.P., Li, K., *Internally Staged Permeator for Gas/Vapour Separation: Effect of Annuli of Annular Hollow Fibres*, Chemical Engineering Science, 56 (12), 2001

Pan C. Y., Habgood, H.W., *An Analysis of the Single Stage Gaseous Permeation Process*, Industrial Engineering & Chemistry Fundamentals, 13 1974

Pan, C.Y., Habgood, H.W., *Gas Separation by Permeation. Part I: Calculation Methods and Parametric Analysis*, Canadian Journal of Chemical Engineering, 56 1978a

Pan, C.Y., Habgood, H.W., *Gas Separation by Permeation. Part II: Effect of Pressure Drop and Choice of Permeate Pressure*, Canadian Journal of Chemical Engineering, 56 1978b

Sidhoum, M.S., S. Majumdar, R.R. Brave, A., Sengupta, K.K. Sirkar, *Experimental Behaviour of Asymmetric CA Membranes and Its Use in a Novel Separation Schemes*, AIChE Symposium Series, 84 (261) 1988

Sidhoum, M., Majumdar, S., Sirkar, K.K., *An Internally Staged Hollow Fiber Permeator for gas Separation*, AIChE Journal, 35 1989

Sirkar, K.K., *Membrane Separation Technologies: Current Developments*, Chemical Engineering Communications, 157 1996

8.8 - Nomenclature

A	-	Membrane area	(m^2)
L	-	Flow rate	(sL/min)
P	-	Pressure	(atm)
Q	-	Permeability	(1 GPU = $10^{-6}cm^3(STP)s^{-1}cm^{-2}cmHg^{-1}$)
y	-	Mole fraction	(Dimensionless)

Greek Characters

α	-	Ideal separation factor	(Dimensionless, defined by Eq. 8.2)
γ	-	Trans-membrane pressure ratio	(Dimensionless, defined by Eq. 85.3)
Φ	-	Stage-cut	(Dimensionless, defined by Eq. 8.5)

Subscripts/Superscripts

*	-	Dimensionless
F	-	Feed
I	-	Feed-shell membrane
II	-	Shell-permeate membrane
Min	-	Minimum
Max	-	Maximum
o	-	Initial
Ov	-	Overall
P	-	Permeate
S	-	Shell

Abbreviations

Conv	-	Conventional module
ISP	-	Internally staged permeator
IVSP	-	Internal variably staged permeator
Ser1	-	Module 1 of the two-stage cascade
Ser2	-	Module 2 of the two-stage cascade

Chapter 9

Summation

9.1 – Discussion

The objective of this work was to evaluate the fundamentals of CO_2 separation technologies and provide a solution pathway for the efficient capture and recovery of carbon dioxide from various point source emitting industries. In order to realize a robust approach to advancing the solution to this global issue, the versatility of the process to the wide range of compounds contained within the stream(s) to be processed must be maintained. More specifically, the effects of water on the CO_2 capacity must be minimized.

The potential of three different process pathways to limiting and/or eliminating CO_2 emissions were identified as: 1) pre-combustion; 2) oxy combustion; and 3) post combustion. The post-combustion approach of adding additional equipment to the end of the pipe was pursued in order to limit the installation *"pain"* and process installation downtime for existing industrial emitters.

The most promising technical approaches for near term deployments are absorption (aqueous amine scrubbing), applied adsorption, and membrane based separations. As discussed in Chapters 2 and 3, all of these processes exhibit positive and negative technical features. Current industrial direction has suggested that amine scrubbing is the most promising technical solution to deploy, given the number of projects currently running or to

be deployed in the near future (as discussed in Chapter 3).

Applied adsorption and membrane based separations are both hindered by their separation media, the materials. For adsorption, the adsorbent itself is not selective enough when challenged with the compounds which are present in the actual industrial streams. This currently requires the use of single or multiple, compound specific, guard adsorption beds, and/or layered adsorbent packing's. Both of these options significantly increase the capital expenditure (CAPEX) and operating expenditure (OPEX) for these process. As a result, these processes have received very little industrial attention, and thus a very low projected adoption/integration rate for near term projects.

Membrane based separations are also greatly hindered by the membrane materials. In most cases, the membrane material may be able to handle the process streams, but at a cost of significantly increased surface area requirements to maintain the required process throughput. As a result, membrane based separation systems are also plagued with high capital expenditure (CAPEX, due to pressure requirements, number of modules) and operating expenditure (OPEX, membrane costs, compression costs). As a result, these processes have also received very little industrial attention, and thus a very low projected adoption/integration rate for near term projects.

It is clear that adsorption, membrane, and aqueous amine based processes are all feasible. However, only wet amine scrubbing appears economically viable at the current stage of development. In order to challenge this, and potentially drive the separation costs lower, this work was focused on hybridizing aqueous amine chemistry and dry adsorption based separations to produce a novel nano-porous material capable of efficient removal of CO_2 from flue gas (5% CO_2 balance N_2 with moisture).

Nano-porous, also known as meso-porous materials, have received a great amount of

development effort over the last few decades. These materials afford the potential of a tuneable pore size, uniform pore channel structure, large pore volume, and surface area. The matrices are assembled with various low cost materials, where silica represents one of these. Silica based nano-porous materials have been gaining a great deal of attention since Mobil's disclosure of MCM-41 in 1992. This novel material with straight hexagonal pores, large surface area and pore volumes, also affords a very reactive surface. The crystalline imperfections result in surface hydroxyl groups which, under the right conditions, are very reactive to surface condensation reactions. Sayari's research group (University of Ottawa) further enhanced this MCM-41 material via a post synthesis pore expansion process. The novel material termed, PE-MCM-41 in this work, exhibited the attractive features of the base material MCM-41, but with exceptionally higher pore volume and pore diameter possibilities. These features were shown to be tuneable based on the swelling agent selection for the post synthesis expansion process, with pore diameters up to 30 nm possible. As a result, PE-MCM-41 was selected for this work as the base support to examine the combination of aqueous amine scrubbing with dry adsorption.

In order to combine aqueous amine scrubbing with dry adsorption, a few approaches were considered and evaluated. These included, amine impregnated within the vast pore volume of PE-MCM-41, surface grafting of various amino silane compounds, and finally, a novel approach of volume based amine functionalization (3D grafting).

The materials produced via amine impregnation exhibited high CO_2 adsorption at reasonable high uptake rates. The most important advancement of this material was its ability to increase the CO_2 capacity, by about 10%, when challenged with humid streams. All other zeolite based adsorbents exhibit a significantly reduced or zero CO_2 capacity in the presence of moisture. Further, the amine impregnated materials did not exhibit any measurable adsorption

capacity for the proxy carrier, N_2. Whereas, most zeolites exhibit some N_2 adsorption capacity.

While this material appeared promising, it also exhibited a loss of impregnated amine over time, and thus long term stability could be questionable. Since the intent of hybridizing aqueous amine scrubbing with dry adsorption was to eliminate the issues which arise from aqueous processing with high pH amine solutions, this loss of amine could result in long term risks with safety, materials of construction, and operability.

In order to address the issues exhibited with amine impregnated within nano-porous silica materials, the more robust method of surface functionalization was examined in detail. The typical art in the field, at the time of this work, was to perform surface functionalization in a very controlled anhydrous manner. This would typically result in a uniform grafted mono-layer of the active group. In this work, mono, di, and tri-amino compounds were tethered to the surface of MCM-41 and PE-MCM-41, under controlled anhydrous conditions, as discussed in Chapters 5, and 6. The results proved that a high quantity of amine content could be obtained with MCM-41, but, higher quantities could be obtained with PE-MCM-41. The resulting materials exhibited a very high rate of CO_2 adsorption relative to zeolite 13X, and the impregnated amine materials presented in Chapter 4.

These amino grafted materials where extremely stable within the feed temperature range of interest (20 – 150 °C). An unexpected result observed with these materials, was the desorption response to a mild thermal pulse. As shown in Chapter 5, when CO_2 was adsorbed at 25 °C, and exposed to 75 °C thermal pulse, almost full equilibrium capacity cyclic adsorption could be realized. However, even with these desirable adsorbent characteristics, the equilibrium adsorption capacity was still too low. For dry CO_2 streams, zeolite 13X still exhibited a higher adsorption capacity. Since the objective of this work to develop a material with a high CO_2 capacity which exceeds all known materials, and not a perfect, predictable

mono-layer, other approaches were sought.

In order to probe the capabilities of this family of grafted silicas further, the concept of 3D grafting was conceptualized. Unlike the water aided mono-layer grafted described by Feng et al., (1997) and Liu et al., (1998), this concept was extended to exploit the pore volume of the PE-MCM-41 supports. The process of grafting the amine functional group to the surface of the silica, a condensation reaction occurs between the methoxy ligands and the surface crystalline defects, the hydroxyl groups. By facilitating the reaction in the aqueous phase, rather than just the surface, a 3D structure was formed. This was achieved by means of partial condensation of the methoxy ligands with an adjacent methoxy ligand from another molecule also in the aqueous phase. While, it was not determined to what extent this aqueous phase condensation (polymerization) reaction occurred, it was speculated that at least one and at most two ligands could condense with the surface, leaving one ligand free to branch into the pore volume, as discussed in Chapter 7.

The results of this modified and optimized grafting procedure (Chapters 6 and 7) resulted in an unprecedented CO_2 adsorption capacity when challenged with 5% CO_2 in N_2 at 1.0 atm total pressure and 25 °C. The equilibrium adsorption capacity was now equal to zeolite 13X for some grafted functional groups, and superior for the optimally grafted TRI-PE-MCM-41 material. The adsorption rate was also far superior with this novel material than zeolite 13X. In an applied process, the very rapid rate of adsorption could translate into a smaller adsorbent mass requirements for the equivalent dry CO_2 removal rate relative to the zeolite 13X performance standard, and thus lower CAPEX. Alternatively, the economically attractive rapid pressure swing adsorption process could be realized, thus lower CAPEX and OPEX.

The TRI-PE-MCM-41 material was also fully stable within the temperature range of

interest (20 – 150 °C). The amount of amine loaded, determined by thermogravimetric analysis, was also unprecedented and determined to equal approximately 8 mol(N)/kg_{ads} (moles of Nitrogen per kilogram of final adsorbent mass).

However, the amine efficiency appeared low, with performance in the 0.20-0.35 (mol(CO_2)/mol(N)) range relative to the stoichiometric ratio of 0.50 (mol(CO_2)/mol(N)). However, this range of amine efficiency has also been observed by many other research groups as discussed in Chapter 7.

A similar humid CO_2 adsorption performance was also observed with the wet grafted material relative to the dry grafted material. A nominal, 10% increase in CO_2 adsorption capacity was measured. This was in addition to the uptake of water.

Overall, a novel amine bearing nano-porous silica based adsorbent was developed and shown to exhibit superior adsorption characteristics relative to all other disclosed adsorbents in the open literature. In recent review by Chen et al., (2014), of amine functionalized nano-porous materials, the optimized TRI-PE-MCM-41 adsorbent developed in this work still outperforms all other silica based amine grafted materials discussed by Chen et al., (2014) under the same processing conditions of 5% CO_2 in N_2, with and without moisture, at 1.0 atm total pressure and 25 °C.

Work has continued on this family of materials with the research group led by Sayari (University of Ottawa). Since the original publication of this novel adsorbent in 2007, 36 additional journal articles have been published by his group as related to the continuation of this work. These have ranged from amine stability – both structural and chemical, insights into effects of moisture, applied adsorption process evaluations – breakthrough curves in pilot scale units, simultaneous H_2S and CO_2 removal, VOC removal, binary mixture adsorption studies (CH_4, CO_2, N_2, H_2, and O_2), base catalysis, and aqueous phase copper removal.

One interesting result of the various studies was discussed by Sayari et al., (2012) about CO_2 induced degradation of the functionalized amine group. They concluded that some amine functionality would be reduced upon introduction of dry CO_2 gas through the creation of stable urea linkages. They conclude that using a humid stream of CO_2 or regeneration gases will eliminate this reaction pathway and provide for very long term stable adsorbent. This concept although not stated in this work to relate to long term amine stability, (see Chapter 7, pg 137-138), was actually employed in this work, and thus the most likely reason for not observing a loss of amine stability, as reported by others.

The development of a novel moisture tolerant, stable adsorbent for CO_2 capture was demonstrated in Chapters 4-7. Even though these materials have demonstrated characteristics attractive for applied adsorption process deployment, consideration was also given to the improvements of membrane based separations.

As discussed in Chapter 8, it is apparent that the current limitations are the membrane material costs required to achieve a specific degree of separation. Typically, multi-staged membrane permeators (operated in parallel, series, or combinations thereof) are required in order to produce the product specifications in terms of purity and flowrate (stage-cut). This results in an increase in CAPEX and OPEX due to re compression and additional units. In Chapter 8 the concept of an internally variably staged permeator was introduced to reduce these issues. A theoretical model was developed and used as the basis for simulation studies. The advantage of the internal variably staged design was shown to permit a very high extent of separation similar to a two stage permeator for purity, while maintaining similar flux rates as per a single stage permeator. This IVSP concept has also taken existing membrane materials and mechanically translated their process performance to a higher level. As such, the unit should prove effective for front end process stream cleanup requirements prior to an

adsorption process with the novel TRI-PE-MCM-41 nano-porous adsorbent.

9.2 – Conclusions

The research project involved several segments. These segments included novel nano-porous materials modification/engineering for CO_2 adsorption, and membrane module development. The following conclusions have been reached:

- Nano-porous silica material PE-MCM-41 can be impregnated with a large quantity of aqueous amine compounds. This enabled the vast quantity of amine groups to be considered for process applications in an adsorption process rather than the challenging aqueous absorption process.
- The CO_2 capacity and uptake rate of the DEA-impregnated PE-MCM-41 reached maximum values at loading levels slightly exceeding pore saturation.
- The CO_2/DEA ratio did not reach the stoichiometric maximum, i.e., 0.5 under dry conditions, due at least partly to deactivation of a portion of the DEA through interactions with the support surface.
- Compared to zeolite 13X, the amine-impregnated adsorbent had superior adsorption capacity below a CO_2 partial pressure of 0.15 atm with similar adsorption kinetics.
- Although the presence of moisture did not improve the performance of the impregnated adsorbent, it did not hinder it as was observed with zeolite 13X.
- Diethanolamine (DEA) impregnated PE-MCM-41 is not cyclically stable for long term use.
- The optimal reaction temperature for amine grafting was found to be 85 °C, which was significantly lower than the temperature of 110 °C typically applied when

grafting with toluene as the solvent

- In comparison to the dry grafting procedure, the wet technique afforded a 33% increase in total amine content and a 43% increase in active amine content, i.e., CO_2/N molar ratio, resulting in a 90% overall improvement
- Water aided amine functionalization of PE-MCM-41 is proposed to result in a 3D structure assembled with the pore volume of the material.
- TRI-PE-MCM-41 will exhibit a dry CO_2 adsorption capacity which is approximately 15-20% higher than the best zeolite CO_2 adsorbent, 13X, with a 5% CO_2 in N_2 stream at 1.0 atm total pressure and 25 °C.
- In the presence of moisture the CO_2 adsorption capacity increased by approximately 10%, whereas the zeolite 13X exhibited no CO_2 adsorption capacity.
- Further review since 2007 has shown that the wet grafted TRI-PE-MCM-41 has still not been surpassed in CO_2 capacity at 25 C, and upto 1 atmosphere pressure
- Parametric analysis of the conventional, two-stage cascade, ISP, and IVSP designs proved that shell pressure control via the IVSP design could enhance the separation capabilities of a dual membrane permeator
- The IVSP should be capable of producing two streams of greater purity than the ISP or two-stage cascade at all stage-cuts
- The IVSP also outperformed the conventional permeator at permeate stage-cuts less than 0.25 and provided the same performance at stage-cuts above 0.25

9.3 – Recommendations

A considerable amount of work has been completed in recent years with respect to amine grafted mess-porous silicas. However, the following work should be undertaken in order to push this novel technology into the industrial domain.

- Measure the effects of adsorption temperature and pressure on CO_2 adsorption characteristics. This should include pressures up to 15 bar and 150 °C.

- Measure the adsorption mass transfer rates as a function of temperature and pressure, as above.

- Measure the pure component, binary, tertiary, etc… Component isotherms for the other major components usually contained within flue gas; NO_x, SO_x, H_2S, CO, VOC's.

- Parametrically evaluate the applied adsorption processes of PSA, TSA, VSA, and combinations thereof, in order to determine the optimal mode of operation.

- Perform in depth economic evaluation of the processes.

- Construct and test the IVSP for CO_2 separations.

9.4 - References

Ahmadalinezhad, A., Tailor, R., Sayari, A., *Molecular-Level Insights into the Oxidative Degradation of Grafted Amines*, Chemistry - A European Journal, 19 (32), 2013

Ahmadalinezhad, A., Sayari, A., *Oxidative Degradation of Silica-Supported Polyethylenimine for CO_2 Adsorption: Insights into the Nature of Deactivated Species*, Physical Chemistry Chemical Physics, 16 (4), 2014

Ahmadalinezhad, A., Tailor, R., Sayari, A., *Molecular-Level Insights into the Oxidative Degradation of Grafted Amines*, Chemistry - A European Journal, 19 (32), 2013

Belmabkhout, Y., Heymans, N., De Weireld, G., Sayari, A., *Simultaneous Adsorption of H_2S and CO_2 on Triamine-Grafted Pore-Expanded Mesoporous MCM-41 Silica*, Energy and Fuels, 25 (3), 2011A

Belmabkhout, Y., Serna-Guerrero, R., Sayari, A., *Adsorption of CO_2-Containing Gas Mixtures over Amine-Bearing Pore-Expanded MCM-41 Silica: Application for CO_2 Separation*, Adsorption, 17 (2), 2011B

Belmabkhout, Y., Serna-Guerrero, R., Sayari, A., *Adsorption of CO_2-Containing Gas Mixtures over Amine-Bearing Pore-Expanded MCM-41 Silica: Application for Gas Purification*, Industrial and Engineering Chemistry Research, 49 (1), 2010A

Belmabkhout, Y., Serna-Guerrero, R., Sayari, A., *Amine-Bearing Mesoporous Silica for CO_2 Removal from Dry and Humid Air*, Chemical Engineering Science, 65 (11), 2010B

Belmabkhout, Y., Sayari, A., *Isothermal versus Non-Isothermal Adsorption-Desorption Cycling of Triamine-Grafted Pore-Expanded MCM-41 Mesoporous Silica for CO_2 Capture From Flue Gas*, Energy and Fuels, 24 (9), 2010

Belmabkhout, Y., De Weireld, G., Sayari, A., *Amine-Bearing Mesoporous Silica for CO_2 and H_2S Removal from Natural Gas and Biogas*, Langmuir, 25 (23), 2009A

Belmabkhout, Y., Serna-Guerrero, R., Sayari, A., *Adsorption of CO_2 from dry gases on MCM-41 silica at ambient temperature and high pressure. 1: Pure CO_2 adsorption*, Chemical Engineering Science, 64 (17), 2009B

Belmabkhout, Y., Sayari, A., *Adsorption of CO_2 from dry gases on MCM-41 silica at ambient temperature and high pressure. 2: Adsorption of CO_2/N_2, CO_2/CH_4 and CO_2/H_2 binary mixtures*, Chemical Engineering Science, 64 (17), 2009A

Belmabkhout, Y., Sayari, A., *Effect of pore expansion and amine functionalization of mesoporous silica on CO_2 adsorption over a wide range of conditions*, Adsorption, 15 (3), 2009B

Chen, C., Kim, J., and Ahn, W., *CO_2 Capture by Amine-Functionalized Nanoporous Materials: A Review*, Korean Journal of Chemical Engineering, 31 (11), 2014

Da'Na, E., Sayari, A., *Modeling Adsorption of Copper on Amine-Functionalized SBA-15: Predicting Breakthrough Curves*, Journal of Environmental Engineering (United States), 139 (1), 2013

Da'na, E., Sayari, A., *Optimization of Copper Removal Efficiency by Adsorption on Amine-Modified SBA-15: Experimental Design Methodology*, Chemical Engineering Journal, 167 (1), 2011A

Da'na, E., Sayari, A., *Adsorption of Heavy Metals on Amine-Functionalized SBA-15 Prepared by Co-Condensation: Applications to Real Water Samples*, Desalination, 285, 2011B

Da'na, E., Sayari, A., *Effect of Regeneration Conditions on the Cyclic Performance of Amine-Modified SBA-15 for Removal of Copper from Aqueous Solutions: Composite Surface Design Methodology*, Desalination, 277 (1-3), 2011C

Da'na, E., De Silva, N., Sayari, A., *Adsorption of Copper on Amine-Functionalized SBA-15 Prepared by Co-Condensation: Kinetics Properties*, Chemical Engineering Journal, 166 (1), 2011

De Canck, E., Ascoop, I., Sayari, A., Van Der Voort, P., *Periodic Mesoporous Organosilicas Functionalized with a Wide Variety of Amines for CO_2 Adsorption*, Physical Chemistry Chemical Physics, 15 (24), 2013

Heydari-Gorji, A., Sayari, A., *Thermal, Oxidative, and CO_2-Induced Degradation of Supported Polyethylenimine Adsorbents*, Industrial and Engineering Chemistry Research, 51 (19), 2012

Heydari-Gorji, A., Belmabkhout, Y., Sayari, A., *Polyethylenimine-Impregnated Mesoporous Silica: Effect of Amine Loading and Surface Alkyl Chains on CO_2 Adsorption*, Langmuir, 27 (20), 2011A

Heydari-Gorji, A., Belmabkhout, Y., Sayari, A., *Degradation of Amine-Supported CO_2 Adsorbents in the Presence of Oxygen-Containing Gases*, Microporous and Mesoporous Materials, 145 (1-3), 2011B

Heydari-Gorji, A., Yang, Y., Sayari, A., *Effect of the Pore Length on CO_2 Adsorption Over Amine-Modified Mesoporous Silicas*, Energy and Fuels, 25 (9), 2011C

Heydari-Gorji, A., Sayari, A., *CO_2 Capture on Polyethylenimine-Impregnated Hydrophobic Mesoporous Silica: Experimental and Kinetic Modeling*, Chemical Engineering Journal, 173 (1), 2011

Sayari, A., Belmabkhout, Y., Da'Na, E., *CO_2 Deactivation of Supported Amines: Does the Nature of Amine Matter?*, Langmuir, 28 (9), 2012

Sayari, A., Heydari-Gorji, A., Yang, Y., *CO_2-Induced Degradation of Amine-Containing Adsorbents: Reaction Products and Pathways*, Journal of the American Chemical Society, 134 (33), 2012

Sayari, A., Belmabkhout, Y., Serna-Guerrero, R., *Flue Gas Treatment via CO_2 Adsorption*, Chemical Engineering Journal, 171 (3), 2011

Sayari, A., Belmabkhout, Y., *Stabilization of Amine-Containing CO_2 Adsorbents: Dramatic Effect of Water Vapor*, Journal of the American Chemical Society, 132 (18), 2010

Sayari, A., Shee, D., Al-Yassir, N., Yang, Y., *Catalysis over Pore-Expanded MCM-41 Mesoporous Materials*, Topics in Catalysis, 53 (3-4), 2010

Serna-Guerrero, R., Belmabkhout, Y., Sayari, A., *Triamine-Grafted Pore-Expanded Mesoporous Silica for CO_2 Capture: Effect of Moisture and Adsorbent Regeneration Strategies*, Adsorption, 16 (6), 2010A

Serna-Guerrero, R., Belmabkhout, Y., Sayari, A., *Influence of Regeneration Conditions on the Cyclic Performance of Amine-Grafted Mesoporous Silica for CO_2 Capture: An Experimental and Statistical Study*, Chemical Engineering Science, 65 (14), 2010B

Serna-Guerrero, R., Belmabkhout, Y., Sayari, A., *Modeling CO_2 Adsorption on Amine-Functionalized Mesoporous Silica: 1. A Semi-Empirical Equilibrium Model*, Chemical Engineering Journal, 161 (1-2), 2010C

Serna-Guerrero, R., Belmabkhout, Y., Sayari, A., *Further Investigations of CO_2 Capture Using Triamine-Grafted Pore-Expanded Mesoporous Silica*, Chemical Engineering Journal, 158 (3), 2010D

Serna-Guerrero, R., Sayari, A., *Modeling Adsorption of CO_2 on Amine-Functionalized Mesoporous Silica. 2: Kinetics and Breakthrough Curves*, Chemical Engineering Journal, 161 (1-2), 2010

Serna-Guerrero, R., Da'na, E., Sayari, A., *New insights into the interactions of CO_2 with amine-functionalized silica*, Industrial and Engineering Chemistry Research, 47 (23), 2008

Tailor, R., Ahmadalinezhad, A., Sayari, A., *Selective Removal of SO_2 Over Tertiary Amine-Containing Materials*, Chemical Engineering Journal, 240, 2014

Tailor, R., Abboud, M., Sayari, A., *Supported polytertiary amines: Highly Efficient and Selective SO_2 Adsorbents*, Environmental Science and Technology, 48 (3), 2014

Appendix A

Publication Copyright Notices

As pertaining to the articles used in this Dissertation

PAGE 201 - As printed from ACS website:
http://pubs.acs.org/userimages/ContentEditor/1218205107465/dissertation.pdf
on April 26, 2015

PAGE 202 - As printed from Elsevier website:
http://www.elsevier.com/about/policies/article-posting-policy#published-journal-article
on April 26, 2015

American Chemical Society's Policy on Theses and Dissertations

If your university requires you to obtain permission, you must use the RightsLink permission system.
See RightsLink instructions at http://pubs.acs.org/page/copyright/permissions.html.

This is regarding request for permission to include **your** paper(s) or portions of text from **your** paper(s) in your thesis. Permission is now automatically granted; please pay special attention to the **implications** paragraph below. The Copyright Subcommittee of the Joint Board/Council Committees on Publications approved the following:

Copyright permission for published and submitted material from theses and dissertations
ACS extends blanket permission to students to include in their theses and dissertations their own articles, or portions thereof, that have been published in ACS journals or submitted to ACS journals for publication, provided that the ACS copyright credit line is noted on the appropriate page(s).

Publishing **implications** of electronic publication of theses and dissertation material
Students and their mentors should be aware that posting of theses and dissertation material on the Web prior to submission of material from that thesis or dissertation to an ACS journal may affect publication in that journal. Whether Web posting is considered prior publication may be evaluated on a case-by-case basis by the journal's editor. If an ACS journal editor considers Web posting to be "prior publication", the paper will not be accepted for publication in that journal. If you intend to submit your unpublished paper to ACS for publication, check with the appropriate editor prior to posting your manuscript electronically.

Reuse/Republication of the Entire Work in Theses or Collections: Authors may reuse all or part of the Submitted, Accepted or Published Work in a thesis or dissertation that the author writes and is required to submit to satisfy the criteria of degree-granting institutions. Such reuse is permitted subject to the ACS' "Ethical Guidelines to Publication of Chemical Research" (http://pubs.acs.org/page/policy/ethics/index.html); the author should secure written confirmation (via letter or email) from the respective ACS journal editor(s) to avoid potential conflicts with journal prior publication*/embargo policies. Appropriate citation of the Published Work must be made. If the thesis or dissertation to be published is in electronic format, a direct link to the Published Work must also be included using the ACS Articles on Request author-directed link – see http://pubs.acs.org/page/policy/articlesonrequest/index.html

* Prior publication policies of ACS journals are posted on the ACS website at
http://pubs.acs.org/page/policy/prior/index.html

If your paper has **not** yet been published by ACS, please print the following credit line on the first page of your article: "Reproduced (or 'Reproduced in part') with permission from [JOURNAL NAME], in press (or 'submitted for publication'). Unpublished work copyright [CURRENT YEAR] American Chemical Society." Include appropriate information.

If your paper has already been published by ACS and you want to include the text or portions of the text in your thesis/dissertation, please print the ACS copyright credit line on the first page of your article: "Reproduced (or 'Reproduced in part') with permission from [FULL REFERENCE CITATION.] Copyright [YEAR] American Chemical Society." Include appropriate information.

Submission to a Dissertation Distributor: If you plan to submit your thesis to UMI or to another dissertation distributor, you should not include the unpublished ACS paper in your thesis if the thesis will be disseminated electronically, until ACS has published your paper. After publication of the paper by ACS, you may release the entire thesis (**not the individual ACS article by itself**) for electronic dissemination through the distributor; ACS's copyright credit line should be printed on the first page of the ACS paper.

10/10/03, 01/15/04, 06/07/06, 04/07/10, 08/24/10, 02/28/11

Sharing

Authors who publish in Elsevier journals can share their research by posting a free draft copy of their article to a repository or website. Researchers who have subscribed access to articles published by Elsevier can share too. There are some simple guidelines to follow, which vary depending on the article version you wish to share.

Help and Support

- Please see our FAQs for further information or download the policy handout (PDF)
- If you are a hosting platform please see our hosting policy
- For questions about permissions please contact the Permissions Helpdesk

Preprint	Accepted Manuscript	Published journal article

Published Journal Article (PJA)

Policies for sharing published journal articles differ for subscription and gold open access articles:

Subscription articles:

- If you are an author, please share a link to your article rather than the full-text. Millions of researchers have access to the formal publications on ScienceDirect, and so links will help your users to find, access, cite, and use the best available version.
- Theses and dissertations which contain embedded PJAs as part of the formal submission can be posted publicly by the awarding institution with DOI links back to the formal publications on ScienceDirect .
- If you are affiliated with a library that subscribes to ScienceDirect you have additional private sharing rights for others' research accessed under that agreement. This includes use for classroom teaching and internal training at the institution (including use in course packs and courseware programs), and inclusion of the article for grant funding purposes.
- Otherwise sharing is by agreement only.

Gold open access articles:

- May be shared according to the author-selected end-user license and should contain a CrossMark logo, the end user license, and a DOI link to the formal publication on ScienceDirect.

Appendix B

Publications: Front Page

As pertaining to the articles used in this Dissertation

Ind. Eng. Chem. Res. **2005,** *44,* 8007−8013 **8007**

Applications of Pore-Expanded Mesoporous Silica. 2. Development of a High-Capacity, Water-Tolerant Adsorbent for CO_2

Robert S. Franchi,[†,‡] Peter J. E. Harlick,[†,‡] and Abdelhamid Sayari[*,†,‡,§]

Centre for Catalysis Research and Innovation (CCRI), Department of Chemistry, University of Ottawa, 10 Marie Curie, Ottawa, Ontario, Canada K1N 6N5, and Department of Chemical Engineering, University of Ottawa, 161 Louis Pasteur, Ottawa, Ontario, Canada K1N 6N5

A novel high-capacity, water-tolerant adsorbent for CO_2 was developed. It consisted of diethanolamine (DEA) loaded pore-expanded MCM-41 silica (PE-MCM-41). Due to its very large pore volume, PE-MCM-41 silica was capable of accommodating a greater quantity of amine resulting in higher CO_2 adsorption capacity compared to the other supports including activated carbon, silica gel, and standard MCM-41 silica. Adsorption measurements were conducted by gravimetry using dry CO_2 to obtain uptake curves and apparent rate data. The capacity and uptake rate reached maxima with respect to amine content and then declined due to the deposition of excess amine on the particle's external surface and within the interparticle voids. At CO_2 partial pressures below 0.15 atm, the current DEA loaded PE-MCM-41 adsorbent was found to be superior to the more conventional zeolite 13X. Adsorption studies with humid CO_2 revealed that the adsorption capacity of the PE-MCM-41-based material was insensitive to the presence of moisture, which represents a major advantage over zeolite 13X. Repeated adsorption−desorption cycles revealed that our novel adsorbent exhibited good cyclic stability.

Introduction

Carbon dioxide is a ubiquitous species that has received much attention recently particularly because of its greenhouse gas effect. Concerns over global warming have caused governments to enact regulations aimed at decreasing emissions of CO_2 to the atmosphere caused largely by industrial manufacturing and stationary power sources.[1] Whether because of environmental constraints or technical reasons, various industries are faced with the task of removing CO_2 from gas mixtures containing a wide range of species in different concentrations. The space industry and military establishments require the removal of CO_2 from enclosed areas[2−5] such as space shuttles and submarines. The natural gas processing and fuel cell industries require CO_2 to be removed from gaseous fuel sources to increase the purity and energy density of the feedstock.[6−10]

Amine−CO_2 chemistry has been employed for decades as a method to selectively remove CO_2 from such gas streams, mainly in the form of gas−liquid absorption columns. Aqueous solutions of monoethanolamine (MEA), diethanolamine (DEA), and methyldiethanolamine (MDEA) are commonly used absorbents.[11] Though these systems are effective, they suffer from numerous drawbacks such as corrosion, high energy consumption,[11] and limited amine concentration in the aqueous phase due to viscosity and foaming issues.

To remedy these problems, recent research has focused on gas−solid adsorption as a promising alternative separation technique. Various zeolitic and non zeolitic adsorbents have been examined; however, many of the adsorbents developed thus far suffer from problems such as low capacity, poor selectivity, poor tolerance to water, and high-temperature regeneration or activation. An example of a commercialized adsorbent for CO_2 removal from gas streams is zeolite 13X. When used for CO_2 separation, this adsorbent requires very stringent moisture control in the inlet gas stream due to its high affinity and adsorption capacity for water. When exposed to water, the material should be regenerated at temperatures between 300 and 400 °C to retain its high CO_2 adsorption capacity.

The idea of combining amines with solid supports to afford CO_2 adsorbents has been examined by several groups.[4,5,9−10,12−15] The materials were prepared either by grafting of amine-containing alkoxysilanes onto the surface of the support or by deposition of amine-containing molecules onto the support. Common problems encountered when developing amine loaded solid supports are low capacity for CO_2 due the limited quantity of amine retained on the support, operation in a narrow temperature range, and poor thermal stability (i.e., volatility). The rate and capacity of CO_2 adsorption on such adsorbents depend chiefly on the amine loading and the porosity of the material, which are not completely independent since higher amine loadings may be obtained with higher pore volumes. To achieve this goal of dry CO_2 scrubbing (absorption−adsorption hybrid), we used as a support a periodic mesoporous silica whose pores have been further expanded through postsynthesis treatment as described elsewhere by Sayari et al.[16−21] As shown in Figure 1, the PE-MCM-41 silica used in this study was prepared using a two-step methodology consisting of (i) synthesis of MCM-41 at relatively low temperature, typically 70−100 °C, and then (ii) postsynthesis hydrothermal treatment of the as-synthesized silica mesophase in an aqueous emulsion of long-chain *N,N*-dimethylalkylamine, typically at 120−130 °C for different periods of time. Depending on the conditions of both steps, materi-

* To whom correspondence should be addressed. Tel.: 613 562 5483. E-mail: abdel.sayari@science.uottawa.ca.
† CCRI.
‡ Department of Chemical Engineering.
§ Department of Chemistry.

10.1021/ie0504194 CCC: $30.25
Published on Web 09/09/2005

3248 *Ind. Eng. Chem. Res.* **2006,** *45,* 3248−3255

Applications of Pore-Expanded Mesoporous Silicas. 3. Triamine Silane Grafting for Enhanced CO_2 Adsorption

Peter J. E. Harlick and Abdelhamid Sayari*

Centre for Catalysis Research and Innovation (CCRI), Department of Chemical Engineering and Department of Chemistry, University of Ottawa, Ottawa, Ontario, K1N 6N5, Canada

Conventional MCM-41 and pore-expanded MCM-41 (PE-MCM-41) silicas have been used as supports for grafting 3-[2-(2-aminoethylamino)ethylamino]propyl trimethoxysilane (TRI) and tested for CO_2 adsorption. The effects of the quantity of triamine silane added to the grafting mixture on the CO_2 adsorption capacity and apparent adsorption rate have been examined. The results showed that when both supports were grafted under the same conditions, PE-MCM-41 was grafted with slightly larger quantities of amine than MCM-41, for all controlled silane additions. Based on the adsorption performance of the materials using a dry 5% CO_2/N_2 feed mixture, the optimal quantity of triamine silane added to the grafting mixture was determined to be ca. 3.0 $cm^3/g(SiO_2)$, for both MCM-41 and PE-MCM-41. The CO_2 adsorption capacity of TRI−PE-MCM-41 was significantly higher than that of TRI−MCM-41. Furthermore, the dynamic adsorption performance of TRI−PE-MCM-41 was far superior to TRI−MCM-41. In comparison to 13X zeolite, TRI−PE-MCM-41 exhibited higher adsorption capacities in the initial time frame of exposure, even though the 13X zeolite exhibited a higher equilibrium adsorption capacity. The result of this behavior is largely due to the rapid CO_2−amine interaction and the open pore structure of TRI−PE-MCM-41 over that of the 13X zeolite. When these adsorbents were exposed to a humid stream of 5% CO_2/N_2 (28% relative humidity), both grafted materials exhibited a slight increase in the adsorption capacity, whereas, 13X zeolite did not retain any significant CO_2 adsorption capacity. These results suggest that the TRI−PE-MCM-41 material may be most suitable for use in a rapid cyclic adsorption process under humid feed conditions.

Introduction

Although there are several compounds that contribute to the greenhouse effect, carbon dioxide has received the most attention, because of its abundance as an effluent in industrial processes. Therefore, because of the global concern over rising atmospheric temperatures, the recent literature has shown that there is a keen interest in developing materials and processes that can efficiently and economically capture and isolate the effluent CO_2. Although the present state-of-the-art methods for CO_2 removal allow for such a process to be applied, the economics of the process may not be favorable enough to offset the capture cost.

Carbon dioxide scrubbing is currently practiced on a large scale for the purification of industrial gases (natural gas, syngas, etc.) and also in life support systems in confined spaces such as submarines, space vehicles, and other inhabited vessels for space exploration platforms). These processes use mainly alkanolamine aqueous solutions,[1] the most common being monoethanolamines and diethanolamines (MEA and DEA) and *N*-methyl diethanol amine (MDEA). The process is reversible and can be represented as shown in Scheme 1.

Because the reactions are exothermic, the formation of carbamate and bicarbonate is favored at low temperature, whereas their dissociation into amine and CO_2 prevails at elevated temperatures.[2]

The use of aqueous solutions of low-molecular-weight alkanolamines suffers many drawbacks.[3,4] Under typical scrubbing conditions, (i) a fraction of the amine and its decomposition products is lost by evaporation, which, in addition to reducing the absorption capacity, may cause problems because of their toxicity; (ii) the amine undergoes oxidative degradation, leading to decreased capacity, increased viscosity, and excessive foaming; and (iii) excessive corrosion occurs, thus posing severe operational problems.

Scheme 1. CO_2 Reaction Pathways with Primary Amines

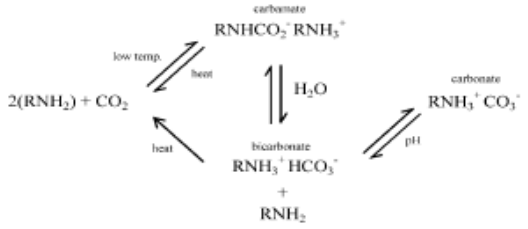

In addition to liquid-phase systems, there were attempts to use reactive solids or amine-impregnated solids, particularly for air revitalization in manned space shuttles.[5−7] Some of the drawbacks of these impregnated materials were the quantity of amine that could be occluded. Because of the nature of the support material, only limited quantities could be loaded, and, thus, the materials did not exhibit sufficiently high adsorption capacities. In our previous work,[8] we developed a material that could occlude a large quantity of amine (up to 7.5 mmol(N)/g, based on diethanol amine), and thus exhibit a high adsorption capacity. However, since the amine loading was achieved through impregnation, the material could only be applied in low-temperature applications, i.e., <100 °C.

In this study, the development of novel adsorbent materials has been achieved with the specific task of CO_2 separation from N_2 by combining the favorable properties of *liquid amine absorption* and *gas−solid adsorption*. The main goal was to develop a material with CO_2 adsorption characteristics that

* To whom correspondence should be addressed. E-mail: abdel.sayari@science.uottawa.ca.

10.1021/ie051286p CCC: $33.50
Published on Web 03/22/2006

Studies in Surface Science and Catalysis, volume 158
J. Čejka, N. Žilková and P. Nachtigall (Editors)

Amine grafted, pore-expanded MCM-41 for acid gas removal: Effect of grafting temperature, water, and amine type on performance

P.J.E. Harlick and A. Sayari*

Centre for Catalysis Research and Innovation (CCRI)
Department of Chemical Engineering and Department of Chemistry
University of Ottawa, Ottawa, Ontario, K1N 6N5, Canada

The application of pore-expanded MCM-41 mesoporous silica coated with various aminosilanes has been examined by the adsorption of CO_2 from N_2. Extremely high levels of active amine content were achieved with pre-hydrated surfaces and reaction at temperatures below reflux in order to facilitate surface polymerization of the silanes. The various coated materials exhibited CO_2 adsorption capacities, which all exceeded the literature reported values, for both meso-porous and micro-porous materials. Further, the apparent adsorption/desorption rate with the amine functionalized materials was exceedingly high even at low regeneration temperatures. When considering the amine type, the adsorption capacity was found to be dependent on the type and quantity of grafted amine. However, the difference between the diamine and triamine silane was only significant in the apparent adsorption rate as the triamine outperformed the diamine. These properties will result in a large decrease in the cyclic temporal and thermal parameters, and therefore an increase in the gas processed per unit time, when exploited in an adsorption process.

1. INTRODUCTION

The term greenhouse gas has been mentioned quite often in the recent literature, as a result of society's global concern over rising atmospheric temperatures. While there are several compounds which contribute to the greenhouse effect, carbon dioxide (CO_2) has received the most attention, due to its abundance as an effluent in industrial processes. Therefore, the literature has shown a concentration on developing a separation scheme. While the present state of the art for CO_2 removal allows for such a process to be applied, the economics of the process are not favorable enough to offset the capture cost. The major obstacle to these processes is the dynamic efficiency of the separation medium being employed. Various techniques have been applied which exploit the properties of membranes, absorbents, or adsorbents. The most common method of CO_2 removal presently used on a large scale is via wet scrubbing (liquid phase absorption).

To meet the present and future constraints placed on the allowable emissions of CO_2 the solution lies with point source reduction and recovery. Therefore, a treatment process must be developed. For this approach to succeed, it must be capable of effective and efficient removal, concentration, and recovery of CO_2 from various sources for industrial applications. Periodic cyclic adsorption processes can be designed to overcome these constraints if a suitable adsorbent is available. In this study, the development of novel adsorbent materials

446 Ind. Eng. Chem. Res. 2007, 46, 446−458

Applications of Pore-Expanded Mesoporous Silica. 5. Triamine Grafted Material with Exceptional CO_2 Dynamic and Equilibrium Adsorption Performance

Peter J. E. Harlick and Abdelhamid Sayari*

Centre for Catalysis Research and Innovation (CCRI), Department of Chemical Engineering and Department of Chemistry, University of Ottawa, Ottawa, Ontario K1N 6N5, Canada

Application of pore-expanded MCM-41 (PE-MCM-41) mesoporous silica coated with 3-[2-(2-aminoethylamino)ethylamino]propyltrimethoxysilane (TRI) has been extensively examined for the adsorption of CO_2 from N_2. A systematic study of the amine loading as a function of the relative amounts of TRI and water used during the grafting procedure and the temperature of the grafting reaction was carried out. Extremely high levels of active amine content were achieved using prehydrated silica surfaces at grafting temperatures below reflux in order to facilitate thermally controlled water-aided surface polymerization of the aminosilanes. The CO_2 adsorption capacities and rates were determined for all materials as a function of the amount of TRI and water per gram of support added to the grafting mixture. The optimal TRI grafted PE-MCM-41 adsorbent exhibited a 2.65 mmol/g adsorption capacity at 25 °C and 1.0 atm for a dry 5% CO_2 in N_2 feed mixture, which exceeded all literature reported values, for both meso- and microporous materials under the conditions used in this study. Further, the apparent adsorption and desorption rates with the amine functionalized materials were exceedingly high. When considering the grafted amine quantity, the adsorption capacity and rate were found to be mutually dependent on each other, exhibiting an apparent optimal combination. In comparison to zeolite 13X, the optimally loaded TRI-PE-MCM-41 was far superior in terms of dynamic adsorption and desorption performance. These results were further enhanced when the adsorbents were challenged with a humid stream of 5% CO_2/N_2. The TRI-PE-MCM-41 exhibited a 10% increase in CO_2 adsorption capacity, whereas the 13X zeolite did not retain any significant CO_2 adsorption capacity.

Introduction

The term greenhouse gas has been mentioned quite often in the recent literature, as a result of society's concern over rising atmospheric temperatures. While there are several compounds which contribute to the greenhouse effect, carbon dioxide (CO_2) has received the most attention, because of its abundance as part of the effluent from many industrial processes. Carbon dioxide emission is largely based on the combustion of carbon containing fuels, as in the heating and transportation markets. Therefore, much effort has been focused on developing viable separation schemes. While the present state of the art for CO_2 removal offers feasible processes for certain applications, the process economics are often not favorable enough to offset the capture cost. The major obstacle to separation processes is the dynamic efficiency of the separation medium being employed. Various techniques have been applied that exploit the properties of membranes, absorbents, or adsorbents, while the most common method of CO_2 removal presently used on a large scale is wet scrubbing (liquid-phase absorption).

To meet the present and future constraints placed on the allowable emissions of CO_2, an immediate solution lies with point-source reduction and recovery. Therefore, a treatment process must be developed. For this separation process to succeed, it must be capable of effective and efficient removal, concentration, and recovery of CO_2 from various sources for industrial applications. Periodic cyclic adsorption processes can be designed to overcome these process requirements if a suitable adsorbent is available. In this study, the development of novel adsorbent materials has been achieved with the specific task of CO_2 separation from N_2 by exploiting the favorable properties of *gas−liquid absorption* and *gas−solid adsorption* via the grafting of amine functionality to a mesoporous solid support.

* To whom correspondence should be addressed. E-mail: abdel.sayari@science.uottawa.ca.

Periodic mesoporous silicas, discovered in 1992 by Mobil researchers[1,2] and extensively studied by others (for example, see refs 3−7), appeared to be an excellent starting point for the synthesis of silicas with large pore volume and pore size. Previously, our research group developed a method to further enlarge the pore size and volume of MCM-41 silica from typically 4 nm and 0.8 cm^3/g up to 25 nm and 3.5 cm^3/g, respectively, through a postsynthesis hydrothermal treatment in the presence of long chain alkyldimethylamines.[8−11] This profound transformation occurs without any significant loss of surface area. This achievement allows us to exploit the internal space of this type of material for different adsorption[12−14] and catalytic applications.[15−17]

In our initial work dealing with CO_2 removal,[13] we exploited the high pore volume and diameter of pore-expanded MCM-41 silica (PE-MCM-41) to impregnate a large quantity of diethanolamine (ca. 8.0 mmol/g). With this material, very high amine loadings were obtained and resulted in CO_2 adsorption capacities as high as 2.93 mmol/g for a 5% CO_2/N_2 feed at 25 °C and 101 kPa total pressure. However, since the amine was loaded by simple impregnation, the interaction between the support and the occluded species was weak; hence, the material could be operated only at relatively low temperature.

In order to overcome the limitations of the amine impregnated PE-MCM-41, we focused our attention on the design of more robust amine containing PE-MCM-41 adsorbents via the grafting of aminosilanes.[14] In this work, we showed that the effect of the amine surface density of the material has a profound impact on the adsorption efficiency. Intuitively, a high amine density would be desirable; however, we demonstrated that a high amine loading does not necessarily allow for the optimal use of the grafted amine for CO_2 adsorption from N_2. This efficiency was defined as the point at which the rate of adsorption was optimal while considering the magnitude of the adsorption capacity.

10.1021/ie060774+ CCC: $37.00
Published on Web 12/20/2006

Appendix C

US Patent 7,767,004; 2010

As pertaining to the work compilation from this Dissertation

US007767004B2

(12) **United States Patent**
Sayari et al.

(10) **Patent No.: US 7,767,004 B2**
(45) **Date of Patent: Aug. 3, 2010**

(54) **FUNCTIONALIZED ADSORBENT FOR REMOVAL OF ACID GASES AND USE THEREOF**

(75) Inventors: **Abdelhamid Sayari**, Ottawa (CA); **Peter J. E. Harlick**, Gatineau (CA)

(73) Assignee: **University of Ottawa**, Ottawa, Ontario (CA)

(*) Notice: Subject to any disclaimer, the term of this patent is extended or adjusted under 35 U.S.C. 154(b) by 0 days.

(21) Appl. No.: **11/908,248**

(22) PCT Filed: **Mar. 13, 2006**

(86) PCT No.: **PCT/CA2006/000372**

§ 371 (c)(1),
(2), (4) Date: **Jul. 18, 2008**

(87) PCT Pub. No.: **WO2006/094411**

PCT Pub. Date: **Sep. 14, 2006**

(65) **Prior Publication Data**

US 2008/0276804 A1 Nov. 13, 2008

Related U.S. Application Data

(60) Provisional application No. 60/660,783, filed on Mar. 11, 2005.

(51) **Int. Cl.**
B01D 53/02 (2006.01)

(52) **U.S. Cl.** **95/285**; 95/136; 96/108; 55/524; 264/48; 428/305.5; 428/310.5

(58) **Field of Classification Search** 96/108; 95/136, 285; 55/524; 264/48; 428/305.5, 428/310.5

See application file for complete search history.

(56) **References Cited**

U.S. PATENT DOCUMENTS

2,818,323	A	12/1957	Haensel
3,491,031	A	1/1970	Stoneburner
4,810,266	A	3/1989	Zinnen et al.
4,999,175	A	3/1991	Vansant et al.
5,087,597	A	2/1992	Leal et al.

(Continued)

FOREIGN PATENT DOCUMENTS

CA	2 510 235	A1	12/2003

OTHER PUBLICATIONS

Attard et al. "Liquid-crystalline phases as templates for the synthesis of mesoporous silica" Nature 378:366-368 (1995).

(Continued)

Primary Examiner—Robert J Hill, Jr.
Assistant Examiner—Christopher P Jones
(74) *Attorney, Agent, or Firm*—Morgan Lewis & Bockius LLP

(57) **ABSTRACT**

The present invention provides a functionalized adsorbent for removal of acid gases, which comprises a pore-expanded mesoporous support having a pore volume of between 0.7 and 3.6 cc/g, a median pore diameter of between 1 and 25 nm, and a BET surface area of between 500 and 1600 m^2/g. The support is functionalized by addition of acid-gas reactive functional groups within the pores and external surface of said support material. Also provided are methods of manufacturing the adsorbent and methods of use.

22 Claims, 14 Drawing Sheets

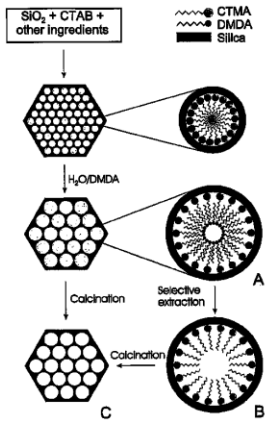

Appendix D

Google Scholar Report – May 2015

As printed from Google Scholar website:
http://scholar.google.com/
on May 20, 2015

Peter Harlick

Unknown affiliation
Chemical engineering, adsorption, catalysis, cellulosic ethanol

Google Scholar

Citation indices	All	Since 2010
Citations	1266	984
h-index	12	9
i10-index	13	9

Title 1–20	Cited by	Year
Applications of pore-expanded mesoporous silica. 5. Triamine grafted material with exceptional CO2 dynamic and equilibrium adsorption performance PJE Harlick, A Sayari Industrial & Engineering Chemistry Research 46 (2), 446-458	311	2007
Applications of pore-expanded mesoporous silica. 2. Development of a high-capacity, water-tolerant adsorbent for CO2 RS Franchi, PJE Harlick, A Sayari Industrial & engineering chemistry research 44 (21), 8007-8013	240	2005
Applications of pore-expanded mesoporous silicas. 3. Triamine silane grafting for enhanced CO2 adsorption PJE Harlick, A Sayari Industrial & Engineering Chemistry Research 45 (9), 3248-3255	239	2006
An experimental adsorbent screening study for CO 2 removal from N 2 PJE Harlick, FH Tezel Microporous and Mesoporous Materials 76 (1), 71-79	198	2004
Adsorption of carbon dioxide, methane and nitrogen: pure and binary mixture adsorption for ZSM-5 with SiO 2/Al 2 O 3 ratio of 280 PJE Harlick, FH Tezel Separation and purification technology 33 (2), 199-210	84	2003
Adsorption of carbon dioxide, methane, and nitrogen: pure and binary mixture adsorption by ZSM-5 with SiO2/Al2O3 ratio of 30 PJE Harlick, FH Tezel Separation science and technology 37 (1), 33-60	46	2002
Applications of pore-expanded MCM-41 silica: 4. Synthesis of a highly active base catalyst DD Das, PJE Harlick, A Sayari Catalysis Communications 8 (5), 829-833	28	2007
A novel solution method for interpreting binary adsorption isotherms from concentration pulse chromatography data PJE Harlick, FH Tezel Adsorption 6 (4), 293-309	28	2000
	20	2005

Title 1–20	Cited by	Year
Amine grafted, pore-expanded MCM–41 for acid gas removal: Effect of grafting temperature, water, and amine type on performance PJE Harlick, A Sayari Studies in Surface Science and Catalysis 158, 987-994		
CO2 N2 and CO2 CH4 binary adsorption isotherms with H-ZSM5: The importance of experimental data regression with the concentration pulse method PJE Harlick, FH Tezel The Canadian Journal of Chemical Engineering 79 (2), 236-245	17	2001
Use of concentration pulse chromatography for determining binary isotherms: comparison with statically determined binary isotherms PJE Harlick, FH Tezel Adsorption 9 (3), 275-286	15	2003
A high capacity, water tolerant adsorbent for CO 2: diethanolamine supported on pore-expanded MCM-41 R Franchi, PJE Harlick, A Sayari Studies in Surface Science and Catalysis 156, 879-886	12	2005
Non-oxidative conversion of ethane to ethylene over transition metals supported on Mg–Al mixed oxide: Preliminary screening of catalytic activity and coking ability A Tsyganok, PJE Harlick, A Sayari Catalysis Communications 8 (5), 850-854	10	2007
Equilibrium analysis of cyclic adsorption processes: CO2 working capacities with NaY PJE Harlick, FH Tezel Separation science and technology 40 (13), 2569-2591	9	2005
Adsorption of tetrafluoromethane and nitrogen by various adsorbents S Singh, FH Tezel, PJE Harlick Separation science and technology 37 (12), 2763-2784	6	2002
Functionalized adsorbent for removal of acid gases and use thereof A Sayari, PJE Harlick US Patent 7,767,004	2	2010
Method for introducing cellulase enzyme to lignocellulosic feedstock slurry PJE Harlick US Patent 8,603,789	1	2013
Process for improving the hydrolysis of cellulose in high consistency systems using one or more unmixed and mixed hydrolysis reactors PJE Harlick, W Zheng US Patent 8,709,770		2014

Title 1–20	Cited by	Year
System for hydrolyzing a cellulosic feedstock slurry using one or more unmixed and mixed reactors PJE Harlick, W Zheng US Patent App. 14/203,769		2014
18-O-01-An experimental adsorbent screening study for CO 2 removal from flue gas PJE Harlick, H Halsall-Whitney, FH Tezel Studies in Surface Science and Catalysis 135, 143		2001

Dates and citation counts are estimated and are determined automatically by a computer program.